LASL EXPLOSIVE PROPERTY DATA

LOS ALAMOS SERIES ON DYNAMIC MATERIAL PROPERTIES

LOS ALAMOS DATA CENTER FOR DYNAMIC MATERIAL PROPERTIES

TECHNICAL COMMITTEE

Charles L. Mader	Program Manager
Terry R. Gibbs	Explosive Data Editor
Charles E. Morris	Shock Wave Profile Editor
Stanley P. Marsh	Equation of State Editor
Alphonse Popolato	Explosive Data Editor
Martha S. Hoyt	Computer Applications Analyst
Kasha V. Thayer	Technical Editor
Sharon L. Crane	Technical Editor

John F. Barnes
Richard D. Dick
John W. Hopson, Jr.
James N. Johnson
Elisabeth Marshall
Timothy R. Neal
Suzanne W. Peterson
Raymond N. Rogers
John W. Taylor
Melvin T. Thieme
Jerry D. Wackerle
John M. Walsh

LASL EXPLOSIVE PROPERTY DATA

Editors — Terry R. Gibbs
Alphonse Popolato

CONTRIBUTORS
John F. Baytos
Bobby G. Craig
Arthur W. Campbell
William E. Deal
Jerry J. Dick
Robert H. Dinegar
Raymond P. Engelke
Thomas E. Larson
Elisabeth Marshall
John B. Ramsay
Raymond N. Rogers
Diane Soran
Manuel J. Urizar
Jerry D. Wackerle

UNIVERSITY OF CALIFORNIA PRESS
Berkeley • Los Angeles • London

University of California Press
Berkeley and Los Angeles, California

University of California Press, Ltd.
London, England

ISBN 0-520-04012-0
Series ISBN 0-520-04007-4
Library of Congress Catalog Card Number: 80-53635
Printed in the United States of America

1 2 3 4 5 6 7 8 9

CONTENTS

PREFACE

This volume of the Los Alamos Series on Dynamic Materials Properties is designed to provide a single source of reliable data on high explosives in use or formerly used at the Los Alamos National Scientific Laboratory (LASL). These are the best LASL data available and, as revisions are made, new or better data will be added.

The volume is divided into two major parts for the user's convenience. Part I presents in one place the properties of explosives by explosive and summarizes all the property data and the results of various tests generally used to characterize explosives. It covers only pure explosives and explosive formulations that have been well characterized. However, for many of these materials there are some properties or test results that have not been determined and in those cases the section normally used to list the property or test result has been omitted. Part II presents the properties of explosives by property or method of determination. It covers many more materials, often those for which only one property has been determined. Part II permits ready comparison of explosives and, for a number of properties, contains detailed data that permit use of other data reduction methods, such as the user's own fitting techniques.

Because many explosives properties depend upon the exact details of charge preparation, and their determination depends upon the exact details of the testing procedures, many of the test procedures used in gathering these data are described. References on the test procedures and data are cited where possible; however, much of the data has been taken from unpublished internal LASL reports. If more than one group of data or conflicting data were available, we selected the most credible. Also, because almost all of these explosives are heterogeneous polycrystalline materials, some of their properties, especially initiation by strong shocks, depend upon such factors as charge density, the particle size distribution of the crystals, and the degree of crystal perfection. Therefore, Part II includes detailed descriptions of the test explosives wherever possible.

In Part I the explosives are discussed alphabetically and the various plastic-bonded explosives, PBXs, and extrudable explosives, XTXs, are discussed in numerical order. Part II, because it covers many more explosives formulations,

treats pure explosives first, alphabetically; then castables; then plastic-bonded explosives, alphabetically by major explosive constituent; and, finally, propellants. An explosives table gives the composition of each material covered in this volume, and a glossary defines acronyms and unusual terms.

The authors gratefully acknowledge the help that was provided by Margaret M. Cox and Jeanne Stein in producing many of the graphics.

PART I
EXPLOSIVES PROPERTIES BY EXPLOSIVE

EXPLOSIVES PROPERTIES BY EXPLOSIVE

BARATOL

1. GENERAL PROPERTIES

1.1 Chemical and Physical Description. Baratol, a mixture of barium nitrate, $Ba(NO_3)_2$, and TNT, $C_7H_5N_3O_6$, is off-white to gray.

1.2 Common Use. During World War II, the British developed baratols that contained about 20 wt% barium nitrate to replace TNT. The United States used baratols that contained slightly more barium nitrate in depth charges and other limited munitions. Baratols that contain up to 76 wt% barium nitrate are now used as the low detonation velocity explosive in waveshaping devices such as plane-wave lenses.

1.3 Toxicity.[1] Barium nitrate can irritate skin and mucous membranes.

2. MANUFACTURE AND PROCUREMENT

2.1 Manufacture. Finely ground barium nitrate is added to molten TNT to form a castable slurry. To lower the slurry viscosity, which increases with the percentage of barium nitrate, about 0.1 wt% of nitrocellulose (11.8-12.2 wt% nitrogen, 18-25 centipoise) is added to the TNT before the addition of the barium nitrate. After the barium nitrate is added, just before vacuum is applied to the melt, 0.05-0.1 wt% of either decylgallophenone or stearoxyacetic acid is added to prevent cracking. Vacuum is applied to the melt just before casting to remove dissolved and occluded gas and to provide higher, more uniform density. Carefully controlled cooling of the casting also promotes uniform density and composition.

2.2 Procurement. There are no purchase specifications for baratol. It is produced to the user's specific requirements at ordnance plants that have TNT-casting facilities.

2.3 Shipping.[2] Baratol is shipped as a Class A explosive, as defined by the Code of Federal Regulations.

2.4 Storage.[3] Baratol is stored in Compatibility Group D, Storage Class 1.1, as required by US Army Materiel Command regulation.

3. CHEMICAL PROPERTIES

3.1 Composition. Unless otherwise specified, the properties given are for the following composition.

Constituent	Weight Percent	Volume Percent
Barium nitrate	76.0	62.8
TNT	24.0	37.2

3.2 Molecular Weight.

Constituent	Structure	Molecular Weight
Barium nitrate	$Ba(NO_3)_2$	261.38
TNT	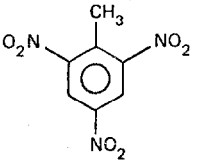 $C_7H_5N_3O_6$	227.13

3.3 Solubility. Barium nitrate solubility in water is given.

Temperature (°C)	Solubility (g/100 ml of solvent)
20	8.7

4. PHYSICAL PROPERTIES

4.2 Density.

	Density (g/cm^3)
Theoretical	2.634
Vacuum cast	2.60-2.62

4.3 Infrared Spectrum. See Fig. 1.

5. THERMAL PROPERTIES

5.1 Phase Changes.

Type	Temperature (°C)	Latent Heat (cal/g)
Solid-to-liquid	79-80	6.1

5.3 Heat Capacity.

Heat Capacity at Constant Pressure (cal/g-°C)	Temperature Range (°C)
0.192	$18 < T < 75$

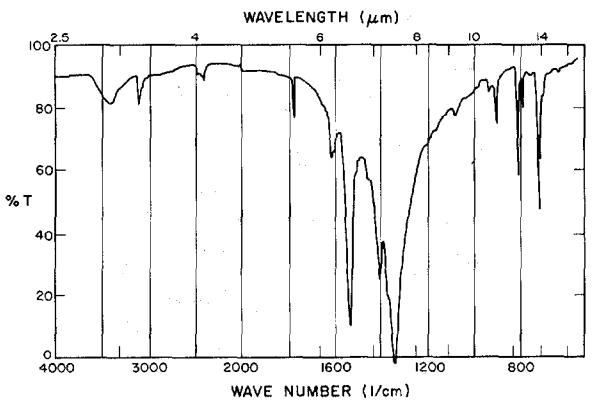

Fig. 1. Infrared spectrum.

5.4 Thermal Conductivity.

Conductivity (cal/s-cm-°C)	Temperature Range (°C)
11.84×10^{-4}	$18 < T < 75$

5.5 Coefficient of Thermal Expansion.

Coefficient of Expansion (1/C°)	Temperature Range (°C)
$3.4 \times 10^{-5} + 2.8 \times 10^{-7}$ T	$-40 < T < 60$

5.6 Heats of Combustion and Formation.[4]

Constituent	ΔH_c° (kcal/mole)	ΔH_f° (kcal/mole)
TNT	−817.2	−12.0
$Ba(NO_3)_2$	---	−238.23

5.8 Other Thermal Stability Test Results.

Test	Results
Vacuum	0.1-0.4 ml/g of gas evolved after 48 h at 120°C
DTA and pyrolysis	See Fig. 2

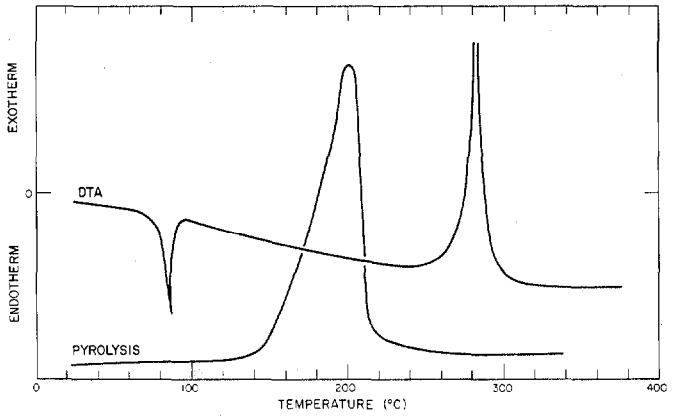

Fig. 2. Baratol DTA and pyrolysis test results.

6. DETONATION PROPERTIES

6.1 Detonation Velocity. The composition of baratol cast to approximately 97% of its theoretical density affects its detonation velocity as follows.

Effect of Composition

Weight Percent $Ba(NO_3)_2$	Detonation Velocity (mm/μs)
70	5.12
72	5.03
74	4.95
76	4.86

6.2 Detonation Pressure.

Weight Percent $Ba(NO_3)_2$	Density (g/cm^3)	Detonation Velocity ($mm/\mu s$)	Pressure (GPa)
76	2.61	4.925	14

6.4 Plate Dent Test Results.

Charge Diameter (mm)	Density (g/cm^3)	Dent Depth (mm)	Charge Height (mm)
41.3	2.61	3.21	203

7. SHOCK INITIATION PROPERTIES

7.1 Gap Test Results.

Weight Percent $Ba(NO_3)_2$	Density g/cm^3	G_{50} (mm)	L_{95} (mm)
	Large Scale		
76	2.597	27.3	0.20
	Small Scale		

No data because sample was below failure diameter.

7.2 Wedge Test Results.

Density (g/cm^3)	Distance, x*, and Time, t*, to Detonation (mm and μs)	Pressure Range (GPa)
2.61	$\log P = (1.2 \pm 0.03) - (0.30 \pm 0.03) \log x^*$ $\log P = (1.01 \pm 0.01) - (0.27 \pm 0.02) \log t^*$, where P= pressure in gigapascals.	$6.9 < P < 11.8$

7.3 Shock Hugoniots.[5]

Density (g/cm^3)	Shock Hugoniot ($mm/\mu s$)	Particle Velocity Range ($mm/\mu s$)
2.611	$U_s = 2.40 + 1.66\,U_p$,	$0 < U_p < 0.75$
	$U_s = 1.50 + 2.16\,U_p$,	$0.75 < U_p < 1.2$
2.63	$U_s = 2.79 + 1.25\,U_p$,	$0 < U_p < 1$

where U_s = shock velocity
and U_p = particle velocity.

8. SENSITIVITY

8.1 Drop Weight Impact Height.

Tool Type	H_{50} (cm)
12	110
12B	140

9. MECHANICAL PROPERTIES

9.2 Tensile Strength and Modulus.

Ultimate Tensile Strength (psi)
380-450

9.3 Compressive Strength and Modulus.

Ultimate Compressive Strength (psi)	Compressive Modulus (psi)
5700-8100	(1.5 to 2.0) x 10^6

REFERENCES

1. N. I. Sax, *Dangerous Properties of Industrial Materials,* 4th Ed. (Van Nostrand Reinhold Company, New York, 1975).

2. *Code of Federal Regulations, 49, Transportation Parts 100-199, Rev. 12-1-76* (Office of the Federal Register, General Services Administration, Washington, DC, 1976).

3. US Army Materiel Command, Regulation No. AMCR 385-100 (1977).

4. Prince E. Rouse, Jr., Journal of Chemical and Engineering Data **21**, 16-20 (1976).

5. V. M. Boyle, R. L. Jameson, and M. Sultanoff, *Proceedings—Fourth Symposium (International) on Detonation, White Oak, Maryland, October 12-15, 1965* (Office of Naval Research, Department of the Navy, ACR-126, 1965), pp. 241-247.

COMPOSITION B

1. GENERAL PROPERTIES

1.1 Chemical and Physical Description. Composition B (Comp B), a mixture of 60 wt% RDX and 40 wt% TNT, with or without a wax desensitizer, is yellow-brown. Mixtures of RDX and TNT are generally called cyclotols in the United States, Hexolite in France, Füllpulver in Germany, Tritolite in Italy, Tritolita in Spain, and Hexotol in Sweden.

Comp B desensitized with 1 wt% wax is available in grades A and B. Grade A is more fluid than Grade B when molten. Comp B-3 contains no desensitizer. It is more viscous than Grade A or B when molten because its median RDX particle diameter is smaller.

1.2 Common Use. Comp B is used as the explosive fill in almost all types of explosive ordnance.

1.3 Toxicity.[1] The toxicity of Comp B is like that of RDX and TNT.

Workers who inhaled RDX dust for several months have become unconscious and have suffered loss of reflexes. The suggested maximum permissible airborne concentration is 1.5 mg/m^3.

Inhaled TNT vapor or dust may irritate mucous membranes and cause sneezing, coughing, and sore throat. TNT may produce toxic hepatitis and aplastic anemia, and it yellows the exposed skin, hair, and nails of workers. Dermatitis, erythema, papules, and itchy eczema can be severe. Ingestion of 1-2 g of TNT is estimated to be an acute fatal dose to humans. The suggested maximum permissible airborne dust concentration is 0.5 mg/m^3.

2. MANUFACTURE AND PROCUREMENT

2.1 Manufacture. Comp B-type explosives, including cyclotols, are manufactured from TNT and water-wet RDX. The TNT is melted in a steam-jacketed kettle equipped with a stirrer and is brought to about 100°C. The wet RDX is added

slowly. Heating and stirring are continued until most of the water is evaporated. The appropriate desensitizing wax or other additive is then thoroughly mixed with the other ingredients. After cooling to satisfactory fluidity, the Comp B is cast into strips or chips. The chips are shipped to an ordnance plant, remelted, and cast into ammunition or into desired shapes. During this melting, other additives may be introduced. To increase the density of cast charges, a vacuum may be applied to the molten Comp B before casting.

2.2 Procurement. Comp B is purchased from the US Army Armament Readiness Command under military specification MIL-C-401C, dated May 15, 1968, or, as Comp B-3, under MIL-C-45113, dated June 19, 1958.

2.3 Shipping.[2] Comp B is shipped as a Class A explosive.

2.4 Storage.[3] Comp B is stored in Compatibility Group D, Storage Class 1.1.

3. CHEMICAL PROPERTIES

3.1 Composition.

	Comp B, Grades A and B		Comp B-3	
Constituent	Weight Percent	Volume Percent	Weight Percent	Volume Percent
RDX	59.5	56.9	60.0	57.8
TNT	39.5	41.2	40.0	42.2
Wax	1.0	1.9	0.0	0.0

3.2 Molecular Weight.

Constituent	Structure	Molecular Weight
RDX	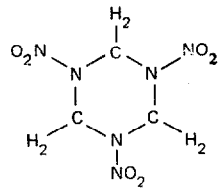 $C_3H_6N_6O_6$	222.13
TNT	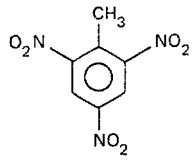 $C_7H_5N_3O_6$	227.13
Wax	$CH_3(CH_2)_n\,CH_3$	$30.07 + (14.02)_n$

3.3 Solubility.[4] The solubility is that of the components RDX and TNT.

Solvent	Grams of RDX Dissolved/100 g of Solvent		
	20°C	40°C	60°C
Acetic acid			
99.6%	0.46	0.56	1.22
71.0%	0.22	0.37	0.74
Acetone	6.81	10.34	---
Isoamyl alcohol	0.026	0.060	0.210
Benzene	0.045	0.085	0.195
Chlorobenzene	0.33	0.554	---
Cyclohexanone	4.94	9.20	13.9
Dimethylformamide	---	41.5	60.6
Ethanol	0.12	0.24	0.58
Methyl acetate	2.9	4.1	---
Methylcyclohexanone	6.81	10.34	---
Methyl ethyl ketone	3.23	---	---
Toluene	0.020	0.050	0.125
Trichloroethylene	0.20	0.24	---
Water	0.005	0.0127	0.03

Solvent	Grams of TNT Dissolved/100 g of Solvent		
	20°C	40°C	60°C
Acetone	109.0	228.0	600.0
Benzene	67.0	180.0	478.0
Butyl carbinol acetate	24.0	---	---
Carbon disulfide	0.48	1.53	---
Carbon tetrachloride	0.65	1.75	6.90
Chlorobenzene	33.9	---	---
Chloroform	19.0	66.0	302.
Diethyl ether	3.29	---	---
Ethanol (95%)	1.23	2.92	8.30
Ethylene chloride	18.7	---	---
Hexane	0.16	---	---
Methyl acetate	72.1	---	---
Toluene	55.0	130.0	367.0
Trichloroethylene	3.04	---	---
Water	0.0130	0.0285	0.0675

4. PHYSICAL PROPERTIES

4.2 Density

Material	Theoretical Density (g/cm^3)	Density of Typical Casting (g/cm^3)	
		Open Melt	Vacuum Melt
Comp B, Grades A and B	1.737	1.68-1.70	1.715-1.720
Comp B-3	1.750	---	1.725-1.730

4.3 Infrared Spectrum. See Fig. 1.

5. THERMAL PROPERTIES

5.1 Phase Change.

Type	Temperature (°C)	Latent Heat (cal/g)
Solid-to-slurry	79	14.1

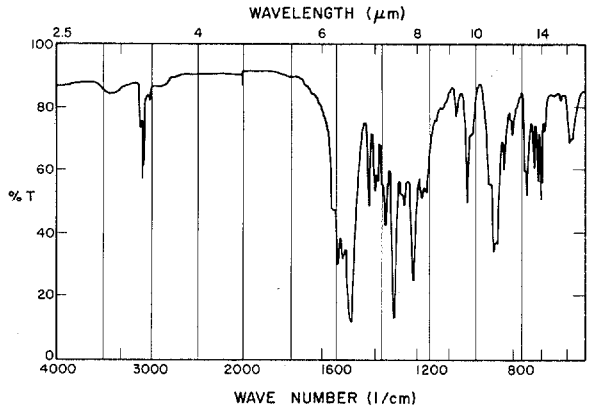

Fig. 1. Infrared spectrum.

5.3 Heat Capacity.

Heat Capacity at Constant Pressure (cal/g-°C)	Temperature Range (°C)
$0.234 + 1.03 \times 10^{-3}$ T	$7 < T < 76$

5.4 Thermal Conductivity.

Density (g/cm^3)	Conductivity (cal/s-cm-°C)
1.730	5.23×10^{-4}

5.5 Coefficient of Thermal Expansion.

Coefficient of Expansion (1/°C)	Temperature Range (° C)
5.46×10^{-5}	$6 < T < 25$

5.6 Heats of Combustion and Formation.[5]

Constituent	ΔH_c° (kcal/mole)	ΔH_f° (kcal/mole)
TNT	-817.2	-12.0
RDX	-501.8	14.7

5.7 Thermal Decomposition Kinetics.[6]

	TNT	RDX
Decomposition energy	300 cal/g	500 cal/g
Activation energy	34.4 kcal/mole	47.1 kcal/mole
Pre-exponential factor	2.51×10^{11}/s	2.02×10^{18}/s

5.8 Other Thermal Stability Test Results.

Test	Results
Vacuum	0.2-0.6 ml/g of gas evolved after 48 h at 120°C
DTA and pyrolysis	See Fig. 2
Critical temperature, Tm	214°C
Charge radius, a	3.0 mm

6. DETONATION PROPERTIES

6.1 Detonation Velocity.[7]

Effect of Charge Radius

Charge radius affects the detonation velocity of unconfined Grade A Comp B, cast to a density of 1.700 g/cm³, as follows.

$$D(R) = 7.859[(1 - 2.84 \times 10^{-2}/R) - 5.51 \times 10^{-2}/R(R - 1.94)],$$

where D = detonation velocity in millimeters per microsecond

and R = charge radius in millimeters.

The experimentally determined failure diameter is 4.28 mm.

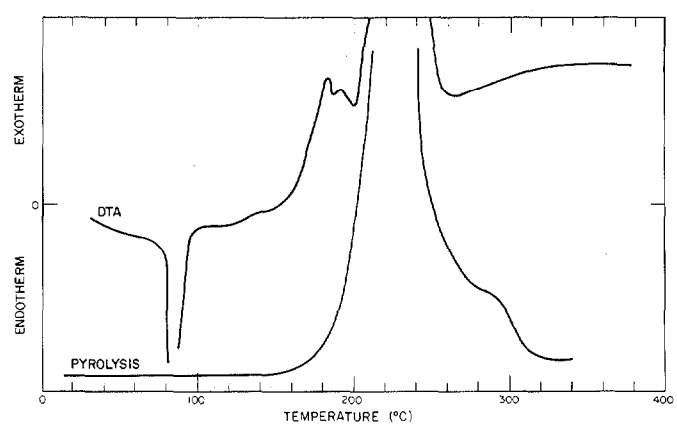

Fig. 2. Comp B DTA and pyrolysis test results.

6.2 Detonation Pressure.[8]

Grade A Comp B (Weight Percent RDX)	Density (g/cm³)	Detonation Velocity (mm/μs)	Detonation Pressure (GPa)
64.0	1.713	8.018	29.22

6.3 Cylinder Test Results.

Density[a] (g/cm³)	Detonation Velocity (mm/μs)	Cylinder Wall Velocity (mm/μs) at	
		$R-R_o = 5$ mm	$R-R_o = 19$ mm
1.700[b]	7.915	1.377	1.625
1.715	7.911	1.378	1.628

[a]Grade A Comp B.
[b]Scaled from a 4-in.-diam shot.

6.4 Plate Dent Test Results.[9]

Charge Diameter (mm)	Weight Percent RDX	Density (g/cm³)	Dent Depth (mm)	Charge Height (mm)
41:3	60:7	1.730	8:64	203
41.3	64.0	1:714	8.47	203

7. SHOCK INITIATION PROPERTIES

7.1 Gap Test Results.[10]

Type	Density (g/cm^3)	Weight Percent RDX	G_{50} (mm)	L_{95} (mm)
		Large Scale		
Comp B-3	1.727	60.0	50.34	0.81
Grade A Comp B	1.710	64.0	45.69	0.45
Grade A Comp B	1.714	64.0	45.18	0.08
		Small Scale		
Comp B-3	1.720	60.0	1.22	---
Grade A Comp B	1.710	---	1.5	0.08

7.2 Wedge Test Results.[11]

Density (g/cm^3)	Distance, x*, to Detonation (mm)	Pressure Range[a] (kbar)
1.72	$2100\ P^{-1.34}$,	$40 < P < 100$
	where P = pressure in kilobars.[a]	

[a]Users should note that this is the only wedge data fit in this volume where pressure is in units of kilobars.

7.3 Shock Hugoniots.[12,13]

Comp B-3 Density (g/cm³)	Shock Hugoniot (mm/μs)	Particle Velocity Range (mm/μs)
1.680	$U_s = 2.71 + 1.86\,U_p$,	$0 < U_p < 1.0$
1.70	$U_s = 3.03 + 1.73\,U_p$,	$0 < U_p < 1.0$

where U_s = shock velocity
and U_p = particle velocity.

7.4 Minimum Priming Charge.[10]

Density (g/cm³)	W_{50} (mg of XTX 8003)	L_{95} (± log mg)
1.727[a]	245	0.070
1.725[b]	623	0.027

[a]Comp B-3.
[b]Grade A Comp B.

7.5 Detonation Failure Thickness.[10]

Density (g/cm³)	Failure Thickness (mm)	L_{95} (mm)
1.729[a]	0.785	0.086
1.729[a]	0.881	0.297
1.727[a]	0.805	0.081
1.727[a]	0.813	0.051
1.713[b]	1.42	0.07

[a]Comp B-3
[b]Grade A Comp B.

8. SENSITIVITY

8.1 Drop Weight Impact Height

Tool Type	H_{50} (cm)
12	59
12B	109

8.2 Large-Scale Drop Test Height.

Density (g/cm^3)	H_{50} (ft)	Reaction
1.725	85	Partial

8.3 Skid Test Results.

Density (g/cm^3)	Impact Angle (degrees)	Target Surface	H_{50} (ft)	Reaction Overpressure (psi)
1.727	15	Sand and epoxy	9.8	< 0.5

8.4 Susan Test Results.[14]

Projectile Impact Velocity (ft/s)	Relative Energy Release (%)
600	0
800	5
1000	20
1200	30
1400	38

9. MECHANICAL PROPERTIES

9.2 Tensile Strength and Modulus.

Ultimate Tensile Strength (psi)
135-150

9.3 Compressive Strength and Modulus.

Temperature (°C)	Ultimate Compressive Strength (psi)	Compressive Modulus (psi x 10^{-6})
50	1400 ± 96	0.63 ± 0.1
0	1860 ± 200	2.40 ± 0.3
-40	2150 ± 280	2.50 ± 0.2

REFERENCES

1. C. R. Buck and S. E. Wilson, Jr., US Army report USEHA-32-049 (1975).

2. *Code of Federal Regulations, 49, Transportation Parts 100-199, Rev. 12-1-76* (Office of the Federal Register, General Services Administration, Washington, DC, 1976).

3. US Army Materiel Command, Regulation No. AMCR 385-100 (1977).

4. A. Seidell, *Solubilities of Organic Compounds,* 3rd Ed., Vol. II, (D. Van Nostrand Co., Inc., New York, 1941).

5. Prince E. Rouse, Jr., Journal of Chemical Engineering Data **21**, 16-20 (1976).

6. R. N. Rogers, Thermochimica Acta **11**, 131-139 (1975).

7. A. W. Campbell and Ray Engelke, *Proceedings—Sixth Symposium (International) on Detonation, Coronado, California, August 24-27, 1976* (Office of Naval Research, Department of the Navy, ACR-221, 1976), pp. 642-652.

8. W. E. Deal, Journal of Chemical Physics **27**, 796-800 (1957).

9. L. C. Smith, Explosivstoffe **15**, 106-130 (1967).

10. Manuel J. Urizar, Suzanne W. Peterson, and Louis C. Smith, Los Alamos Scientific Laboratory report LA-7193-MS (April 1978).

11. J. B. Ramsay and A. Popolato, *Proceedings—Fourth Symposium (International) on Detonation, White Oak, Maryland, October 12-15, 1965* (Office of Naval Research, Department of the Navy, ACR-126, 1965), pp. 233-238.

12. N. L. Coleburn and T. P. Liddiard, Journal of Chemical Physics 44, 1929-1936 (1966).

13. V. M. Boyle, R. L. Jameson, and M. Sultanoff, *Proceedings—Fourth Symposium (International) on Detonation, White Oak, Maryland, October 12-15, 1965* (Office of Naval Research, Department of the Navy, ACR-126, 1965), pp. 241-247.

14. L. G. Green and G. D. Dorough, *Proceedings—Fourth Symposium (International) on Detonation, White Oak, Maryland, October 12-15, 1965* (Office of Naval Research, Department of the Navy, ACR-126, 1965), pp. 477-486.

CYCLOTOL

1. GENERAL PROPERTIES

1.1 Chemical and Physical Description. Cyclotol is the generic term for mixtures of TNT and RDX. In the United States, the term is used for mixtures of 75 wt% RDX and 25 wt% TNT (Type I) or 70 wt% RDX and 30 wt% TNT (Type II), also called Cyclotol 75/25 and Cyclotol 70/30. Neither mixture contains a desensitizer. To improve the flow of the molten form, a bimodal distribution of RDX crystals generally is used.

1.2 Common Use. Cyclotol is generally used as an explosive fill in military applications that require slightly more energy than Comp B can provide.

1.3 Toxicity.[1] Cyclotol toxicity is like that of RDX and TNT.

Workers who inhaled RDX dust for several months have become unconscious and have suffered loss of reflexes. The suggested maximum permissible airborne concentration of RDX is 1.5 mg/m^3.

Inhaled TNT vapor or dust may irritate mucous membranes and cause sneezing, coughing, and sore throat. TNT may produce toxic hepatitis and aplastic anemia, and it yellows the exposed skin, hair, and nails of workers. Dermatitis, erythema, papules, and itchy eczema can be severe. Ingestion of 1-2 g of TNT is estimated to be an acute fatal dose to humans. The suggested maximum permissible airborne dust concentration is 0.5 mg/m^3.

2. MANUFACTURE AND PROCUREMENT

2.1 Manufacture. Cyclotols are manufactured from TNT and water-wet RDX. The TNT is melted in a steam-jacketed kettle equipped with a stirrer and is brought to about 100°C. The wet RDX is added slowly, and heating and stirring are continued until the water is evaporated. Upon cooling to satisfactory fluidity, the cyclotol is cast into strips or chips. The chips are shipped to an ordnance plant, remelted, and cast into ammunition or into desired shapes. During this melting, other additives may be introduced. To increase the density of cast charges, a vacuum may be applied to the molten cyclotol before casting.

2.2 Procurement. Cyclotol is purchased from the US Army Armament Readiness Command under military specification MIL-C-13477A, dated March 31, 1965.

2.3 Shipping.[2] Cyclotol is shipped as a Class A explosive.

2.4 Storage.[3] Cyclotol is stored in Compatibility Group D, Storage Class 1.1.

3. CHEMICAL PROPERTIES

3.1 Composition.

	Type I		Type II	
Constituent	Weight Percent	Volume Percent	Weight Percent	Volume Percent
RDX	75.0	73.2	70.0	68.0
TNT	25.0	26.8	30.0	32.0

3.2 Molecular Weight.

Constituent	Structure	Molecular Weight
RDX	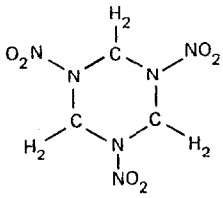 $C_3H_6N_6O_6$	222.13
TNT	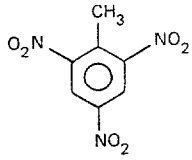 $C_7H_5N_3O_6$	227.13

3.3 Solubility.[4] The solubility is that of the components, RDX and TNT.

	Grams of RDX Dissolved/100 g of Solvent		
Solvent	**20°C**	**40°C**	**60°C**
Acetic acid			
99.6%	0.46	0.56	1.22
71.0%	0.22	0.37	0.74
Acetone	6.81	10.34	---
Benzene	0.045	0.085	0.195
Chlorobenzene	0.33	0.554	---
Cyclohexanone	4.94	9.20	13.9
Dimethylformamide	---	41.5	60.6
Ethanol	0.12	0.24	0.58
Isoamyl alcohol	0.026	0.060	0.210
Methyl acetate	2.9	4.1	---
Methylcyclohexanone	6.81	10.34	---
Methyl ethyl ketone	3.23	---	---
Toluene	0.020	0.050	0.125
Trichloroethylene	0.20	0.24	---
Water	0.005	0.0127	0.03

Solvent	Grams of TNT Dissolved/100 g of Solvent		
	20°C	40° C	60°C
Acetone	109.0	228.0	600.0
Benzene	67.0	180.0	478.0
Butyl carbinol acetate	24.0	---	---
Carbon disulfide	0.48	1.53	---
Carbon tetrachloride	0.65	1.75	6.90
Chlorobenzene	33.9	---	---
Chloroform	19.0	66.0	302.0
Diethyl ether	3.29	---	---
Ethanol (95%)	1.23	2.92	8.30
Ethylene chloride	18.7	---	---
Hexane	0.16	---	---
Methyl acetate	72.1	---	---
Toluene	55.0	130.0	367.0
Trichloroethylene	3.04	---	---
Water	0.013	0.0285	0.0675

4. PHYSICAL PROPERTIES

4.2 Density.

Material	Theoretical Density (g/cm^3)	Density of Typical Casting (g/cm^3)	
		Open Melt	Vacuum Melt
Type I, Cyclotol 75/25	1.776	---	1.74-1.75
Type II, Cyclotol 70/30	1.765	1.71-1.73	---

4.3 Infrared Spectrum. See Fig. 1.

5. THERMAL PROPERTIES

5.1 Phase Changes.

Type	Temperature (°C)	Latent Heat (cal/g) 75/25	Latent Heat (cal/g) 70/30
Solid-to-slurry	79	5.87	7.05

5.4 Thermal Conductivity.

Type	Density (g/cm^3)	Conductivity (cal/s-cm-°C)
75/25	1.760	5.41×10^{-4}

5.6 Heats of Combustion and Formation.[5]

Constituent	ΔH_c° (kcal/mole)	ΔH_f° (kcal/mole)
TNT	-817.2	-12.0
RDX	-501.8	14.7

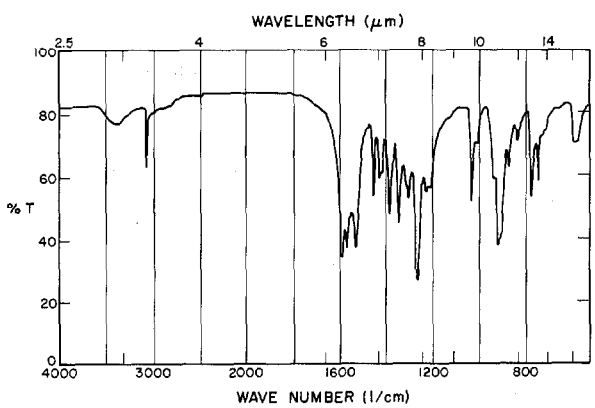

Fig. 1. Infrared spectrum.

5.7 Thermal Decomposition Kinetics.[6]

	TNT	RDX
Decomposition energy	300 cal/g	500 cal/g
Activation energy	34.4 kcal/mole	47.1 kcal/mole
Pre-exponential factor	2.51×10^{11}/s	2.02×10^{18}/s

5.8 Other Thermal Stability Test Results.

Test	Results
Vacuum	0.4-0.5 ml/g of gas evolved after 48 h at 120°C
DTA and pyrolysis	See Fig. 2
Critical temperature, Tm	208°C
Charge radius, a	3.5 mm

6. DETONATION PROPERTIES

6.1 Detonation Velocity.[7]

Effect of Charge Radius

Charge radius affects the detonation velocity of unconfined Cyclotol 75/25 cast to a density of 1.740 g/cm³ as follows.

$$D(R) = 8.210[(1 - 4.89 \times 10^{-2}/R) - 0.119/R(R - 2.44)],$$

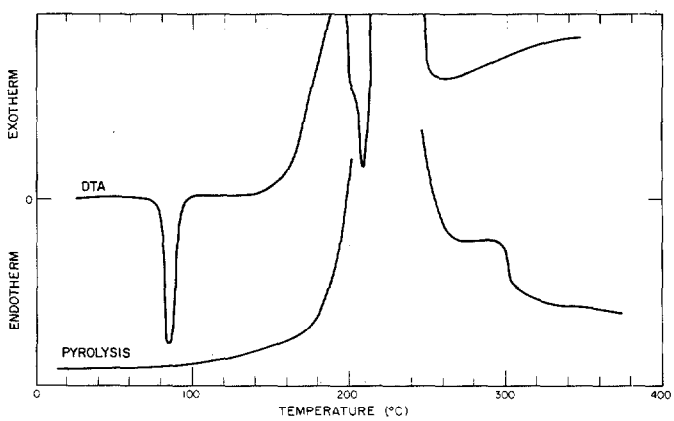

Fig. 2. Cyclotol 75/25 DTA and pyrolysis test results.

where D = detonation velocity in millimeters per microsecond,

and R = charge radius in millimeters.

The experimentally determined failure diameter is 6.0 mm.

6.2 Detonation Pressure.[8]

Weight Percent RDX	Density (g/cm³)	Detonation Velocity (mm/μs)	Detonation Pressure (GPa)
77.0	1.743	8.252	31.25

6.4 Plate Dent Test Results.[9] (See Part II for additional data.)

Charge Diameter (mm)	Weight Percent RDX	Density (g/cm³)	Dent Depth (mm)	Charge Height (mm)
41.3	77	1.200	5.38	203
41.3	77	1.743	9.24	203

7. SHOCK INITIATION PROPERTIES

7.1 Gap Test Results.[10]

Density (g/cm³)	Weight Percent RDX	G_{50} (mm)	L_{95} (mm)
	Large Scale		
1.756	77.0	42.85	0.23
1.757	76.1	43.15	0.15
1.744	77.3	44.93	0.08
1.750	77.9	44.17	1.30
	Small Scale		
1.737	---	0.38	0.05
1.746	77	0.18	0.05
1.752	77	0.34	0.06

7.3 Shock Hugoniot

Density (g/cm³)	Shock Hugoniot (mm/μs)	Particle Velocity Range (mm/μs)
1.752	$U_s = 2.63 + 1.85\ U_p$ where U_s = shock velocity and U_p = particle velocity.	$0 < U_p < 1.0$

7.4 Minimum Priming Charge.[10]

Density (g/cm³)	Weight Percent RDX	W_{50} (mg of XTX 8003)	L_{95} (± log mg)
1.749	75	785	0.054
1.739	70	898	0.024

7.5 Detonation Failure Thickness.[10]

Density (g/cm³)	Weight Percent RDX	Failure Thickness (mm)	L_{95} (mm)
1.752	77	1.51	0.11

8. SENSITIVITY

8.1 Drop Weight Impact Height.

Tool Type	H_{50} (cm)
12	36
12B	108

8.2 Large-Scale Drop Test Height.[11]

Density (g/cm³)	H_{50} (ft)	Reaction
1.750	>150	No events

8.3 Skid Test Results.

Density (g/cm^3)	Weight Percent RDX	Impact Angle (degrees)	Target Surface	H_{50} (ft)	Overpressure (psi)
1.758	77	15	Sand and epoxy	4	< 1.0

8.4 Susan Test Results.[12]

Projectile Impact Velocity (ft/s)	Relative Energy Release (%)
200	5
500	25
1000	50

8.5 Spark Sensitivity.

Electrode	Lead Foil Thickness (mils)	Sample Size (mg)	Energy (J)	Occurrence of Explosion (%)
Brass	3	27	0.38	23
Brass	10	27	3.29	23

9. MECHANICAL PROPERTIES

9.3 Compressive Strength and Modulus.

Temperature (°C)	Ultimate Compressive Strength (psi)	Compressive Modulus (psi x 10^{-6})
50	650 ± 150	0.74 ± 0.3
0	856 ± 200	2.39 ± 0.3
-40	993 ± 354	1.47 ± 0.06

REFERENCES

1. C. R. Buck and S. E. Wilson, Jr., US Army report USEHA-32-049 (1975).

2. *Code of Federal Regulations, 49, Transportation Parts 100-199, Rev. 12-1-76* (Office of the Federal Register, General Services Administration, Washington, DC, 1976).

3. US Army Materiel Command, Regulation No. AMCR 385-100 (1977).

4. A. Seidell, *Solubilities of Organic Compounds,* 3rd Ed., Vol. II (D. Van Nostrand Co., Inc., New York, 1941).

5. Prince E. Rouse, Jr., Journal of Chemical and Engineering Data **21**, 16-20 (1976).

6. R. N. Rogers, Thermochimica Acta **11,** 131-139 (1975).

7. A. W. Campbell and Ray Engelke, *Proceedings—Sixth Symposium (International) on Detonation, Coronado, California, August 24-27, 1976* (Office of Naval Research, Department of the Navy, ACR-221, 1976), pp. 642-652.

8. W. E. Deal, Journal of Chemical Physics **27**, 796-800 (1957).

9. L. C. Smith, Explosivstoffe **15,** 106-130 (1967).

10. Manuel J. Urizar, Suzanne W. Peterson, and Louis C. Smith, Los Alamos Scientific Laboratory report LA-7193-MS (April 1978).

11. A. Popolato, Proceedings of the International Conference on Sensitivity and Hazards of Explosives, Ministry of Aviation, Waltham Abbey, Essex (October 1963).

12. L. Green, Lawrence Livermore Laboratory, private communication (1975).

DATB

1. GENERAL PROPERTIES

1.1 Chemical and Physical Description. DATB (1,3-diamino-2,4,6-trinitrobenzene), $C_6H_5N_5O_6$, is a yellow crystalline solid.

1.2 Common Use. DATB is a relatively insensitive, temperature-resistant high explosive of limited military application. To be used effectively, it must be coated with a plastic (plastic-bonded explosive) or be mixed with liquid ingredients.

1.3 Toxicity. Industrial health data on DATB toxicity are virtually nil. Animal exposure indicated no immediate hazard even at 80°C. Although DATB is relatively safe, it is from a homologous group that has caused skin sensitivity, cancer, and internal physical damage.

2. MANUFACTURE AND PROCUREMENT

2.1 Manufacture. DATB is synthesized from m-nitroaniline in two steps. The nitroaniline is nitrated with mixed sulfuric and nitric acids to give tetranitroaniline, which is then aminated using ammonia in methanol. DATB is insoluble in methanol and precipitates as it is formed. It may be recrystallized from dimethylformamide or dimethylsulfoxide.

2.2 Procurement. There is no dedicated DoD facility for DATB manufacture. It can be procured, on special order, from a few US chemical companies that have facilities for synthesizing energetic materials.

2.3 Shipping.[1] DATB is shipped as a Class A explosive.

2.4 Storage.[2] DATB is stored dry in Compatibility Group D, Storage Class 1.1.

3. CHEMICAL PROPERTIES

3.1 Structural Formula.

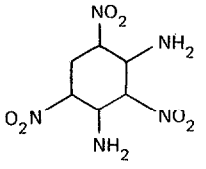

$C_6H_6N_6O_6$

3.2 Molecular Weight. 243.14

3.3 Solubility.

Solvent	Grams Dissolved/100 g of Solvent	
	40°C	60°C
Acetic anhydride	0.492	---
γ-Butyrolactone	0.810	---
Cyclohexanone	0.355	---
Dimethylformamide	2.96	4.88
Dimethylsulfoxide	4.56	8.15
Formamide	0.282	---
Nitromethane	0.362	---
Sulfuric acid	22.2	22.9

4. PHYSICAL PROPERTIES

4.1 Crystal Structure.[3,4] Two crystalline polymorphs of DATB have been identified. The cell parameters of Form I, stable to 217°C, and of Form II are given.

Cell Parameters	Form I	Form II
Unit cell edge length (Å)		
a	7.30 ± 0.01	7.76
b	5.20 ± 0.01	9.04
c	11.63 ± 0.02	12.84
Angle β	95.90 ± 0.3°	103.0
Molecules per unit cell	2	4

4.2 Density.[3,4]

Method of Determination	State	Temperature (C°)	Density (g/cm³)	
			Form I	Form II
X-ray	Solid	23	1.838	1.84
Direct measurement	Solid	23	1.837	1.815

DATB powder can be pressed into pellets. No quantitative pressing data is available.

4.3 Infrared Spectrum. See Fig. 1.

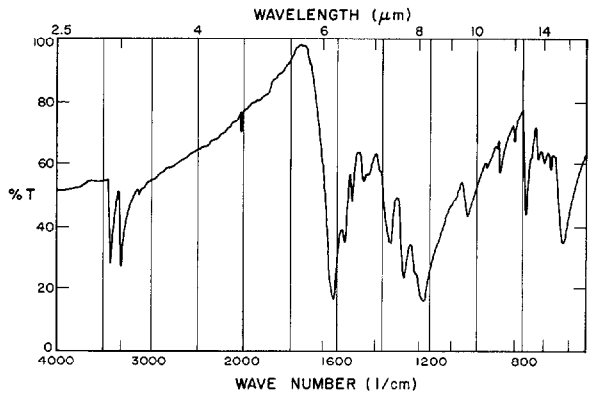

Fig. 1. Infrared spectrum.

5. THERMAL PROPERTIES

5.1 Phase Changes.[3-5]

Type	Temperature (°C)	Latent Heat (kcal/mole)
Solid-to-solid		
Form I to Form II	217	---
Solid-to-liquid	286	---
Solid-to-gas		
Form I	---	33.47[a]

[a]Computed from vapor pressure data presented in Sec. 5.2.

5.2 Vapor Pressure.[5]

Temperature (°C)	Vapor Pressure (mm Hg × 10^7)
62.6	0.081
78.2	0.879
85.3	2.09-2.36
97.6	9.12-9.80
108.1	34

A least squares fit to these data gives

$$\log_{10} P(\text{mm Hg}) = 13.73 - 33\,470/4.576\,T(K)$$

5.3 Heat Capacity.

Heat Capacity at Constant Pressure (cal/g-°C)
$0.261 + 1.11 \times 10^{-3}\,T$

5.4 Thermal Conductivity.

Conductivity (cal/s-cm-°C)
6.19×10^{-4}

5.6 Heats of Combustion and Formation at 25°C.[6]

ΔH_c° (kcal/mole)	ΔH_f° (kcal/mole)
−711.5	−23.6

5.7 Thermal Decomposition Kinetics.[7]

Decomposition energy	300 cal/g
Activation energy	46.3 kcal/mole
Pre-exponential factor	1.17×10^{15}/s

5.8 Other Thermal Stability Test Results.

Test	Results
Vacuum	0.1-0.3 ml/g of gas evolved after 48 h at 120°C
DTA and pyrolysis	See Fig. 2
Critical temperature, Tm	322 °C
Charge radius, a	3.5 mm
Density, ρ	1.74 g/cm^3

6. DETONATION PROPERTIES

6.1 Detonation Velocity.[8,9]

Effect of Density

The infinite-diameter detonation velocity as a function of density is given by

$$D = 2.480 + 2.852\,\rho_o\ ,$$

where D = detonation velocity in millimeters per microsecond

and ρ_o = charge density in grams per cubic centimeter.

The failure diameter of unconfined DATB pressed to a density of 1.816 g/cm³ is approximately 5.3 mm.

6.2 Detonation Pressure.

Density (g/cm³)	Detonation Velocity (mm/μs)	Detonation Pressure (GPa)
1.780	7.60	25.1

7. SHOCK INITIATION PROPERTIES

7.1 Gap Test Results.[10]

Density (g/cm³)	G_{50} (mm)	L_{95} (mm)
	Large Scale	
0.81	49.27	0.23
1.705	45.36	0.08
1.786	41.68	0.18
	Small Scale	
1.801	0.36	0.10

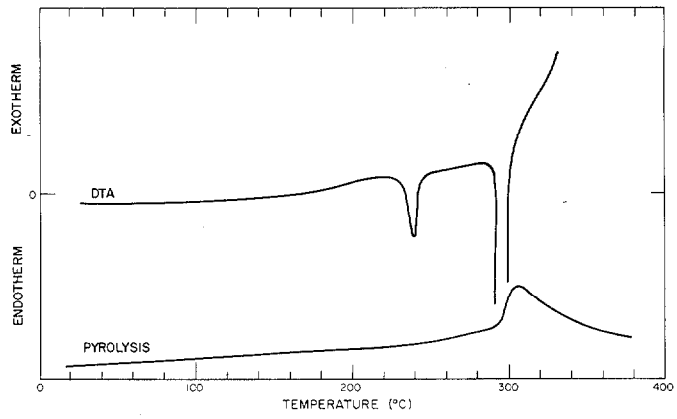

Fig. 2. DATB DTA and pyrolysis test results.

7.3 Shock Hugoniot.[9]

Density (g/cm^3)	Shock Hugoniot ($mm/\mu s$)
1.780	$U_s = (2.449 \pm 0.043) + (1.892 \pm 0.058)\ U_p$, where U_s = shock velocity and U_p = particle velocity.

7.4 Minimum Priming Charge.

Density (g/cm^3)	W_{50} (mg of XTX 8003)	L_{95} ($\pm$ log mg)
1.783	57.1	0.108

7.5 Detonation Failure Thickness.

Density (g/cm^3)	Failure Thickness (mm)	L_{95} (mm)
1.708	0.630	0.069
1.724	0.732	0.145

8. SENSITIVITY

8.1 Drop Weight Impact Height.

Tool Type	H_{50} (cm)
12	>320
12B	230

REFERENCES

1. *Code of Federal Regulations, 49, Transportation Parts 100-199, Rev. 12-1-76* (Office of the Federal Register, General Services Administration, Washington, DC, 1976).

2. US Army Materiel Command, Regulation No. AMCR-385-100 (1977).

3. J. R. Holden, Acta Crystallographica **22**, 545-550 (1967).

4. J. R. Holden, A. H. Rosen, and J. M. Rosen, Naval Ordnance Laboratory, private communication (March 1959).

5. J. M. Rosen and C. Dickenson, Naval Ordnance Laboratory report NOLTR-69-67 (April 1969).

6. Prince E. Rouse, Jr., Journal of Chemical and Engineering Data **21**, 16-20 (1976).

7. R. N. Rogers, Thermochimica Acta **11**, 131-139 (1975).

8. N. L. Coleburn, B. E. Drimmer, and T. P. Liddiard, Naval Ordnance Laboratory, private communication (October 1960).

9. N. L. Coleburn and T. P. Liddiard, Jr., Journal of Chemical Physics **44**, 1929-1936 (1966).

10. Manuel J. Urizar, Suzanne W. Peterson, and Louis C. Smith, Los Alamos Scientific Laboratory report LA-7193-MS (April 1978).

HMX*

1. GENERAL PROPERTIES

1.1 Chemical and Physical Description. HMX, an explosive similar to RDX, was a byproduct in the production of RDX by the process that W. E. Bachmann and J. E. Sheehan developed. It has a higher density and much higher melting point than RDX. It was named HMX for High Melting eXplosive.

HMX, $C_4H_8N_8O_8$, is a colorless polycrystalline material. It is also known as octahydro-1,3,5,7-tetranitro-1,3,5,7-tetrazocine, cyclotetramethylene-tetranitramine, and Octogen.

1.2 Common Use. Because of its higher density, HMX has replaced RDX in explosive applications for which energy and volume are important. It is used in castable TNT-based binary explosives called Octols; as the main ingredient in high-performance plastic-bonded explosives, and in high-performance solid propellants.

1.3 Toxicity.[1] The suggested maximum concentration of HMX in air is 1.5 mg/m^3.

---

*Unless otherwise specified, the properties listed are for the β polymorph.

2. MANUFACTURE AND PROCUREMENT

2.1 Manufacture. A modified Bachmann batch process is used to produce HMX. Solutions of hexamine in acetic acid and ammonium nitrate in nitric acid are added to a base of acetic acid, acetic anhydride, and paraformaldehyde. A first period of continuous addition is followed by 15 minutes of aging, and a second period of continuous addition is followed by 1 hour of aging. Then the reaction mixture is diluted with hot water and heated to boiling to destroy all linear compounds. Cooling, filtering, and water washing complete preparation of the product. The crude HMX is purified by recrystallization from acetone solution to give a final product that is up to 99% beta HMX.

2.2 Procurement. HMX is purchased from the US Army Armament Readiness Command under Military Specification MIL-H-45448, Amendment 1, dated July 15, 1975.

2.3 Shipping.[2] HMX is shipped as a Class A explosive and must be shipped wet with not less than 10% water.

2.4 Storage.[3] HMX may be stored dry in Compatibility Group A or wet in Compatibility Group D. Either wet or dry, it is in Storage Class 1.1.

3. CHEMICAL PROPERTIES

3.1 Structural Formula.

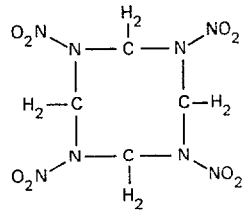

$C_4H_8N_8O_8$

3.2 Molecular Weight. 296.17

3.3 Solubility.

Solvent	Grams Dissolved/100 g of Solvent		
	20°C	40°C	60° C
Acetic acid			
Glacial	0.037	0.044	0.090
70%	---	0.033	0.103
Acetic anhydride	---	1.29	1.94
Acetone			
Anhydrous	2.4	3.4	---
70%	0.66	1.20	---
Acetonitrile	---	3.07	4.34
Cyclohexanone	---	5.91	7.17
Dimethylformamide	---	6.1	11.1
Dimethylsulfoxide	---	45.5	47.2

4. PHYSICAL PROPERTIES

4.1 Crystal Structure.[4-6] The cell parameters of the four polymorphic forms of HMX are given.

Cell Parameters	α	β	γ	δ
Unit cell edge length (Å)				
a	15.14	6.54	10.95	7.66
b	23.89	11.05	7.93	---
c	5.91	7.37	14.61	32.49
Angle β	---	102.8°	119.4°	---
Molecules per unit cell	8	2	4	6

4.2 Density.[4]

Method of Determination	State	Density (g/cm³) α	β	γ	δ
X-ray	Solid	1.838	1.902	1.78	1.786
Direct measurement	Solid	1.84	1.905	1.76	1.80

HMX cannot be consolidated into charges by conventional pressing. Obtaining large pieces of polycrystalline HMX requires solvent pressing techniques.

4.3 Infrared Spectrum. See Fig. 1.

4.4 Refractive Index.[7] The refractive indices of the four polymorphs in sodium light are shown.

Face	HMX Polymorph α	β	γ	δ
Alpha	1.561-1.565	1.589	1.537	---
Beta	1.562-1.566	1.594-1.595	1.585	---
Gamma	1.720-1.740	1.730-1.773	1.666	---
Epsilon	---	---	---	1.566
Omega	---	---	---	1.607
Double refraction	pos	pos	pos	neg

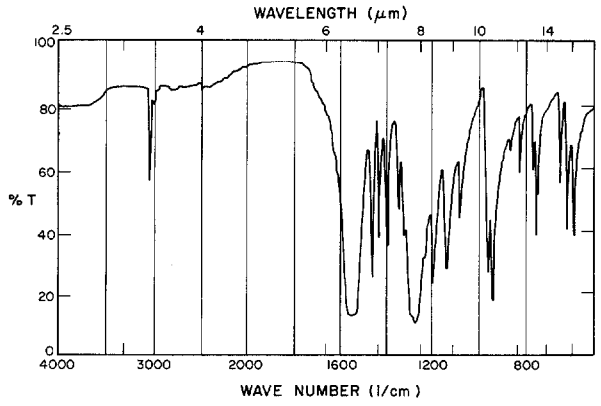

Fig. 1. Infrared spectrum.

5. THERMAL PROPERTIES

5.1 Phase Changes.[6-8]

Type	Temperature[a] (°C)	Latent Heat (cal/g)	Latent Heat (kcal/mole)
Solid-to-solid			
β to α	102-104	2.0	0.6
α to γ	Metastable	---	---
α to δ	160-164	7.8	2.3
Solid-to-liquid			
α	256-257	---	---
β	246-247	50.0	17.0
γ	279-280	---	---
δ	280-281	---	---
Solid-to-gas	---	141.4	41.89[b]

[a]There is some controversy about the temperature stability ranges of the four HMX polymorphs. These data are from Ref. 8.
[b]Computed from the vapor pressure data presented in Sec. 5.2.

5.2 Vapor Pressure.[9]

Temperature (°C)	Vapor Pressure (mm Hg x 10^7)
97.6	0.032
108.2	0.164
115.6	0.385-0.419
129.3	2.830-2.870

A least squares fit to these data gives

$$\log_{10} P(\text{mm Hg}) = 16.18 - 41\ 890/4.576\ T(K)\ .$$

5.3 Heat Capacity.

Heat Capacity at Constant Pressure (cal/g-°C)	Temperature Range (°C)
$0.231 + 5.5 \times 10^{-4}\,T$	$37 < T < 167$

5.4 Thermal Conductivity.[10]

Conductivity (cal/s-cm-°C)	Temperature (°C)
1.2×10^{-3}	25
9.7×10^{-4}	160

5.6 Heats of Combustion and Formation at 25°C.[11]

ΔH_c° kcal/mole	ΔH_f° kcal/mole
−660.7	11.3

5.7 Thermal Decomposition Kinetics.[12].

Decomposition energy	500 cal/g
Activation energy	52.7 kcal/mole
Pre-exponential factor	5×10^{19}/s

5.8 Other Thermal Stability Test Results.

Test	Results
Vacuum	0.1-0.4 ml/g of gas evolved after 48 h at 120°C
DTA and pyrolysis	See Fig. 2
Critical temperature, Tm	253°C
Charge radius, a	3.3 mm
Density, ρ	1.81 g/cm³

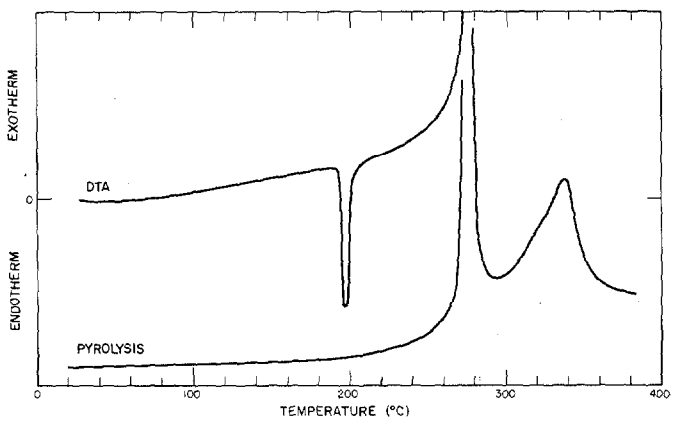

Fig. 2. HMX DTA and pyrolysis test results.

6. DETONATION PROPERTIES

6.1 Detonation Velocity.[13]

Density (g/cm^3)	Detonation Velocity[a] ($mm/\mu s$)
1.89	9.110

[a]Because HMX is a high-density version of RDX, their detonation velocities should be identical if they are compared at the same density.

6.2 Detonation Pressure.[13]

Density (g/cm^3)	Computed Detonation Pressure (GPa)
1.900	39.5

6.3 Cylinder Test Results.[14]

Density (g/cm³)	Cylinder Wall Velocity (mm/μs) at	
	R − R$_o$ = 5 mm	R − R$_o$ = 19 mm
1.891	1.65	1.86

7. SHOCK INITIATION

7.1 Gap Test Results.

Density (g/cm³)	G$_{50}$ (mm)	L$_{95}$ (mm)
	Large Scale	
1.07	70.68	0.71
	Small Scale	
1.20	8.53	0.05
1.79	4.23	0.10
1.83	4.04	0.13

7.2 Wedge Test Results.

Density (g/cm³)	Distance, x*, to Detonation (mm)	Pressure Range (GPa)
1.891	log P = (1.18±0.02)-(0.59±0.03) log x*, where P = pressure in gigapascals.	4.41 < P < 9.55

7.3 Shock Hugoniots.[15]

Density (g/cm³)	Shock Hugoniot (mm/μs)	Particle Velocity Range (mm/μs)
1.903	$U_s = 2.74 + 2.6\,U_p$,[a]	
1.89	$U_s = (2.901 \pm 0.407) + (2.058 \pm 0.490)\,U_p$,	$0.59 < U_p < 1.04$

where U_s = shock velocity
and U_p = particle velocity.

[a]Computed from isothermal compression data,

$$U_{st} = 2.67 + 2.6\,U_{pt},$$

where the subscripts "st" and "pt" indicate the shock and particle velocities, respectively, at constant temperature.

8. SENSITIVITY

8.1 Drop Weight Impact Height.

Tool Type	H_{50} (cm)
12	26
12B	37

8.5 Spark Sensitivity.

Electrode	Lead Foil Thickness (mils)	Sample Size (mg)	Energy (J)	Occurrence of Explosion (%)
Brass	3	66.9	0.2	50
Brass	10	66.9	1.03	50
Steel	1	75.0	0.12	50
Steel	10	75.0	0.87	50

REFERENCES

1. Committee on Threshold Limit Values: *Documentation of Threshold Limit Values*, 3rd Ed. (American Conference of Governmental Industrial Hygienists, 1014 Broadway, Cincinnati, Ohio, 1971).

2. *Code of Federal Regulations, 49, Transportation Parts 100-199, Rev. 12-1-76* (Office of the Federal Register, General Services Administration, Washington, DC, 1976).

3. US Army Materiel Command, Regulation No. AMCR-385-100 (1977).

4. H. H. Cady, A. C. Larson, and D. T. Cromer, Acta Crystallographica **16,** 617-623 (1963).

5. W. C. McCrone, Analytical Chemistry **22,** 1225-1226 (1950).

6. Anna S. Teetsov and W. C. McCrone, Microscope **15,** 13-29 (1965).

7. W. E. Beatty and B. Gilbert, Explosives Research and Development Establishment report ERDE 7/R/59 (October 1959).

8. Howard H. Cady and Louis C. Smith, Los Alamos Scientific Laboratory report LAMS-2652 (1961).

9. J. M. Rosen and C. Dickenson, Naval Ordnance Laboratory report NOLTR-69-67 (April 1969).

10. C. M. Tarver, Lawrence Livermore Laboratory report UCID-17272-78-4 (September 1978).

11. O. H. Johnson, Naval Ordnance Laboratory report NAVORD-4371 (October 1956).

12. R. N. Rogers, Thermochimica Acta **11,** 131-139 (1975).

13. C. L. Mader, Los Alamos Scientific Laboratory report LA-2900 (July 1963).

14. J. W. Kury, H. C. Hornig, E. L. Lee, J. L. McDonnel, D. L. Ornellas, M. Finger, F. M. Strange, and M. L. Wilkins, *Proceedings—Fourth Symposium (International) on Detonation, White Oak, Maryland, October 12-15, 1965* (Office of Naval Research, Department of the Navy, ACR-126, 1965), pp. 3-12.

15. Bart Olinger, Brad Roof, and Howard Cady, Symposium (International) on High Dynamic Pressures, Paris, France, August 1978, pp. 3-8 (1978).

NITROGUANIDINE

1. GENERAL PROPERTIES

1.1 Chemical and Physical Description. Nitroguanidine (NQ), $CH_4N_4O_2$, is a colorless polycrystalline material, generally in the form of a low-density matted structure. It is also known as Picrite.

1.2 Common Use. NQ is used extensively as an ingredient in gun propellants, because the combustion products of such propellants are less erosive than those of other propellants of equivalent energy.

2. MANUFACTURE AND PROCUREMENT

2.1 Manufacture.[1,2] The procedures used to produce NQ are the British aqueous fusion (BAF) and the urea/ammonium nitrate processes. The United States uses a modified BAF process. Calcium carbide is reacted with nitrogen to form calcium cyanamide. The calcium cyanamide is reacted with carbon dioxide and water to form cyanamide. This is reacted with ammonium nitrate to form guanidine nitrate (GuN). GuN is reacted with 40 wt% oleum to form nitroguanidine. Final purification of the NQ is by crystallization from water.

2.2 Procurement. NQ is purchased from the US Army Armament Readiness Command under military specification MIL-N-494A, dated January 31, 1964.

2.3 Shipping.[3] NQ is shipped dry as a Class A explosive.

2.4 Storage.[4] NQ is stored dry in Compatibility Group D, Storage Class 1.1.

3. CHEMICAL PROPERTIES

3.1 Structural Formula.[5,6]

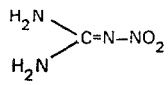

$CH_4N_4O_2$

3.2 Molecular Weight. 104.1

3.3 Solubility.

Solvent	Grams Dissolved/100 g of Solvent		
	20°C	40°C	60°C
Water	0.36	0.75	1.6
Dimethyl sulfoxide	24	25	28
Dimethyl formamide	14	---	20
Methanol	0.3	0.6	---
Methyl ethyl ketone	0.13	0.20	---
Butyl acetate	0.07	0.08	0.1
n-octane	0.003	0.008	---

4. PHYSICAL PROPERTIES

4.1 Crystal Structure.[7,8] Only one polymorph of NQ has been observed. The orthorhombic unit cell parameters are given.

Cell Parameters	
Length of unit cell edge (Å)	
a	17.58
b	24.84
c	3.58
Molecules per unit cell	16

4.2 Density.[7]

Crystal

Method of Determination	State	Temperature (°C)	Density (g/cm³)
X-ray	Solid	---	1.78
Direct measurement	---	25	1.77

Pressed

NQ can be pressed to a density of 1.70 g/cm³ at a pressure of 20 000 psi.

4.3 Infrared Spectrum. See Fig. 1.

4.4 Refractive Index.[7]

	Refractive Index in 5893-Å Light
α	1.526
β	1.694
γ	1.81

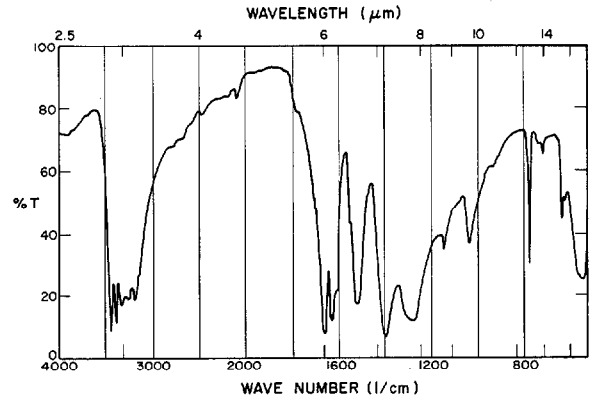

Fig. 1. Infrared spectrum.

5. THERMAL PROPERTIES

5.1 Phase Change.

Type	Temperature (°C)
Solid-to-liquid	245-250[a]

[a]Melting is usually preceded by decomposition, which is very rapid in the liquid phase.

5.3 Heat Capacity.

Material	Heat Capacity at Constant Pressure (cal/g-°C)	Temperature Range (°C)
LBD NQ[a]	0.242 + 0.0011 T(°C)	37 < T < 167
HBD NQ[b]	0.269 + 0.0007 T(°C)	37 < T < 167

[a]Low-bulk density, in accordance with material specification MIL-N-494A.
[b]High-bulk density NQ recrystallized from water, median particle diameter ~300 μm.

5.4 Thermal Conductivity.

Material	Density (g/cm^3)	Conductivity (cal/cm-s-°C)	Temperature Range (C°)
LBD NQ	1.65	10.1×10^{-4}	25 < T < 50
	1.69	9.8×10^{-4}	25 < T < 50

5.6 Heats of Combustion and Formation at 25°C.[9]

ΔH_c° (kcal/mole)	ΔH_f° (kcal/mole)
−210.4	−20.29

5.7 Thermal Decomposition Kinetics.[10,11]

	Source	
	Ref. 10	Ref. 11
Decomposition energy	500 cal/g	---
Activation energy	20.9 kcal/mole	57.1 kcal/mole
Pre-exponential factor	2.84×10^7/s	8.75×10^{22}/s

5.8 Other Thermal Stability Test Results.

Test	Results
Vacuum	Gas evolved after 48 h at 120°C (ml/g)
NQ per MIL-N-494A	0.0-1.0
Water recrystallized HBD NQ	1.4-3.6
DMF recrystallized HBD NQ	0.6-1.2
DTA and pyrolysis	See Fig. 2
Critical temperature, Tm	198°C
Charge radius, a	3.9 mm
Density, ρ	1.63 g/cm^3

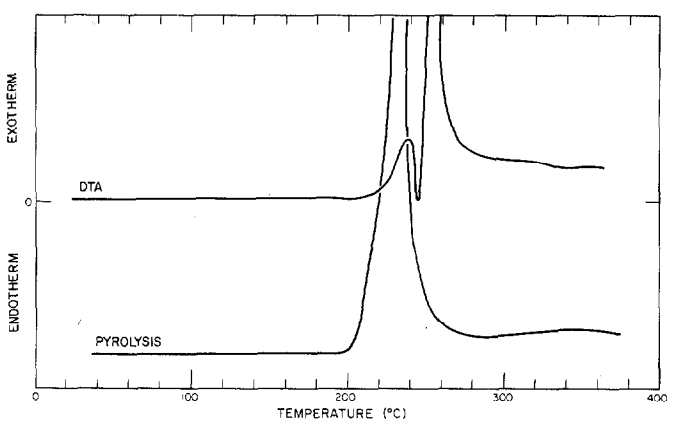

Fig. 2. NQ DTA and pyrolysis test results.

6. DETONATION PROPERTIES

6.1 Detonation Velocity.[12]

Effect of Density

The effect of density on the infinite-diameter detonation velocity is given by

$D_\infty = 1.44 + 4.015\,\rho_o$ for $0.3 < \rho_o < 1.78$,

where D_∞ = infinite-diameter detonation velocity in millimeters per microsecond,

and ρ_o = density in grams per cubic centimeter.

Failure Diameter

The LBD NQ failure diameter as a function of charge density is shown.

Charge Density (g/cm^3)	Charge Diameter (mm)	
	Detonates	Fails
1.0	25.4	---
1.21	15.9	14.3
1.52	14.3	12.7

6.2 Detonation Pressure. There are no experimental data on NQ detonation pressure. However, there is one data point from a mixture of 95 wt% NQ and 5 wt% Estane. The results are as follows.

Material	Density (g/cm^3)	Detonation Velocity ($mm/\mu s$)	Detonation Pressure (GPa)
95 wt% NQ/ 5 wt% Estane	1.704	8.28	26.8

6.4 Plate Dent Test Results.

Charge Diameter (mm)	Density (g/cm^3)	Dent Depth (mm)	Charge Height (mm)
12.7	0.25	0.56	76.2
12.7	0.40	0.79	76.2

7. SHOCK INITIATION PROPERTIES

7.1 Gap Test Results.

Density (g/cm^3)	G_{50} (mm)	L_{95} (mm)
	Large Scale	
1.609	5.00	0.5

7.2 Wedge Test Results.

Density (g/cm^3)	Distance, x*, and Time, t*, to Detonation (mm and μs)	Pressure Range (GPa)
1.659 to 1.723[a]	$\log P = (1.44 \pm 0.07) - (0.15 \pm 0.08) \log x^*$ $\log P = (1.32 \pm 0.03) - (0.15 \pm 0.07) \log t^*$	$13.35 < P < 26.28$
1.688[b]	$\log P = (1.51 \pm 0.02) - (0.26 \pm 0.03) \log x^*$	$21.2 < P < 27.1$

[a]NQ median particle diameter, 300 μm, as cubic crystals.
[b]NQ as long needle crystals with a needle diameter of a few micrometers.

7.3 Shock Hugoniots.

Density (g/cm^3)	Shock Hugoniots (mm/μs)	Particle Velocity Range (mm/μs)
1.659 to 1.723[a]	$U_s = (3.544 \pm 0.524) + (1.459 \pm 0.276)\ U_p$,	$1.337 < U_p < 2.220$
1.688[b]	$U_s = (3.048 \pm 0.254) + (1.725 \pm 0.135)\ U_p$,	$1.172 < U_p < 2.336$

where U_s = shock velocity
and U_p = particle velocity.

[a]NQ median particle diameter, 300 μm, as cubic crystals.
[b]NQ as long needle crystals with a needle diameter of a few micrometers.

NQ

8. SENSITIVITY

8.1 Drop Weight Impact Height.

Tool Type	H_{50} (cm)
12	>320
12B	>320

REFERENCES

1. C. H. Nichols, Picatinny Arsenal Technical report PA-TR-4566 (May 1974).

2. G. Cowan, US Army Armament Materiel Command, private communication (1977).

3. *Code of Federal Regulations, 49, Transportation Parts 100-199, Rev. 12-1-76* (Office of the Federal Register, General Services Administration, Washington, DC, 1976).

4. US Army Armament Materiel Command, Regulation No. AMCR 385-100 (1977).

5. W. D. Kumler and P. P. T. Sah, Journal of Organic Chemistry **18,** 669-675 (1953).

6. W. D. Kumler, Journal of the American Chemical Society **76,** 814-816 (1954).

7. W. C. McCrone, Analytical Chemistry **23,** 205-206 (1951).

8. J. Donohue and J. H. Bryden, Acta Crystallographica 8, 314-316 (1955).

9. L. Medard and M. T. Thomas, Memorial des Poudres **31,** 173-196 (1949).

10. R. N. Rogers, Thermochimica Acta **11,** 131-139 (1975).

11. J. L. Block, US Naval Ordnance Laboratory report NAVORD-2705 (January 1953).

12. D. Price and A. R. Clairmont, US Naval Ordnance Laboratory report NOLTR 67-169 (February 1968).

OCTOL

1. GENERAL PROPERTIES

1.1 Chemical and Physical Description. Octol is the generic term for mixtures of TNT and HMX. In the United States, the mixtures consist of 75 wt% HMX and 25 wt% TNT (Type I) or 70 wt% HMX and 30 wt% TNT (Type II), also called Octol 75/25 and Octol 70/30. Neither mixture contains a desensitizer. To improve the flow characteristics of the molten form, a bimodal distribution of HMX crystals generally is used.

1.2 Common Use. Octol is often used as an explosive fill in military applications that require more energy than either Comp B or Type I Cyclotol can provide.

1.3 Toxicity.[1,2] Octol toxicity is like that of HMX and TNT.

The suggested maximum concentration of HMX in air is 1.5 mg/m^3.

Inhaled TNT vapor or dust may irritate mucous membranes and cause sneezing, coughing, and sore throat. TNT may produce toxic hepatitis and aplastic anemia. TNT yellows the exposed skin, hair, and nails of workers. Dermatitis, erythema, papules, and itchy eczema can be severe. Ingestion of 1-2 g of TNT is estimated to be an acute fatal dose to humans. The suggested maximum permissible airborne dust concentration is 0.5 mg/m^3.

2. MANUFACTURE AND PROCUREMENT

2.1 Manufacture. Octols are manufactured from TNT and water-wet HMX. The TNT is melted in a steam-jacketed kettle equipped with a stirrer and brought to about 100°C. The wet HMX is added slowly, and stirring is continued until the water is evaporated. The slurry temperature is reduced until the viscosity is satisfactory for casting. The octol is cast onto a continuous belt as strips or chips.

These are shipped to an ordnance plant, remelted, and cast into ammunition or into other desired shapes. During this melting, other additives may be introduced. To increase the density of the cast charges, a vacuum may be applied to the molten octol before casting.

2.2 Procurement. Octol is purchased from the US Army Armament Command under military specification MIL-O-45445A, dated September 30, 1962.

2.3 Shipping.[3] Octol is shipped as a Class A explosive.

2.4 Storage.[4] Octol is stored in Compatibility Group D, Storage Class 1.1.

3. CHEMICAL PROPERTIES

3.1 Composition.

	Type I		Type II	
Constituent	Weight Percent	Volume Percent	Weight Percent	Volume Percent
HMX	75	72.3	70	66.9
TNT	25	27.7	30	33 1

3.2 Molecular Weight.

Constituent	Structure	Molecular Weight
HMX	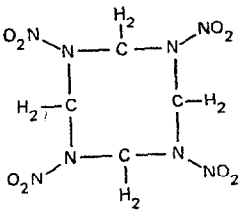 $C_4H_8N_8O_8$	296.17
TNT	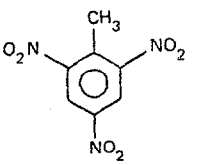 $C_7H_5N_3O_6$	227.13

3.3 Solubility.[5] The solubility is that of the components, HMX and TNT.

Solvent	Grams of HMX Dissolved/100 g of Solvent		
	20°C	40°C	60°C
Acetic acid			
Glacial	0.037	0.044	0.090
70%	---	0.033	0.103
Acetic anhydride	---	1.29	1.94
Acetone			
Anhydrous	2.4	3.4	---
70%	0.66	1.20	---
Acetonitrile	---	3.07	4.34
Cyclohexanone	---	5.91	7.17
Dimethylformamide	---	6.1	11.1
Dimethylsulfoxide	---	45.5	47.2

Solvent	Grams of TNT Dissolved/100 g Solvent		
	20°C	40° C	60°C
Acetone	109.0	228.0	600.0
Benzene	67.0	180.0	478.0
Butyl carbinol acetate	24.0	---	---
Carbon disulfide	0.48	1.53	---
Carbon tetrachloride	0.65	1.75	6.90
Chlorobenzene	33.9	---	---
Chloroform	19.0	66.0	302.0
Diethyl ether	3.29	---	---
Ethanol (95%)	1.23	2.92	8.30
Ethylene chloride	18.7	---	---
Hexane	0.16	---	---
Methyl acetate	72.1	---	---
Toluene	55.0	130.0	367.0
Trichloroethylene	3.04	---	---
Water	0.0130	0.0285	0.0675

4. PHYSICAL PROPERTIES

4.2 Density.

Material	Theoretical Density (g/cm^3)	Density of Typical Casting (g/cm^3)	
		Open Melt	Vacuum Melt
Type I, Octol 75/25	1.835	1.800	1.810-1.825
Type II, Octol 70/30	1.822	1.790	1.805-1.810

4.3 Infrared Spectrum. See Fig. 1.

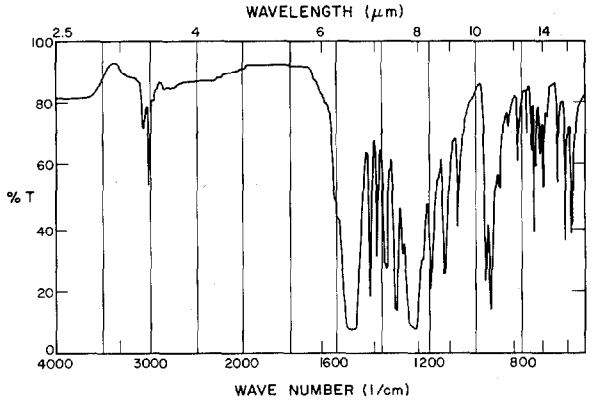

Fig. 1. Infrared spectrum.

5. THERMAL PROPERTIES

5.1 Phase Changes.

Type	Temperature (°C)	Latent Heat (cal/g)	
		75/25	70/30
Solid-to-slurry	79	5.87	7.05

5.6 Heats of Combustion and Formation.[6]

Constituent	ΔH_c^o (kcal/mole)	ΔH_f^o (kcal/mole)
TNT	−817.2	−12.2
HMX	−660.7	11.3

5.7 Thermal Decomposition Kinetics.[7]

	TNT	HMX
Decomposition energy	300 cal/g	500 cal/g
Activation energy	34.4 kcal/mole	52.7 kcal/mole
Pre-exponential factor	2.5×10^{11}/s	5×10^{19}/s

5.8 Other Thermal Stability Test Results.

Test	Results
Vacuum	0.1-0.4 ml/g of gas evolved after 48 h at 120°C
DTA and pyrolysis	See Fig. 2
Critical temperature, Tm	281°C
Charge radius, a	3.7 mm
Density, ρ	1.70 g/cm^3

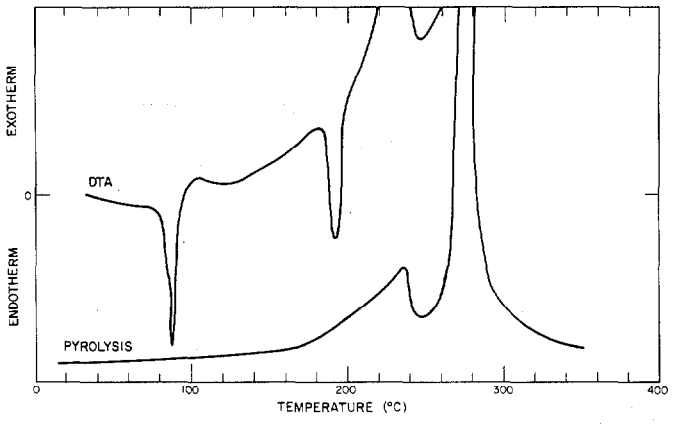

Fig. 2. Octol DTA and pyrolysis test results.

6. DETONATION PROPERTIES

6.1 Detonation Velocity.[8]

Effect of Charge Radius

Charge radius affects the detonation velocity of unconfined Octol 77/23 cast to a density of 1.814 g/cm³ as follows.

$$D(R) = 8.481[(1 - 6.9 \times 10^{-2}/R) - (9.25 \times 10^{-2})/R(R - 1.34)],$$

where D = detonation velocity in millimeters per microsecond

and R = charge radius in millimeters.

The experimentally determined failure diameter is <6.4 mm.

6.2 Detonation Pressure.

Weight Percent HMX	Density (g/cm³)	Detonation Velocity (mm/μs)	Detonation Pressure (GPa)
76.3	1.809	8.452	33.8

6.4 Plate Dent Test Results.

Charge Diameter (mm)	Weight Percent HMX	Density (g/cm³)	Dent Depth (mm)	Charge Height (mm)
41.3	76.3	1.809	10.06	203
41.3	76.4	1.802	9.99	127

7. SHOCK INITIATION PROPERTIES

7.1 Gap Test Results.[9]

Weight Percent HMX	Density (g/cm³)	G_{50} (mm)	L_{95} (mm)
	Large Scale		
76.0	1.822	49.45	0.2
a	1.726	48.59	0.41
a	1.795	43.56	0.46
	Small Scale		
76.0	1.803	0.71	0.08
76.0	1.810	0.58	---
78.6	1.800[b]	0.56	0.06
c	1.775	0.41	0.05
d	1.791	0.36	0.05

[a]UK EDC-1 nominal 75 wt% HMX with some RDX.
[b]With 1 wt% wax.
[c]UK EDC-1 cast in the United Kingdom.
[d]UK EDC-1 vacuum cast in the United States.

7.3 Shock Hugoniots.[10]

Density (g/cm³)	Weight Percent HMX	Shock Hugoniot (mm/μs)	Particle Velocity Range (mm/μs)
1.80	75	$U_s = 3.01 + 1.72\,U_p$, where U_s = shock velocity and U_p = particle velocity	$0 < U_p < 1.5$

7.4 Minimum Priming Charge.[9]

Density (g/cm^3)	Weight Percent HMX	W_{50} (mg of XTX 8003)	L_{95} (± log mg)
1.818	75	292	0.028

7.5 Detonation Failure Thickness.[9]

Density (g/cm^3)	Weight Percent HMX	Failure Thickness (mm)	L_{95} (mm)
1.791	75	1.43	0.21

8. SENSITIVITY

8.1 Drop Weight Impact Height.

Tool Type	H_{50} (cm)
12	38
12B	93

8.2 Large-Scale Drop Test Height.[11]

Density (g/cm^3)	Weight Percent HMX	H_{50} (ft)	Reaction
1.810	75	45	Low-order partial
1.805	75[a]	~150	Low-order partial
1.766	b	~110	Low-order partial

[a]Octol 75/25 with 1 wt% wax.
[b]UK EDC-1 cast in the United Kingdom.

8.3 Skid Test Results.

Density (g/cm³)	Weight Percent HMX	Impact Angle (degrees)	Target Surface	H_{50} (ft)	Reaction Overpressure (psi)
1.810	75	45	Sand and epoxy	~75	0.1
1.805	a	45	Sand and epoxy	>150	---

[a]Cast with 1 wt% wax.

8.4 Susan Test Results.[12]

Projectile Impact Velocity (ft/s)	Relative Energy Release (%)
200	0
400	20
1000	60

8.5 Spark Sensitivity.

Electrode	Lead Foil Thickness (mils)	Sample Size (mg)	Energy (J)	Occurrence of Explosion (%)
Brass	3	29	0.82	17
Brass	10	29	4.36	17

9. MECHANICAL PROPERTIES

9.3 Compressive Strength and Modulus.

Temperature (°C)	Density (g/cm³)	Weight Percent HMX	Ultimate Compressive Strength (psi)	Compressive Modulus (psi x 10^{-5})
Ambient	1.821-1.824	76	2000-2340	8.0 to 13.4

REFERENCES

1. Commitee on Threshold Limit Values, *Documentation of Threshold Limit Values*, 3rd Ed. (American Conference of Governmental Industrial Hygienists, 1014 Broadway, Cincinnati, Ohio, 1971).

2. C. R. Buck and S. E. Wilson, Jr., US Army report USEHA-32-049 (1975).

3. *Code of Federal Regulations, 49, Transportation Parts 100-199, Rev. 12-1-76* (Office of the Federal Register, General Services Administration, Washington, DC, 1976).

4. US Army Materiel Command, Regulation No. AMCR 385-100 (1977).

5. A. Seidell, *Solubilities of Organic Compounds,* 3rd Ed., Vol II, (D. Van Nostrand Co., Inc., New York, 1941).

6. Prince E. Rouse, Jr., Journal of Chemical and Engineering Data **21,** 16-20 (1976).

7. R. N. Rogers, Thermochimica Acta **11,** 131-139 (1975).

8. A. W. Campbell and Ray Engelke, *Proceedings—Sixth Symposium (International) on Detonation, Coronado, California, August 24-27, 1976* (Office of Naval Research, Department of the Navy, ACR-221, 1976), pp. 642-652.

9. Manuel J. Urizar, Suzanne W. Peterson, and Louis C. Smith, Los Alamos Scientific Laboratory report LA-7193-MS (April 1978).

10. V. M. Boyle, R. L. Jameson, and M. Sultanoff, *Proceedings—Fourth Symposium (International) on Detonation, White Oak, Maryland, October 12-15, 1965* (Office of Naval Research, Department of the Navy, ACR-126, 1965), pp. 241-247.

11. A. Popolato, Proceedings of the International Conference on Sensitivity and Hazards of Explosives, Ministry of Aviation, Waltham Abbey, Essex (October 1963).

12. L. Green, Lawrence Livermore Laboratory, private communication (1975).

PBX 9011

1. GENERAL PROPERTIES

1.1 Chemical and Physical Description. PBX 9011 is composed of HMX bonded with Estane 5703. The molding powder is off-white to light brown.

1.2 Common Use. PBX 9011 is a high-performance explosive that is used in a variety of special applications in nuclear ordnance.

1.3 Toxicity.[1] Estane 5703 is not toxic. The suggested maximum concentration of HMX in air is 1.5 mg/m^3.

2. MANUFACTURE AND PROCUREMENT

2.1 Manufacture. PBX-9011 molding powder is prepared by the water slurry process. An Estane lacquer is prepared in a water-immiscible solvent. This is added to a water slurry containing a bimodal distribution of HMX crystals. During solvent removal by distillation, the plastic uniformly coats and agglomerates the HMX crystals in the water phase. The process variables must be controlled closely to produce satisfactory agglomerates, composition, and bulk density.

2.2 Procurement. PBX 9011 is purchased from the US Army Armament Readiness Command under LASL material specification 13Y-101030 Rev. B, dated January 9, 1967.

2.3 Shipping.[2] PBX-9011 molding powder is shipped as a Class A explosive.

2.4 Storage.[3] PBX 9011 is stored in Compatibility Group D, Storage Class 1.1.

3. CHEMICAL PROPERTIES

3.1 Composition.

Constituent	Weight Percent	Volume Percent
HMX	90	84.9
Estane 5703	10	15.1

3.2 Molecular Weight.

Constituent	Structure	Molecular Weight
HMX	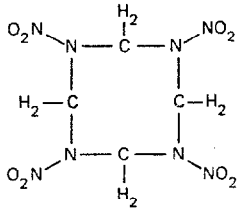 $C_4H_8N_8O_8$	296.17
Estane	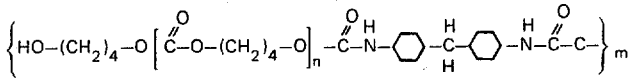 $C_{5.14}H_{7.5}N_{0.187}O_{1.76}$	100.0

3.3 Solubility. The solubility is that of HMX.

Solvent	Grams of HMX Dissolved/100 g of Solvent		
	20°C	40° C	60°C
Acetic acid			
Glacial	0.037	0.044	0.090
70%	-----	0.033	0.103
Acetic anhydride	----	1.29	1.94
Acetone			
Anhydrous	2.4	3.4	---
70%	0.66	1.20	
Acetonitrile	----	3.07	4.34
Cyclohexanone	----	5.91	7.17
Dimethylformamide	----	6.1	11.1
Dimethylsulfoxide	-----	45.5	47.2

4. PHYSICAL PROPERTIES

4.2 Density.

Theoretical Density (g/cm^3)	Density of Typical Pressed Charges (g/cm^3)
1.795	1.770

The following densities are obtained by vacuum pressing (residual pressure $<10^3$ μm Hg) molding powder with a 3-min dwell.

Pressure (psi)	Density (g/cm^3) with Powder Preheated to	
	70°C	100°C
10 000	1.762	1.768
12 500	1.759	1.770
15 000	1.759	1.771
20 000	1.760	1.772

4.3 Infrared Spectrum. See Fig. 1.

5. THERMAL PROPERTIES

5.1 Phase Changes.

Type	Temperature (°C)	Latent Heat (cal/g)
β-to-δ solid-to-solid in HMX	190	9.2

5.3 Heat Capacity.

Heat Capacity at Constant Pressure (cal/g-°C)	Temperature Range (°C)
$0.259 + 6.3 \times 10^{-4} T$	$17 < T < 167$

5.4 Thermal Conductivity.

Density (g/cm^3)	Conductivity (cal/s-cm-°C)
1.772	9.08×10^{-4}

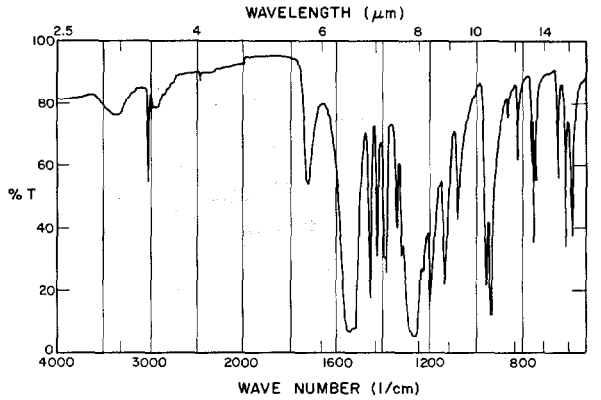

Fig. 1. Infrared spectrum.

5.5 Coefficient of Thermal Expansion.

Density (g/cm^3)	Coefficient of Expansion (1/°C)	Temperature Range (°C)
1.752	22.2×10^{-6}	$25 < T < 74$

5.6 Heats of Combustion and Formation.

Constituent	ΔH_c° (kcal/mole)	ΔH_f° (kcal/mole)
HMX	-660.7	11.3

5.7 Thermal Decomposition Kinetics.[4]

Property	HMX
Decomposition energy	500 cal/g
Activation energy	52.7 kcal/mole
Pre-exponential factor	5×10^{19}/s

5.8 Other Thermal Stability Test Results.

Test	Results
Vacuum	0.3-0.9 ml/g of gas evolved after 48 h at 120°C
DTA and pyrolysis	See Fig. 2

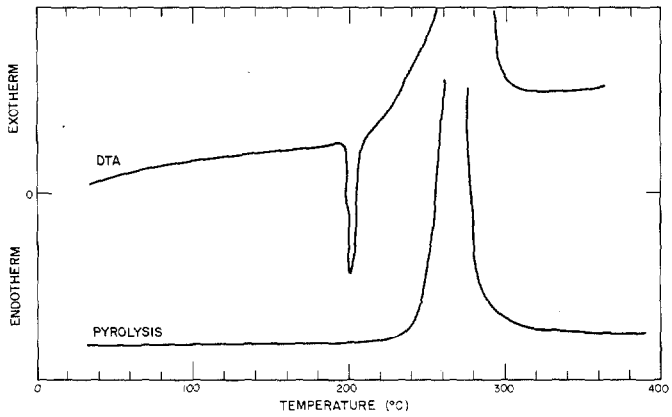

Fig. 2. PBX 9011 DTA and pyrolysis test results.

6. DETONATION PROPERTIES

6.1 Detonation Velocity.

Effect of Charge Radius

At a density of 1.767 g/cm^3, the infinite-radius detonation velocity of unconfined charges is 4.25 mm/μs. The failure radius has not been determined.

6.2 Detonation Pressure.

Density (g/cm^3)	Detonation Velocity (mm/μs)	Detonation Pressure (GPa)
1.767	8.5	29.8

6.3 Cylinder Test Results.[5]

Density (g/cm³)	Detonation Velocity (mm/μs)	Cylinder Wall Velocity (mm/μs) at	
		$R-R_0 = 5$ mm	$R-R_0 = 19$ mm
1.777	8.50	1.46	1.69

6.4 Plate Dent Test Results.

Density (g/cm³)	Dent Depth (mm)
1.785	9.86

7. SHOCK INITIATION PROPERTIES

7.1 Gap Test Results.

Density (g/cm³)	G_{50} (mm)	L_{95} (mm)
Large Scale		
0.85	67.81	0.20
1.761	51.97	0.41
1.766	51.96	0.33
Small Scale		
0.88	5.16	0.07
1.759	1.19	0.15
1.766	1.27	0.13
1.775	0.64	0.08
1.788	0.56	0.08

7.2 Wedge Test Results.

Density (g/cm^3)	Distance, x*, and Time, t*, to Detonation (mm and μs)	Pressure Range (GPa)
1.790	$\log P = (1.18 \pm 0.01) - (0.66 \pm 0.02) \log x^*$, $\log P = (0.74 \pm 0.01) - (0.55 \pm 0.01) \log t^*$, where P = pressure in gigapascals.	$4.82 < P < 15.65$

7.3 Shock Hugoniot.

Density (g/cm^3)	Shock Hugoniot ($mm/\mu s$)	Particle Velocity Range ($mm/\mu s$)
1.790	$U_s = (2.363 \pm 0.131) + (2.513 \pm 0.141)\, U_p$ where U_s = shock velocity and U_p = particle velocity.	$0.65 < U_p < 1.43$

7.4 Minimum Priming Charge.[6]

Density (g/cm^3)	W_{50} (mg of XTX 8003)	L_{95} ($\pm$ log mg)
1.772	153	0.021
1.765[a]	58	0.058

[a]Prepared with 1/4 Class A and 3/4 Class B HMX.

7.5 Detonation Failure Thickness.[6]

Density (g/cm^3)	Failure Thickness (mm)	L_{95} (mm)
1.770	0.610	0.081

8. SENSITIVITY

8.1 Drop Weight Impact Height.

Tool Type	H_{50} (cm)
12	55
12B	67

8.2 Large-Scale Drop Test Height.

Density (g/cm^3)	H_{50} (ft)	Reaction
1.773	96	Very small partial, overpressure, <0.2 psi

8.3 Skid Test Results.

Density (g/cm^3)	Impact Angle (degrees)	Target Surface	H_{50} (ft)	Reaction Overpressure (psi)
1.773	45	Garnet paper	78	<0.5
1.773	45	Garnet paper	4[a]	<0.5

[a]HE cooled to −29°C.

8.4 Susan Test Results.[7]

Projectile Impact Velocity (ft/s)	Relative Energy Release (%)
190	0
400	5
600	22
800	40
1000	50

8.5 Spark Sensitivity.

Electrode	Lead Foil Thickness (mils)	Sample Size (mg)	Energy (J)	Occurrence of Explosion (%)
Brass	3	30	1.09	33
Brass	10	30	2.77	33

9. MECHANICAL PROPERTIES

9.2 Tensile Strength and Modulus.

Temperature (°C)	Density (g/cm^3)	Ultimate Tensile Strength (psi)	Tensile Modulus ($psi \times 10^{-4}$)
74	1.780	52	0.7
49	1.780	108	3.0
24	1.780	508	29.0
-18	1.780	920	91.0
-54	1.780	1118	138.0

9.3 Compressive Strength and Modulus

Temperature (°C)	Density (g/cm^3)	Ultimate Compressive Strength (psi)	Compressive Modulus (psi x 10^{-4})
74	1.783	180	2.1
49	1.786	370	3.0
24	1.782	1070	17.9
-18	1.786	3520	48.0
-54	1.783	9580	124.0

9.4 Shear Strength and Modulus.

Temperature (°C)	Density (g/cm^3)	Ultimate Shear Strength (psi)
74	1.780	130
49	1.780	190
24	1.780	530
−18	1.780	910
−54	1.780	2790

REFERENCES

1. Committee on Threshold Limit Values, *Documentation of Threshold Limit Values,* 3rd Ed. (American Conference of Governmental Industrial Hygienists, 1014 Broadway, Cincinnati, Ohio, 1971).

2. *Code of Federal Regulations, 49, Transportation Parts 100-199, Rev. 12-1-76* (Office of the Federal Register, General Services Administration, Washington, DC, 1976).

3. US Army Materiel Command, Regulation No. AMCR 385-100 (1977).

4. R. N. Rogers, Thermochimica Acta **11,** 131-139 (1975).

5. J. W. Kury, H. C. Hornig, E. L. Lee, J. L. McDonnel, D. L. Ornellas, M. Finger, F. M. Strange, and M. L. Wilkins, *Proceedings—Fourth Symposium (International) on Detonation, White Oak, Maryland, October 12-15, 1965* (Office of Naval Research, Department of the Navy, ACR-126, 1965), pp. 3-12.

6. Manuel J. Urizar, Suzanne W. Peterson, and Louis C. Smith, Los Alamos Scientific Laboratory report LA-7193-MS (April 1978).

7. L. G. Green and G. D. Dorough, *Proceedings—Fourth Symposium (International) on Detonation, White Oak, Maryland, October 12-15, 1965* (Office of Naval Research, Department of the Navy, 1965), pp. 477-486.

PBX 9404

1. GENERAL PROPERTIES

1.1 Chemical and Physical Description. Plastic-bonded explosive PBX 9404 is composed of HMX bonded with nitrocellulose (NC) and with tris-beta chloroethylphosphate (CEF) as the plasticizer. A small quantity of diphenylamine (DPA) is added to stabilize the NC. The molding powder is off-white at time of manufacture. As the NC decomposes, the DPA reacts with the decomposition products, and the color changes from white to light blue, dark blue, and finally a yellow-brown. The color can be used to estimate the temperature storage history of the powder or molded piece.

1.2 Common Use. PBX 9404 is a high-performance high explosive used in nuclear ordnance.

1.3 Toxicity.[1,2] The suggested maximum concentration of HMX in air is 1.5 mg/m^3. We have no data on NC toxicity. The toxicity of CEF is unknown; DPA is highly toxic if inhaled or absorbed through the skin.

2. MANUFACTURE AND PROCUREMENT

2.1 Manufacture. PBX-9404 molding powder is prepared by the water slurry process. A lacquer of NC, CEF, and DPA is prepared in a water-immiscible solvent. This is added to a water slurry containing a bimodal distribution of HMX crystals. During solvent removal by distillation, the plastic, plasticizer, and stabilizer uniformly coat and agglomerate the HMX crystals in the water phase. The process variables must be closely controlled to produce satisfactory agglomerates, composition, and bulk density.

2.2 Procurement. PBX 9404 is purchased from the US Army Armament Readiness Command under LASL material specification 13Y-103159 Rev. B, dated June 16, 1970.

2.3 Shipping.[3] PBX-9404 molding powder is shipped as a Class A explosive.

2.4 Storage.[4] PBX 9404 is stored in Compatibility Group D, Storage Class 1.1.

3. CHEMICAL PROPERTIES

3.1 Composition.

Constituent	Weight Percent	Volume Percent
HMX	94.0	92.5
NC	3:0	3.6
CEF	3.0	3.9
DPA	0.1	0.1

3.2 Molecular Weight.

Constituent	Structure	Molecular Weight
HMX	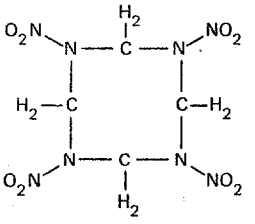	296.17
	$C_4H_8N_8O_8$	
NC	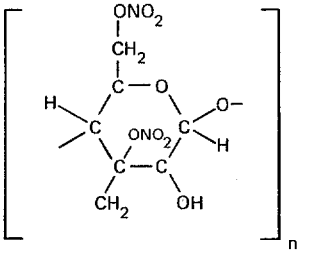	$(262.64)_n$
	$[C_7H_8N_2O_9]_n$	
CEF	$(ClCH_2CH_2O)_3-P=0$ $C_6H_{12}O_4Cl_3P$	286.0
DPA	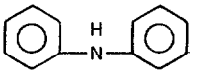	
	$C_{12}H_{11}N$	169.22

3.3 Solubility. The solubility is that of HMX.

Solvent	Grams of HMX Dissolved/100 g of Solvent		
	20°C	40°C	60°C
Acetic acid			
Glacial	0.037	0.044	0.090
70%	---	0.033	0.103
Acetic anhydride	---	1.29	1.94
Acetone			
Anhydrous	2.4	3.4	---
70%	0.66	1.20	---
Acetonitrile	---	3.07	4.34
Cyclohexanone	---	5.91	7.17
Dimethylformamide	---	6.1	11.1
Dimethylsulfoxide	---	45.5	47.2

4. PHYSICAL PROPERTIES

4.2 Density.

Theoretical Density (g/cm^3)	Density of Typical Pressed Charges (g/cm^3)
1.873	1.840

The following densities are obtained by vacuum pressing (residual pressure $\leq 10^3$ μm Hg) hot (80°C) molding powder with a 4-min dwell.

Pressure (psi)	Density (g/cm^3)
10 000	1.820-1.825
12 000	1.830-1.835
15 000	1.835-1.845

4.3 Infrared Spectrum. See Fig. 1.

5. THERMAL PROPERTIES

5.1 Phase Changes.

Type	Temperature (°C)	Latent Heat (cal/g)
β-to-δ solid-to-solid in HMX	190	9.2

5.3 Heat Capacity.

Heat Capacity at Constant Pressure (cal/g-°C)	Temperature Range (°C)
$0.224 + 7 \times 10^{-4} T$	$7 < T < 147$

5.4 Thermal Conductivity.

Density (g/cm^3)	Conductivity (cal/s-cm-°C)
1.845	9.2×10^{-4}

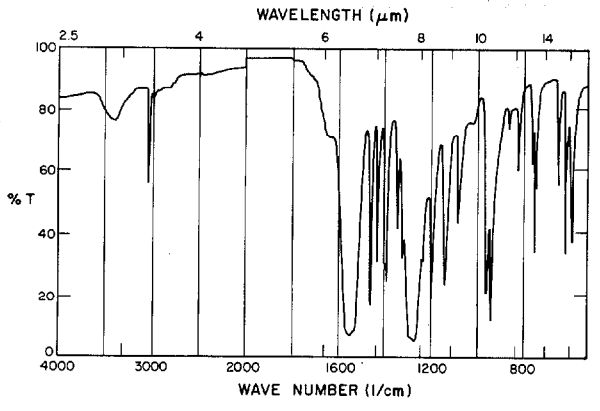

Fig. 1. Infrared spectrum.

5.5 Coefficient of Thermal Expansion.

Density (g/cm^3)	Coefficient of Expansion (1/°C)	Temperature Range (°C)
1.840	4.7×10^{-5}	$25 < T < 70$

5.6 Heats of Combustion and Formation.

Constituent	ΔH_c° (kcal/mole)	ΔH_f° (kcal/mole)
HMX	−660.7	11.3
NC	---	−200
CEF	---	−300.0

5.7 Thermal Decomposition Kinetics.[5]

	Constituent	
Property	PBX 9404[a]	HMX
Decomposition energy	---	500 cal/g
Activation energy	31.3 kcal/mole	52.7 kcal/mole
Pre-exponential factor	4.3×10^{12}/s	5×10^{19}/s

[a]Reflects NC decomposition.

5.8 Other Thermal Stability Test Results.

Test	Results
Vacuum	1.3-4.0 ml/g of gas evolved after 48 h at 120°C
DTA and pyrolysis	See Fig. 2

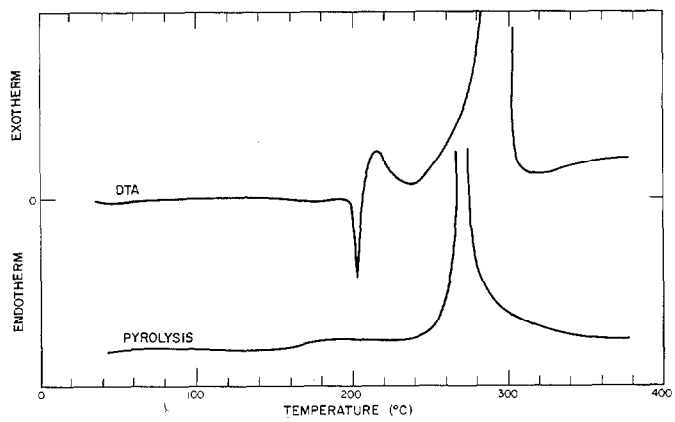

Fig. 2. PBX 9404 DTA and pyrolysis test results.

6. DETONATION PROPERTIES

6.1 Detonation Velocity.[6]

Effect of Charge Radius

Charge radius affects the detonation velocity of unconfined PBX-9404 charges pressed to a density of 1.846 g/cm³ as follows.

$$D(R) = 8.776[(1 - 0.89 \times 10^{-2}/R) - 4.9 \times 10^{-3}/R(R - 0.533)],$$

where D = detonation velocity in millimeters per microsecond

and R = charge radius in millimeters.

The experimentally determined failure diameter is 1.18 mm.

6.2 Detonation Pressure.

Density (g/cm³)	Detonation Velocity (mm/μs)	Detonation Pressure (GPa)
1.844	8.802[a]	36.8

[a]Note that this value is greater than the infinite-diameter velocity reported in Section 6.1.

6.3 Cylinder Test Results.

Density (g/cm³)	Detonation Velocity (mm/μs)	Cylinder Wall Velocity (mm/μs) at	
		$R - R_o = 5$ mm	$R - R_o = 19$ mm
1.846	8.781	1.556	1.787

6.4 Plate Dent Test Results.[7]

Charge Diameter (mm)	Density (g/cm³)	Dent Depth (mm)	Charge Height (mm)
41.3	1.844	10.9	203

7. SHOCK INITIATION PROPERTIES

7.1 Gap Test Results.[8]

Density (g/cm^3)	G_{50} (mm)	L_{95} (mm)
	Large Scale	
0.920	68.43	0.20
1.230	64.16	1.85
1.400	63.07	0.18
1.585	62.76	0.30
1.798	59.21	0.30
1.821	58.34	0.56
1.825	56.46	0.38
1.833	56.44	0.51
1.847	55.86	0.10
1.865	51.94	0.51
	Small Scale[a]	
0.96	0.58	0.10
1.792	3.40	0.15
1.812	3.23	0.13
1.826	3.23	0.10
1.830	2.90	0.08
1.836	2.69	0.18
1.843	2.67	0.13
1.860	2.36	0.25

[a]These results seem inconsistent.

7.2 Wedge Test Results.

Density (g/cm³)	Distance, x*, and Time, t*, to Detonation (mm and μs)	Pressure Range (GPa)
1.84	$\log P = (1.11 \pm 0.01) - (0.65 \pm 0.02) \log x^*$ $\log P = (0.69 \pm 0.01) - (0.54 \pm 0.01) \log t^*$,	$2.27 < P < 25.72$
1.72	$\log P = (0.96 \pm 0.03) - (0.71 \pm 0.04) \log x^*$ $\log P = (0.54 \pm 0.01) - (0.57 \pm 0.02) \log t^*$,	$1.19 < P < 6.34$

where P = pressure in gigapascals.

7.3 Shock Hugoniots.

Density (g/cm³)	Shock Hugoniot (mm/μs)	Particle Velocity Range (mm/μs)
1.840	$U_s = (2.494 \pm 0.039) + (2.093 \pm 0.045) U_p$,	$0.133 < U_p < 2.063$
1.721	$U_s = (1.890 \pm 0.197) + (1.565 \pm 0.353) U_p$,	$0.172 < U_p < 0.995$

where U_s = shock velocity
and U_p = particle velocity.

7.4 Minimum Priming Charge.[8]

Density (g/cm³)	W_{50} (mg of XTX 8003)	L_{95} (±log mg)
1.800	16.2	0.108
1.840	23.9	0.132

7.5 Detonation Failure Thickness.[8]

Density (g/cm^3)	Failure Thickness (mm)	L_{95} (mm)
1.785	0.439	0.069
1.800	0.589	0.074
1.814	0.404	0.056
1.828	0.510	0.061
1.844	0.503	0.185
1.844	0.368	0.028
1.844	0.396	0.112
1.845	0.457	0.033

8. SENSITIVITY

8.1 Drop Weight Impact Height.

Tool Type	H_{50} (cm)
12	42
12B	47

8.2 Large-Scale Drop Test Height.[9]

Density (g/cm^3)	H_{50} (ft)	Reaction
1.835	49	Explosion
1.800[a]	110	Explosion

[a]PBX 9404 + 1wt% wax.

8.3 Skid Test Results.[9,10]

Density (g/cm^3)	Impact Angle (degrees)	Target Surface	H_{50} (ft)	Reaction Overpressure (psi)
1.847	45	Sand and epoxy	~4.5	>20
1.837	45	Garnet paper	~4.0	15
1.866	45	Garnet paper	~5.0	8
1.837	15	Garnet paper	~3.0	15
1.838	15	Quartz	1.8	15
1.838	15	Alumina[a]	~11.0	15
1.838	15	Alumina[b]	19.0	15
1.838	45	Gold	>150.0	---

[a]Surface finish, 1.2-2.0 μm.
[b]Surface finish, 0.5-0.9 μm.

8.4 Susan Test Results.[11]

Projectile Impact Velocity (ft/s)	Relative Energy Release (%)
90	0
110	82
>110	82

8.5 Spark Sensitivity.

Electrode	Lead Foil Thickness (mils)	Sample Size (mg)	Energy (J)	Occurrence of Explosion (%)
Brass	3	28	0.42	0
Brass	10	28	3.13	0

9. MECHANICAL PROPERTIES

9.2 Tensile Strength and Modulus.

Temperature (°C)	Density (g/cm^3)	Ultimate Tensile Strength[a] (psi)	Tensile Modulus[a] (psi × 10^{-5})
74	1.848	97	1.3
49	1.848	170	1.4
24	1.848	482	2.5
−18	1.848	698	11.75
−54	1.848	533	15.40

[a]These properties vary with the HMX particle-size distribution. They are time dependent; if PBX 9404 is exposed to temperatures >40°C for long periods, its strength and modulus decrease.

9.3 Compressive Strength and Modulus.

Temperature (°C)	Density (g/cm³)	Ultimate Compressive Strength[a] (psi)	Compressive Modulus[a] (psi × 10^{-5})
74	1.848	658	1.2
49	1.848	1289	2.6
24	1.848	2479	2.9
−18	1.848	4859	9.9
−54	1.848	8510	16.0

[a]These properties vary with the HMX particle-size distribution. They are time dependent; if PBX 9404 is exposed to temperatures >40°C for long periods, its strength and modulus decrease.

9.4 Shear Strength and Modulus.

Temperature (°C)	Density (g/cm³)	Ultimate Shear Strength[a] (psi)
74	1.844	523
49	1.844	834
24	1.844	1251
−18	1.844	1454
−54	1.844	2261

[a]This property varies with the HMX particle-size distribution. It is time dependent; if PBX 9404 is exposed to temperatures >40°C for long periods, its strength decreases.

REFERENCES

1. Committee on Threshold Limit Values, *Documentation of Threshold Limit Values,* 3rd Ed. (American Conference of Governmental Industrial Hygienists, 1014 Broadway, Cincinnati, Ohio, 1971).

2. N. I. Sax, *Dangerous Properties of Industrial Materials,* 4th Ed. (Van Nostrand Reinhold Company, New York, 1975).

3. *Code of Federal Regulations, 49, Transportation Parts 100-199, Rev. 12-1-76,* (Office of the Federal Register, General Services Administration, Washington, DC, 1976).

4. US Army Materiel Command, Regulation No. AMCR 385-100 (1977).

5. R. N. Rogers, Thermochemica Acta **11**, 131-139 (1975).

6. A. W. Campbell and Ray Engelke, *Proceedings—Sixth Symposium (International) on Detonation, Coronado, California, August 24-27, 1976* (Office of Naval Research, Department of the Navy, ACR-221, 1976), pp. 642-652.

7. L. C. Smith, Explosivstoffe **15**, 106-130 (1967).

8. Manuel J. Urizar, Suzanne W. Peterson, and Louis C. Smith, Los Alamos Scientific Laboratory report LA-7193-MS (April 1978).

9. A. Popolato, Proceedings of the International Conference on Sensitivity and Hazards of Explosives, Ministry of Aviation, Waltham Abbey, Essex (October 1963).

10. A. D. Randolph, L. E. Hatler, and A. Popolato, Industrial and Engineering Chemistry Fundamentals **15**, 1 (1976).

11. L. G. Green and G. D. Dorough, *Proceedings—Fourth Symposium (International) on Detonation, White Oak, Maryland, October 12-15, 1965* (Office of Naval Research, Department of the Navy, ACR-126, 1965), pp. 477-486.

PBX 9407

1. GENERAL PROPERTIES

1.1 Chemical and Physical Description. PBX 9407 is composed of RDX coated with Exon 461, a chlorotrifluoroethylene/tetrafluoroethylene/vinylidene fluoride copolymer. The molding powder is off-white.

1.2 Common Use. PBX 9407 is generally used as a booster explosive.

1.3 Toxicity.[1] Workers who inhaled RDX dust for several months have become unconscious and have suffered loss of reflexes. The suggested maximum permissible airborne concentration is 1.5 mg/m^3. Inhaling hot Exon vapor should be avoided.

2. MANUFACTURE AND PROCUREMENT

2.1 Manufacture. PBX-9407 molding powder is prepared by the water slurry process. An Exon lacquer is prepared in a water-immiscible solvent and added to a water slurry containing Type II Class 5 RDX crystals. During solvent removal by distillation, the plastic uniformly coats and agglomerates the RDX crystals in the water phase. The process variables must be carefully controlled to produce satisfactory agglomerates, composition, and bulk density.

2.2 Procurement. PBX 9407 is purchased from the US Army Armament Readiness Command under LASL material specification 13Y-109098 Rev. C, dated August 24, 1978.

2.3 Shipping.[2] PBX-9407 molding powder is shipped as a Class A explosive.

2.4 Storage.[3] PBX 9407 is stored in Compatibility Group D, Storage Class 1.1.

3. CHEMICAL PROPERTIES

3.1 Composition.

Constituent	Weight Percent	Volume Percent
RDX	94.0	93.6
Exon 461	6.0	6.4

3.2 Molecular Weight.

Constituent	Structure	Molecular Weight
RDX	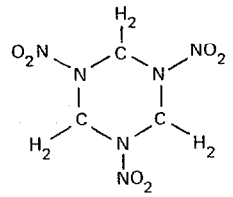 $C_3H_6N_6O_6$	222.13
Exon 461	$[(CF_2CFCl)_{0.64}/CH_2CHCl)_{0.36}]_n$	$(97.05)_n$

3.3 Solubility. The solubility is like that of RDX.

Solvent	Grams RDX Dissolved/100 g of Solvent		
	20°C	40°C	60°C
Acetic acid			
99.6%	0.46	0.56	1.22
71.0%	0.22	0.37	0.74
Acetone	6.81	10.34	---
Isoamyl alcohol	0.026	0.060	0.210
Benzene	0.045	0.085	0.195
Chlorobenzene	0.33	0.554	---
Cyclohexanone	4.94	9.20	13.9
Dimethylformamide	---	41.5	60.6
Ethanol	0.12	0.24	0.58
Methyl acetate	2.9	4.1	---
Methylcyclohexanone	6.81	10.34	---
Methyl ethyl ketone	3.23	---	---
Toluene	0.020	0.050	0.125
Trichloroethylene	0.20	0.24	---
Water	0.005	0.0127	0.03

4. PHYSICAL PROPERTIES

4.2 Density.

Theoretical Density (g/cm^3)	Density of Typical Pressed Charge (g/cm^3)
1.809	1.65

4.3 Infrared Spectrum. See Fig. 1.

5. THERMAL PROPERTIES

5.1 Phase Changes.

Type	Temperature (°C)	Latent Heat (cal/g)
RDX (solid-to-liquid)	204.1	33.37

5.3 Heat Capacity.

Density (g/cm^3)	Heat Capacity at Constant Pressure (cal/g-°C)	Temperature Range (°C)
1.66	$0.241 + 7.7 \times 10^{-4}$ T	$37 < T < 167$

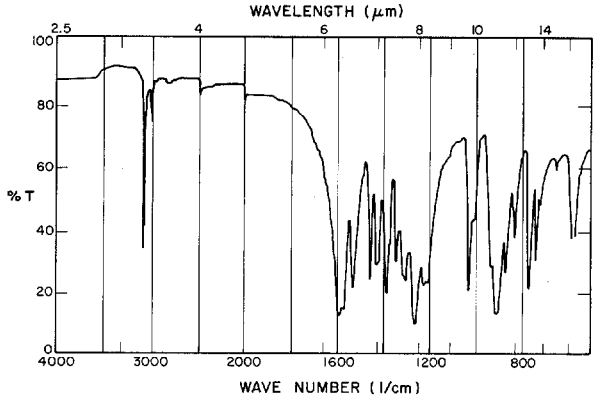

Fig. 1. Infrared spectrum.

5.4 Thermal Conductivity.

Conductivity (cal/s-cm-°C)	Temperature Range (°C)
$0.241 + 7.7 \times 10^{-4}$	$37 < T < 167$

5.6 Heats of Combustion and Formation.

Constituent	ΔH_c° (kcal/mole)	ΔH_f° (kcal/mole)
RDX	−501.8	14.7

5.7 Thermal Decomposition Kinetics.[4]

Property	RDX
Decomposition energy	500 cal/g
Activation energy	47.1 kcal/mole
Pre-exponential factor	2.02×10^{18}/s

5.8 Other Thermal Stability Test Results.

Test	Results
Vacuum	0.1-0.3 ml/g of gas evolved after 48 h at 120°C
DTA and pyrolysis	See Fig. 2

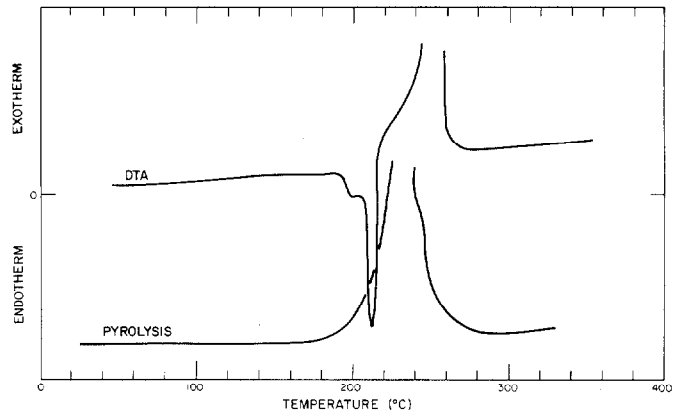

Fig. 2. PBX 9407 DTA and pyrolysis test results.

6. DETONATION PROPERTIES

6.1 Detonation Velocity.[5] A detonation velocity of 8.1 mm/μs was obtained at a density of 1.60 g/cm^3. The charge radius was unspecified.

7. SHOCK INITIATION PROPERTIES[5]

7.1 Gap Test Results.

Density (g/cm^3)	G_{50} (mm)	L_{95} (mm)
	Large Scale	
0.60	62.4	---
1.772	54.72	0.15
1.773	53.85	0.08
	Small Scale	
1.538	4.75	0.25
1.555	4.80	0.15
1.598[a]	5.13	0.08
1.598	4.95	0.13
1.603	4.75	0.18
1.650[a]	4.72	0.10
1.663[b]	4.72	0.10
1.664	4.78	0.13
1.696	3.91	0.13

[a]Cold pressed.
[b]With 0.8 wt% graphite added.

7.2 Wedge Test Results.

Density (g/cm³)	Distance, x*, and Time, t*, to Detonation (mm and μs)	Pressure Range (GPa)
1.60	$\log P = (0.57 \pm 0.02) - (0.49 \pm 0.03) \log x^*$ $\log P = (0.33 \pm 0.13) - (0.41 \pm 0.03) \log t^*$, where P = pressure in gigapascals.	$1.14 < P < 4.69$

7.3 Shock Hugoniot.[6]

Density (g/cm³)	Shock Hugoniot (mm/μs)	Particle Velocity Range (mm/μs)
1.60	$U_s = 1.328 + 1.993\ U_p$, where U_s = shock velocity and U_p = particle velocity.	$0.35 < U_p < 0.93$

7.4 Minimum Priming Charge.

Density (g/cm³)	W_{50} (mg of XTX 8003)	L_{95} (±log mg)
1.764	12.4	0.054

7.5 Detonation Failure Thickness.[5]

Density (g/cm³)	Failure Thickness (mm)	L_{95} (mm)
1.767	0.305	0.089

8. SENSITIVITY

8.1 Drop Weight Impact Height.

Tool Type	H_{50} (cm)
12	33
12B	35

8.5 Spark Sensitivity.

Electrode	Lead Foil Thickness (mils)	Sample Size (mg)	Energy (J)	Occurrence of Explosion (%)
Brass	3	30	0.77	50
Brass	10	30	1.50	50

9. MECHANICAL PROPERTIES

9.2 Tensile Strength and Modulus.

Temperature (°C)	Density (g/cm^3)	Ultimate[a] Tensile Strength (psi)	Tensile Modulus ($psi \times 10^{-5}$)
74	1.653	287	8.88
24	1.653	364	10.87
−18	1.653	747	---

[a]The ultimate strength varies as much as 75 psi.

9.3 Compressive Strength and Modulus.

Temperature (°C)	Ultimate[a] Compressive Strength (psi)	Compressive Modulus (psi × 10^{-5})
74	1729	3.81
49	3250	5.75
20	6770	12.47
−18	8970	12.48
−54	9300	13.18

[a]The ultimate strength varies as much as a few hundred psi.

9.4 Shear Strength and Modulus.

Temperature (°C)	Density (g/cm^3)	Ultimate[a] Shear Strength (psi)
74	1.636	1080
60	1.636	1775
24	1.636	2120
−18	1.636	1840
−54	1.636	1990

[a]The ultimate shear strength varies as much as a few hundred psi below 0°C, and about 100 psi above 0°C.

REFERENCES

1. C. R. Buck and S. E. Wilson, Jr., US Army report USEHA-32-049 (1975).

2. *Code of Federal Regulations, 49, Transportation Parts 100-199, Rev. 12-1-76* (Office of the Federal Register, General Services Administration, Washington, DC, 1976).

3. US Army Materiel Command, Regulation No. AMCR 385-100 (1977).

4. R. N. Rogers, Thermochimica Acta **11**, 131-139 (1975).

5. Manuel J. Urizar, Suzanne W. Peterson, and Louis C. Smith, Los Alamos Scientific Laboratory report LA-7193-MS (April 1978).

6. I. E. Lindstrom, Journal of Applied Physics **37**, 4873-4880 (1966).

PBX 9501

1. GENERAL PROPERTIES

1.1 Chemical and Physical Description. PBX 9501 is composed of HMX bonded with Estane and the eutectic mixture of bis(2,2-dinitropropyl)acetal and bis(2,2-dinitropropyl)formal (BDNPA/BDNPF). At time of manufacture the molding powder is off-white. With time, it changes to a light buff.

1.2 Common Use. PBX 9501 is a high-performance explosive more thermally stable and less hazardous to handle then any other explosive of equivalent energy. It is used in nuclear ordnance.

1.3 Toxicity. The suggested maximum airborne HMX concentration[1] is 1.5 mg/m^3. BDNPA/BDNPF is considered slightly to moderately toxic,[2] and Estane is not toxic.

2. MANUFACTURE AND PROCUREMENT

2.1 Manufacture. PBX-9501 molding powder is prepared by the slurry process. A lacquer of Estane and BDNPA/ BDNPF is prepared in a solvent partially immiscible in water. This is added to a solvent-saturated water slurry containing a bimodal distribution of HMX crystals. During solvent removal by distillation, the Estane and BDNPA/ BDNPF uniformly coat and agglomerate the HMX crystals in the water phase. The process variables must be controlled closely to produce satisfactory agglomerates, composition, and bulk density.

2.2 Procurement. PBX 9501 is purchased from the US Army Armament Readiness Command under LASL material specification 13Y-109643 Rev. C, dated March 1, 1977. The DOE furnishes the BDNPA/ BDNPF.

2.3 Shipping.[3] PBX-9501 molding powder is shipped as a Class A explosive.

2.4 Storage.[4] PBX 9501 is stored in Compatibility Group D, Storage Class 1.1.

3. CHEMICAL PROPERTIES

3.1 Composition.

Constituent	Weight Percent	Volume Percent
HMX	95.0	92.7
Estane	2.5	3.9
BDNPA/BDNPF	2.5	3.3

3.2 Molecular Weight.

Constituent	Structure	Molecular Weight
HMX	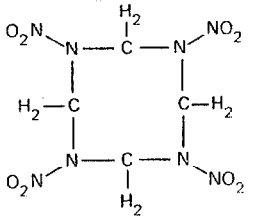	296.17
Estane 5703 F-1	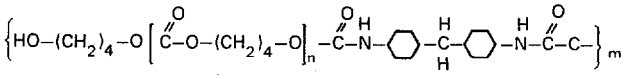 $C_{5.14}H_{7.5}N_{0.187}O_{1.76}$	100.0
BDNPA/BDNPF	$\{[CH_3\text{-}C\text{-}(NO_2)_2\text{-}CH2\text{-}O]_2CH_2/$ $[CH_3\text{-}C(NO_2)_2\text{-}CH_2\text{-}O]_2CH_2CH_3\}$ $C_{2.35}H_{4.07}N_{1.25}O_{3.14}$	100.0

3.3 Solubility. The solubility is that of HMX.

Solvent	Grams of HMX Dissolved/100 g of Solvent		
	20°C	40°C	60°C
Acetic acid			
Glacial	0.037	0.044	0.090
70%	---	0.033	0.103
Acetic anhydride	---	1.29	1.94
Acetone			
Anhydrous	2.4	3.4	---
70%	0.66	1.20	---
Acetonitrile	---	3.07	4.34
Cyclohexanone	---	5.91	7.17
Dimethylformamide	---	6.1	11.1
Dimethylsulfoxide	---	45.5	47.2

4. PHYSICAL PROPERTIES

4.2 Density.

Theoretical Density (g/cm^3)	Density of Typical Pressed Charge (g/cm^3)
1.860	1.830

The following densities are obtained by vacuum pressing (residual pressure $\leq 10^3$ μm of Hg) with three 3-min intensifications.

Pressure (psi)	Density (g/cm^3) with Powder Preheated to	
	85°C	95°C
15 000	1.836	1.836
20 000	1.840	1.840

5. THERMAL PROPERTIES

5.1 Phase Changes.

Type	Temperature (°C)	Latent Heat (cal/g)
β-to-δ solid-to-solid in HMX	190	9.2

5.3 Heat Capacity.

Heat Capacity at Constant Pressure (cal/g-°C)	Temperature Range (°C)
$0.238 + 7.9 \times 10^{-4} T$	$5 < T < 175$

5.4 Thermal Conductivity.

Density (g/cm^3)	Conductivity (cal/s-cm-°C)
1.847	1.084×10^{-3}

5.5 Coefficient of Thermal Expansion.

Density (g/cm^3)	Coefficient of Expansion (1/°C)	Temperature Range (°C)
1.835	49.1×10^{-6}	$54 < T < 74$

5.6 Heats of Combustion and Formation.

Constituent	ΔH_c° (kcal/mole)	ΔH_f° (kcal/mole)
HMX	−660.7	11.3

5.7 Thermal Decomposition Kinetics.[5]

Property	Constituent	
	PBX 9501	HMX
Decomposition energy	----	500 cal/g
Activation energy	40.1 kcal/mole	52.7 kcal/mole
Pre-exponential factor	5.9×10^{14}/s	5×10^{19}/s

5.8 Other Thermal Stability Test Results

Test	Results
Vacuum	0.3-0.7 ml/g of gas evolved after 48 h at 120°C
DTA and pyrolysis	See Fig. 1

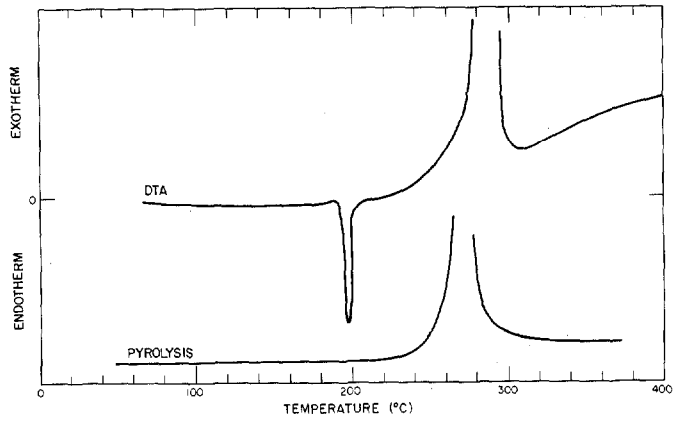

Fig. 1. PBX 9501 DTA and pyrolysis test results.

6. DETONATION PROPERTIES

6.1 Detonation Velocity.[6]

Effect of Charge Radius

Charge radius affects the detonation velocity of unconfined PBX 9501 charges pressed to a density of 1.832 g/cm³ as follows.

$$D(R) = 8.802\ [(1 - 1.9 \times 10^{-2})/R - 9.12 \times 10^{-3}/R(R - 0.48)]$$

where D = detonation velocity in millimeters per microsecond

and R = charge radius in millimeters.

The experimentally determined failure diameter is slightly less than 1.52 mm.

6.3 Cylinder Test Results.

Density (g/cm³)	Detonation Velocity (mm/μs)	Cylinder Wall Velocity (mm/μs)at	
		$R - R_o = 5$ mm	$R - R_o = 19$ mm
1.834	8.792	1.534	1.776

6.4 Plate Dent Test Results.

Density (g/cm³)	Dent Depth (mm)
1.853	10.47

7. SHOCK INITIATION PROPERTIES

7.1 Gap Test Results.[7]

Density (g/cm^3)	G_{50} (mm)
Large Scale	
1.834	55.52
Small Scale	
1.843	1.52

7.2 Wedge Test Results.

Density (g/cm^3)	Distance, x*, and Time, t*, to Detonation (mm and μs)	Pressure Range (GPa)
1.833	$\log P = (1.15 \pm 0.05) - (0.64 \pm 0.06) \log x^*$ $\log P = (0.73 \pm 0.01) - (0.53 \pm 0.03) \log t^*$,	$2.38 < P < 7.32$
1.844	$\log P = (1.10 \pm 0.04) - (0.51 \pm 0.03) \log x^*$ $\log P = (0.76 \pm 0.01) - (0.45 \pm 0.03) \log t^*$,	$2.47 < P < 7.21$

where P = pressure in gigapascals.

7.3 Shock Hugoniot.

Density (g/cm^3)	Shock Hugoniot ($mm/\mu s$)	Particle Velocity Range ($mm/\mu s$)
1.833	$U_s = (2.501 \pm 0.131) + (2.261 \pm 0.233)\, U_p$	$0.07 < U_p < 0.89$
1.844	$U_s = (2.953 \pm 0.098) + (1.507 \pm 0.179)\, U_p$,	$0.1 < U_p < 0.9$

where U_s = shock velocity
and U_p = particle velocity.

7.4 Minimum Priming Charge.[7]

Density (g/cm^3)	W_{50} (mg of XTX 8003)	L_{95} ($\pm$log mg)
1.837	67.0	0.04
1.834	44.8	0.05

8. SENSITIVITY

8.1 Drop Weight Impact Height.

Tool Type	H_{50} (cm)
12	48
12B	44

8.2 Large-Scale Drop Test Height.

Density (g/cm^3)	H_{50} (ft)	Reaction
1.830	>150	One partial reaction in eight 150-ft drops

8.3 Skid Test Results.

Density (g/cm^3)	Impact Angle (degrees)	Target Surface	H_{50} (ft)	Reaction Overpressure (psi)
1.830	45	Garnet paper	26	1.0
1.830	15	Quartz[a]	>14	---

[a]200-μ in. finish on quartz.

8.4 Susan Test Results.

Projectile Impact Velocity (ft/s)	Relative Energy Release (%)
175	0
200	40
210	60

9. MECHANICAL PROPERTIES*

9.2 Tensile Strength and Modulus.

Temperature (°C)	Density (g/cm³)	Ultimate Tensile Strength (psi)	Tensile Modulus (psi × 10^{-5})
74	1.844	100	1.05
24	1.844	320	2.24
−18	1.844	645	7.63
−54	1.845	1000	13.38

9.3 Compressive Strength and Modulus.

Temperature (°C)	Density (g/cm³)	Ultimate Compressive Strength (psi)	Compressive Modulus (psi × 10^{-5})
74	1.844	520	0.64
24	1.844	1140	1.93
−18	1.843	2100	3.30
−54	1.843	4700	6.52

*Above 50°C, the polyester polyurethane, Estane, depolymerizes so its strength decreases with time. The data given are initial values.

REFERENCES

1. Committee on Threshold Limit Values, *Documentation of Threshold Limit Values*, 3rd Ed. (American Conference of Governmental Industrial Hygienists, 1014 Broadway, Cincinnati, Ohio, 1971).

2. D. M. Smith, J. E. London, G. A. Drake, and R. G. Thomas, Los Alamos Scientific Laboratory report LA-7206-MS (March 1978).

3. *Code of Federal Regulations, 49, Transportation Parts 100-199, Rev. 12-1-76* (Office of the Federal Register, General Services Administration, Washington, DC, 1976).

4. US Army Materiel Command, Regulation No. AMCR 385-100, (1977).

5. R. N. Rogers, Thermochimica Acta **11,** 131-139 (1975).

6. A. W. Campbell and Ray Engelke, *Proceedings—Sixth Symposium (International) on Detonation, Coronado, California, August 24-27, 1976* (Office of Naval Research, Department of the Navy, ACR-221, 1976), pp. 642-652.

7. Manuel J. Urizar, Suzanne W. Peterson, and Louis C. Smith, Los Alamos Scientific Laboratory report LA-7193-MS (April 1978).

PBX 9502

1. GENERAL PROPERTIES

1.1 Chemical and Physical Properties. PBX 9502 is a plastic-bonded explosive composed of TATB bonded with Kel-F 800. The molding powder is yellow to tan or light brown.

1.2 Common Use. PBX 9502 is extremely difficult to initiate either deliberately or accidentally. It is used as the explosive in nuclear ordnance.

1.3 Toxicity. The toxicity is that of TATB. The maximum permissible concentration of TATB in air is 1.5 mg/m^3. TATB was not mutagenic when tested in five strains of *Salmonella typhimurium* and in *Escherichia coli* strain WP.

2. MANUFACTURE AND PROCUREMENT

2.1 Manufacture. PBX-9502 molding powder is prepared by the water slurry process. A Kel-F 800 lacquer is prepared in a solvent that is partially immiscible in water. This is added to a water slurry containing TATB. The solvent is extracted from the lacquer by adding water. The TATB particles are plastic coated and agglomerated during the extraction process. A simmering period is used to adjust the agglomerate size. The process variables must be carefully controlled to produce satisfactory agglomerates, composition, and bulk density.

2.2 Procurement. PBX 9502 is purchased from the US Army Armament Readiness Command under LASL material specification 13Y-188727, Rev. A, dated September 12, 1977. The DOE supplies the TATB.

2.3 Shipping.[1] PBX-9502 molding powder is shipped as a Class A explosive.

2.4 Storage.[2] PBX 9502 is stored in Compatibility Group D, Storage Class 1.1

3. CHEMICAL PROPERTIES

3.1 Composition.

Constituent	Weight Percent	Volume Percent
TATB	95	95.2
Kel-F 800	5	4.8

3.2 Molecular Weight.

Constituent	Structure	Molecular Weight
TATB	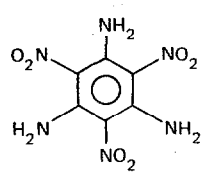 $C_6H_6N_6O_6$	258.18
Kel-F 800	$(CFClCF_2CH_2CF_2)_n$ $(C_4H_2F_5Cl)_n$	$(180.51)_n$

3.3 Solubility. The solubility is like that of TATB, which is practically insoluble in all organic solvents but is soluble in some superacids.

Solubility in Organic Solvents

Solvent	Solubility[a] (ppm)
Methanesulfonic acid	820
Hexamethylphosphoric triamide	150
Ethanesulfonic acid	120
Dimethylsulfoxide	100
Hexafluoroacetone sesquihydrate	68
N-methyl-2-pyrrolidinone	58
N, N-dimethylacetamide	33
N, N-dimethylacetamide	27
Dimethylformamide	26

[a]Temperature not reported.

Solubility in Sulfuric Acid and Water Mixtures

Acid (vol%)	Maximum Quantity Dissolved (grams of TATB/100 ml)
50	<0.02
66.7	<0.02
80	0.24
85	0.32
87.5	>1.28
90	3.84
100	>24.0

4. PHYSICAL PROPERTIES

4.2 Density.

Theoretical Density (g/cm^3)	Density of Typical Pressed Charges (g/cm^3)
1.942	1.895

The following densities are obtained by vacuum pressing (residual pressure $\leq 10^3$ μm Hg) hot molding powder (110°C) with a 4-min dwell and three pressure intensifications.

Pressure ($lb/in.^2$)	Density (g/cm^3)
15 000	1.890 ± 0.005
20 000	1.895 ± 0.005

5. THERMAL PROPERTIES

5.1 Phase Changes.[3]

Type	Temperature (°C)	Latent Heat (cal/g)
Solid-to-liquid in TATB	448-449	---
Solid-to-gas in TATB	---	163.9

5.3 Heat Capacity.

Heat Capacity at Constant Pressure (cal/g-°C)
$0.249 + 5.9 \times 10^{-4} T$

5.4 Thermal Conductivity.

Conductivity (cal/cm-s-°C)
13.4×10^{-4}

5.6 Heats of Combustion and Formation.[4]

Constituent	ΔH_c° (kcal/mole)	ΔH_f° (kcal/mole)
TATB	−735.9	−33.4

5.7 Thermal Decomposition Kinetics.[5]

Property	TATB
Decomposition energy	600 cal/g
Activation energy	59.9 kcal/mole
Pre-exponential factor	3.18×10^{19}/s

5.8 Other Thermal Stability Test Results.

Test	Results
Vacuum	0.0-0.2 ml/g of gas evolved after 48 h at 120°C
DTA and pyrolysis	See Fig. 1
Critical temperature, Tm	331°C
Charge radius, a	3.3 mm
Density, ρ	1.84 g/cm^3

6. DETONATION PROPERTIES

6.1 Detonation Velocity.[6]

Effect of Charge Radius

Charge radius affects the detonation velocity of unconfined PBX-9502 charges pressed to a density of 1.895 g/cm^3 as follows.

$$D(R) = 7.706(1 - 19.4 \times 10^{-2}/R) ,$$

where D = detonation velocity in millimeters per microsecond

and R = charge radius in millimeters.

The experimentally determined failure diameter is 9 mm.

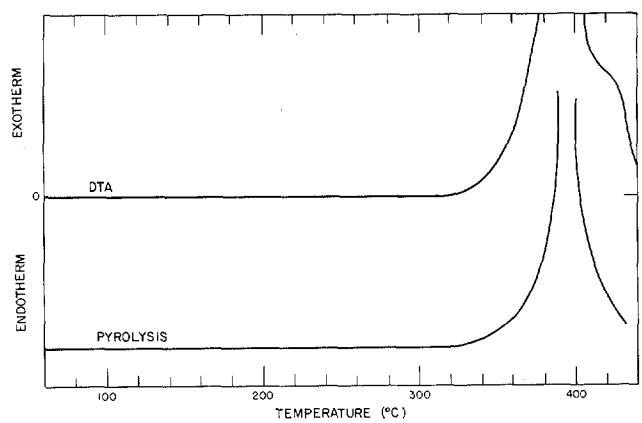

Fig. 1. PBX 9502 DTA and pyrolysis test results.

6.3 Cylinder Test Results.

Density (g/cm³)	Detonation Velocity (mm/μs)	Cylinder Wall Velocity (mm/μs) at	
		$R - R_o = 5$ mm	$R - R_o = 19$ mm
1.894	7.589	1.241	1.436

7. SHOCK INITIATION PROPERTIES

7.1 Gap Test Results.

Density (g/cm³)	G_{50} (mm)	L_{95} (mm)
	Large Scale	
1.895	22.33	1.0
	Small Scale	

This scale is too close to the detonation failure diameter.

7.2 Wedge Test Results.

Density (g/cm³)	Distance, x*, and Time, t*, to Detonation (mm and μs)	Pressure Range (GPa)
1.896	$\log P = (1.37 \pm 0.05) - (0.31 \pm 0.05) \log x^*$ $\log P = (1.15 \pm 0.01) - (0.28 \pm 0.04) \log t^*$, where P = pressure in gigapascals.	$10.05 < P < 14.95$

7.3 Shock Hugoniot.

Density (g/cm³)	Shock Hugoniot (mm/μs)	Particle Velocity Range (mm/μs)
1.896	$U_s = (3.263 \pm 0.977) + (1.678 \pm 0.777)\, U_p$, where U_s = shock velocity and U_p = particle velocity.	$1.08 < U_p < 1.42$

7.4 Minimum Priming Charge.[7]

Density (g/cm³)	W_{50} (mg of XTX 8003)
1.920[a]	$>1.53 \times 10^4$

[a]For 90 wt% TATB and 10 wt% Kel-F 800. Pure TATB gave a similar result.

8. SENSITIVITY

8.1 Drop Weight Impact Height.

Tool Type	H_{50} (cm)
12	>320
12B	>320

8.3 Skid Test Results. A formulation of 50 wt% HMX, 40 wt% TATB, and 10 wt% Kel-F gave no events in four 64-ft drops at a 45° impact angle on a garnet-paper target.

8.4 Susan Test Results. At an impact velocity of 1500 ft/s, the relative energy release was equivalent to the kinetic energy of the test vehicle. A similar result was obtained with an inert fill.

9. MECHANICAL PROPERTIES

9.2 Tensile Strength and Modulus.

Temperature (°C)	Density (g/cm³)	Ultimate Tensile Strength (psi)	Tensile Modulus (psi × 10^{-5})
−54	1.884	1340	6.51
24	1.886	1000	5.60
74	1.886	430	2.38

9.3 Compressive Strength and Modulus.

Temperature (°C)	Density (g/cm³)	Ultimate Compressive Strength (psi)	Compressive Modulus (psi × 10^{-5})
−54	1.886	5170	4.97
24	1.886	3360	3.41
74	1.885	1640	1.67

REFERENCES

1. *Code of Federal Regulations, 49, Transportation Parts 100-199, Rev. 12-1-76,* (Office of the Federal Register, General Services Administration, Washington, DC, 1976).

2. US Army Materiel Command, Regulation No. AMCR 385-100 (1977).

3. J. M. Rosen and C. Dickenson, US Naval Ordnance Laboratory report NOLTR 69-67 (April 1969).

4. Prince E. Rouse, Journal of Chemical and Engineering Data **21**, 16-20 (1976).

5. R. N. Rogers, Thermochimica Acta **11**, 131-139 (1975).

6. A. W. Campbell and Ray Engelke, *Proceedings—Sixth Symposium (International) on Detonation, Coronado, California, August 24-27, 1976* (Office of Naval Research, Department of the Navy, ACR-221, 1976), pp. 642-652.

7. Manuel J. Urizar, Suzanne W. Peterson, and Louis C. Smith, Los Alamos Scientific Laboratory report LA-7193-MS (April 1978).

PENTAERYTHRITOL TETRANITRATE (PETN)

1. GENERAL PROPERTIES

1.1 Chemical and Physical Description.[1] PETN, $C_5H_8N_4O_{12}$, forms colorless prismatic crystals that together appear white and opaque. Its name differs in various countries: PETN, Penthrite, and Penta in English-speaking countries; Pentrit, Niperyth, Nitropenta, and NP in Germany; and TEN in the Union of Soviet Socialist Republics.

1.2 Common Use. PETN is used extensively in detonators, detonating fuzes, and priming compositions. Mixed with another explosive or an inert material, it is used as the main explosive charge in grenades, small-caliber projectiles, and demolition devices. For example, Primacord, a detonating fuze, consists of a tube of waterproofed textile filled with finely powdered PETN.

1.3 Toxicity.[2] Because PETN is insoluble in water, it is slightly toxic. The recommended maximum atmospheric concentration for an 8-h period is 15 mg/m^3.

2. MANUFACTURE AND PROCUREMENT

2.1 Manufacture.[3] Acetaldehyde, aldol, or crotonaldehyde is condensed with formaldehyde in aqueous solution, in the presence of lime, to form pentaerythritol, which is nitrated with 96% nitric acid at 22-23°C to give PETN. The PETN is filtered, washed with water, and recrystallized from acetone by running acetone solution into water.

2.2 Procurement. Purchase is under Military Specification MIL-P-387B, dated November 7, 1967.

2.3 Shipping.[4] Bulk PETN is shipped by common carrier as a Class A explosive. It must be shipped wet with at least 40 wt% water.

2.4 Storage.[5] PETN is stored wet in Compatibility Group D. In certain conditions, it may be stored dry in Compatibility Group A. Wet or dry, PETN is in Storage Class 1.1.

3. CHEMICAL PROPERTIES

3.1 Structural Formula.

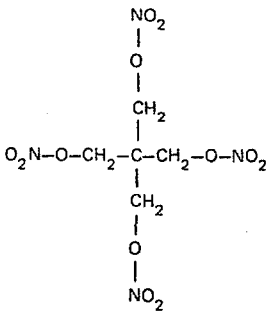

$C_5H_8N_4O_{12}$

3.2 Molecular Weight. 316.15

3.3 Solubility.[6]

Solvent	Grams Dissolved/ 100 g of Solvent		
	20°C	40°C	60°C
Acetone	24.8	44.92	---
Acetone and water (wt% water)			
6.23	16.29	31.42	---
12.30	9.31	20.25	---
18.22	5.22	12.66	---
23.99	2.87	7.66	---
35.11	0.68	2.33	---
55.80	0.03	0.13	---
Benzene	0.27	0.83	2.58
Ethanol	0.13	0.37	1.19
Ethyl acetate	10.6	18.50	---

4. PHYSICAL PROPERTIES

4.1 Crystal Structure.[7] There are two polymorphs of PETN. The most common, PETN I, transforms to PETN II at 130°C. Unit cell parameters for the two forms are as follows.

Cell Parameters	Polymorphic Form	
	PETN I at 22°C	PETN II at 136°C
Unit cell edge length (Å)		
a	9.38	13.29
b	9.38	13.49
c	6.71	6.83
Molecules per unit cell	2.0	4.0

4.2 Density.

Crystal Density[7]

Method of Determination	Temperature (°C)	Crystal Form	Crystal Density (g/cm^3)
X-ray calculation	22	I	1.778
X-ray calculation	136	II	1.716
Experimental	22	I	1.778

Compression gives the following densities.[1]

Pressure (psi)	Density (g/cm^3)
5 000	1.58
10 000	1.64
20 000	1.71
30 000	1.73
40 000	1.74

4.3 Infrared Spectrum. See Fig. 1.

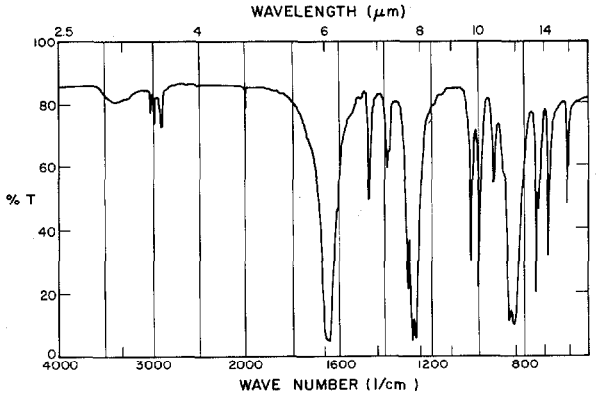

Fig. 1. Infrared spectrum.

4.4 Refractive Indices.[8]

	PETN Polymorph[a]	
	Form I	**Form II**
Omega	1.556	1.556
Epsilon	1.551	1.551
Birefringence	0.005	0.02
Double refraction	negative	---

[a]Form I is also called Alpha, and Form II is also called Beta.

5. THERMAL PROPERTIES

5.1 Phase Changes.[7,9,10]

Type	Temperature (°C)	Latent Heat (cal/g)	Latent Heat (kcal/mole)
PETN I-to-PETN II	130.0	---	---
Solid-to-liquid	142.9	37.4[a]	11.82
Solid-to-gas	---	91.9[b]	29.1

[a]Reference 9 indicates that the heat of fusion varies with the method of crystallization. Imperfect or very disordered crystals had heats of fusion as low as 31 kcal/g.

[b]The latent heat of sublimation was computed from the vapor pressure data given in Ref. 10.

5.2 Vapor Pressure.[10,11]

$$\log_{10} P(\text{mm Hg}) = 14.44 - 6352/T(\text{K}) \quad \text{for } 323 < T < 371 \text{ K.}$$

$$\log_{10} P(\text{mm Hg}) = 17.73 - 7750/T(\text{K}) \quad \text{for } 383 < T < 412 \text{ K.}$$

5.3 Heat Capacity.

Heat Capacity at Constant Pressure (cal/g-°C)	Temperature Range (°C)
$0.239 + 0.008\ T$	$32 < T < 127$

5.5 Coefficients of Thermal Expansion.[12]

Linear Expansion Coefficient

Crystal Face	Coefficient of Expansion (1/°C)	Temperature Range (°C)
$\alpha(001)$	$8.55 \times 10^{-5} + 1.82 \times 10^{-7}\ T + 6.30 \times 10^{-10}\ T^2 + 2.17 \times 10^{-12}\ T^3$	$-160 < T < 100$
$\alpha(100)$	$6.75 \times 10^{-5} + 1.28 \times 10^{-7}\ T + 0.74 \times 10^{-10}\ T^2 + 1.27 \times 10^{-12}\ T^3$	$-160 < T < 100$

Volume Expansion Coefficient

Coefficient of Expansion (1/°C)	Temperature Range (°C)
$22.05 \times 10^{-5} + 4.38 \times 10^{-7}\ T + 7.78 \times 10^{-10}\ T^2 + 4.71 \times 10^{-12}\ T^3$	$-160 < T < 100$

5.6 Heats of Combustion and Formation at 25°C.

ΔH_c° kcal/mole	ΔH_f° kcal/mole
−618.7	−110.34

5.7 Thermal Decomposition Kinetics.[13]

Decomposition energy	300 cal/g
Activation energy	47.0 kcal/mole
Frequency factor	6.3×10^{19}/s

5.8 Other Thermal Stability Test Results.

Test	Results
Vacuum	0.2-0.5 ml/g of gas evolved after 48 h at 100°C
DTA and pyrolysis	See Fig. 2
Critical temperature, Tm	192 °C
Charge radius, a	3.4 mm
Density, ρ	1.74 g/cm^3

6. DETONATION PROPERTIES

6.1 Detonation Velocity.[14]

Effect of Density

$D = 1.608 + 3.933\,\rho$ for $0.57 < \rho < 1.585$,

where D is in millimeters per microsecond,

and ρ is in grams per cubic centimeter.

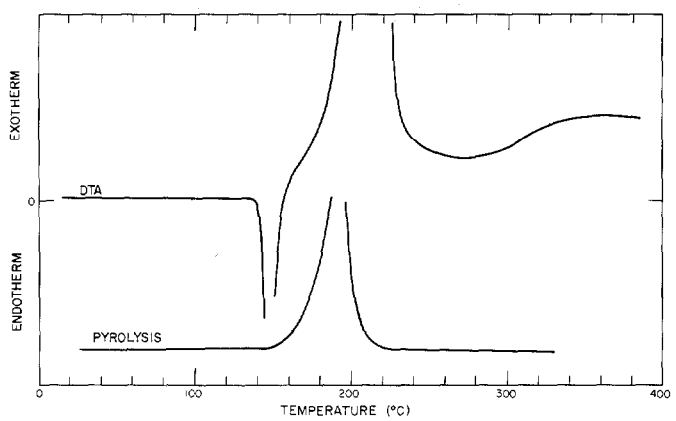

Fig. 2. PETN DTA and pyrolysis test results.

6.2 Detonation Pressure.[15]

Density (g/cm^3)	Detonation Velocity ($mm/\mu s$)	Detonation Pressure (GPa)
1.67	7.975	31

6.3 Cylinder Test Results.[16]

Density (g/cm^3)	Detonation Velocity ($mm/\mu s$)	Cylinder Wall Velocity ($mm/\mu s$) at	
		$R - R_o = 5$ mm	$R - R_o = 19$ mm
1.765	8.16	1.56	1.79

6.4 Plate Dent Test Results.[17]

Density (g/cm^3)	Dent Depth (mm)	Charge Height (mm)
1.670	9.80	---
1.665	9.75	203

7. SHOCK INITIATION PROPERTIES

7.1 Gap Test Results.[18]

Small Scale	
Density (g/cm^3)	G_{50} (mm)
1.757	5.21

7.2 Wedge Test Results.

Density (g/cm^3)	Distance, x*, and Time, t*, to Detonation (mm and μs)	Valid Pressure Range (GPa)
1.4	$\log P = (0.14 \pm 0.03) - (0.4 \pm 0.05) \log x^*$ $\log P = (0.04 \pm 0.02) - (0.33 \pm 0.04) \log t^*,$	$0.66 < P < 0.99$
1.6	$\log P = (0.40 \pm 0.03) - (0.54 \pm 0.05) \log x^*$ $\log P = (0.18 \pm 0.02) - (0.44 \pm 0.09) \log t^*,$	$1.2 < P < 2.0$
1.72	$\log P = (0.61 \pm 0.03) - (0.49 \pm 0.05) \log x^*$ $\log P = (0.34 \pm 0.02) - (0.50 \pm 0.09) \log t^*,$	$1.7 < P < 3.9$
1.75	$\log P = (0.57 \pm 0.04) - (0.41 \pm 0.06) \log x^*$ $\log P = (0.33 \pm 0.02) - (0.22 \pm 0.16) \log t^*,$	$1.7 < P < 2.54$

where P = pressure in gigapascals.

7.3 Shock Hugoniots.

Density (g/cm^3)	Shock Hugoniot[19] (mm/μs)	Particle Velocity Range (mm/μs)
1.60	$U_s = 1.32 + 2.58\, U_p$	$0.1 < U_p < 0.7$
1.72	$U_s = 1.83 + 3.45\, U_p$	$0.1 < U_p < 0.7$
1.77	$U_s = 2.87 + 1.69\, U_p$	$0.5 < U_p < 1.5$
	Isothermal Hugoniot[20]	
1.774	$U_s = 2.24 + 2.95\, U_p$ $-0.605\, U_p^2,$	$U_p < 1.0$
	$U_s = 2.81 + 1.75\, U_p,$	$U_p > 1.0$

where U_s = shock velocity
and U_p = particle velocity.

8. SENSITIVITY

8.1 Drop Weight Impact Height.

Type Tool	H_{50} (cm)
12	12
12B	37

8.5 Spark Sensitivity.

Electrode	Lead Foil Thickness (mils)	Sample Size (mg)	Energy (J)	Occurrence of Explosion (%)
Brass	3	47.2	0.19	50
Brass	10	47.2	0.36	50
Steel	1	50.0	0.10	50
Steel	10	50.0	0.41	50

REFERENCES

1. T. Urbanski, *Chemistry and Technology of Explosives,* Vol. II (Pergamon Press, Oxford, 1965).

2. Committee on Threshold Limit Values, *Documentation of Threshold Limit Values,* 3rd Ed. (American Conference of Governmental Industrial Hygienists, Cincinnati, Ohio, 1971).

3. T. L. Davis, *The Chemistry of Powder and Explosives* (John Wiley and Sons, Inc., New York, 1941).

4. *Code of Federal Regulations, 49, Transportation Parts 100-199, Rev. 12-1-76* (Office of the Federal Register, General Services Administration, Washington, DC, 1976).

5. US Army Materiel Command, Regulation No. AMCR 385-100 (1977).

6. R. N. Roberts and R. H. Dinegar, Journal of Physical Chemistry **62,** 1009-1011 (1958).

7. H. H. Cady and A. C. Larson, Acta Crystallographica **31,** 1864-1869 (1975).

8. A. T. Blomquist, National Defense Research Committee report NDRC-B-3014 (August 1944).

9. R. N. Rogers and R. H. Dinegar, Thermochimica Acta **3,** 367-378 (1972).

10. G. Edwards, Transactions of the Faraday Society **49,** 152-154 (1953).

11. F. T. Crimmons, Lawrence Livermore Laboratory report UCRL-50704 (1969).

12. H. H. Cady, Journal of Chemical and Engineering Data **17,** 369-371 (1972).

13. R. N. Rogers, Thermochimica Acta **11,** 131-139 (1975).

14. G. H. Messerly, Explosives Research Laboratory report OSRD-1219 (February 1943).

15. W. C. Davis, B. G. Craig, and J. B. Ramsay, Physics of Fluids **8,** 2169-2182 (1965).

16. J. W. Kury, H. C. Hornig, E. L. Lee, J. L. McDonnel, D. L. Ornellas, M. Finger, F. M. Strange, and M. L. Wilkins, *Proceedings—Fourth Symposium (International) on Detonation, White Oak, Maryland, October 12-15, 1965* (Office of Naval Research, Department of the Navy, ACR-126, 1965), pp. 3-12.

17. L. C. Smith, Explosivstoffe **15,** 106-130 (1967).

18. Manuel J. Urizar, Suzanne W. Peterson, and Louis C. Smith, Los Alamos Scientific Laboratory report LA-7193-MS (April 1978).

19. Dante Stirpe, James O. Johnson, and Jerry Wackerle, Journal of Applied Physics **41,** 3884-3893 (1970).

20. Bart Olinger, P. M. Halleck, and Howard H. Cady, Journal of Chemical Physics **62,** 4480-4483 (1975).

RDX

1. GENERAL PROPERTIES

1.1 Chemical and Physical Description.[1,2] The British first used "RDX" to identify a new chemical explosive developed for use during World War II. During its development, the new explosive was called "Research Department Explosive."

RDX, $C_3H_6N_6O_6$, is a colorless polycrystalline material. It is also known as hexahydro-1,3,5-trinitro-s-triazine, cyclotrimethylenetrinitramine, 1,3,5-trinitro-1,3,5-triazocyclohexane, Hexogen, cyclonite, and T4.

1.2 Common Use. RDX is used extensively as the base charge in detonators. Its most common uses are as an ingredient in castable TNT-based binary explosives such as cyclotols and Comp B, and as the primary ingredient in plastic-bonded explosives or plastic explosives such as Composition A and Composition C. Either the castable or plastic-coated mixture is used as the explosive fill in almost all types of munitions.

1.3 Toxicity.[3] Workers who inhaled RDX dust for several months have become unconscious and have suffered loss of reflexes. The suggested maximum permissible airborne concentration of RDX is 1.5 mg/m^3.

2. MANUFACTURE AND PROCUREMENT

2.1 Manufacture.[2] RDX is manufactured in two ways. In the British process, hexamethylenetetramine is nitrated directly; in the Bachmann process, it is nitrated by a mixture of nitric acid, ammonium nitrate, acetic anhydride, and acetic acid. The former process produces relatively pure RDX; the latter has been

developed into a continuous high-yield process that gives about 10% HMX as an impurity. The crude RDX is purified by washing it with water and recrystallizing it from either acetone or cyclohexanone.

2.2 Procurement. RDX is purchased from the US Army Armament Readiness Command under Military Specification MIL-R-398C Amendment 3, dated August 14, 1973.

2.3 Shipping.[4] RDX is shipped as a Class A explosive and must be shipped wet with not less than 10% water.

2.4 Storage.[5] RDX may be stored dry in Compatibility Group A or wet in Compatibility Group D. Wet or dry, it is in Storage Class 1.1.

3. CHEMICAL PROPERTIES

3.1 Structural Formula.

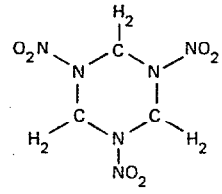

$C_3H_6N_6O_6$

3.2 Molecular Weight. 222.13

3.3 Solubility.

Solvent	Grams of RDX Dissolved/ 100 g of Solvent		
	20°C	40°C	60°C
Acetic acid			
99.6%	0.46	0.56	1.22
71.0%	0.22	0.37	0.74
Acetone	6.81	10.34	---
Isoamyl alcohol	0.026	0.060	0.210
Benzene	0.045	0.085	0.195
Chlorobenzene	0.33	0.554	---
Cyclohexanone	4.94	9.20	13.9
Dimethylformamide	---	41.5	60.6
Ethanol	0.12	0.24	0.58
Methyl acetate	2.9	4.1	---
Methylcyclohexanone	6.81	10.34	---
Methyl ethyl ketone	3.23	---	---
Toluene	0.020	0.050	0.125
Trichloroethylene	0.20	0.24	---
Water	0.005	0.0127	0.03

4. PHYSICAL PROPERTIES

4.1 Crystal Structure.[6,7] RDX is orthorhombic. It also has a very unstable polymorph that has been isolated only in very small quantities for very short periods during fusion.

The cell parameters of orthorhombic form are given.

Cell Parameters	RDX
Unit cell edge length (Å)	
a	13.18
b	11.57
c	10.71
Molecules per unit cell	8

4.2 Density.[7]

Crystal

Method of Determination	State	Temperature (°C)	Density (g/cm³)
X-ray data	Solid	---	1.806
Direct measurement	Solid	22.8	1.799

Pressed Charges

RDX powder can be pressed to various densities. The pressures required to produce a given density are as follows.

Pressure (psi)	Density[a] (g/cm³)
5 000	1.52
10 000	1.60
20 000	1.68
30 000	1.70

[a]These data are typical and will vary with particle-size distribution, time under pressure, and temperature.

4.3 Infrared Spectrum. See Fig. 1.

4.4 Refractive Index.[6] In light whose wave length varied between 4470 and 6680 Å, the following refractive indices have been reported.

	Refractive Index
α	1.597-1.572
β	1.620-1.591
γ	1.624-1.596

5. THERMAL PROPERTIES

5.1 Phase Changes.[7,8]

Type	Temperature (°C)	Latent Heat (cal/g)	Latent Heat (kcal/mole)
Solid-to-liquid	204.1	35.5	7.89
Solid-to-gas[a] (vaporization)	---	---	31.1

[a]Computed from vapor pressure data taken at 55-98°C.

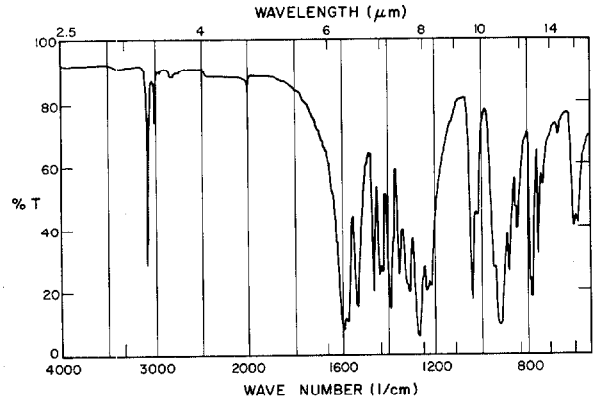

Fig. 1. Infrared spectrum.

5.2 Vapor Pressure.[8]

Temperature (°C)	Vapor Pressure (mm Hg × 10^7)
55.7	3.24-3.5
62.6	7.14-8.6
78.2	69.30-78.7
97.7	667-735

A least squares fit to these data gives the following.

$\log_{10} P(\text{mm Hg}) = 14.18 - 31\,100/4.576\,T(K)$,

where P = vapor pressure in millimeters of mercury

and T = temperature in Kelvin.

5.3 Heat Capacity.

Heat Capacity at Constant Pressure (cal/g-°C)	Temperature Range (°C)
$0.232 + 7.5 \times 10^{-7}\,T$	$37 < T < 167$

5.5 Coefficient of Thermal Expansion.[9]

Coefficient of Expansion (1/°C)	Temperature Range (°C)
$18.33 \times 10^{-5} + 3.625 \times 10^{-7}\,T + 5.48 \times 10^{-10}\,T^2$	$-100 < T < 135$

5.6 Heats of Combustion and Formation at 25°C.[10]

ΔH_c^o	ΔH_f^o
−501.8 kcal/mole	14.7 kcal/mole

5.7 Thermal Decomposition Kinetics.[11]

Decomposition energy	500 cal/g
Activation energy	47.1 kcal/mole
Pre-exponential factor	2.02×10^{18}/s

5.8 Other Thermal Stability Test Results.

Test	Results
Vacuum	0.1-0.3 ml/g of gas evolved after 48 h at 120°C
DTA and pyrolysis	See Fig. 2
Critical temperature, Tm	217°C
Charge radius, a	3.5 mm
Density, ρ	1.72 g/cm^3

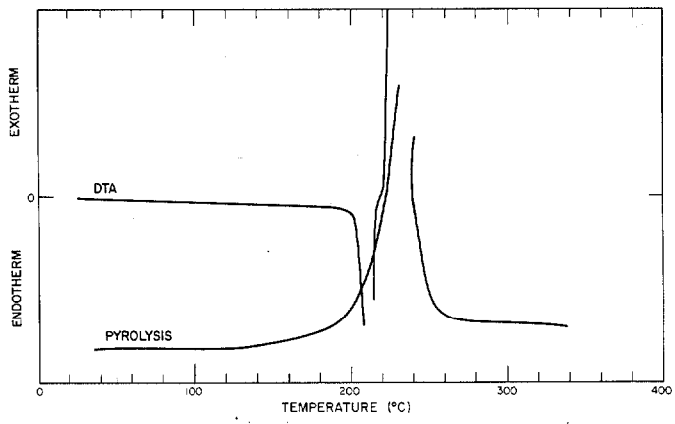

Fig. 2. RDX DTA and pyrolysis test results.

6. DETONATION PROPERTIES

6.1 Detonation Velocity.

Effect of Density

$D = 2660 + 3400\,\rho_o$,

where D = detonation velocity in meters per second

and ρ_o = density in grams per cubic centimeter.

6.2 Detonation Pressure.[12]

Density (g/cm^3)	Detonation Velocity ($mm/\mu s$)	Detonation Pressure (GPa)
1.767 ± 0.011	8.639 ± 0.041	33.79 ± 0.31

6.4 Plate Dent Test Results.

Charge Diameter (mm)	Density (g/cm^3)	Dent Depth (mm)	Charge Height (mm)
41.3	1.754	10.35	203
41.3	1.744	10.14	203
41.3	1.537	8.20	203

7. SHOCK INITIATION

7.1 Gap Test Results.[13]

Density (g/cm³)	Gap_{50} (mm)	L_{95} (mm)
	Large Scale	
1.09	7.02	0.10
1.750	6.17	0.01
	Small Scale	
1.00[a]	7.82	0.15
1.11[b]	8.86	0.15
1.704	0.50	---
1.735	5.18	0.18
1.752	0.36	0.01

[a]Median RDX particle diameter is ~110 μm.

[b]Median RDX particle diameter is ~25 μm.

7.3 Shock Hugoniot.[14]

Density (g/cm³)	Shock Hugoniot[a] (mm/μs)
1.799	$U_s = 2.78 + 1.9\,U_p$

[a]Computed from the isothermal volume compression data. Two RDX phases were observed in the course of determining its isothermal volume compression. The shock Hugoniot tabulated is that for the orthorhombic form described previously in Sec. 4.1. Another RDX polymorph, Form III, occurs at pressures of 4.4 GPa. The volume change between the two polymorphs was about 1.6% (from 0.4651 to 0.4566 cm³/g). The isothermal Hugoniots of the two polymorphs were

RDX(I) $U_{st} = 2.68 + 1.9\,U_{pt}$
and
RDX(II) $U_{st} = 2.49 + 1.8\,U_{pt}$,
where the subscript "t" denotes isothermal conditions.

8. SENSITIVITY

8.1 Drop Weight Impact Height.

Tool Type	H_{50} (cm)
12	22
12B	41

8.5 Spark Sensitivity.

Electrode	Lead Foil Thickness (mils)	Sample Size (mg)	Energy (J)	Occurrence of Explosion (%)
Brass	3	61.1	0.22	50
Brass	10	61.1	0.55	50
Steel	1	64.0	0.12	50
Steel	10	64.0	0.87	50

REFERENCES

1. J. E. Ablard, US Naval Ordnance Laboratory report NAVSEA-03-TR-058 (July 1977).

2. T. Urbanski, *The Chemistry and Technology of Explosives* 3rd Ed. (Pergamon Press, Oxford, 1965).

3. C. R. Buck and S. E. Wilson, Jr., US Army report USEHA-32-049 (1975).

4. *Code of Federal Regulations, 49, Transportation Parts 100-199, Rev. 12-1-76* (Office of the Federal Register, General Services Administration, Washington, DC, 1976).

5. US Army Materiel Command, Regulation No. AMCR-385-100 (1977).

6. W. C. McCrone, Analytical Chemistry **22,** (7), 954-955 (1950).

7. C. S. Choi and E. Prince, Acta Crystallographica **B28,** 2857-2862 (1972).

8. J. M. Rosen and C. Dickenson, Naval Ordnance Laboratory report NOLTR-69-67 (April 1969).

9. H. H. Cady, Journal of Chemical and Engineering Data **17,** (3), 369-371 (1972).

10. O. H. Johnson, Naval Ordnance Laboratory report NAVORD-4371 (October 1956).

11. R. N. Rogers, Thermochimica Acta **11,** 131-139 (1975).

12. W. E. Deal, Journal of Chemical Physics **27,** (1), 796-800 (1957).

13. Manuel J. Urizar, Suzanne W. Peterson, and Louis C. Smith, Los Alamos Scientific Laboratory report LA-7193-MS (April 1978).

14. Bart Olinger, Brad Roof, and Howard Cady, Symposium (International) on High Dynamic Pressures, Paris, France (August 1978).

TATB

1. GENERAL PROPERTIES

1.1 Chemical and Physical Description. TATB (1,3,5-trinitrobenzene), $C_6H_6N_6O_6$, is a yellow polycrystalline material. Exposure to sunlight or UV light turns it light green, and prolonged exposure eventually turns it dark brown to black.

1.2 Common Use. The excellent thermal stability and extreme resistance to accidental initiation by impact or shock make TATB useful for special applications. To be used effectively, it is generally coated with a thermoplastic polymer and pressed into desired shapes.

1.3 Toxicity. The maximum permissible concentration of TATB in air is 1.5 mg/m^3. It was not mutagenic when tested in five strains of *Salmonella typhimurium* and in *Escherichia coli* strain WP.

2. MANUFACTURE AND PROCUREMENT

2.1 Manufacture.[1] TATB is synthesized by reacting 1,3,5,-trichlorobenzene with SO_3 (30% oleum) and sodium nitrate to give 1,3,5-trichloro-2,4,6-trinitrobenzene. The reaction mixture is then quenched in a large volume of ice, and the 1,3,5,-trichloro-2,4,6-trinitrobenzene is recovered by filtration and reacted with ammonia gas in the presence of toluene to give TATB.

2.2 Procurement. There is no dedicated DoD or DOE facility for TATB manufacture. It can be procured, on special order, from a few chemical companies in the United States which have facilities for synthesizing energetic materials. The DOE procures TATB under LASL material specification 13Y-188025, dated August 23, 1978.

2.3 Shipping.[2] TATB is shipped dry or wet as a Class A explosive.

2.4 Storage.[3] TATB is stored dry or wet in Compatibility Group D, Storage Class 1.1.

3. CHEMICAL PROPERTIES

3.1 Structural Formula.

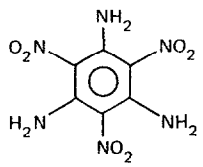

$C_6H_6N_6O_6$

3.2 Molecular Weight. 258.18

3.3 Solubility.[4] TATB is practically insoluble in all organic solvents, but it is soluble in some superacids.

Solvent	Solubility[a] (ppm)
Methanesulfonic acid	820
Hexamethylphosphoric triamide	150
Ethanesulfonic acid	120
Dimethylsulfoxide	100
Hexafluoroacetone sesquihydrate	68
N-methyl-2-pyrrolidinone	58
N, N-dimethylacetamide	27
Dimethylformamide	26

[a]Temperature not reported.

TATB solubility in sulfuric acid and water mixtures.

Acid (vol%)	Maximum Quantity Dissolved (grams of TATB/100 ml)
50	<0.02
66.7	<0.02
80	0.24
85	0.32
87.5	>1.28
90	3.84
100	>24.0

4. PHYSICAL PROPERTIES

4.1 Crystal Structure.[5] Only one TATB polymorph has been observed. The triclinic unit cell parameters are given.

Cell Parameters	TATB
Length of unit cell edge (Å)	
a	9.010 ± 0.003
b	9.028 ± 0.003
c	6.812 ± 0.003
Angle (°)	
α	108.590 ± 0.02
β	91.820 ± 0.03
γ	119.970 ± 0.01
Molecules per unit cell	2

4.2 Density.

Crystal

Method of Determination	State	Temperature (°C)	Density (g/cm³)
X-ray	Solid	23	1.937
Direct measurement	Solid	23	1.93 ± 0.01

Pressed

TATB powder at 120°C can be pressed to a density of 1.860 g/cm³ at a pressure of 30 000 psi.

4.3 Infrared Spectrum. See Fig. 1.

4.4 Refractive Index.[5] TATB crystals are pleochroic, being colorless parallel to the X-axis and yellow in the Y-Z plane. They are anisotropic. The indices of refraction are $N_x = 1.45$, $N_y = 2.3$, and $N_z = 3.1$.

5. THERMAL PROPERTIES

5.1 Phase Change.

Type	Temperature (°C)	Latent Heat (kcal/mole)
Solid-to-liquid[a]	448-449	---
Solid-to-gas[b] (vaporization)	---	40.21

[a]Determined on a hot bar melting apparatus. Rapid decomposition was observed in both solid and liquid states.

[b]Determined from the vapor pressure data listed in Section 5.2.

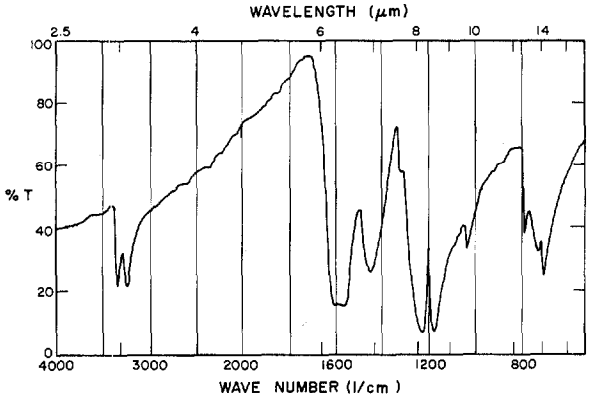

Fig. 1. Infrared spectrum.

5.2 Vapor Pressure.[6]

Temperature (°C)	Vapor Pressure (mm Hg × 10^7)
129.3	4.06-4.10
136.2	6.36-6.50
150.0	10.41-11.02
161.4	29.00-29.28
166.4	42.09
177.3	49.16

A least squares fit to the data gives

$\log_{10} P = 14.73 - 402\,100/4.576\,T(K)$

5.3 Heat Capacity.

Heat Capacity at Constant Pressure (cal/g-°C)
$0.215 + 1.324 \times 10^{-3} T$

5.4 Thermal Conductivity.

Conductivity (cal/s-cm-°C)
1.3×10^{-3}

5.5 Coefficient of Thermal Expansion.[7] The TATB crystals are extremely anisotropic. The linear coefficient of expansion in the three unit cell directions has been estimated from the following x-ray data.

Cell Direction	Coefficient of Expansion (1/°C)	Temperature Range (°C)
a	9.50×10^{-6}	−60 to +100
b	2.10×10^{-5}	−60 to +100
c	2.25×10^{-4}	−60 to +100

The volume coefficient of expansion is estimated from the same x-ray data.

Coefficient of Expansion (1/°C)	Temperature Range (°C)
2.36×10^{-4}	−60 to +10
3.67×10^{-4}	10 to 100

5.6 Heats of Combustion and Formation at 25°C.[8]

ΔH_c°	ΔH_f°
−735.9 kcal/mole	−33.4 kcal/mole

5.7 Thermal Decomposition Kinetics.[9]

Decomposition energy	600 cal/g
Activation energy	59.9 kcal/mole
Pre-exponential factor	3.18×10^{19}/s

5.8 Other Thermal Stability Test Results.

Test	Results
Vacuum	0.0-0.2 ml/g of gas evolved after 48 h at 120°C
DTA and pyrolysis	See Fig. 2
Critical temperature, Tm	347°C
Charge radius, a	3.3 mm
Density, ρ	1.84 g/cm^3

6. DETONATION PROPERTIES

6.1 Detonation Velocity.[10]

Density (g/cm^3)	Charge Diameter (mm)	Average Detonation Velocity (mm/μs)	Confinement
1.860	25.35	7.619 ± 0.001	Copper tube with a 2.54-mm wall

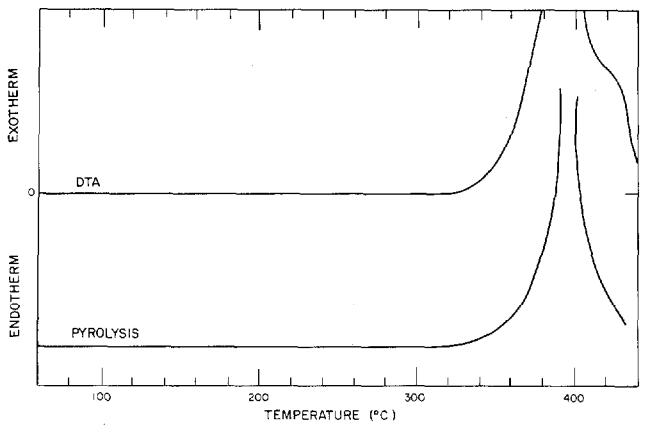

Fig. 2. TATB DTA and pyrolysis test results.

Effect of Densities

Density affects the infinite diameter detonation velocity as follows:

$D = 2.480 + 2.852\,\rho_0$,

where D = infinite diameter velocity in millimeters per microseconds,

and ρ_0 = density in grams per cubic centimeter.

Effect of Charge Diameter

Charge diameter affects the detonation velocity of unconfined TATB pressed to a density of 1.860 g/cm³ as follows:

$D = 7.758 - 0.472/d$ for $d \geq 4$ mm

where D = the detonation velocity in millimeters per microsecond,

and d = charge diameter in millimeters.

Failure Diameter

The failure diameter of TATB pressed to a density of 1.860 g/cm³ is 4.0 mm.

6.2 Detonation Pressure.[11]

Density (g/cm³)	Detonation Velocity (mm/μs)	Detonation Pressure (GPa)
1.847	7.66	25.9
1.50	---	17.5

6.3 Cylinder Test Results.

Density (g/cm³)	Cylinder Wall Velocity (mm/μs) at	
	R − R_o = 5 mm	R − R_o = 19 mm
1.860	1.268	1.446

6.4 Plate Dent Test Results.

Charge Diameter (mm)	Density (g/cm³)	Dent Depth (mm)	Charge Height (mm)
41.3	1.87	8.31	203

7. SHOCK INITIATION PROPERTIES

7.1 Gap Test Results.

Density (g/cm³)	G_{50} (mm)	L_{95} (mm)
	Large Scale	
1.870	21.92	0.43
	Small Scale	
1.872	0.127	0.10

7.2 Wedge Test Results.

Density (g/cm³)	Distance, x*, and Time, t*, to Detonation (mm and μs)	Pressure Range (GPa)
1.714	$\log P = (1.09 \pm 0.02) - (0.41 \pm 0.17) \log x^*$ $\log P = (0.8 \pm 0.07) - (0.32 \pm 0.12) \log t^*$,	$3.27 < P < 5.64$
1.841	$\log P = (1.39 \pm 0.07) - (0.52 \pm 0.07) \log x^*$ $\log P = (1.01 \pm 0.02) - (0.46 \pm 0.05) \log t^*$,	$5.93 < P < 16.5$
1.876	$\log P = (1.42 \pm 0.02) - (0.40 \pm 0.03) \log x^*$ $\log P = (1.11 \pm 0.01) - (0.36 \pm 0.03) \log t^*$,	$11.4 < P < 16.22$

where P = pressure in gigapascals.

7.3 Shock Hugoniots.[11-13] A number of TATB shock Hugoniots at various densities have been determined using different experimental techniques.

Density (g/cm³)	Shock Hugoniot (mm/μs)	Particle Velocity Range (mm/μs)	Technique
1.847	$U_s = 2.34 + 2.316\,U_p$	$0 < U_p < 1.5$	a
1.876	$U_s = 1.46 + 3.68\,U_p$ $U_s = 2.037 + 2.497\,U_p$	$0 < U_p < 0.48$ $0.48 < U_p < 1.54$	a
	$U_s = (1.663 \pm 0.123) + (2.827 \pm 0.132)\,U_p$	$0.15 < U_p < 1.47$	a
1.937	$U_s = 1.73 + 6.56\,U_p - 4.14\,U_p^2$ $U_s = 2.93 + 1.69\,U_p$	$0 < U_p < 0.35$ $0.35 < U_p$	b

[a]Direct measurement of shock velocity.
[b]Isothermal compression x-ray computation.

7.4 Minimum Priming Charge.[14]

Density (g/cm³)	W_{50} (mg of XTX 8003)	Remarks
1.876	$>1.53 \times 10^4$	Pressed charge

8. SENSITIVITY

8.1 Drop Weight Impact Height.

Tool Type	H_{50} (cm)
12	>320
12B	>320

8.4 Susan Test Results.

Projectile Impact Velocity (m/s)	Relative Energy Release[a]
500	Threshold for reaction

[a]Measured in terms of overpressure relative to the overpressure achieved in a detonation.

8.5 Spark Sensitivity.

Lead Foil Thickness (mils)	Sample Size (mg)	Energy (J)	Occurrence of Explosion (%)
3	31	4.25	0
10	31	18.1	0

9. MECHANICAL PROPERTIES

9.2 Tensile Strength and Modulus.

Temperature (°C)	Density (g/cm^3)	Ultimate Tensile Strength (psi)	Tensile Modulus ($psi \times 10^{-5}$)
24	1.864	370	6.91

9.3 Compressive Strength and Modulus.

Density (g/cm^3)	Ultimate Compressive Strength (psi)	Compressive Modulus ($psi \times 10^{-5}$)
1.804	1360	2.62

REFERENCES

1. T. M Benziger and R. K. Rohwer, Los Alamos Scientific Laboratory report LA-3632 (January 1967).

2. *Code of Federal Regulations, 49, Transportation Parts 100-199, Rev. 12-1-76,* (Office of the Federal Register, General Services Administration, Washington, DC, 1976.)

3. US Army Materiel Command, Regulation No. AMCR-385-100 (1977).

4. W. Selig, Lawrence Livermore Laboratory report UCID-17412 (April 1977).

5. H. H. Cady and A. C. Larson, Acta Crystallographica **18,** 485-496 (1965).

6. J. M. Rosen and C. Dickenson, US Naval Ordnance Laboratory report NOLTR 69-67 (April 1969).

7. J. R. Kolb, Lawrence Livermore Laboratory, private communication (1978).

8. Prince E. Rouse, Journal of Chemical and Engineering Data **21,** 16-20 (1976).

9. R. N. Rogers, Thermochimica Acta **11,** 131-139 (1975).

10. A. W. Campbell, Los Alamos Scientific Laboratory, private communication (1975).

11. N. L. Coleburn and T. P. Liddiard, Journal of Chemical Physics **44,** 1929-1936 (1966).

12. B. G. Craig, Los Alamos Scientific Laboratory, private communication (1978).

13. B. W. Olinger, Los Alamos Scientific Laboratory, private communication (1978).

14. Manuel J. Urizar, Suzanne W. Peterson, and Louis C. Smith, Los Alamos Scientific Laboratory report LA-7193-MS (April 1978).

TETRYL

1. GENERAL PROPERTIES

1.1 Chemical and Physical Description.[1] Tetryl (2,4,6-trinitrophenylmethylnitramine), $C_7H_5N_5O_8$ is a light yellow crystalline solid. Other accepted names are 2,4,6- trinitro-N-methylaniline; picrylmethylnitramine; Tetrylite; Tetralite; Tetralita; and C. E.

1.2 Common Use. Tetryl is no longer commonly used as a US military explosive. It was used as a booster explosive, in binary mixtures of TNT and tetryl (Tetratols), and as the base charge in detonators.

1.3 Toxicity.[2] Tetryl can yellow human skin and sometimes cause dermatitis. Some workers' eyes and nasal membranes may become irritated, which can lead to excessive sneezing and nosebleeds. The suggested maximum permissible concentration of tetryl dust in air is 1.5 mg/m^3.

2. MANUFACTURE AND PROCUREMENT

2.1 Manufacture.[3] Two processes have been used extensively in tetryl production. In the first, N,N-dimethylaniline is dissolved in concentrated sulfuric acid and the mixture is run slowly into nitric acid. Cooling precipitates the crude tetryl, which is then purified by washing with water and recrystallization from benzene or

acetone. In the second process, methylamine is reacted with 2,4- or 2,6-dinitrochlorobenzene to dinitrophenyl methylamine, which is then nitrated to tetryl.

2.2 Procurement. Purchase is under Joint Army-Navy Specification MIL-T-339C, dated February 9, 1973.

2.3 Shipping.[4] Tetryl may be shipped dry as a Class A explosive.

2.4 Storage.[5] Tetryl is stored dry in Compatibility Group D, Storage Class 1.1.

3. CHEMICAL PROPERTIES

3.1 Structural Formula.

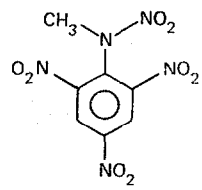

$C_7H_5N_5O_8$

3.2 Molecular Weight. 287.15

3.3 Solubility.[6]

Solvent	Grams of Tetryl Dissolved/100 g of solvent			
	20°C	50°C	60°C	75°C
Water	0.0075	0.0195	0.035	0.066
Ethanol (95 vol%)	0.563	1.72	2.64	5.33
Carbon tetrachloride	0.025	0.095	0.154	0.297
Chloroform	0.57	1.78	2.65	---
Ethylene chloride	3.8	12.0	18.8	45.0
Carbon disulfide	0.021	---	---	---
Ether	0.418	---	---	---

4. PHYSICAL PROPERTIES

4.1 Crystal Structure.[7] The tetryl crystal is monoclinic and has the following cell parameters.

Cell Parameters	
Length of unit cell edge (Å)	
a	14.129
b	7.374
c	10.614
Angle β	95.07°
Molecules per unit cell	4

4.2 Density.[7,8]

Method of Determination	State	Temperature (°C)	Density (g/cm³)
X-ray data	Solid	21	1.731
Flotation	Solid	21	1.74

Pressed Tetryl

Compression usually gives the following densities.

Pressure (psi)	Density (g/cm³)
3 000	1.40
5 000	1.47
10 000	1.57
20 000	1.67
30 000	1.71

4.3 Infrared Spectrum. See Fig. 1.

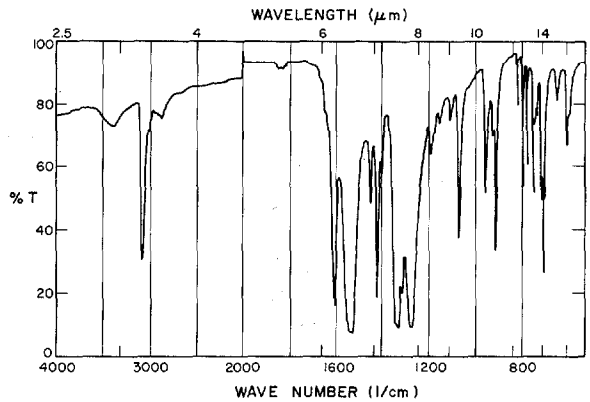

Fig. 1. Infrared spectrum.

4.4 Refractive Indices.[9]

alpha	1.546
beta	1.632

5. THERMAL PROPERTIES

5.1 Phase Changes.[8]

Type	Temperature (°C)	Latent Heat (cal/g)	Latent Heat (kcal/mole)
Solid-to-liquid	129.45	22.2	6.37

5.3 Heat Capacity.[8]

Heat Capacity at Constant Pressure (cal/g-°C)	Temperature Range (°C)
$0.211 + 2.6 \times 10^{-4} T$	$-100 < T < 100$

5.4 Thermal Conductivity.[8]

Density (g/cm^3)	Conductivity (cal/s−cm−°C)
1.53	6.83×10^{-4}
1.39	5.81×10^{-4}

5.6 Heats of Combustion and Formation at 25°C.[10]

ΔH_c^o	ΔH_f^o
−836.8 kcal/mole	7.6 kcal/mole

5.7 Thermal Decomposition Kinetics.[11]

Activation energy	38.4 k cal/mole
Frequency factor	2.51×10^{15}/s

5.8 Other Thermal Stability Test Results.

Test	Results
Vacuum stability	0.4-1.0 ml/g of gas evolved after 48 h at 120°C
DTA and pyrolysis	See Fig. 2
Critical temperature, Tm	187°C

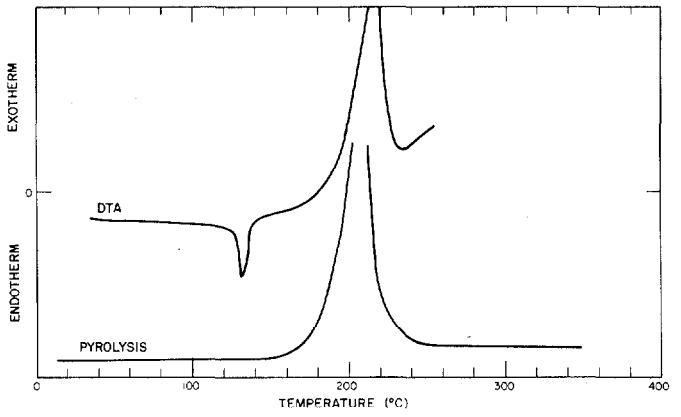

Fig. 2. Tetryl DTA and pyrolysis test results.

6. DETONATION PROPERTIES

6.1 Detonation Velocity.

Effect of Density

$D = 2.742 + 2.935\,\rho_o \qquad (1.3 \leq \rho_o \leq 1.69)$,

where D = detonation velocity in millimeters per microsecond,

and ρ_o = charge density in grams per cubic centimeter.

6.2 Detonation Pressure.[12]

Density (g/cm^3)	Detonation Pressure (GPa)
1.614	22.64

6.4 Plate Dent Test Results.

Charge Diameter (mm)	Density (g/cm^3)	Dent Depth (mm)	Charge Height (mm)
41.3	1.681	8.10	203

7. SHOCK INITIATION PROPERTIES

7.1 Gap Test Results.[13]

Density (g/cm^3)	G_{50} (mm)	L_{95} (mm)
	Large Scale	
0.85	69.21	0.61
1.666	60.60	0.63
1.682	59.38	0.18
	Small Scale	
0.93	7.44	0.05
1.678	4.04	0.20
1.684	3.83	0.30

7.2 Wedge Test Results.

Density (g/cm^3)	Distance, x*, and Time, t*, to Detonation (mm and μs)	Pressure Range (GPa)
1.70	$\log P = (0.79 \pm 0.01) - (0.42 \pm 0.01) \log x^*$ $\log P = (0.55 \pm 0.01) - (0.39 \pm 0.01) \log t^*$,	$2.22 < P < 8.53$
1.60	$\log P = (0.73 \pm 0.01) - (0.65 \pm 0.01) \log x^*$ $\log P = (0.4 \pm 0.01) - (0.55 \pm 0.01) \log t^*$,	$1.08 < P < 8.02$
1.50	$\log P = (0.75 \pm 0.01) - (0.81 \pm 0.01) \log x^*$ $\log P = (0.35 \pm 0.01) - (0.64 \pm 0.01) \log t^*$,	$0.62 < P < 7.09$
1.40	$\log P = (0.84 \pm 0.01) - (0.99 \pm 0.02) \log x^*$ $\log P = (0.35 \pm 0.01) - (0.75 \pm 0.01) \log t^*$,	$0.51 < P < 6.84$
1.30	$\log P = (0.87 \pm 0.05) - (1.11 \pm 0.07) \log x^*$ $\log P = (0.33 \pm 0.02) - (0.83 \pm 0.03) \log t^*$,	$0.37 < P < 6.91$

where P = pressure in gigapascals.

7.3 Shock Hugoniots.[14]

Density (g/cm^3)	Shock Hugoniot (mm/μs)	Particle Velocity Range (mm/μs)
1.70	$U_s = 2.476 + 1.416\,U_p$	$0.428 < U_p < 1.195$
1.60	$U_s = 2.362 + 1.528\,U_p - 0.255/U_p$	$0.324 < U_p < 1.232$
1.50	$U_s = 2.167 + 1.662\,U_p - 0.341/U_p$	$0.287 < U_p < 1.231$
1.40	$U_s = 1.611 + 1.966\,U_p - 0.278/U_p$	$0.297 < U_p < 1.253$
1.30	$U_s = 2.162 + 1.427\,U_p - 0.499/U_p$	$0.296 < U_p < 1.399$

7.4 Minimum Priming Charge.[13]

Density (g/cm^3)	W_{50} (mg of XTX 8003)
1.692	1.5

7.5 Detonation Failure Thickness.[13]

Density (g/cm^3)	Failure Thickness (mm)	L_{95} (mm)
1.684	0.267	0.079

8. SENSITIVITY

8.1 Drop Weight Impact Height.

Tool Type	H_{50} (cm)
12	420
12B	490

8.5 Spark Sensitivity.

Electrode	Lead Foil Thickness (mils)	Sample Size (mg)	Energy (J)	Occurrence of Explosion (%)
Brass	3	48.2	0.54	50
Brass	10	48.2	2.79	50
Steel	1	54.0	0.19	50
Steel	10	54.0	3.83	50

REFERENCES

1. T. Urbanski, *The Chemistry and Technology of Explosives,* Vol. III, (Pergamon Press, Oxford, England, 1965).

2. Committee on Threshold Limit Values, *Documentation of Threshold Limit Values,* 3rd Ed. (American Conference of Governmental Industrial Hygienists, 1014 Broadway, Cincinnati, Ohio, 1971).

3. T. L. Davis, *The Chemistry of Powder and Explosives* (John Wiley and Sons, Inc., New York, 1941).

4. *Code of Federal Regulations, 49, Transportation Parts 100-199, Rev. 12-1-76* (Office of the Federal Register, General Services Administration, Washington, DC, 1976).

5. US Army Materiel Command, Regulation No. 385-100 (1977).

6. Dept. of the Army and Air Force, Technical Manual 9-1300-214 TO11A-1-34 (November 1967).

7. H. H. Cady, Acta Crystallographica **23** (2), 601-609 (1967).

8. W. R. Tomlinson, Picatinny Arsenal Technical report 1740 (April 1958).

9. A. T. Blomquist, National Defense Research Committee report NDRC-B-3014 (August 1944).

10. G. Stegeman, National Defense Research Committee report OSRD 5603 (July 1945).

11. E. K. Rideal and A. J. B. Robertson, Proceedings of the Royal Society of London, Series A, **195**, 135-150 (1948).

12. N. L. Coleburn, US Naval Ordnance Laboratory report NOLTR-64-58 (1964).

13. Manuel J. Urizar, Suzanne W. Peterson, and Louis C. Smith, Los Alamos Scientific Laboratory report LA-7193-MS (April 1978).

14. I. E. Lindstrom, Journal of Applied Physics **41**(1), 337-350 (1970).

TNT

1. GENERAL PROPERTIES

1.1 Chemical and Physical Description.[1] TNT (2,4,6-trinitrotoluene), $C_7H_5N_3O_6$, is a light yellow or buff crystalline solid. This isomer, also known as TNT in the United States, is the compound used in miltary explosives. TNT is also known by a variety of other names: Tolite in France; Tri, Trotyl, Tutol, Trinol, and Füllpulver 1902 in Germany; Tritolo in Italy; Tol, Trotil, TNT in the Union of Soviet Socialist Republics; and TNT in the United Kingdom.

1.2 Common Use. TNT is the most common military explosive because of its ease of manufacture and its suitability for melt loading, either as the pure explosive or as binary mixtures. The most common binary mixtures are cyclotols (mixtures with RDX), octols (mixtures with HMX), amatols (mixtures with ammonium nitrate), and tritonals (mixtures with aluminum).

1.3 Toxicity.[2] Inhaled TNT vapor or dust may irritate mucous membranes and cause sneezing, coughing, and sore throat. TNT may produce toxic hepatitis and aplastic anemia. TNT yellows the exposed skin, hair, and nails of workers. Dermatitis, erythema, papules, and itchy eczema can be severe. Ingestion of 1-2 g of TNT is estimated to be an acute fatal dose to humans. The suggested maximum permissible airborne dust concentration is 0.5 mg/m^3.

2. MANUFACTURE AND PROCUREMENT

2.1 Manufacture.[1] Toluene is nitrated to TNT in one, two, or three stages with a mixture of nitric and sulfuric acids. The crude TNT is purified by washing with a water solution of sodium sulfite (the Sellite process). The sulfite reacts with the 2,3,4- and 2,3,5-isomers of TNT to form water-soluble compounds, which are then removed.

2.2 Procurement. TNT is purchased from the US Army Armament Materiel Command under MIL-T-248C, dated November 8, 1974.

2.3 Shipping.[3] TNT may be shipped dry as a Class A explosive.

2.4 Storage.[4] TNT is stored dry in compatibility Group D, Storage Class 1.1.

3. CHEMICAL PROPERTIES

3.1 Structural Formula.

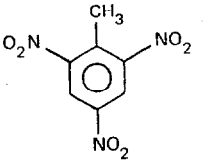

$C_7H_5N_3O_6$

3.2 Molecular Weight. 227.13

3.3 Solubility.[5]

Solvent	Grams of TNT Dissolved/100 g of Solvent		
	20°C	40°C	60°C
Acetone	109.0	228.0	600.0
Benzene	67.0	180.0	478.0
Butyl carbinol acetate	24.0	---	---
Carbon disulfide	0.48	1.53	---
Carbon tetrachloride	0.65	1.75	6.90
Chlorobenzene	33.9	---	---
Chloroform	19.0	66.0	302.0
Diethyl ether	3.29	---	---
Ethanol (95%)	1.23	2.92	8.30
Ethylene chloride	18.7	---	---
Hexane	0.16	---	---
Methyl acetate	72.1	---	---
Toluene	55.0	130.0	367.0
Trichloroethylene	3.04	---	---
Water	0.0130	0.0285	0.0675

4. PHYSICAL PROPERTIES

4.1 Crystal Structure.[6-9] Both orthorhombic and monoclinic TNT have been observed. The monoclinic form is obtained by annealing cast TNT. Crystallization of TNT from most solvents gives complex mixed-phase intergrowth and twinned crystals that usually show structural disorder. Good monocrystals of TNT have been obtained from cyclohexanone.

Cell parameters of the two polymorphs are given.

Cell Parameters	Monoclinic	Orthorhombic[a]
Length of unit cell edges (Å)		
a	21.275	15.007
b	6.093	20.029
c	15.025	6.098
Angle β	110.14°	---
Molecules per unit cell	8.0	---

[a]There is some controversy about existence of the orthorhombic polymorph, which may be a disordered version of the monoclinic one (Ref. 8).

4.2 Density.[6,10,11]

Solid and Liquid

Method of Determination	State	Temperature (°C)	Density (g/cm³)	
			Monoclinic	Orthorhombic
X-ray data	Solid	21	1.653	1.646
Direct measurement	Solid	21	1.654	---
Direct measurement	Liquid	83-120	$1.545 - 1.016 \times 10^{-3}$ T(°C)	

Pressed Charges. The density of TNT in large billets or in ammunition varies with the method of preparation. Compression without application of a vacuum to remove the residual air gives the following densities.

Pressure (psi)	Density (g/cm^3)
3 000	1.35
5 000	1.40
10 000	1.45
15 000	1.52
20 000	1.55
50 000	1.60

Compaction with the residual air removed and the TNT preheated to 70°C gives the following density.

Pressure (psi)	Powder Temperature (°C)	Density (g/cm^3)
12 000	70	1.63-1.64

Cast Charges. The density of cast TNT depends on the procedures used to melt, cast, and solidify it. Typical densities are as follows.

Preparative Procedure			Density (g/cm^3)
Melting[a]	Casting[b]	Solidification	
Open	100% liquid	Ambient	1.56-1.59
Open	75% liquid	Ambient	1.59-161
Vacuum	50-75% liquid	Ambient	1.61-1.62

[a]In an open melt the TNT is melted in atmospheric conditions. In a vacuum melt, the molten TNT is subjected to a vacuum (~20 mm Hg) for a few minutes.

[b]Because of the ~7% volume change associated with the liquid-to-solid transition, solid TNT is usually added to the liquid TNT. The TNT, either as a liquid or as a mixture of liquid and solids, is cast at a temperature within a degree or two of the melting point (80-82°C).

4.3 Infrared Spectrum. See Fig. 1.

4.4 Refractive Indices.[11] The following refractive indices in sodium light have been reported.

α	1.5430
β	1.6742
γ	1.717

5. THERMAL PROPERTIES

5.1 Phase Changes.[10,12]

Type	Temperature (°C)	Latent Heat (cal/g)	Latent Heat (kcal/mole)
Solid-to-liquid	80.9	23.53	5.35
Solid-to-gas (sublimation)	---	---	28.3[a]

[a]Computed from the solid-phase vapor pressure data in Sec. 5.2.

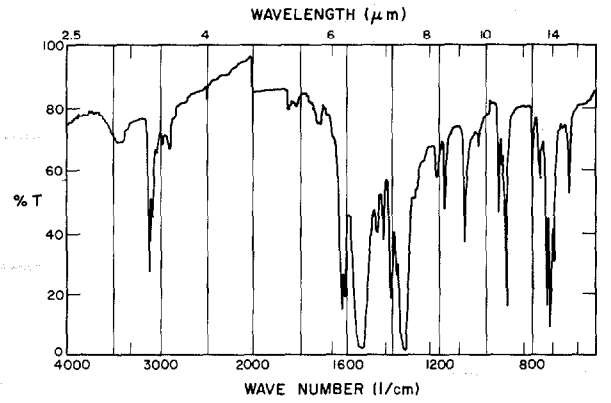

Fig. 1. Infrared spectrum.

5.2 Vapor Pressure.[12]

Temperature (°C)	Vapor Pressure (mm Hg)
60.1	5.43×10^{-4}
78.5	6.44×10^{-3}
80.2	7.16×10^{-3}
82.4	7.96×10^{-3}
99.5	4.07×10^{-2}
110.6	8.26×10^{-2}
131.1	3.48×10^{-1}
141.4	6.21×10^{-1}

A least squares fit to these data gives

$\log_{10} P(\text{mm Hg}) = 15.43 - 6180/T(K)$.

5.3 Heat Capacity.

Heat Capacity at Constant Pressure (cal/g-°C)	Temperature Range (°C)
$0.254 + 7.5 \times 10^{-4} T(°C)$	$17 < T < 67$
$0.309 + 5.5 \times 10^{-4} T(°C)$	$97 < T < 150$

5.4 Thermal Conductivity.

Density (g/cm^3)	Conductivity (cal/s-cm-°C)	Temperature Range (°C)
1.59	6.22×10^{-4}	$10 < T < 45$
1.59	5.89×10^{-4}	$45 < T < 75$

5.5 Coefficient of Thermal Expansion.

Coefficient of Expansion (1/°C)	Temperature Range (°C)
$5.0 \times 10^{-5} + 7.8 \times 10^{-8}\,T$	$-40 < T < 60$

5.6 Heats of Combustion and Formation at 25°C.[13]

ΔH_c°	ΔH_f°
−817.2 kcal/mole	−12.0 kcal/mole

5.7 Thermal Decomposition Kinetics.[14,15]

Decomposition energy	300 cal/g[a]
Activation energy	34.4 kcal/mole
Pre-exponential factor	2.51×10^{11}/s

[a]The complexities of the decomposition reaction are described in Ref. 15.

5.8 Other Thermal Stability Test Results.

Test	Results
Vacuum	0.2 ml/g of gas evolved after 48 h at 120°C
DTA and pyrolysis	See Fig. 2
Critical temperature, Tm	288°C
Charge radius, a	0.38 mm
Density, ρ	1.57 g/cm^3

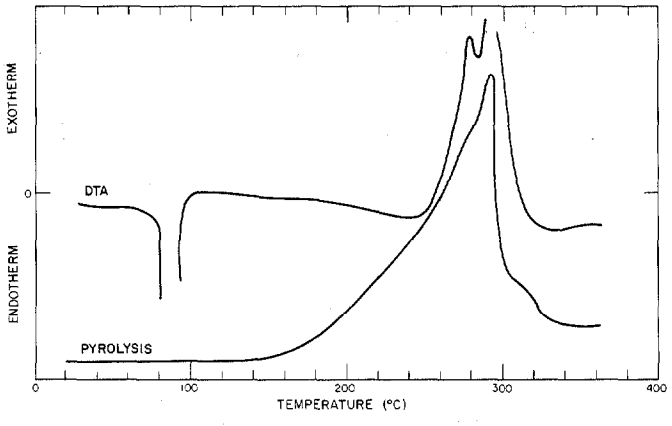

Fig. 2. TNT DTA and pyrolysis test results.

6. DETONATION PROPERTIES

6.1 Detonation Velocity.[16-18]

Effect of Density

	Density Range (g/cm^3)
$D = 1.873 + 3.187\ \rho_0$,	$0.9 < \rho_0 < 1.534$
and	
$D = 6.762 + 3.187\ (\rho_0 - 1.534) - 25.1\ (\rho_0 - 1.534)^2$,	$1.534 < \rho_0 < 1.636$

where D = detonation velocity in millimeters per microsecond and

ρ_0 = density in grams per cubic centimeter.

$+ 115.056\ (\rho - 1.534)^3$ Cubic term - ?. missing

The charge preparation method affects the infinite-diameter detonation velocity and failure diameter of unconfined cylindrical charges as follows.

Method of Charge Preparation	Charge Density (g/cm^3)	Detonation Velocity at Infinite "D" ($mm/\mu s$)	Critical Diameter (mm)
Vacuum melting	---	---	---
Creaming and casting	1.615	6.942 ± 0.028	14.6 ± 2.0
Vacuum melting and casting	1.620	6.999 ± 0.011	14.5 ± 0.5
Pressing	1.620	7.045 ± 0.170	2.6 ± 0.6
Liquid	1.443	6.574 ± 0.001	62.6 ± 2.6

Effect of Charge Radius

Detonation velocity varies with charge radius and preparation procedure as follows.

Method of Charge Preparation	Density (g/cm^3)	Effect of Charge Radius on Detonation Velocity ($mm/\mu s$)
Creaming and casting	1.615	$D(R) = 6.942\ [(1-5.67 \times 10^{-2}/R) - 4.2 \times 10^{-1}/R\ (R - 7.41)]$
Vacuum melting and casting	1.620	$D(R) = 6.999\ [(1 - 1.3 \times 10^{-2}/R) - 6.2 \times 10^{-1}/R\ (R - 5.5)]$
Pressing	1.620	$D(R) = 7.045\ [(1 - 6.1 \times 10^{-2}/R) - 3.5 \times 10^{-2}/R\ (R - 0.57)]$
Liquid	1.443	$D(R) = 6.574\ (1 - 0.291/R)$

The detonation velocity of liquid TNT at 81°C is given.

Temperature (°C)	Density (g/cm³)	Velocity (mm/μs)
81	1.462	6.633

6.2 Detonation Pressure.[19]

Density (g/cm³)	Detonation Velocity (mm/μs)	Pressure (GPa)
1.637	6.942 ± 0.016	18.91 ± 0.1

6.3 Cylinder Test Results.[20]

Density g/cm³)	Detonation Velocity (mm/μs)	Cylinder Wall Velocity (mm/μs) at	
		$R - R_o = 5$ mm	$R - R_o = 19$ mm
1.630	6.940	1.18	1.40

6.4 Plate Dent Test Results.

Charge Diameter (mm)	Density (g/cm³)	Dent Depth (mm)	Charge Height (mm)
12.7	1.63	1.57	12.7
		1.70	16.9
		1.93	84.58-508
		2.90	203.0
25.4	1.631	1.73	12.7
		2.90	25.4
		3.20	31.7
		4.04	42.4
		4.19	50.8
		4.27	63.5
		4.14	72.6
		4.19	84.6
		4.09	101.6
		4.11	127.0
		4.14	169.4
		4.06	254.0
		4.09	508.0
	1.626	6.73	63.5
		7.01	101.6
		6.60	169.4
		7.01	203.0
	1.640	6.88	203.0
41.3	1.626	3.02	16.9
		4.01	25.4
		4.67	31.8
		5.41	42.4
		6.05	50.8
		6.90	63.5
		7.06	72.6
		7.14	76.2
		7.18	101.6
		7.06	127.0
		6.81	169-203
		6.93	254.0
		6.78	304.8
		6.96	508.0
		6.99	1016.0

7. SHOCK INITIATION PROPERTIES

7.1 Gap Test Results.[21]

Density (g/cm³)	G_{50} (mm)	L_{95} (mm)	Remarks
	Large Scale		
0.800	61.49	0.38	Bulk density flake
1.024	61.54	0.20	Pressed
1.220	56.26	0.08	Pressed
1.356	55.02	0.25	Pressed
1.505	54.92	0.30	Pressed
1.551	54.46	0.28	Pressed
1.595	52.53	0.18	Pressed
1.631	46.43	0.30	Pressed
1.615	28.30	0.64	Cast
	Small Scale[a]		
0.77	4.11	0.08	Granular at bulk density
0.84	No go at zero gap		Flake at bulk density
1.628	0.33	0.05	Pressed at 65°C

[a]The failure diameter of cast TNT is 14.5 mm, so it cannot be initiated in the small-scale gap test.

7.2 Wedge Test Results.[22]

Density (g/cm³)	Distance, x*, and Time, t*, to Detonation (mm and μs)	Pressure Range (GPa)
1.62 to 1.634	$\log P = (1.40 \pm 0.03) - (0.32 \pm 0.03) \log x^*$ $\log P = (1.16 \pm 0.03) - (0.31 \pm 0.05) \log t^*,$	$9.17 < P < 17.1$

where P = pressure in gigapascals.

7.3 Shock Hugoniots.[23,24]

Density (g/cm³)	Shock Hugoniot (mm/μs)	Particle Velocity Range (mm/μs)
1.614	$U_s = 2.390 + 2.50\,U_p$,	---
1.63	$U_s = 2.57 + 1.88\,U_p$,	$0 < U_p < 2.0$

where U_s = shock velocity
and U_p = particle velocity.

7.4 Minimum Priming Charge.

Density (g/cm³)	W_{50} (mg of XTX 8003)	Remarks
1.59	394	Pressed at 65°C
1.63	1260	Pressed at 65°C

7.5 Detonation Failure Thickness.[21]

Density (g/cm³)	Failure Thickness (mm)	Remarks
1.568	1.82	Pressed at 65°C
1.627	2.16	Pressed at 65°C
1.629	1.76	Pressed at 65°C
1.631	2.00	Pressed at 72°C
1.635	2.59	Pressed at 72°C

8. SENSITIVITY

8.1 Drop Weight Impact Height.

Tool Type	H_{50} (cm)	Remarks
12	212	Flake TNT
12B	>320	Flake TNT
12	154	Granular TNT
12B	>320	Granular TNT

8.5 Spark Sensitivity.

Electrode	Lead Foil Thickness (mils)	Sample Size (mg)	Energy (J)	Occurrence of Explosion (%)
Brass	3	47.9	0.46	50
Brass	10	47.9	2.75	50
Steel	1	53.0	0.19	50
Steel	10	53.0	4.00	50

9. MECHANICAL PROPERTIES

9.1 Viscosity.

Temperature (°C)	Viscosity (cp)
85	12.0-13.7
90	10.6-11.8
95	9.4-10.2
100	8.6-9.0

9.3 Compressive Strength and Modulus.

Density (g/cm^3)	Ultimate Compressive Strength[a] (psi)	Compressive Modulus[a] (psi)
1.60	1400	7.9×10^4

[a]Compressive strength is a function of density and method of charge preparation. These are cast TNT data.

REFERENCES

1. T. Urbanski, *Chemistry and Technology of Explosives,* Vol. I, Pergamon Press, Oxford, 1965).

2. C. R. Buck and S. E. Wilson, Jr., US Army report USEHA-32-049 (1975).

3. *Code of Federal Regulations, 49, Transportation Parts 100-199, Rev. 12-1-76* (Office of the Federal Register, General Services Administration, Washington, DC, 1976).

4. US Army Materiel Command, Regulation No. AMCR 385-100 (1977).

5. A. Seidell, *Solubilities of Organic Compounds,* 3rd Ed., Vol. II, (D. Van Nostrand Co., Inc., New York, 1941).

6. J. R. C. Duke, Explosives Research and Development Establishment informal report, Waltham Abbey (September 1974).

7. L. A. Burkardt and J. H. Bryden, Acta Crystallographica **7,** 135-137 (1954).

8. D. G. Grabar, F. C. Rauch, and A. J. Fanelli, Journal of Physical Chemistry **73** (5), 3514-3518 (1969).

9. W. Connick, F. G. J. May, and B. W. Thorpe, Australian Journal of Chemistry **22,** 2685-2688 (1969).

10. Howard H. Cady and William H. Rogers, Los Alamos Scientific Laboratory report LA-2696 (1962).

11. Department of the Army and Air Force, Technical Manual 9-1300-214 and TO11A-1-34 (November 1967).

12. G. Edwards, Transactions of the Faraday Society **46,** 423-427 (1950).

13. Prince E. Rouse, Jr., Journal of Chemical and Engineering Data **21,** 16-20 (1976).

14. R. N. Rogers, Thermochimica Acta **11,** 131-139 (1975).

15. J. C. Dacons, H. G. Adolph, and M. J. Kamlet, Journal of Physical Chemistry **74** (5), 3035-3040 (1970).

16. M. J. Urizar, E. James, Jr., and L. C. Smith, Physics of Fluids **4,** 262-274 (1961).

17. A. W. Campbell and Ray Engelke, *Proceedings—Sixth Symposium (International) on Detonation, Coronado, California, August 24-27, 1976* (Office of Naval Research, Department of the Navy, ACR-221, 1976) pp. 642-652.

18. W. B. Garn, Journal of Chemical Physics **30,** 819-822 (1959).

19. W. E. Deal, Journal of Chemical Physics **27** (1), 796-800 (1957).

20. J. W. Kury, H. C. Hornig, E. L. Lee, J. L. McDonnel, D. L. Ornellas, M. Finger, F. M. Strange, and M. L. Wilkins, *Fourth Symposium (International) on Detonation, White Oak, Maryland, October 12-15, 1965* (Office of Naval Research, Department of the Navy, ACR-126, 1965), pp. 3-12.

21. Manuel J. Urizar, Suzanne W. Peterson, and Louis C. Smith, Los Alamos Scientific Laboratory report LA-7193-MS (April 1978).

22. J. B. Ramsay and A. Popolato, *Proceedings—Fourth Symposium (International) on Detonation, White Oak, Maryland, October 12-15, 1965* (Office of Naval Research, Department of the Navy, ACR-126, 1965), pp. 233-238.

23. N. L. Coleburn and T. P. Liddiard, Jr., Journal of Chemical Physics **44** (3), 1929-1936 (1966).

24. V. M. Boyle, R. L. Jameson, and M. Sultanoff, *Proceedings—Fourth Symposium (International) on Detonation, White Oak, Maryland, October 12-15, 1965,* (Department of the Navy, ACR-126, 1965), pp. 241-247.

XTX 8003

1. GENERAL PROPERTIES

1.1 Chemical and Physical Description. XTX (Extex) 8003 consists of PETN coated with a low-temperature vulcanizing silicone resin, Sylgard 182. Uncured XTX 8003 is putty-like and can be extruded through small openings at modest pressures. After curing, it is white and rubbery.

1.2 Common Use. XTX 8003 is used in special applications that require explosives with small detonation failure diameters.

1.3 Toxicity.[1,2] There are no known toxicity problems associated with the use of Sylgard 182. PETN, because it is insoluble in water, is slightly toxic. The recommended maximum atmospheric concentration over an 8-h period is 15 mg/m^3.

2. MANUFACTURE AND PROCUREMENT

2.1 Manufacture. Sylgard 182 resin and its curing agent are mixed with PETN in a high-shear vertical mixer to the consistency of wet sea sand. This material is passed through a three-roll differential paint mill until it is the consistency of glazier's putty. After milling, XTX 8003 has a shelf life of 24 h at 25°C. Storage at −30°C increases the shelf life to 8 months. When it is to be used, the XTX 8003 is extruded into molds of the desired configuration. Curing or polymerization is achieved by exposure to 65°C for 8-12 h.

2.2 Procurement. XTX 8003 can be purchased from the DOE under LASL material specification 13Y-104481 Rev. F, dated February 6, 1978.

2.3 Shipping.[3] Cured or uncured XTX 8003 is shipped as a Class A explosive.

2.4 Storage.[4] Uncured XTX 8003 is in Storage Compatibility Group A. When cured, it is stored in Compatibility Group D. Either cured or in a device, it is in Storage Class 1.1.

3. CHEMICAL PROPERTIES

3.1 Composition.

Constituent	Weight Percent	Volume Percent
PETN	80	69.9
Sylgard 182	20	30.1

3.2 Molecular Weight.

Constituent	Structure	Molecular Weight
PETN	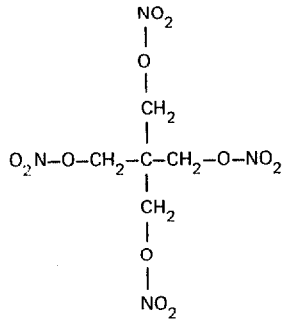 $C_5H_8N_4O_{12}$	316.15
Sylgard 182	Proprietary	---

3.3 Solubility.[5] The solubility is that of PETN.

Solvent	Grams of PETN Dissolved/100 g of Solvent		
	20°C	40°C	60°C
Acetone	24.8	44.92	---
Acetone and water (wt% water)			
6.23	16.29	31.42	---
12.30	9.31	20.25	---
18.22	5.22	12.66	---
23.99	2.87	7.66	---
35.11	0.68	2.33	---
55.80	0.03	0.13	---
Benzene	0.27	0.83	2.58
Ethanol	0.13	0.37	1.19
Ethyl acetate	10.6	18.50	---

4. PHYSICAL PROPERTIES

4.2 Density.

Theoretical Density (g/cm^3)	Density of Typical Charges (g/cm^3)
1.556	1.50

4.3 Infrared Spectrum. See Fig. 1.

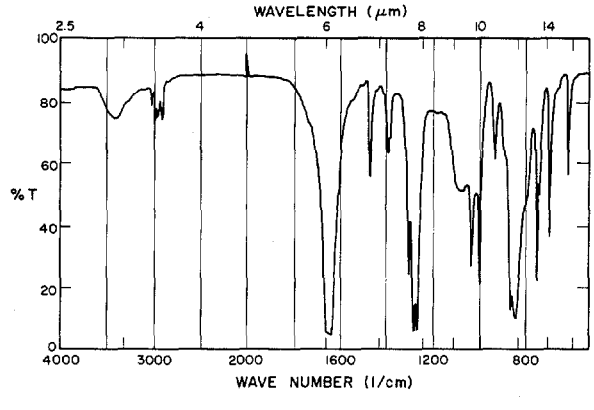

Fig. 1. Infrared spectrum.

5. THERMAL PROPERTIES

5.1 Phase Change.

Type	Temperature (°C)	Latent Heat (cal/g mix)
PETN (solid-to-liquid)	142.9	29.9

5.3 Heat Capacity.

Density (g/cm^3)	Heat Capacity at Constant Pressure (cal/g-°C)	Temperature Range (°C)
1.50	$0.252 + 8.5 \times 10^{-4} T$	$37 < T < 127$

5.5 Coefficient of Thermal Expansion.[6]

Density (g/cm^3)	Coefficient of Expansion (1/°C)	Temperature Range (°C)
1.50	1.65×10^{-6}	$-50 < T < 25$

5.6 Heats of Combustion and Formation.

	ΔH_c° (kcal/mole)	ΔH_f° (kcal/mole)
PETN	−618.7	−110.34

5.7 Thermal Decomposition Kinetics.[7]

Property	PETN
Decomposition energy	300 cal/g
Activation energy	47.0 kcal/mole
Pre-exponential factor	6.3×10^{19}/s

5.8 Other Thermal Stability Test Results.

Test	Results
Vacuum	0.2 ml/g of gas evolved after 48 h at 100°C
DTA and pyrolysis	See Fig. 2

6. DETONATION PROPERTIES[8]

6.1 Detonation Velocity.

Effect of Charge Radius

Charge radius affects the detonation velocity of XTX 8003 at a density of 1.53 g/cm³, confined in polycarbonate plastic in a hemicylinder configuration, as follows.

$$D(R) = 7.260[(1 - 0.191 \times 10^{-2}/R) - 2.12 \times 10^{-4}/R\ (R - 0.111)]$$

where D = detonation velocity in millimeters per microsecond,

and R = charge radius in millimeters.

The experimentally determined failure diameter in polycarbonate confinement is 0.36 mm.

7. SHOCK INITIATION PROPERTIES

7.1 Gap Test Results.[9]

Small Scale		
Density (g/cm³)	G_{50} (mm)	L_{95} (mm)
1.50	4.42	0.28

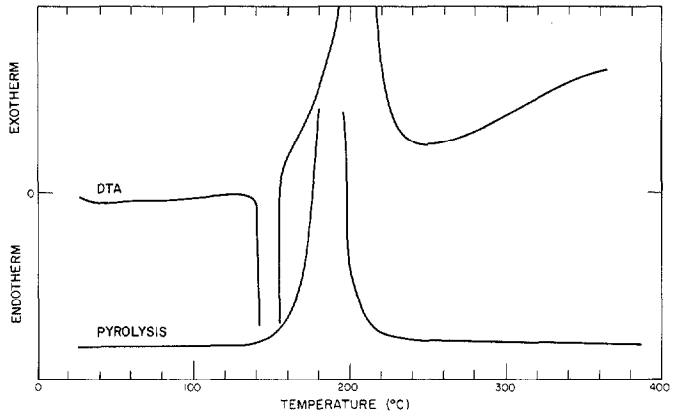

Fig. 2. XTX 8003 DTA and pyrolysis test results.

7.2 Wedge Test Results.

Density (g/cm^3)	Distance, x*, and Time, t*, to Detonation (mm and μs)	Pressure Range (GPa)
1.53	$\log P = (0.74 \pm 0.01) - (0.37 \pm 0.02) \log x^*$ $\log P = (0.53 \pm 0.008) - (0.33 \pm 0.02) \log t^*$, where P = pressure in gigapascals.	$2.5 < P < 8.2$

7.3 Shock Hugoniot.[10]

Density (g/cm^3)	Shock Hugoniot (mm/μs)	Particle Velocity Range (mm/μs)
1.50	$U_s = 1.49 + 3.03\ U_p$ (Ref. 10)	$0 < U_p < 0.8$
1.53	$U_s = (1.59 \pm 0.39) + (3.24 \pm 0.63)\ U_p$	$0.48 < U_p < 0.78$

7.4 Minimum Priming Charge. XTX 8003 is used as the donor explosive in this test.

8. SENSITIVITY

8.1 Drop Weight Impact Height.

Tool Type	H_{50}^{a} (cm)
12	30
12B	35

[a]Cured or uncured.

8.4 Susan Test Results.

Projectile Impact Velocity (ft/s)	Relative Energy Release (%)
160	<1
750	~5-8

9. MECHANICAL PROPERTIES

9.2 Tensile Strength and Modulus.

Temperature (°C)	Density[a] (g/cm³)	Ultimate Tensile Strength (psi)	Tensile Modulus psi x 10^{-5}
22	1.50	90 ± 20	[b]

[a]Cured.

[b]Strain-to-failure of a 0.25-in.-diam charge tested at a load rate of 0.05/min occurs after 5% elongation.

REFERENCES

1. D. M. Smith, J. E. London, G. A. Drake, and R. G. Thomas, Los Alamos Scientific Laboratory report LA-7368-MS (June 1978).

2. Committee on Threshold Limit Values, *Documentation of Threshold Limit Values,* 3rd Ed., (American Conference of Governmental Industrial Hygienists, Cincinnati, Ohio, 1971).

3. *Code of Federal Regulations, 49, Transportation Parts 100-199, Rev. 12-1-76* (Office of the Federal Register, General Services Administration, Washington, DC, 1976).

4. US Army Materiel Command, Regulation No. AMCR 385-100 (1977).

5. R. N. Roberts and R. H. Dinegar, Journal of Physical Chemistry **62**, 1009-1011 (1958).

6. A. Popolato, Los Alamos Scientific Laboratory report LA-3210-MS (March 1965).

7. R. N. Rogers, Thermochimica Acta **11**, 131-139 (1975).

8. A. W. Campbell and Ray Engelke, *Proceedings—Sixth Symposium (International) on Detonation, Coronado, California, August 24-27, 1976* (Office of Naval Research, Department of the Navy, ACR-221, 1976), pp. 642-652.

9. Manuel J. Urizar, Suzanne W. Peterson, and Louis C. Smith, Los Alamos Scientific Laboratory report LA-7193-MS (April 1978).

10. Dante Stirpe, James O. Johnson, and Jerry Wackerle, Journal of Applied Physics **41**, 3884-3893 (1970).

XTX 8004

1. GENERAL PROPERTIES

1.1 Chemical and Physical Description. XTX (Extex) 8004 consists of RDX coated with a low-temperature vulcanizing silicone resin, Sylgard 182. Uncured XTX 8004 is putty-like and can be extruded through small openings at modest pressures. After curing, it is white and rubbery.

1.2 Common Use. XTX 8004 is used in special applications that require more thermal stability than XTX 8003 can give. The detonation failure diameter is slightly greater than that of XTX 8003.

1.3 Toxicity. Sylgard 182 is not known to be toxic. Workers who inhaled RDX dust for several months have become unconscious with loss of reflexes. The suggested maximum permissible airborne concentration of RDX is 1.5 mg/m^3 (Ref. 1).

2. MANUFACTURE AND PROCUREMENT

2.1 Manufacture. Sylgard 182 resin and its curing agent are mixed with RDX in a high-shear vertical mixer to the consistency of wet sea sand. This material is passed through a three-roll differential paint mill until it reaches the consistency of glazier's putty. Milled XTX 8004 has a 24-h shelf life at 25°C. Storage at -30°C increases the shelf life to 8 months. When it is to be used, the XTX 8004 is extruded into molds of the desired configuration. Curing or polymerization is achieved by exposure to 65°C for 8-12 h.

2.2 Procurement. XTX 8004 can be purchased from the DOE under LASL material specification 13Y-189496 Rev. A, dated November 22, 1978.

2.3 Shipping.[2] Cured or uncured, XTX 8004 is shipped as a Class A explosive.

2.4 Storage.[3] Uncured or cured, XTX 8004 is in Storage Compatibility Group D and Storage Class 1.1.

3. CHEMICAL PROPERTIES

3.1 Composition

Constituent	Weight Percent	Volume Percent
RDX	80	69.9
Sylgard 182	20	30.1

3.2 Molecular Weight.

Constituent	Structure	Molecular Weight
RDX	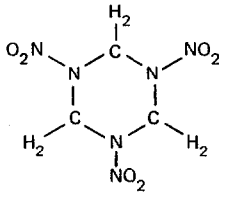 $C_3H_6N_6O_6$	222.13
Sylgard 182	Proprietary	

3.3 Solubility. The solubility is that of RDX.

Solvent	Grams of RDX Dissolved/100 g of Solvent		
	20°C	40°C	60°C
Acetic acid			
99.6%	0.46	0.56	1.22
71.0%	0.22	0.37	0.74
Acetone	6.81	10.34	---
Isoamyl alcohol	0.026	0.060	0.210
Benzene	0.045	0.085	0.195
Chlorobenzene	0.33	0.554	---
Cyclohexanone	4.94	9.20	13.9
Dimethylformamide	---	41.5	60.6
Ethanol	0.12	0.24	0.58
Methyl acetate	2.9	4.1	---
Methylcyclohexanone	6.81	10.34	---
Methyl ethyl ketone	3.23	---	---
Toluene	0.020	0.050	0.125
Trichloroethylene	0.20	0.24	---
Water	0.005	0.0127	0.03

4. PHYSICAL PROPERTIES

4.2 Density.

Theoretical Density (g/cm^3)	Density of Typical Charge (g/cm^3)
1.584	1.5

5. THERMAL PROPERTIES

5.3 Heat Capacity.

Density (g/cm^3)	Heat Capacity at Constant Pressure (cal/g)	Temperature Range (°C)
1.5	$0.247 + 6.2 \times 10^{-4}$	$25 < T < 187$

5.4 Thermal Conductivity.

Density (g/cm^3)	Conductivity (cal/cm-s-°C)
1.5	3.4×10^{-4}

5.6 Heats of Combustion and Formation.

	ΔH_c° (kcal/mole)	ΔH_f° (kcal/mole)
RDX	−660.7	11.3

5.7 Thermal Decomposition Kinetics.

Property	RDX
Decomposition energy	500 cal/g
Activation energy	47.1 kcal/mole
Pre-exponential factor	2.02×10^{18}/s

5.8 Other Thermal Stability Test Results.

Test	Results
Vacuum	0.1-0.3 ml/g of gas evolved after 48 h at 120°C
DTA and pyrolysis	See Fig. 1

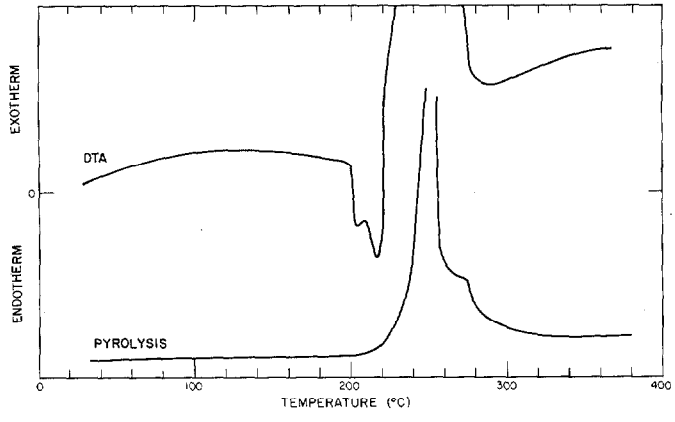

Fig. 1. XTX-8004 DTA and pyrolysis test results.

6. DETONATION PROPERTIES

6.1 Detonation Velocity.

Effect of Charge Radius

Charge radius affects the detonation velocity of 1.5-g/cm³ XTX 8004 confined in polycarbonate plastic in a hemispherical configuration as follows.

Diameter (mm)	Detonation Velocity (mm/μs)
∞	7.45
4.5	7.35
3.13	7.30
2.0	7.22
1.75	7.15
1.6	Failure

7. SHOCK INITIATION PROPERTIES

7.1 Gap Test Results.

Small Scale	
Density (g/cm³)	G_{50} (mm)
1.52	1.96

8. SENSITIVITY

8.1 Drop Weight Impact Height.

	H_{50} (cm)	
Tool Type	Cured	Uncured
12	70	65
12B	170	145

REFERENCES

1. C. R. Buck and S. E. Wilson, Jr., US Army report USEHA-32-049 (1975).

2. *Code of Federal Regulations, 49, Transportation Parts 100-199 Rev. 12-1-76* (Office of the Federal Register, General Services Administration, Washington, DC, 1976).

3. US Army Materiel Command, Regulation No. AMCR 385-100 (1977).

PART II
EXPLOSIVES PROPERTIES BY PROPERTIES

Table 1.01 CHEMICAL DESCRIPTION

Explosive	Constituents	Weight Percent	Volume Percent	Molecular Formula	Molecular Weight
Alex/20	RDX	44	44.07	$C_3H_6N_6O_6$	222.13
	TNT	32	34.93	$C_7H_5N_3O_6$	227.13
	Al	20	12.96	Al	26.97
	Wax	4	8.04	$CH_3(CH_2)_nCH_3$	$30.07 + (14.02)_n$
Alex/30	RDX	37	38.72	$C_3H_6N_6O_6$	222.13
	TNT	28	31.92	$C_7H_5N_3O_6$	227.13
	Al	31	20.98	Al	26.97
	Wax	4	8.37	$CH_3(CH_2)_nCH_3$	$30.07 + (14.02)_n$
Amatex/20	Ammonium nitrate	40	39.5	NH_4NO_3	80.05
	TNT	40	41.5	$C_7H_5N_3O_6$	227.13
	RDX	20	19.0	$C_3H_6N_6O_6$	222.13
Amatex/30	Ammonium nitrate	30	29.8	NH_4NO_3	80.05
	TNT	40	41.7	$C_7H_5N_3O_6$	227.13
	RDX	30	28.5	$C_3H_6N_6O_6$	222.13
Amatex/40	Ammonium nitrate	20	19.9	NH_4NO_3	80.05
	TNT	40	41.8	$C_7H_5N_3O_6$	227.13
	RDX	40	38.2	$C_3H_6N_6O_6$	222.13
AP	Ammonium picrate	100	100	$C_6H_2(NO_2)_3ONH_4$	246.14
ANFO	Ammonium nitrate	94	89.1	NH_4NO_3	80.05
	No. 2 diesel oil	6	10.9	$CH_3(CH_2)_nCH_3$	$30.07 + (14.02)_n$
Baratol	Barium nitrate	76	62.8	$Ba(NO_3)_2$	261.36
	TNT	24	37.2	$C_7H_5N_3O_6$	227.13
Boracitol	Boric acid	60	63.3	H_3BO_3	61.84
	TNT	40	36.7	$C_7H_5N_3O_6$	227.13
BTF	Benzotrifuroxan	100	100	$C_6N_6O_6$	252.12
BTX	5.7-Dinitro-1-picrylbenzo-triazole	100	100	$C_{12}H_2N_8O_{10}$	418.21

Comp A-3	RDX	91	83.5	$C_3H_6N_6O_6$	222.13
	Wax	9	16.5	$CH_3(CH_2)_nCH_3$	$30.07 + (14.02)_n$
Comp B	RDX	59.5	56.9	$C_3H_6N_6O_6$	222.13
	TNT	39.5	41.2	$C_7H_5N_3O_6$	227.13
	Wax	1.0	1.9	$CH_3(CH_2)_nCH_3$	$30.07 + (14.02)_n$
Comp B-3	RDX	60	57.8	$C_3H_6N_6O_6$	222.13
	TNT	40	42.2	$C_7H_5N_3O_6$	227.13
Cyclotol	RDX	75	73.2	$C_3H_6N_6O_6$	222.13
75/25	TNT	25	26.8	$C_7H_5N_3O_6$	227.13
DATB	Diaminotrinitro-benzene	100	100.	$C_6H_5N_5O_6$	243.10
DIPAM	Diaminohexanitro-biphenyl	100	100	$C_{12}H_6N_8O_{12}$	454.25
DNPA	Dinitropropyl-acrylate	100	100	$(C_6H_6N_6O_6)_n$	$(258.15)_n$
HMX	Cyclotetra-methylene-tetranitramine	100	100.	$C_4H_8N_8O_8$	296.17
HNS	Hexanitrostilbene	100	100	$C_{14}H_4N_6O_{12}$	448.23
HNDS	Hexanitrodipicrylsulfone	100	100.	$C_{12}H_4N_6O_{14}S$	488.27
NM	Nitromethane	100	100	CH_3NO_2	61.04
NP	Nitroplasticizer dinitropropyl formal	50	50.8	$C_7H_{12}N_4O_{10}$	312.21
	Nitroplasticizer dinitropropyl acetal	50	49.2	$C_8H_{14}N_4O_{10}$	326.22
NQ	Nitroguanidine	100	100	$CH_4N_4O_2$	104.1
Octol	HMX	75	72.3	$C_4H_8N_8O_8$	296.17
	TNT	25	27.7	$C_7H_5N_3O_6$	227.14
PATO	Picrylamino-triazole	100	100	$C_8H_5N_6O_6$	281.18

Table 1.01 (continued)

Explosive	Constituents	Weight Percent	Volume Percent	Molecular Formula	Molecular Weight
PBX 9007	RDX	90	83.7	$C_3H_6N_6O_6$	222.13
	Polystyrene	8.5	13.6	$(C_8H_8)_n$	$(104.15)_n$
	Dioctylphthalate (DOP)	1.5	2.5	$C_{24}H_{34}O_4$	386.53
PBX 9010	RDX	90	90	$C_3H_6N_6O_6$	222.13
	Kel-F 3700	10	10	$(CFClCF_2CH_2CF_2)_n$	$(180.51)_n$
PBX 9011	HMX	90	84.9	$C_4H_8N_8O_8$	296.17
	Estane 5703F1	10	15.1	$C_{5.1}H_{7.5}N_{0.19}O_{1.76}$	100
PBX 9205	RDX	92	86.8	$C_3H_6N_6O_6$	222.13
	Polystyrene	6	9.7	$(C_8H_8)_n$	$(104.14)_n$
	DOP	2	3.5	$C_{24}H_{34}O_4$	386.51
PBX 9404	HMX	94	92.5	$C_4H_8N_8O_8$	296.17
	Nitrocellulose (NC)	3	3.6	$(C_6H_7N_{2.25}O_{9.5})_n$	$(262.64)_n$
	Chloroethyl phosphate (CEF)	3	3.9	$C_6H_{12}O_4Cl_3$ P	285.51
PBX 9407	RDX	94	93.6	$C_3H_6N_6O_6$	222.13
	Exon-461	6	6.4	$[(CF_2CFCl)_{0.64}$ $(CH_2CHCl)_{0.36}]_n$	$(97.05)_n$
PBX 9501	HMX	95	92.7	$C_4H_8N_8O_8$	296.17
	Estane 5703F1	2.5	3.9	$C_{5.1}H_{7.5}N_{0.19}O_{1.76}$	100
	Nitroplasticizer	2.5	3.3	$C_7H_{12}N_4O_{10}$/ $C_8H_{14}N_4O_{10}$	312.21/ 326.22
PBX 9502	TATB	95	95.2	$C_6H_6N_6O_6$	258.16
	Kel-F 800	5	4.8	$(CFClCF_2CH_2CF_2)_n$	$(180.51)_n$
PETN	Pentaerythritol-tetranitrate	100	100	$C_5H_8N_4O_{12}$	316.15
RDX	Cyclotrimethylene-trinitramine	100	100	$C_3H_6N_6O_6$	222.13

TATB	Triaminotrinitro-benzene	100	100	$C_6H_6N_6O_6$	258.18
Tetryl	Trinitrophenylmethyl nitramine	100	100	$C_7H_5N_5O_8$	287.15
TNT	Trinitrotoluene	100	100	$C_7H_5N_3O_6$	227.14
TPM	Tripicrylmelamine	100	100	$C_{24}H_9N_{15}O_{18}$	795.46
XTX 8003	PETN	80	70.3	$C_5H_8N_4O_{12}$	316.15
	Sylgard	20	29.6	Proprietary	
XTX 8004	RDX	80	69.9	$C_3H_6N_6O_6$	222.13
	Sylgard	20	30.1	Proprietary	
		Plastic-Bonded DATB			
X-0243	DATB	95	91.5	$C_6H_5N_5O_6$	243.14
	Polystyrene	3.5	5.8	$(C_8H_8)_n$	$(104.15)_n$
	DOP	1.5	2.7	$C_{24}H_{34}O_4$	386.53
X-0300	DATB	95	92.4	$C_6H_5N_5O_6$	243.10
	Estane	5	7.5	$C_{5.1}H_{7.5}N_{0.19}O_{1.76}$	100
X-0247	DATB	95	95	$C_6H_5N_5O_6$	243.14
	Kel-F	5	5	$(CFClCF_2CH_2CF_2)_n$	$(180.51)_n$
X-0299	DATB	95	94.9	$C_6H_5N_5O_6$	243.10
	Viton A	5	5.1	$(C_5H_{3.5}F_{6.5})$	$(187.07)_n$
		Plastic-Bonded HMX			
X-0217	HMX	94	92.2	$C_4H_8N_8O_8$	296.17
	DNPA	3.6	4.6	$(C_6H_6N_6O_6)_n$	$(258.06)_n$
	NP	2.4	3.2	$C_7H_{12}N_4O_{10}$/ $C_8H_{14}N_4O_{10}$	312.21/ 326.22
X-0234-50	HMX	94	92.3	$C_4H_8N_8O_8$	296.17
	DNPA	3	3.8	$(C_6H_6N_6O_6)_n$	$(258.06)_n$
	CEF	3	3.9	$C_6H_{12}O_4Cl_3P$	285.52

Table 1.01 (continued)

Explosive	Constituents	Weight Percent	Volume Percent	Molecular Formula	Molecular Weight
X-0234-60	HMX	94	92.3	$C_4H_8N_8O_8$	296.17
	DNPA	3.6	4.5	$(C_6H_6N_6O_6)_n$	$(258.06)_n$
	CEF	2.4	3.2	$C_6H_{12}O_4Cl_3P$	285.52
X-0234-70	HMX	94	92.3	$C_4H_8N_8O_8$	296.17
	DNPA	4.2	5.3	$(C_6H_6N_6O_6)_n$	$(258.06)_n$
	CEF	1.8	2.4	$C_6H_{12}O_4Cl_3P$	285.52
X-0234-80	HMX	94.0	92.3	$C_4H_8N_8O_8$	296.17
	DNPA	4.8	6.1	$(C_6H_6N_6O_6)_n$	$(258.06)_n$
	CEF	1.2	1.6	$C_6H_{12}O_4Cl_3P$	285.52
X-0286	HMX	97	93.8	$C_4H_8N_8O_8$	296.17
	Kraton	1.35	2.7	Proprietary	
	Oil	1.65	3.5	$(CH_2)_n$	$(14.03)_n$
X-0287	HMX	97.5	93.8	$C_4H_8N_8O_8$	296.17
	Kraton	1.43	3.9	Proprietary	
	Wax	1.17	2.3	$(CH_2)_n$	$(14.03)_n$
X-0298	HMX	97.5	93.7	$C_4H_8N_8O_8$	296.17
	Kraton	1.43	3.9	Proprietary	
	High Vacuum Oil	1.17	2.4	$(CH_2)_n$	$(14.03)_n$
X-0233-13-85	HMX	13.2	55	$C_4H_8N_8O_8$	296.17
	W	85.5	35	W	183.85
	Polystyrene	0.8	6	$[C_8H_8]_n$	$[104.14]_n$
	DOP	0.5	4	$C_{24}H_{34}O_4$	386.51
X-0118	HMX	29.7	27.4	$C_4H_8N_8O_8$	296.17
	NQ	64.9	64.6	$CH_4N_4O_2$	104.1
	Estane	5.4	8	$C_{5.1}H_{7.5}N_{0.19}O_{1.76}$	100
X-0114	HMX	65.7	64.3	$C_4H_8N_8O_8$	296.17
	NQ	26.4	27.8	$CH_4N_4O_2$	104.1
	Kel-F	7.9	7.9	$(CFClCF_2CH_2CF_2)_n$	$(180.51)_n$

PBX 9207	HMX	92	90.7	$C_4H_8N_8O_8$	296.17
	Exon-461	6	6.7	$[(CF_2CFCl)_{0.64}(CH_2CHCl)_{0.36}]/_n$	$(97.05)_n$
	CEF	2	2.6	$C_6H_{12}O_4Cl_3P$	285.51
X-0204	HMX	83	84.3	$C_4H_8N_8O_8$	296.17
	Teflon	17	15.7	$(CF_2)_n$	$[40.01]_n$
X-0007	HMX	86.4	79.9	$C_4H_8N_8O_8$	296.17
	Estane	13.6	20	$C_{5.1}H_{7.5}N_{0.19}O_{1.76}$	100
X-0009	HMX	93.4	89.7	$C_4H_8N_8O_8$	296.17
	Estane	6.6	10.3	$C_{5.1}H_{7.5}N_{0.19}O_{1.76}$	100

Table 1.02 DENSITIES AND MELTING POINTS

Explosive	Densities of Constituents		Mixture		Melting Point of Explosive (C°)
			Theoretical	Typical	
Alex/20	RDX	1.802	1.805	1.762	79
	TNT	1.654			
	Al	2.708			
	Wax	0.93			
Alex/30	RDX	1.802	1.885	1.864	79
	TNT	1.654			
	Al	2.708			
	Wax	0.93			
Amatex/20	NH_4NO_3	1.725	1.706	1.615	79
	TNT	1.654			
	RDX	1.802			
Amatex/30	NH_4NO_3	1.725	1.714	1.625	79
	TNT	1.654			
	RDX	1.802			
Amatex/40	NH_4NO_3	1.725	1.721	1.850	79
	TNT	1.654			
	RDX	1.802			
Ammonium Picrate	$C_6H_2(NO_2)_3ONH_4$	1.72			
ANFO	NH_4NO_3	1.725	1.635	0.9-1.0	
	No. 2 Diesel Oil	0.90			
Baratol	$Ba(NO_3)_2$	3.24	2.634	2.60	79
	TNT	1.654			
Boracitol	H_3BO_3	1.435	1.515	1.49	79
	TNT	1.654			
BTF	Benzotrifuroxan	1.901	1.901	1.84	195
BTX	5,7-Dinitro-1-picrylbenzo-triazole	1.74			263

Comp A-3	RDX Wax	1.802 0.90	1.653	1.5-1.6	200
Comp B	RDX TNT Wax	1.802 1.654 0.9	1.720	1.71-1.72	79
Comp B-3	RDX TNT	1.816 1.654	1.748	1.72-1.73	79
Cyclotol 75/25	RDX TNT	1.816 1.654	1.773	1.74-1.75	79
DATB	Diamino-trinitro-benzene	1.837			
DIPAM	Diamino-hexanitro-biphenyl	1.79			303
DNPA	Dinitro-propyl-acrylate	1.477			
HMX	Cyclotetra-methylene-tetranitramine	1.905			278.d[a]
HNS	Hexanitrostilbene	1.74			315
HNDS	Hexanitro-dipicrylsulfone	1.841			304
NM	Nitromethane	1.130[b]			−29
NP	Nitroplasticizer dinitropropyl formal	1.366^{25} [c]			14
	Nitroplasticizer dinitropropyl acetal	1.410^{35} [c]			

[a]Melts with decomposition.
[b]Specific gravities.
[c]At superscript temperature (°C).

Table 1.02 (continued)

Explosive	Densities of Constituents		Mixture		Melting Point of Explosive (°C)
			Theoretical	Typical	
NQ	Nitroguanidine	1.76-1.78			240
Octol	HMX	1.905	1.835	1.820	
	TNT	1.654			
PATO	Picrylamino-triazole	1.936			310d
PBX 9007	RDX	1.816	1.683	1.63	
	Polystyrene	1.054			
	Dioctylphthalate (DOP)	0.986[20c]			
PBX 9010	RDX	1.816	1.819	1.80	200d
	Kel-F 3700	1.85			
PBX 9011	HMX	1.905	1.797	1.770	278d
	Estane 5703F1	1.19			
PBX 9205	RDX	1.816	1.713	1.68	200d
	Polystyrene	1.054			
	DOP	0.986[24c]			
PBX 9404	HMX	1.905	1.873	1.840	278d
	Nitrocellulose (NC)	1.54-1.58			180d
	Chloroethyl phosphate (CEF)	1.425			−60
PBX 9407	RDX	1.816	1.809	1.65	200d
	Exon-461	1.7			
PBX 9501	HMX	1.905	1.860	1.830	278d
	Estane 5703F1	1.19			
	Nitroplasticizer	1.39			
PBX 9502	TATB	1.939	1.942	1.895	>400
	Kel-F 800	2.02			

PETN	Pentaerythritol-tetranitrate	1.77			141.3d
RDX	Cyclotrimethylene trinitramine	1.802			204d
TATB	Triaminotrinitro-benzene	1.939	1.937	1.860	450d
Tetryl	Trinitrophenyl-methylnitramine	1.74			129.5
TNT	Trinitrotoluene	1.654	1.654	1.620	80.9
TPM	Tripicrylmelamine				
XTX 8003	PETN	1.77	1.556	1.50	140d
	Sylgard	1.05			
XTX 8004	RDX	1.816	1.584	1.5	200d
	Sylgard	1.05			
DATB-Bonded Explosives					
X-0243	DATB	1.837	1.786	1.750	285d
	Polystyrene	1.054			
	DOP	0.986			
X-0300	DATB	1.837	1.789	1.750	285d
	Estane	1.19			
X-0247	DATB	1.837	1.845	1.810	285d
	Kel-F	2.02			
X-0299	DATB	1.837	1.835	1.800	285d
	Viton A	1.815			
HMX-Bonded Explosives					
X-0217	HMX	1.905	1.869	1.835	278d
	DNPA	1.477			
	NP	1.39			
X-0234-50	HMX	1.905	1.870	1.847	278d
	DNPA	1.477			
	CEF	1.425			

Table 1.02 (continued)

Explosive	Densities of Constituents		Mixture		Melting Point
			Theoretical	Typical	(°C)
X-0234-60	HMX	1.905	1.870	1.845	278d
	DNPA	1.477			
	CEF	1.425			
X-0234-70	HMX	1.905	1.870	1.843	278d
	DNPA	1.477			
	CEF	1.425			
X-0234-80	HMX	1.905	1.870	1.840	278d
	DNPA	1.477			
	CEF	1.425			
X-0286	HMX	1.905	1.842		278d
	Kraton	0.91			
	Oil	$0.873^{25/25\ c}$			
X-0287	HMX	0.905	1.833		278d
	Kraton	0.91			
	Wax	0.93			
X-0298	HMX	1.905	1.830		278d
	Kraton	0.91			
	High Vacuum Oil	$0.87^{25/25\ c}$			
X-0233-13-85	HMX	1.905	7.903	7.5-7.9	278d
	W	19.3			
	Polystyrene	1.054			
	DOP	0.986			
X-0118	HMX	1.905	1.761	1.712	278d
	NQ	1.76-1.78			
	Estane	1.19			
X-0114	HMX	1.905	1.863	1.815	240d
	NQ	1.76-1.78			
	Kel-F	1.85			

PBX 9207	HMX	1.905	1.878	1.837	278d
	Exon-461	1.70			
	CEF	1.425			
X-0204	HMX	1.905	1.953	1.915	278d
	Teflon	2.1			

2. THERMAL PROPERTIES

2.1 Heat Capacity Determination. Heat capacity was measured by use of a differential scanning calorimeter (DSC)[1]. In this instrument, a sample of explosive is subjected to a linearly increasing temperature and the heat flow rate, dH/dt, is monitored continuously. The heat capacity of the sample can be found from $dH/dt = mC_p(dT/dt)$, where dH/dt = heat flow rate in calories per second, m = sample mass in grams, C_p = heat capacity in calories per gram per degree Celsius, T = temperature in degree Celsius, and t = time. In using this equation to find C_p, one must know both dH/dt and the rate at which the temperature is increased or, more commonly, use a material of known heat capacity to calibrate the instrument.

Synthetic sapphire, whose heat capacity is well known, is used as a reference

Table 2.01 HEAT CAPACITY DATA

Explosive	Density (g/cm³)	Heat Capacity, C_p (cal/g-°C)	Valid Temperature Range (°C)
		Pure Explosives	
DATB	1.834	$0.20 + (1.11 \times 10^{-3})T - (1.81 \times 10^{-6})T^2$	---
DIPAM	1.79	$0.235 + (6.2 \times 10^{-4})T - (4.75 \times 10^{-7})T^2$	---
HNS	1.74	$0.201 + (1.27 \times 10^{-3})T - (2.39 \times 10^{-6})T^2$	---
HMX	1.90	$0.231 + (5.5 \times 10^{-4})T$	$37 < T < 167$
PETN	1.770	$0.239 + (8.0 \times 10^{-4})T$	$37 < T < 127$
RDX	1.804	$0.232 + (7.2 \times 10^{-4})T$	$37 < T < 167$
TATB	1.938	$0.215 + (1.324 \times 10^{-3})T - (2 \times 10^{-6})T^2$	---
Tetryl	1.73	$0.213 + (2.18 \times 10^{-4})T - (3.73 \times 10^{-7})T^2$	---
		Castable Mixtures	
Comp B-3	1.725	$0.234 + (1.03 \times 10^{-3})T$	$7 < T < 67$
		$0.137 + (2.09 \times 10^{-3})T$	$97 < T < 157$
TNT	---	$0.254 + (7.5 \times 10^{-4})T$	$17 < T < 67$
		$0.329 + (5.50 \times 10^{-4})T$	$97 < T < 157$
		Plastic-Bonded Explosives	
HMX-Based			
PBX 9011	1.772	$0.259 + (6.3 \times 10^{-4})T$	$17 < T < 167$
PBX 9404	1.845	$0.224 + (7.0 \times 10^{-4})T$	$17 < T < 147$
PBX 9501	1.835	$0.238 + (7.9 \times 10^{-4})T$	$50 < T < 175$
PETN-Based			
XTX 8003	---	$0.252 + (8.5 \times 10^{-4})T$	$37 < T < 127$
RDX-Based			
PBX 9010	1.785	$0.247 + (6.4 \times 10^{-4})T$	$37 < T < 167$
PBX 9407	1.660	$0.241 + (7.7 \times 10^{-4})T$	$37 < T < 167$
XTX 8004	---	$0.247 + (6.2 \times 10^{-4})T$	$25 < T < 187$

standard. To determine the heat capacity of an explosive, one must establish a base line that indicates the differential heat loss of the two aluminum sample containers at the initial temperature. This is done by placing two empty sample containers in the DSC sample holders and subjecting them to a linearly increasing temperature. Next, a weighed sample of test explosive is placed in one container, both containers are subjected to the linearly increasing temperature, and the heat flow rate is recorded as a function of temperature. Then the procedure is repeated with a weighed sample of synthetic sapphire.

The heat capacity at any temperature is calculated by using $C_p = C_{pl}(m_l) \times (h)/mh_l$, where C_p = heat capacity of the explosive at temperature T, C_{pl} = heat capacity of the sapphire at temperature T, m = weight of the explosive sample, m_l = weight of the sapphire, h = baseline deflection of the explosive sample, and h_l = baseline deflection of the sapphire.

2.2 Thermal Conductivity. Two steady-state procedures have been used to determine the thermal conductivity of explosives. The first is the guarded hot plate (GHP) procedure that the American Society for Testing and Materials (ASTM) uses and describes[2] to test insulating materials in ASTM Source C-177. The second procedure involves a differential scanning calorimeter.[1] The DSC sample is much smaller and more suitable for testing high explosives than is the GHP sample.

The DSC method requires two identical right circular cylinders, one of the test material and the other of a reference material. The thermal conductivity is determined, under steady-state conditions, from the heat flow and temperature drop along the cylinder length. The following equations apply.

$$q_1 = \frac{k_1 A_1 \Delta T}{L_1}$$

and

$$q_2 = \frac{k_2 A_2 \Delta T}{L_2} ,$$

where

$q_1 - q_2$ = DSC output,
A = area of cylinder base,
L = cylinder length,
ΔT = temperature drop along the cylinder length,
k_1 = thermal conductivity of reference material,

and

k_2 = thermal conductivity of unknown.

Because ΔT, A, and L of both the reference and unknown are indentical, the thermal conductivity of the unknown is given by

$$k_2 = k_1 - \frac{(q_1 - q_2)\ L}{A\ \Delta T}$$

For thermal conductivity measurements, the DSC must have a sample-mounting structure consisting of a common metal plate or heat sink, an insulating block, an aluminum radiation shield, and sample holders. The unknown and reference samples are placed in good thermal contact with the sample holder plate and are surrounded by an aluminum radiation shield. An insulating block separates the heat sink and shield. The tops of the samples make thermal contact with a copper heat sink through two circular holes in the insulating block. Thermocouples in the heat sink and sample holders measure the temperature at the sample surfaces.

2.3 Coefficient of Thermal Expansion. Two procedures were used to measure the coefficient of thermal expansion. That used for large specimens was the

Table 2.02 THERMAL CONDUCTIVITY

Explosive	Density (g/cm³)	Thermal Conductivity (cal/cm-s-°C)	Test Temperature or Temperature Range (°C)	Method
		Pure Explosives		
DATB	1.834	6×10^{-4}	---	DSC[a]
HMX	1.91	1×10^{-3}	---	DSC
NQ	1.65	1.014×10^{-3}	41	DSC
RDX	1.806	2.53×10^{-4}	---	GHP[b]
TATB	1.938	1.3×10^{-3}	---	GHP
Tetryl	1.73	6.83×10^{-4}	---	GHP
TNT	1.654	6.22×10^{-4}	---	GHP
TPM	1.75	5×10^{-4}	---	GHP
		Castable Mixtures		
Comp B	1.730	5.23×10^{-4}	30-46	GHP
Cyclotol 75/25	1.760	5.41×10^{-4}	45	GHP
		Plastic-Bonded Explosives		
HMX-Based				
PBX 9011	1.772	9.08×10^{-4}	43.4	GHP
PBX 9404	1.845	9.2×10^{-4}	46.2	GHP
PBX 9501	1.847	1.084×10^{-3}	55	GHP
PETN-Based				
XTX 8003	1.54	3.42×10^{-4}	39.8	GHP
RDX-Based				
PBX 9010	1.875	5.14×10^{-4}	48.8	GHP

[a]Differential scanning calorimeter.
[b]Guarded hot plate method.

American Society for Testing and Materials procedure D696-70, "Coefficient of Linear Expansion of Plastics." A DuPont Model 900 thermal analyzer equipped with a Model 941 thermomechanical analyzer (TMA) was used for single crystals and small specimens. They are denoted by ASTM and TMA in the following tables.

2.4 Thermal Decomposition Kinetics. The thermal decomposition rate constants of explosives, discussed in detail by R. N. Rogers,[3,4] are found using a differential scanning calorimeter at constant temperature.

The kinetic constants were determined using a Perkin-Elmer DSC-1B or DSC-2. Samples were sealed in Perkin-Elmer No. 219-0062 aluminum cells perforated by a single 0.15-mm-diam hole. Differential and average temperature calibrations of the DSC-1B were checked before the runs.

The recorder and the DSC with two empty cells on its supports are set at the test temperature. The sample cell is removed, and the instrument is allowed to equilibrate. The recorder is started, the instrument range switch is set, and the sample is dropped onto the support. The sharp break on the record is used to mark zero time. (The absolute position of the zero point on the time axis is unimportant because rate constants are determined from the slope of the ln deflection, b, vs time, t, plot.)

The DSC deflection above the base line, b, is directly proportional to the rate of energy evolution or absorption by the sample, dq/dt, which is proportional in turn, to the reaction rate da/dt. Therefore,

$$\alpha b = \beta dq/dt = da/dt = k(1 - a) , \tag{1}$$

where α and β are proportionality constants and k is the rate constant. Hence,

$$\ln b = \ln k/\alpha + \ln(1 - a) . \tag{2}$$

For a first-order reaction,

$$-\ln(1 - a) = kt + C , \tag{3}$$

where C is a constant. Substituting Eq. (3) into Eq. (2) and combining constants gives

$$\ln b = C - kt .$$

Therefore, rate constants for first-order reactions can be obtained directly from a plot of ln deflection vs time. This provides the rate constant, k, as a function of temperature, since k is given by

$$k = Ze^{-E/RT},$$

where

Table 2.03 COEFFICIENT OF THERMAL EXPANSION

Explosive	Density (g/cm^3)	Coefficient of Thermal Expansion (1/°C)	Valid Temperature Range (° C)	Procedure
		Pure Explosives		
PETN	---	$(8.55 \times 10^{-5}) + (1.82 \times 10^{-7})T + (6.30 \times 10^{-10})T^2 + (2.17 \times 10^{-12})T^3$	$-160 < T < 100$	TMA[a]
	---	$(6.75 \times 10^{-5}) + (1.28 \times 10^{-2})T + (0.74 \times 10^{-10})T^2 + (1.27 \times 10^{-12})T^3$	$-160 < T < 100$	TMA[b]
	---	$(2.205 \times 10^{-4}) + (4.38 \times 10^{-7})T + (7.78 \times 10^{-10})T^2 + 4.71 \times 10^{-12})T^3$	$-160 < T < 100$	TMA[c]
RDX	---	$(1.833 \times 10^{-4}) + (3.625 \times 10^{-7})T + (5.48 \times 10^{-10})T^2$	$-100 < T < 135$	TMA
TNT	---	$(5.0^{-} \times 10^{-5}) + (7.8 \times 10^{-8})T$	$-40 < T < 60$	ASTM
		Castable Mixtures		
Baratol	---	$(3.4 \times 10^{-5}) + (2.8 \times 10^{-7})T$	$-40 < T < 60$	ASTM
Comp B	---	5.46×10^{-5}	$6 < T < 25$	ASTM
		Plastic-Bonded Explosives		
HMX-Based				
PBX 9011	1.722	2.22×10^{-5}	$25 < T < 74$	ASTM
PBX 9404	1.840	4.7×10^{-5}	$25 < T < 74$	ASTM
PBX 9501	1.835	4.91×10^{-5}	$-54 < T < 74$	ASTM
PETN-Based				
XTX 8003	---	1.65×10^{-4}	$-50 < T < 25$	ASTM

[a]Linear expansion along 001-axis.
[b]Linear expansion along 100-axis.
[c]Volume coefficient of expansions.

Z = the pre-exponential factor in reciprocal seconds,

and

E = energy in kilocalories per mole.

The chemical Arrhenius data plot, ln k as a function of 1/T, was used to obtain Z and E.

The fraction decomposed is determined by Simpson's Rule integration using closely spaced deflection measurements.

Table 2.04 DECOMPOSITION KINETICS

Explosive	State	Density (g/cm^3)	Heat of Reaction, Q (cal/g)	Z (1/s)	Activation Energy, E (kcal/mole)
		Pure Explosives			
BTF	Liquid	1.901	600	4.11×10^{12}	37.2
DATB	Liquid	1.834	300	1.17×10^{15}	46.3
DIPAM	Liquid	1.79	---	2.22×10^{9}	29.2
HMX	Liquid	1.81	500	5×10^{19}	52.7
	Vapor	---	---	1.51×10^{20}	52.9
HNS	Liquid	1.65	500	1.53×10^{9}	30.3
NQ	Liquid	1.74	500	2.84×10^{7}	20.9
PATO	Liquid	1.70	500	1.51×10^{10}	32.2
PETN	Liquid	1.74	300	6.3×10^{19}	47.0
RDX	Liquid	1.72	500	2.02×10^{18}	47.1
	Vapor	---	---	3.14×10^{13}	34.1
TATB	Solid	1.84	600	3.18×10^{19}	59.9
Tetryl	Liquid	1.73	---	2.5×10^{15}	38.4
TNT	Liquid	1.57	300	2.51×10^{11}	34.4
TPM	Liquid	1.75	---	1.05×10^{16}	48.5

2.5 Heats of Combustion and Formation. Combustion experiments were conducted in a stationary oxygen-bomb calorimeter that had an automatically controlled adiabatic jacket. The calorimeter was calibrated by burning standard benzoic acid to determine its effective energy equivalent.

The standard heat of combustion of the explosive (in kilocalories per mole) was calculated by use of

$$\Delta H_c^\circ = \Delta E_c^\circ + 0.593 \left(\frac{d}{2} - \frac{b}{4} + \frac{c}{2}\right),$$

where b, c, and d are subscripts in the chemical formula $C_aH_bN_cO_d$,

ΔH_c° = standard heat of combustion at 25°C,

and

ΔE_c° = standard internal energy of combustion at 25°C.

The standard heat of formation of the explosive (in kilocalories per mole) was calculated by the use of

$$\Delta H_f^\circ = a\Delta H_f^\circ(CO_2,g) + \frac{b}{2}\Delta H_f^\circ (H_2O,1) - \Delta H_c^\circ$$

where ΔH_f° = the standard heat of formation of sample,

$\Delta H_f^\circ(CO_2,g) = -94.051$ kcal/mole,

$\Delta H_f^\circ(H_2O,l) = -68.315$ kcal/mole,

and a and b are the same subscripts as above.

Table 2.05 STANDARD HEATS OF COMBUSTION AND FORMATION

Explosive	Heat of Combustion, ΔH_c° (kcal/mole)	Heat of Formation, ΔH_f° (kcal/mole)
ABH	−2578.4	116.3
BTF	−708.1	143.8
BTX	−1336.2	70.9
DATB	−711.5	−23.6
DIPAM	−1326.8	−6.8
DODECA	−2512.8	50.6
HMX	−660.7	11.3
HNAB	−1333.2	67.9
bis-HNAB	−2653.3	191.1
HNBP	−1279.9	14.6
HNS	−1540.3	18.7
NONA	−1891.2	27.4
NQ	−210.4	−20.29
ONT	−1917.6	19.7
PADP	−1917.4	147.7
PATO	−959.5	36.3
PENCO	−1366.9	−26.6
PETN	618.7	110.34
PYX	−1858.8	20.9
RDX	−501.8	14.7
T-TACOT	−1377.7	112.4
Z-TACOT	1375.7	110.5
TATB	−735.9	−33.4
Tetryl	−836.8	7.6
TNN	−1090.0	12.3
TNT	−817.2	−12.0
TPB	−2502.6	−62.1

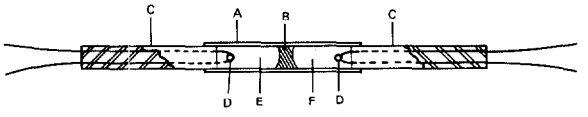

Fig. 2.01. Differential thermal analysis cell.
A. Stainless steel tube
B. Plug
C. Thermocouple insulator
D. Thermocouple junction
E. Sample compartment

2.6 Differential Thermal Analysis and Pyrolysis Test. Smothers and Chiang[5] give a complete discussion of the differential thermal analysis technique, and its theory and a complete review is given in the Analytical Reviews edition of *Analytical Chemistry*.[6]

Figure 2.01 shows the DTA cell design. The 0.139-in.-o.d., 1.25-in.-long stainless steel hypodermic tube, A, is reamed to accept the 0.115-in.-o.d. thermocouple insulators, C. The relatively low thermal conductivity of stainless steel allows use of the axial cell arrangement. The plug, B, between the sample and reference sides of the cell is made by impregnating a small wad of quartz wool with Sauereisen cement and packing it into the center of the tube. After the cement is dry, the cell is ignited in a burner flame. The thermocouples, D, made from 28-gauge Chromel/Alumel, are arc-welded against a carbon rod at the clipped end of a single twist of both wires.

Expendable tube furnaces are a 75-ohm helical coil of Nichrome wire distributed on a helically grooved, 3-in.-long, 11/16-in.-i.d. Alundum tube. A 21/32-in.-o.d. by 3/8-in.-i.d. by 3-in.-long graphite tube is used as a furnace liner for thermal ballast. A 1/4-in.-o.d. aluminum tube is inserted into the furnace liner but is isolated from it by asbestos "O" rings at each end. The natural tubing-cutter constrictions at the ends of the aluminum tube support the thermocouple insulators of the DTA cell and keep it from touching the aluminum walls. A 6-in. cube of foamed glass contains and insulates the assembly. The entire assembly is placed in a blast shield box before a run is started.

The reference thermocouple that indicates cell temperature is connected to the abscissa terminal of a Moseley Autograf Model 2 X-Y recorder. A Leeds and Northrup Model 9835-B dc microvolt amplifier amplifies the differential thermocouple output, which is then connected to the ordinate terminal of the X-Y recorder. An F&M Model 40 linear temperature programmer, which provides a constant heating rate to the cell, is controlled by a thermocouple placed between the Alundum furnace shell and the graphite liner.

Five- to twenty-milligram samples give the best results, but samples as small as 3 mg can be tested. The differential temperature scale normally used is ± 5°C, but the sensitivity can be increased to record differential temperatures of ± 0.5°C.

A deflagration usually does not damage the DTA cell beyond repair. A low-order explosion will destroy the sample thermocouple, but the thermocouple can be replaced without changing the zero-line characteristics of the cell. Detonation of a 10-mg sample will destroy the entire assembly, often including the insulation.

Pyrolysis. Figure 2.02 shows the apparatus used to obtain the pyrolysis curves, and Fig. 2.03 gives details of the pyrolysis block. In this test an ~10-mg sample of

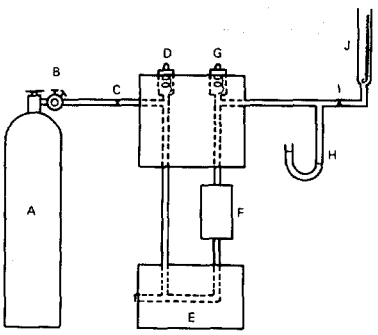

Fig. 2.02. Pyrolysis apparatus.
A. Carrier gas supply
B. Pressure regulator
C. Flow control needle valve
D. Reference thermal conductivity cell
E. Pyrolysis chamber
F. Combustion tube
G. Active cell
H. Manometer
I. Pressure control needle valve
J. Rotameter

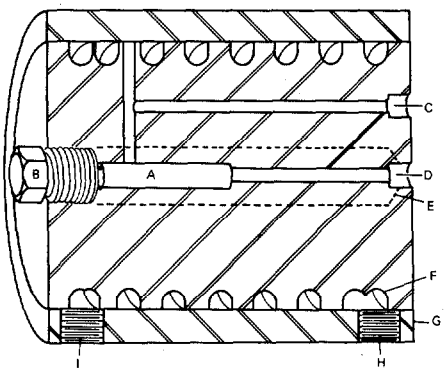

Fig. 2.03. Pyrolysis block.
A. Pyrolysis chamber
B. Nickel plug
C. Carrier gas inlet
D. Carrier gas outlet
E. Cartridge heater wells (2)
F. Helical threads cut in inner body of block
G. Outer shell of block
H. Cooling jacket inlet
I. Cooling jacket outlet

test material is weighed into a small combustion boat and placed in the pyrolysis chamber, initially at room temperature. A 10- to 15-ml/min flow of helium is then started, and when the air has been swept out, the pyrolysis chamber temperature is raised at a constant rate, usually 10°C/min. The helium stream carries gases evolved from the sample through the combustion tube and into the thermal conductivity cell, G. The two cells, D and G, form two arms of a Wheatstone bridge whose output varies with the concentration of impurities (decomposition products, etc.) in the effluent helium stream. The bridge output is fed to one axis of an X-Y recorder, and the pyrolysis chamber temperature is fed to the other. In this manner, the rate of gas evolution from the sample as a function of chamber temperature is determined.

The combustion chamber converts the more complex products, such as undecomposed but vaporized explosive, to simple molecules. This increases the bridge sensitivity and also keeps these products from condensing in the cooler parts of the apparatus.

Data Presentation. All the DTA curves were determined at a heating rate of 11°C/min with granular NaCl as the reference sample. All the pyrolysis curves were determined at a heating rate of 10°C/min. Gas-solid interactions were minimimized because gaseous products were swept away from the sample in the pyrolysis apparatus as rapidly as they were formed.

Any possible contribution to the reaction from atmospheric oxygen also was eliminated, because the carrier gas was helium.

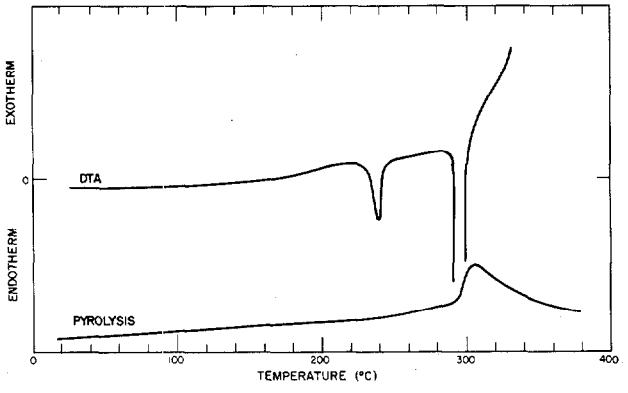
EXOTHERM
0
ENDOTHERM
DTA
PYROLYSIS
0
100
200
300
400
TEMPERATURE (°C)

DATB

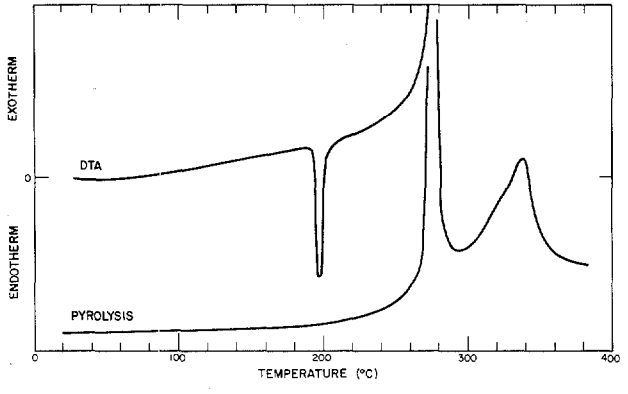
EXOTHERM
0
ENDOTHERM
DTA
PYROLYSIS
0
100
200
300
400
TEMPERATURE (°C)

HMX

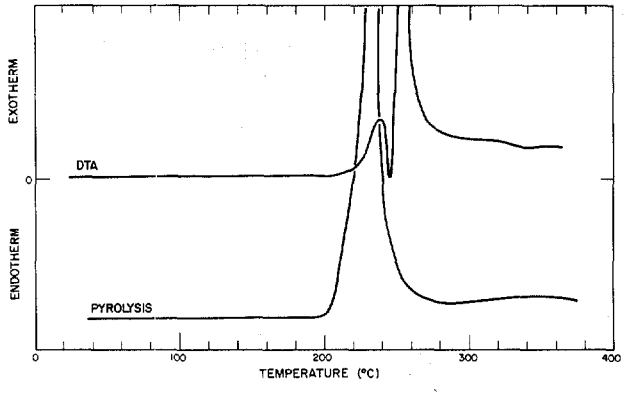
EXOTHERM
0
ENDOTHERM
DTA
PYROLYSIS
0
100
200
300
400
TEMPERATURE (°C)

NQ

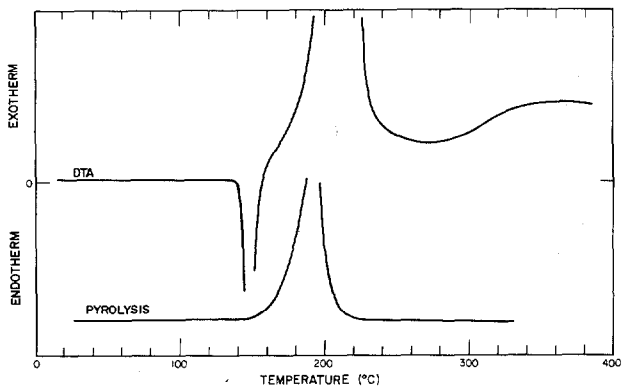

PETN

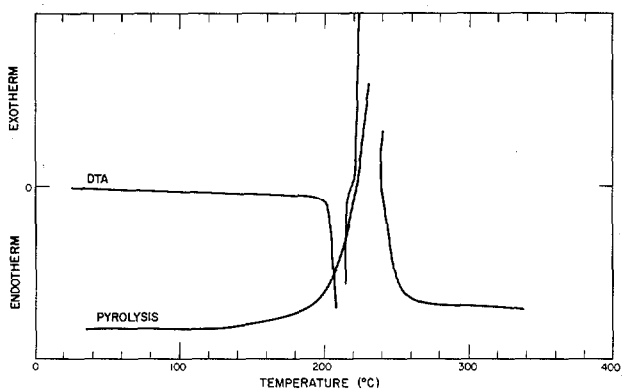

RDX

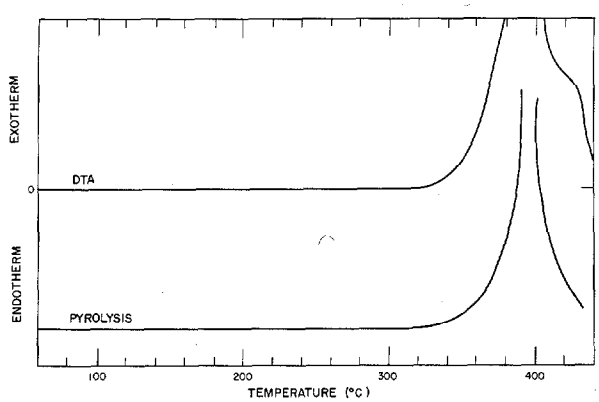

TATB

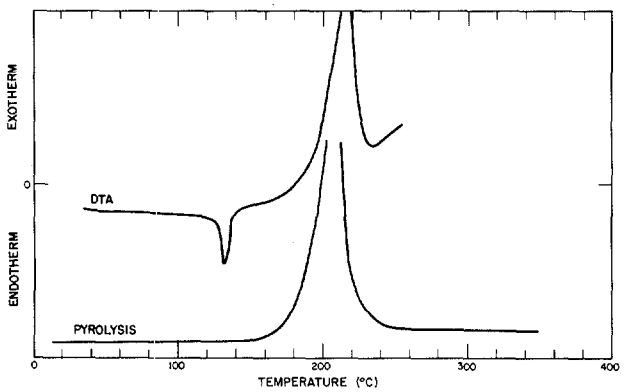

Tetryl

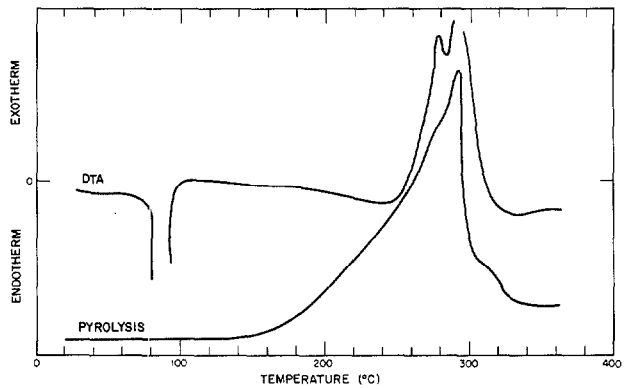

TNT

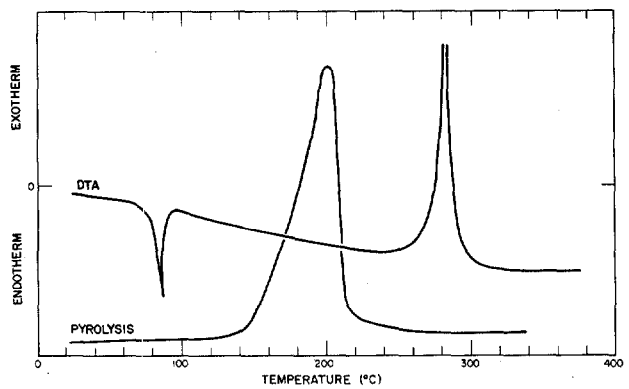

Baratol

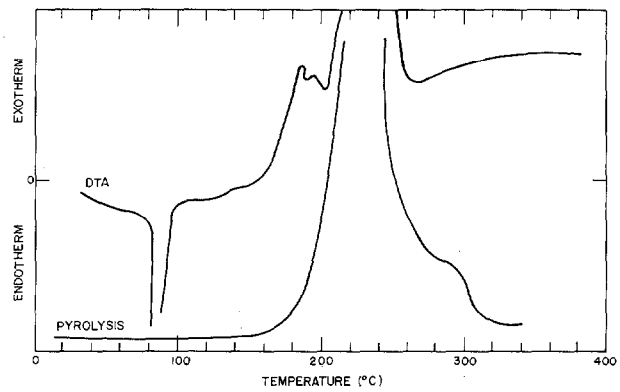

Composition B

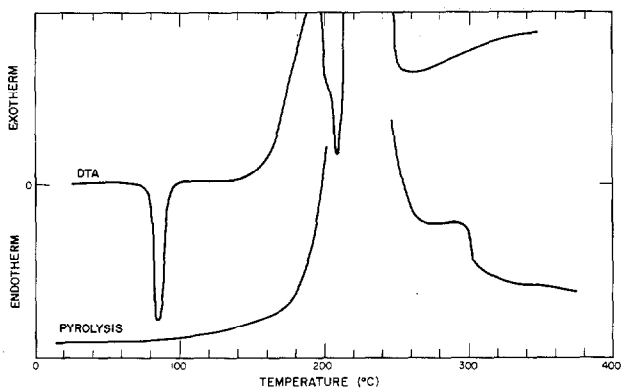

Cyclotol 75/25

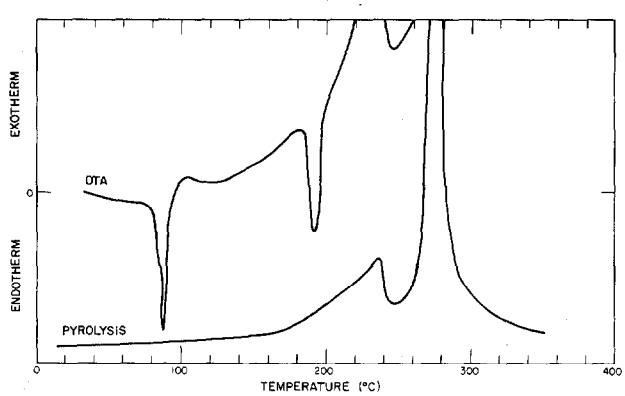

Octol

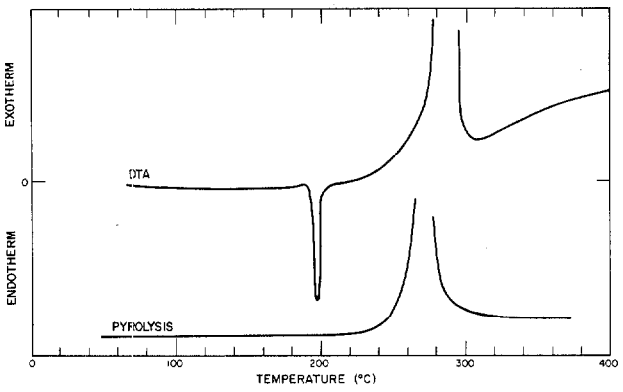

PBX 9501

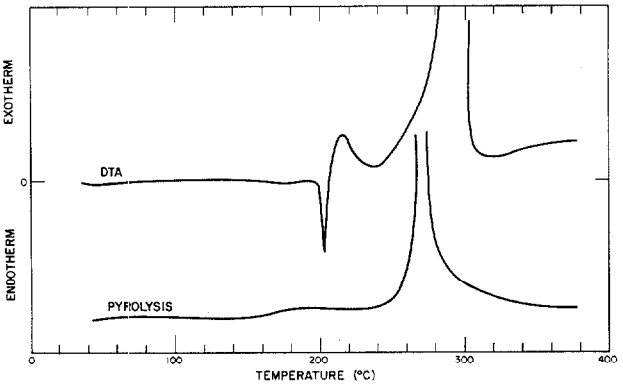

PBX 9404

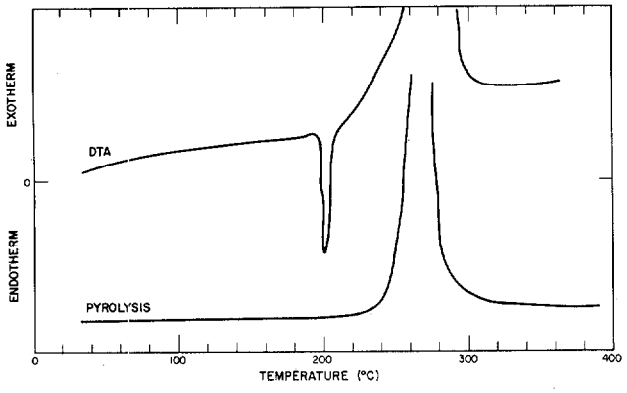

PBX 9011

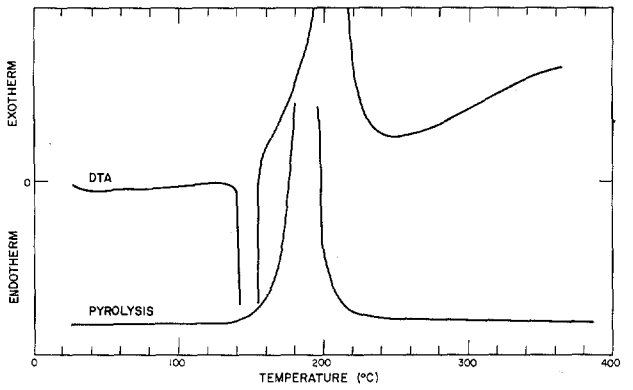

XTX 8003

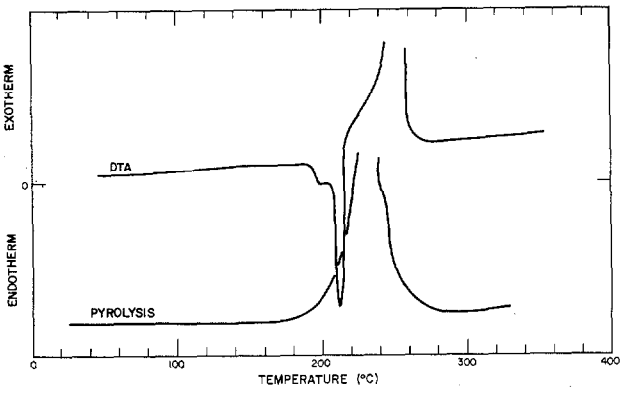

PBX 9407

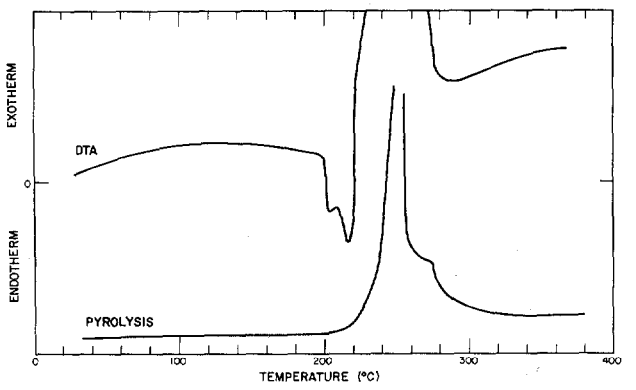

XTX 8004

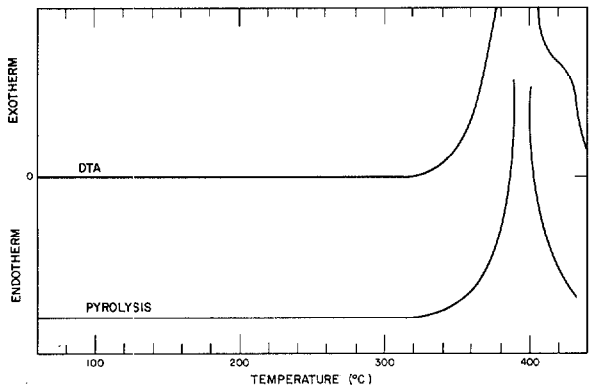

PBX 9502

2.7 Time-to- Explosion Test. All explosives decompose exothermally at temperatures above absolute zero. When chemical decomposition produces heat faster than it can be dissipated to the surroundings, the explosive mass self-heats to explosion. In steady-state conditions, the temperature at which a thermal explosion is produced is called the critical temperature, Tm. A relatively simple expression for the critical temperature has been derived[7] in terms of the kinetic and physical parameters.

$$Tm = \frac{E}{R \ln \frac{A^2 \rho Q Z E}{Tm^2 \lambda \delta R}} ,$$

where

R = gas constant, 1.987 cal/mole,
A = radius of sphere, cylinder, or half-thickness of a slab,
ρ = density,
Q = heat of decomposition reaction,
Z = pre-exponential factor,
E = activation energy,
λ = thermal conductivity,
δ = shape factor (0.58 for infinite slabs, 2.0 for infinite cylinders, 3.32 for spheres).

The LASL method for determining critical temperatures is based on a time-to-explosion test that Henkin[8] developed. The explosive sample, usually 40 mg, is pressed into a DuPont E-83 aluminum blasting-cap shell and covered with a hollow, skirted plug. A conical punch is used to expand the plug and apply a reproducible 400-lb force. This plug expansion forms a positive seal and confines the sample in a known geometry. The density, which can be calculated from a sample thickness measurement, is usually about 90% of the crystal density.

This assembly is dropped into a preheated liquid metal bath, and the time to explosion is measured as the time to the sound created by the rupture of the blasting cap or unseating of the plug. The lowest temperature at which a runaway reaction can be obtained is the Tm. Many tests are required to determine Tm with confidence, because it is necessary to raise and lower the bath temperature across the apparent Tm, make many separate tests, and allow enough time for a reaction. A safe failure criterion for 40-mg samples is no explosion in 1000 seconds. We have never obtained an explosion after 10 000 seconds.

Because the reactions can be violent, the metal-bath enclosure shown in Fig. 2.04 is used. The baffles keep most of the hot metal in the chamber, and the test can be made behind a shield in a fume hood.

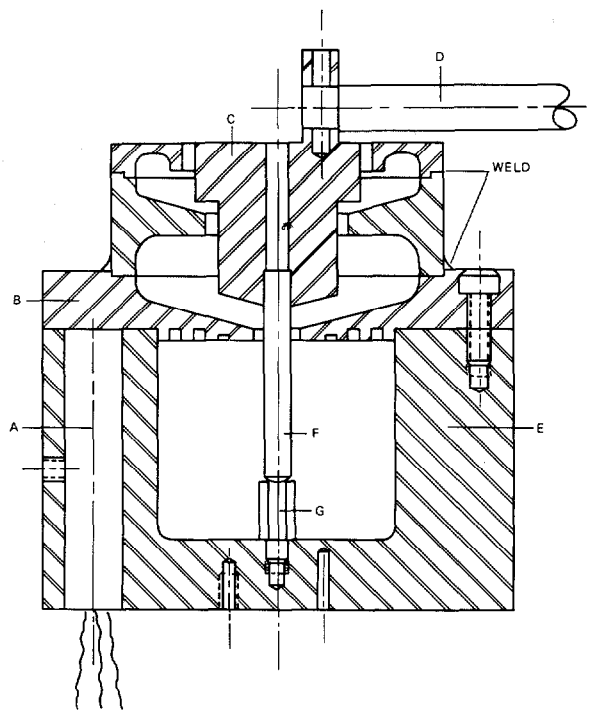

Fig. 2.04. Time-to-explosion test metal-bath assembly.
A. Cartridge heaters (3 each)
B. Top assembly, bolted to base
C. Sample-cell holder (the sample cell is insulated from the holder by a band of glass tape around its top)
D. Sample-cell holder pivot arm, which allows cell and holder to be inserted remotely into the lower assembly
E. Metal-bath container, made from mild steel for stability when containing molten metal
F. Sample cell
G. Sample cell support pedestal, whose length is adjusted to the sample cell length

Table 2.06 TIME-TO-EXPLOSION TEST

Explosive	T_m (°C)	a (mm)	Density (g/cm^3)
	Pure Explosives		
BTF	249 ± 1	0.33	1.81
DATB	321 ± 2	0.35	1.74
HMX	253 ± 1	0.33	1.81
HNS	320 ± 1	0.37	1.65
NQ	202 ± 2	0.39	1.63
PATO	281 ± 1	0.37	1.70
PETN	201 ± 2	0.34	1.74
RDX	216 ± 1	0.35	1.72
TATB	331 ±P 1	0.331.84	
TNT	288 ± 1	0.38	1.57
TPM	316 ± 2	0.72	1.66
	Castable Explosives		
Amatex/20	226 ± 4	0.35	---
Comp B	214	0.35	---
Cyclotol 75/24	208	0.35	---
	Plastic-Bonded Explosives		
PBX 9404	236 ± 1		

REFERENCES

1. John F. Baytos, Los Alamos Scientific Laboratory report LA-8034-MS (September 1979).

2. W. P. Brennan, B. Miller, and J. C. Whitwell, Journal of Applied Polymer Science **12**, 1800-1902 (1968).

3. R. N. Rogers, Thermochimica Acta **3**, 437-447 (1972).

4. R. N. Rogers, Analytical Chemistry **44**, 1336-1337 (1972).

5. W. J. Smothers and Ya O. Chiang, *Differential Thermal Analysis* (Chemical Publishing Co., Inc., New York, 1958).

6. C. B. Murphy, Analytical Chemistry **32**, 168 R-171R (1960).

7. John Zinn and Charles L. Mader, Journal of Applied Physics **31**, 323-328 (1960).

8. H. Henkin and R. McGill, Industrial Engineering Chemistry **44**, 1391 (1952).

3. DETONATION PROPERTIES

3.1 Detonation Velocity and Diameter Effect. The velocity with which a steady detonation travels through an explosive is measured by using a broomstick-shaped piece of the explosive, called a rate stick. A standard rate stick is a right cylinder, usually composed of a number of shorter cylinders that have been cast, pressed, or machined to a predetermined diameter. The stick is detonated at one end, and the progress of the detonation is measured at discrete points along the stick length. The locations of the measurement points are determined with a micrometer. The times at which the detonation front reaches these points are determined by using the high conductivity or pressure at the detonation front to close an electrical switch called a pin. The switch closure allows a capacitor to discharge, and the associated signal is recorded on a fast oscilloscope. The detonation velocity can be calculated from the measured distances and times by using an appropriate numerical procedure.

Sometimes optical records of the detonation trajectory along the stick have been obtained with a smear camera, but this less precise method is used only in special circumstances, as for very small diameter sticks in which pins might perturb the detonation wave significantly.

When a rate stick is detonated initially, there usually are velocity transients for some distance along its length. Therefore, the data from the first part of the run, a distance equal to six rate stick diameters, usually are discarded. Detonation velocities in plastic-bonded explosives pressed to more than 95% of theoretical density commonly are measured to within 0.1% by these techniques.

Liquid-explosive rate sticks must be contained in rigid cylinders. The way in which this container affects the detonation velocity and the explosive diameter at which failure occurs is called the confinement effect. When measuring the detonation velocity of a confined explosive, one should make the container walls thick enough to represent infinitely thick walls, to simplify data interpretation.

Details of these techniques are given in A. W. Campbell and Ray Engelke, *Sixth Symposium (International) on Detonation, San Diego, California, August 1976,* Office of Naval Research Symposium report ACR-221, and in other works cited therein.

Diameter-Effect Curve

The velocity of a detonation traveling in a cylindrical stick decreases with the stick diameter until a diameter is reached at which detonation no longer propagates. That is called the failure diameter. The steady detonation velocity as a function of the rate stick radius is given by $D(R) = D(\infty)[1 - A/(R - R_c)]$, where $D(R)$ and $D(\infty)$ are the steady detonation velocities at rate stick radius R and at infinite radius, respectively. A and R_c are fitting parameters. Campbell and Engelke discuss this fitting form. Table 3.01 lists nonlinear least squares fits of this function to empirical data. The fits can be used to interpolate the detonation velocity at any diameter that will allow detonation to propagate.

Table 3.01 PARAMETERS OF THE DIAMETER-EFFECT CURVE[a]

Explosive	Data, Points/ Diameter[b]	Density/TMD[c] (g/cm³)	% TMD[c]	$D(\infty) \pm \sigma_D$ (mm/μs)	$R_c \pm \sigma_{R_c}$ (mm)	$(A \pm \sigma_A) \times 10^2$ (mm)	Experiment Failure[d] Radius (mm)	Comments
Nitromethane (liquid)	9/5	1.128/1.128	100	6.213 ± 0.001	−0.4 ± 0.1	2.6 ± 0.2	1.42 ± 0.21	The fit shows slight upward concavity. Fired in brass tubes with 3.18-mm-thick walls.
Amatex/20	4/4	1.613/1.710	94.3	7.030 ± 0.010	4.4 ± 0.2	59 ± 3.	8.5 ± 0.5	Nominally 20/20/40 RDX/TNT/AN. Median AN particle size was ≈0.5 mm.
Baratol 76	3/3	2.619/2.63	99.6	4.874	4.36	102	21.6 ± 2.5	24/76 TNT/$Ba(NO_3)_2$. Interpolating fit.
Comp A	5/5	1.687/1.704	99.0	8.274 ± 0.003	1.2 ± 0.1	1.39 ± 0.17	<1.1	92/8 RDX/wax. No sticks failed.
Comp B	26/12	1.700/1.742	97.6	7.859 ± 0.010	1.94 ± 0.02	2.84 ± 0.19	2.14 ± 0.03	36/63/1 TNT/RDX/wax
Cyclotol 77/23	8/8	1.740/1.755	99.1	8.210 ± 0.014	2.44 ± 0.12	4.89 ± 0.82	3.0 ± 0.6	77/23 RDX/TNT
Destex	7/4	1.696/1.722	98.5	6.816 ± 0.009	0.0[e]	59.4 ± 0.035	14.3 ± 1.6	75/19/5/1/1 TNT/Al/wax/carbon black. $R_c \equiv 0$.
Octol	8/6	1.814/1.843	98.4	8.481 ± 0.007	1.34 ± 0.21	6.9 ± 0.9	<3.2	77/23 HMX/TNT
PBX 9404	15/13	1.846/1.865	99.0	8.773 ± 0.012	0.553 ± 0.005	0.89 ± 0.08	0.59 ± 0.01	94/3/3 HMX/NC/CEF
PBX 9501	7/5	1.832/1.855	98.8	8.802 ± 0.006	0.48 ± 0.02	1.9 ± 0.1	<0.76	95/2.5/1.25/1.25 HMX/Estane/ BDNPA/BDNPF
X-0219	8/6	1.915/1.946	98.4	7.627 ± 0.015	0.0[e]	26.9 ± 2.3	7.5 ± 0.5	90/10 TATB/Kel-F 800
X-0290	5/5	1.895/1.942	97.6	7.706 ± 0.009	0.0[e]	19.4 ± 0.8	4.5 ± 0.5	95/5 TATB/Kel-F 800
XTX 8003	162/4	1.53/1.556	98.3	7.264 ± 0.003	0.113 ± 0.007	0.018 ± 0.002	0.18 ± 0.05	80/20 PETN/silicone rubber Fired as half-cylinder confined in polycarbonate.

[a]Fired in air confinement, unless otherwise noted.
[b]Number of shots that propagated a steady wave/number of distinct diameters at which observations were made.
[c]TMD = theoretical maximum density.
[d]R_r is the average of the radii from two go/no-go shots, σ_r is one-half the difference in the go/no-go radii.
[e]R_c fired at 0.0 gives the smallest variance of fit.

Table 3.02 DETONATION VELOCITY vs COMMERCIAL-GRADE LIQUID NITROMETHANE[a] RATE STICK DIAMETER

Rate Stick Diameter (mm)	Average Velocity D (mm/μs)[b]	Length/Diameter[c]
95.25	6.210	8
25.40	6.201	30
25.37	6.200	30
12.79	6.188	60
12.70	6.190	60
6.33	6.169	120
6.43	6.166	120
3.00	6.128	254
3.05	6.125	254
2.41	Failed	316

[a]The nitromethane, which had been purified by redistillation, was confined in brass tubes with 3.18-mm-thick walls that were effectively infinite, unless otherwise specified. The firing temperature was 93.0°F and the density was 1.033 g/cm^3.

[b]D is the average velocity through the stick obtained with electrical pins.

[c]The initiation assembly consisted of an SE-1 detonator, a booster pellet, a P-16, and a cube of Comp B bigger than the tube diameter.

Table 3.03 AMATEX/20[a] DETONATION VELOCITY vs RATE STICK DIAMETER

Shot No.	Rate Stick Diameter (mm)	D ± σ (mm/μs)[b]	Density (g/cm³)	Length/ Diameter	Initiation Assembly	Comments
E-3823	101.6	6.937 ± 0.008	1.613	16.5	1E-23 detonator, P-40, 101.6-mm-diam by 12.7-mm-long Comp B	
E-3819	50.8	6.840 ± 0.013	1.613	19	SE-1 detonator, pellet, P-22, 50.8-mm-diam by 12.7-mm-long Comp B	
E-3817	25.4	6.532 ± 0.033	1.613	16	SE-1 detonator, pellet, P-16 25.4-mm-diam by 22.2-mm-long TNT	
E-3983	17.0	6.029 (Failed)	1.613	5.9	SE-1 detonator, pellet, P-16, 25.4-mm-diam by 25.4-mm-long Amatex/20	Two-segment fit; last piece of four segments failed

[a]The prill size of the ammonium nitrate (AN) was ≈0.5 mm.
[b]Unless otherwise noted, D is the average of the segmental velocities and σ is their standard deviation about D.

Table 3.04 BARATOL 76 DETONATION VELOCITY vs RATE STICK DIAMETER

Shot No.	Rate Stick Diameter (mm)	D ± σ (mm/μs)[a]	Density (g/cm³)	Length/ Diameter	Initiation Assembly	Comments
C-4394	101.60	4.767 ± 0.002	2.619	8.2	1E-23 detonator, P-40	
E-4672	65.30	4.700 ± 0.006	2.619	8.4	1E-23 detonator, P-40	
E-4067	48.13	4.625 ± 0.003	2.619	9.3	SE-1 detonator, pellet, 44.5-mm-diam by 51.2-mm-long cyclotol	
E-4066	38.07	Failed	2.619	10.6	SE-1 detonator, pellet, P-16	Failed

[a]Unless otherwise noted, D is the slope of a linear least squares fit to the detonation trajectory as measured by electrical pins, and σ is one standard deviation of the slope of that line.

Table 3.05 COMPOSITION B DETONATION VELOCITY vs RATE STICK DIAMETER

Shot No.	Rate Stick Diameter (mm)	D ± σ (mm/μs)[a]	Density (g/cm³)	Length/ Diameter	Initiation Assembly[b]
B-727	25.5	7.868	1.706	2	
B-728	25.5	7.887	1.706	2	
B-785	24.8	7.869	1.704	5.2	c
B-785	24.8	7.864	1.702	5.2	c
B-785	24.8	7.847	1.698	5.2	c
B-757	12.7	7.816	1.704	4	
B-758	12.7	7.819	1.703	4	
B-790	10.0	7.787	1.703	5	c
B-790	10.0	7.792	1.701	5	c
B-790	10.0	7.755	1.701	5	c
B-749	8.48	7.738	1.704	6.3	
B-738	8.47	7.742	1.708	6	
B-786	7.95	7.738	1.704	6.4	c
B-786	7.95	7.725	1.704	6.4	c
B-786	7.96	7.746	1.704	6.4	c
B-739	6.36	7.648	1.703	10.4	
B-740	6.35	7.650	1.700	8	
B-780	5.61	7.572	1.706		c
B-781	5.61	7.561	1.706		c
B-748	5.10	7.476	1.705	9.2	
B-750	5.08	7.476	1.705	9.9	
B-784	4.64	7.326	1.703	10.9	c
B-778	4.60	7.308	1.706	11.0	c
B-782	4.45	7.092	1.701	11.4	c
B-783	4.43	7.066	1.703	11.5	c
B-771	4.28	6.709	1.704	7.9	c
B-770	4.27	Failed	1.700	11.8	c

[a]Average velocity through the stick.
[b]SE-1 detonator, pellet, >4-diam Comp B runup.
[c]P-15.

Table 3.06
CYCLOTOL DETONATION VELOCITY vs RATE STICK DIAMETER[a]

Rate Stick Diameter (mm)	D (mm/μs)[b]	Density (g/cm³)
101.6	8.217	1.740
50.8	8.204	1.740
25.4	8.160	1.740
16.9	8.107	1.740
12.7	8.116	1.740
8.5	8.012	1.740
7.3	7.859	1.740
6.4	7.664	1.740
5.6	Failed	1.740

[a]Information on the booster, length-to-diameter ratio, and shot numbers was unavailable.
[b]D is probably the average of a set of segmental velocities.

Table 3.07 DESTEX/X-0309 DETONATION VELOCITY vs RATE STICK DIAMETER

Shot No.	Rate Stick Diameter (mm)	D ± σ (mm/μs)[a]	Density (g/cm³)	Length/ Diameter	Initiation Assembly	Comments
B-8199	101.60	6.743 ± 0.001	1.689	7.0	101.6-mm-diam by 946-mm-long Destex[b]	[c]
B-8208	101.60	6.737 ± 0.002	1.698	7.5	101.6-mm-diam by 584-mm-long Destex[b]	[c]
F-4543	76.20	6.698 ± 0.001	1.698	13.5	101.6-mm-diam by 101.6-mm-long TNT[b]	
F-4106	50.80	6.653 ± 0.004	1.690	10.3	50-mm-diam by 6.4-mm-long PBX 9404[d]	
F-4510	50.80	6.654 ± 0.018	1.700	12.0	50.8-mm-diam by 50.8-mm-long Comp B[d]	
B-8203	50.80	6.671 ± 0.004	1.695	8.1	50.8-mm-diam by 25.4-mm-long PBX 9404[d]	Cylinder test, 5.08-mm-thick OFHC copper wall
E-4542	31.75	6.560 ± 0.003	1.698	12.0	50.8-mm-diam by 76.2-mm-long Comp B[d]	
—						
F-4089	25.37	Failed	1.69	10.0	SE-1 detonator, pellet, 25.4-mm-diam by 28.6-mm-long PBX 9404	Failed

[a]Unless otherwise noted, D is the slope of the linear least squares fit to the detonation trajectory as measured by electrical pins, and σ is one standard deviation of the slope of that line.
[b]IE-23 detonator and P-40.
[c]Cylinder Test, 10.16-mm-thick OFHC copper wall.
[d]SE-1 detonator, pellet, and P-22.

Table 3.08 OCTOL DETONATION VELOCITY vs RATE STICK DIAMETER

Shot No.	Rate Stick Diameter (mm)	D ± σ (mm/μs)[a]	Density (g/cm³)[b]	Length/ Diameter	Initiation Assembly[c]
B-3909	50.79	8.452	1.811	12	Pellet, 50.8-mm-diam by 203-mm-long Octol
B-3913	38.11	8.450	1.810	21.3	38.11-mm-diam Octol
B-3915	22.89	8.415	1.813	17.8	22.9-mm-diam by 50.8-mm-long Octol
E-0074	22.89	8.427	1.813	15.6	Pellet, 22.9-mm-diam by 50.8-mm-long Octol
B-3914	16.30	8.402	1.816	24.9	16.3-mm-diam by 50.8-mm-long Octol
B-3912	16.30	8.400	1.817	24.9	16.3-mm-diam by 50.8-mm-long Octol
B-3919	12.72	8.357	1.816	60	12.7-mm-diam by 50.8-mm-long Octol
E-0081	6.34	8.161	1.816	80	Pellet, 6.35-mm-diam by 50.8-mm-long Octol

[a]D is probably an average of a set of segmented velocities.
[b]All entries are corrected to 1.814-g/cm³ density.
[c]SE-1 detonators.

Table 3.09 PBX 9404 DETONATION VELOCITY vs RATE STICK DIAMETER

Shot No.	Rate Stick Diameter (mm)	D ± σ (mm/μs)	Density (g/cm³)	Length/ Diameter	Initiation Assembly	Comments
B-4339	146.0	8.800	1.844	NA	146-mm-diam Comp B[a]	[b]
B-0768	146.0	8.803	1.844	NA	146-mm-diam Comp B[a]	[b]
B-0768	38.1	8.789	1.844	13.3	38.1-mm-diam by 152-mm-long Comp B[a]	[b]
B-8033	25.4	8.774 ± <0.001	1.846	22	1E23 detonator, P-80, 203-mm by 50.8-mm-thick PBX 9404 203-mm-diam by 0.38-mm-thick polyethylene, 25.4-mm air gap, and 203-mm-diam by 2.54-mm-thick magnesium.	Stick was strongly overdriven with a flying plate.[c]
B-8034	25.4	8.775 ± <0.001	1.846	32	[a,d]	Stick was much underdriven.[c]
B-4370	22.9	8.793	1.844	22	22.9-mm-diam by 9.16-mm-long Comp B[a]	[b]
B-4369	16.31	8.789	1.844	31	16.3-mm-diam by 65.2-mm-long Comp B[a]	[b]
E-0769	12.70	8.776	1.844	40	12.7-mm-diam by 50.8-mm-long Comp B[a]	[b]
E-0746	6.38	8.731	1.844	80	6.38-mm-diam by 25.5-mm-long Comp B[a]	[b]

Table 3.09 (cont)

Shot No.	Rate Stick Diameter (mm)	D±σ (mm/μs)[a]	Density (g/cm³)	Length/ Diameter	Initiation Assembly	Comments
E-3977	2.88	8.651 ± 0.031	1.843	69	Pellet, 10.2-mm-dia. by 7.6-mm-long PBX 9404[a]	D is average velocity. σ is the standard deviation of 3 segmental velocities.
B-8008	2.80	8.668	1.844	10	12.6-mm-diam by 12.6-mm-long tetryl, 6.35-mm-diam by 12-mm-long[d] PBX 9404[a]	[c]
B-8009	2.00	8.525	1.844	16	Tetryl pellet, 6.35-mm-diam by 12-mm-long[d] PBX 9404[a]	[e]
B-8010	1.50	8.355	1.844	18	Tetryl pellet, 6.35-mm-diam by 12-mm-long[d] PBX 9404[a]	[e]
C-4352	1.27	7.874	1.84	8.3	Pellet[a]	[e]
C-4351	1.21	7.279	1.84	20.8	Pellet[a]	[e]
F-2989	1.17	Failed	1.84	10.9	Pellet[a]	Failed

[a]SE-1 detonator.
[b]D from linear least squares fit to detonation trajectory.
[c]σ is one standard deviation of slope of the least squares line.
[d]Pellet, P-16, 25.4-mm-diam by 152-mm-long Amatex/20.
[e]D from least squares fit to optical record of the detonation trajectory.

Table 3.10 PBX-9501 DETONATION VELOCITY vs RATE STICK DIAMETER

Shot No.	Rate Stick Diameter (mm)	D ± σ (mm/μs)[a]	Density (g/cm³)	Length/ Diameter	Booster	Comments
C-4431	25.4	8.790 ± 0.004	1.832	14	25.4-mm-diam by 25.4-mm-long PBX 9404[b]	
C-4521	25.4	8.791 ± 0.001	1.834	12	P-16[b]	[c]
C-4525	25.4	8.792 ± 0.001	1.834	12	P-16[b]	[c]
C-4442	5.01	8.728 ± 0.010	1.832	30	9.5-mm-diam by 9.5-mm-long PBX 9404[b]	[d]
C-4427	2.83	8.612 ± 0.011	1.832	21	10.2-mm-diam by 7.6-mm-long PBX 9404[b]	[d]
C-4440	2.01	8.487 ± 0.013	1.832	24	9.5-mm-diam by 9.5-mm-long PBX 9404[b]	[d]
C-4441	1.58	8.259 ± 0.013	1.832	30	9.5-mm-diam by 9.5-mm-long PBX 9404[b]	[d]

[a]Unless otherwise noted, D is the slope of a linear least squares fit to the detonation trajectory as measured by electrical pins, and σ is one standard deviation of the slope of that line.
[b]SE-1 detonator, pellet.
[c]Cylinder test, 2.54-mm-thick OFHC copper wall.
[d]D and σ from least squares fit to optical record of detonation trajectory.

Table 3.11 COMPOSITION A DETONATION VELOCITY vs RATE STICK DIAMETER[a]

Rate Stick Diameter (mm)	D (mm/μs)[b]
25.37	8.262
12.70	8.254
8.46	8.236
6.35	8.213
5.08	8.172
4.24	8.143

[a]Density is 1.687 g/cm³.
[b]Information on the booster, length-to-diameter ratio, and shot numbers was unavailable.
[c]D is probably the average of a set of segmental velocities.

Table 3.12 PBX-9502 DETONATION VELOCITY vs RATE STICK DIAMETER

Shot No.	Rate Stick Diameter (mm)	D ± σ[a] (mm/μs)	Density (g/cm^3)	Length/ Diameter	Booster
E-4081	50.00	7.649 ± <0.001	1.894	12.0	50.9-mm-diam by 50.8-mm-long Comp B[b]
E-4096	17.98	7.528 ± <0.001	1.895	33.3	25.4-mm-diam by 26.3-mm-long PBX 9404[b]
E-4133	14.00	7.483 ± <0.001	1.893	21.4	25.4-mm-diam by 26.3-mm-long PBX 9404[b]
E-4133	12.00	7.455 ± 0.001	1.894	25.0	14-mm-diam by 300-mm-long PBX 9502[b]
F-3768	10.00	7.407 ± 0.001	1.894	30.0	10.2-mm-diam by 15.2-mm-long PBX 9404[b]
F-8074	7.96	Failed	1.894	14.2	[b]

[a]Unless otherwise noted, D is the slope of a linear least-squares fit to the detonation trajectory as measured by electrical pins and σ is one standard deviation of the slope of that line.
[b]SE-1 detonator, pellet.

Table 3.13 X-0219 DETONATION VELOCITY vs RATE STICK DIAMETER

Shot No.	Rate Stick Diameter (mm)	D ± σ (mm/μs)[a]	Density (g/cm³)	Length/ Diameter	Booster	Comments
C-4436	50.8	7.555 ± 0.002	1.912	12	P-22, 50.8-mm-diam by 6.4-mm-long PBX 9404[b]	
E-3621	41.2	7.531 ± 0.018	1.920	6.2	P-22, 38.1-mm-diam by 114-mm-long Comp B[b]	Velocity is average of segmental values and σ is standard deviation of same.
C-4438	25.4	7.462 ± <0.001	1.911	24	P-16, 25.4-mm-diam by 25.4-mm-long PBX 9404[b]	
E-4118	25.4	7.457 ± <0.001	1.913	12	P-16, 25.4-mm-diam by 26.3-mm-long PBX 9404[b]	Test of effect of pressing direction
E-4119	25.4	7.453 ± <0.001	1.916	12	P-16, 25.4-diam by 26.3-mm-long PBX 9404[b]	Test of effect of pressing direction
C-4395	18.0	7.397 ± 0.002	1.915	11.1	P-16, 25.4-mm cube Comp B	
E-4095	15.9	7.380 ± <0.001	1.916	18.9	25.4-mm-diam by 26.3-mm-long PBX 9404[b]	
E-4095	14.0	Failed	1.915	21.4	Shot E-4095 booster plus 300-mm-long by 15.9-mm-diam X-0219[b]	Failed

[a]Unless otherwise noted, D is the slope of a linear least squares fit to the detonation trajectory as measured by electrical pins, and σ is one standard deviation of the slope of that line.
[b]SE-1 detonator, pellet.

Table 3.14 XTX-8003 DETONATION VELOCITY vs RATE STICK DIAMETER

Shot No.	Rate Stick Diameter (mm)	D ± σ (mm/μs)[b]	Density (g/cm³)	Length/ Diameter	Booster
[c]	1.02	7.248 ± 0.014	1.53	199	1E30
	0.45	7.244 ± 0.016	1.53	452	1E30
	0.26	7.167 ± 0.015	1.53	782	1E30
	0.19	7.087 ± 0.021	1.53	1069	1E30

[a]Fired in half-cylinder geometry confined in polycarbonate.
[b]D is the average of the linear least squares detonation velocities obtained from the 41 shots, and σ is the standard deviation of the D values about the average value.
[c]Because these values are average results from 41 shots at each diameter, shot numbers are not listed.

3.2 Cylinder Test Performance. The cylinder test, developed at the Lawrence Livermore Laboratory, is used to compare directly the dynamic performance of explosives or to derive empirical equations of state for their detonation products.

A 1-in.-i.d. OFHC copper tube is filled with the test explosive. The tube wall thickness is controlled to give a nominal loading of 4.0331 grams of copper per cubic centimeter of explosive. The explosive is detonated at one end of the tube, and a rotating mirror camera records tube wall expansion as a function of time. The camera slit is positioned at a point 9 diameters (228.6 mm) along the tube from the detonated end.

The wall position -vs- time record on the camera film is measured in approximately 500 places, and these data are fitted with a seventh-order polynomial or various splines. Wall velocities are then obtained by differentiating the fits. Fine detail in the wall motion can be resolved by increasing the number of knots in the spline-fitting form from 15 to 30 or 50.

Given test explosive diameters at which detonation velocity varies little, the tube wall trajectory scales linearly with cylinder diameter. Therefore data from tests at nonstandard diameters are commonly scaled to 25.4 mm for comparison. For two common nonstandard diameters, 50.8 and 101.6 mm, the camera split is located at a position only six diameters distance along the tube from its detonated end.

The detonation velocity of each explosive is monitored by 12 probes made of 50-μm-diam enameled copper wire and attached to the outside of the copper tube at 25-mm intervals. The charge temperature is kept at 24 ± 2°C, and the charge is fired in a helium atmosphere to minimize shock refraction effects at early time.

Cylinder wall velocity data at early times should be evaluated carefully, because the early expansion consists of a series of shock-induced accelerations accompanied by a pullback. Also the preferred test in a helium atmosphere may give slightly lower wall expansion values and velocity than similar tests in air.

Wall velocity accuracy is thought to be 0.5% or better for high-quality explosives.

Table 3.15 GENERAL CYLINDER TEST SHOT INFORMATION

Explosive	Data Table	Shot Number	Explosive Density (g/cm³)	Detonation Velocity (mm/μs)	Loading[a] (Nominal is 4.0331 g/cm³)	Fitting Form
PBX 9404	3.16	C-4309	1.843	8.768 ± 0.002	Nom.	8-knot spline
PBX 9404	3.16	C-4335	1.848	8.788 ± 0.002	Nom.	[b]
PBX 9404	3.16	C-4526	1.847	8.787 ± 0.001	Nom.	[b]
PBX 9404	3.16	C-4527	1.847	8.783 ± 0.001	Nom.	
PBX 9501	3.17	C-4521	1.834	8.792 ± 0.001	Nom.	
PBX 9501	3.17	C-4525	1.834	8.792 ± 0.001	Nom.	
PBX-9502	3.18	C-4454	1.894	---	Nom.	14-knot spline
PBX 9502	3.18	C-4455	1.894	7.589 ± 0.018	Nom.	14-knot spline
X-0282	3.19	C-4443	1.812	8.773 ± 0.001	Nom.	9-knot spline
X-0282	3.19	C-4529	1.819	8.749 ± 0.001	Nom.	
X-0282	3.19	C-4507	1.827	8.783 ± 0.002	Nom.	7-knot spline
X-0282	3.19	C-4523	1.829	8.792 ± 0.001	Nom.	
X-0284[d]	3.20	C-4453	1.636	6.728 ± 0.003	4.0282	
X-0285	3.21	C-4502	1.831	8.784 ± 0.013	Nom.	[b]
X-0287	3.22	B-8193	1.822	8.874 ± 0.003	Nom.	[b]
X-0298	3.23	B-8310	1.820	8.841 ± 0.001	Nom.	[b]
X-0309[e,f]	3.24	B-8208	1.699	6.737 ± 0.002	4.0284	8-knot spline
X-0309[e,g]	3.25	B-8203	1.694	6.671 ± 0.002	4.035	[b]

[a]Expressed in grams of copper per cubic centimeter of high explosive.
[b]Seventh-order polynomial.
[c]Fifteen-knot spline.
[d]Also called Pamatex/20 and Amatex-20K; 4-in. cylinder test.
[e]Also called Destex.
[f]4-in. cylinder test.
[g]2-in. cylinder test.

Table 3.16 PBX-9404 WALL VELOCITY vs EXPANSION RADIUS IN 1-in. CYLINDER TEST

Expansion Radius (mm)	Wall Velocity (mm/μs)				Average Wall Velocity (mm/μs)	Average Specific Wall Kinetic Energy (mm/μs)²
	C-4309	C-4335	C-4526	C-4527		
4	---	1.508	1.488	1.501	1.499	2.247
5	1.560	1.558	1.551	1.554	1.556	2.420
6	1.596	1.595	1.596	1.593	1.595	2.544
7	1.627	1.627	1.628	1.628	1.628	2.649
8	1.654	1.654	1.652	1.659	1.655	2.738
9	1.676	1.678	1.670	1.681	1.676	2.809
10	1.695	1.699	1.685	1.695	1.694	2.868
11	1.709	1.717	1.697	1.703	1.707	2.914
12	1.721	1.732	1.708	1.713	1.719	2.953
13	1.732	1.743	1.719	1.726	1.730	2.993
14	1.743	1.753	1.729	1.741	1.742	3.033
15	1.755	1.760	1.740	1.753	1.752	3.070
16	1.766	1.768	1.750	1.761	1.761	3.102
17	1.775	1.775	1.761	1.767	1.770	3.131
18	1.783	1.784	1.772	1.774	1.778	3.162
19	1.790	1.794	1.782	1.781	1.787	3.192
20	1.799	1.805	1.792	1.789	1.796	3.227
21	1.811	1.814	1.802	1.799	1.807	3.263
22	1.827	1.817	1.811	1.809	1.816	3.298
23	---	---	1.820	1.820	1.820	3.312
24	---	---	1.828	1.831	1.830	3.347
25	---	---	1.835	1.843	1.839	3.382
26	---	---	1.841	1.856	1.849	3.419
27	---	---	1.847	1.866	1.857	3.447
28	---	---	1.852	1.872	1.862	3.467
29	---	---	1.857	1.875	1.866	3.482
30	---	---	1.861	1.875	1.868	3.489

Table 3.17 PBX-9501 WALL VELOCITY vs EXPANSION RADIUS IN 1-in. CYLINDER TEST

Expansion Radius (mm)	Wall Velocity (mm/μs)		Average Wall Velocity (mm/μs)	Average Specific Wall Kinetic Energy $(mm/\mu s)^2$
	C-4521	C-4525		
4	1.509	1.484	1.497	2.240
5	1.536	1.532	1.534	2.353
6	1.568	1.572	1.570	2.465
7	1.608	1.606	1.607	2.582
8	1.645	1.634	1.640	2.688
9	1.669	1.655	1.662	2.762
10	1.681	1.669	1.675	2.806
11	1.690	1.682	1.686	2.843
12	1.702	1.697	1.700	2.888
13	1.716	1.712	1.714	2.938
14	1.731	1.727	1.729	2.989
15	1.745	1.740	1.743	3.036
16	1.759	1.752	1.756	3.082
17	1.770	1.761	1.766	3.117
18	1.777	1.767	1.772	3.140
19	1.780	1.772	1.776	3.154
20	1.785	1.779	1.782	3.176
21	1.795	1.791	1.793	3.215
22	1.812	1.808	1.810	3.276
23	1.829	1.825	1.827	3.338
24	1.837	1.837	1.837	3.375
25	1.839	1.845	1.842	3.393
26	1.835	1.850	1.843	3.395
27	1.834	1.854	1.844	3.400
28	1.837	1.855	1.846	3.408
29	1.843	1.855	1.849	3.419
30	1.851	1.859	1.855	3.441

Table 3.18 PBX-9502 WALL VELOCITY vs EXPANSION RADIUS IN 1-in. CYLINDER TESTS

Expansion Radius (mm)	Wall Velocity (mm/μs)		Average Wall Velocity (mm/μs)	Average Specific Wall Kinetic Energy (mm/μs)²
	C-4454	C-4455		
4	---	---	---	---
5	1.265	1.216	1.241	1.539
6	1.296	1.305	1.301	1.691
7	1.320	1.327	1.324	1.752
8	1.340	1.334	1.337	1.788
9	1.359	1.348	1.354	1.832
10	1.374	1.366	1.370	1.877
11	1.385	1.382	1.384	1.914
12	1.395	1.393	1.394	1.943
13	1.403	1.401	1.402	1.966
14	1.410	1.408	1.409	1.985
15	1.417	1.414	1.416	2.004
16	1.423	1.420	1.422	2.021
17	1.429	1.425	1.427	2.036
18	1.434	1.429	1.432	2.049
19	1.438	1.432	1.435	2.059
20	1.441	1.437	1.439	2.071
21	1.445	1.443	1.444	2.085
22	1.448	1.451	1.450	2.101
23	1.449	1.457	1.453	2.111
24	1.450	1.461	1.456	2.118
25	1.453	1.462	1.458	2.124
26	1.461	1.464	1.463	2.139
27	1.468	1.467	1.468	2.154
28	1.473	1.471	1.472	2.167
29	1.476	1.475	1.476	2.177
30	1.483	1.477	1.480	2.190

Table 3.19 X-0282 WALL VELOCITY vs EXPANSION RADIUS IN 1-in. CYLINDER TEST

Expansion Radius (mm)	Wall Velocity (mm/μs)				Average Wall Velocity[a] (mm/μs)	Average Specific Wall Kinetic Energy[a] (mm/μs)²
	C-4443	C-4529	C-4507	C-4523		
4	1.464	1.456	1.458	1.469	1.464	2.142
5	1.522	1.510	1.529	1.527	1.528	2.335
6	1.567	1.549	1.579	1.571	1.575	2.481
7	1.602	1.582	1.612	1.603	1.608	2.584
8	1.626	1.608	1.632	1.625	1.629	2.652
9	1.645	1.628	1.650	1.644	1.647	2.713
10	1.662	1.645	1.667	1.660	1.664	2.767
11	1.679	1.659	1.682	1.674	1.678	2.816
12	1.694	1.671	1.697	1.689	1.693	2.866
13	1.703	1.686	1.710	1.705	1.708	2.916
14	1.719	1.704	1.723	1.721	1.722	2.965
15	1.728	1.719	1.734	1.734	1.734	3.007
16	1.736	1.728	1.744	1.743	1.744	3.040
17	1.741	1.732	1.753	1.748	1.751	3.064
18	1.746	1.734	1.762	1.753	1.758	3.089
19	1.752	1.739	1.769	1.759	1.764	3.112
20	1.759	1.747	1.776	1.763	1.770	3.131
21	1.767	1.757	1.782	1.789	1.781	3.172
22	1.775	1.768	1.788	1.793	1.791	3.206
23	1.781	1.781	1.794	1.807	1.801	3.242
24	1.787	1.793	1.800	1.823	1.812	3.282
25	1.791	1.801	1.805	1.835	1.818	3.303
26	1.793	1.806	1.810	1.843	1.827	3.336
27	1.796	1.808	1.815	1.846	1.831	3.351
28	1.799	1.811	1.819	1.847	1.833	3.360
29	1.803	1.815	1.822	1.848	1.835	3.367
30	1.807	1.821	1.825	1.850	1.838	3.376

[a]Shots C-4507 and C-4523.

Table 3.20 X-0284[a]
WALL VELOCITY vs EXPANSION RADIUS IN 4-in. CYLINDER TEST

Expansion Radius (mm)	Wall Velocity C-4453 (mm/μs)	Average Specific Wall Kinetic Energy (mm/μs)²
4	1.103	1.217
5	1.155	1.334
6	1.195	1.428
7	1.228	1.508
8	1.254	1.573
9	1.278	1.633
10	1.298	1.685
11	1.316	1.732
12	1.331	1.772
13	1.345	1.809
14	1.357	1.841
15	1.368	1.871
16	1.377	1.896
17	1.385	1.918
18	1.392	1.938
19	1.399	1.957
20	1.405	1.974
21	1.410	1.988
22	1.416	2.005
23	1.422	2.022
24	1.428	2.039
25	1.433	2.053
26	1.437	2.065
27	1.440	2.074

[a]Also called Pamatex/20 and Amatex-20K.

Table 3.21 X-0285
WALL VELOCITY vs EXPANSION RADIUS
IN 1-in. CYLINDER TESTS

Expansion Radius (mm)	Wall Velocity C-4502 (mm/μs)	Average Specific Wall Kinetic Energy (mm/μs)²
4	1.453	2.111
5	1.520	2.310
6	1.570	2.465
7	1.608	2.586
8	1.637	2.680
9	1.659	2.752
10	1.677	2.812
11	1.692	2.863
12	1.705	2.907
13	1.716	2.945
14	1.726	2.979
15	1.735	3.010
16	1.743	3.038
17	1.751	3.066
18	1.759	3.094
19	1.767	3.122
20	1.774	3.147
21	1.781	3.172
22	1.787	3.193
23	1.793	3.215
24	1.799	3.236
25	1.805	3.258
26	1.810	3.276

Table 3.22 X-0287
WALL VELOCITY vs EXPANSION RADIUS
IN 1-in. CYLINDER TESTS

Expansion Radius (mm)	Wall Velocity B-8193 (mm/μs)	Average Specific Wall Kinetic Energy (mm/μs)²
4	---	---
5	---	---
6	---	---
7	1.617	2.615
8	1.643	2.699
9	1.666	2.776
10	1.686	2.843
11	1.703	2.900
12	1.718	2.952
13	1.731	2.996
14	1.743	3.038
15	1.754	3.077
16	1.764	3.112
17	1.774	3.147
18	1.783	3.179
19	1.791	3.208
20	1.800	3.24
21	1.808	3.269

Table 3.23 X-0298
WALL VELOCITY vs EXPANSION RADIUS
IN 1-in. CYLINDER TESTS

Expansion Radius (mm)	Wall Velocity B-8310 (mm/μs)	Average Specific Wall Kinetic Energy (mm/μs)
4	1.504	2.262
5	1.555	2.418
6	1.592	2.534
7	1.622	2.631
8	1.647	2.713
9	1.669	2.786
10	1.688	2.849
11	1.705	2.907
12	1.719	2.955
13	1.732	3.000
14	1.743	3.058
15	1.753	3.073
16	1.762	3.105
17	1.771	3.136
18	1.781	3.172
19	1.790	3.204
20	1.798	3.233

Table 3.24 X-0309[a]
WALL VELOCITY vs EXPANSION RADIUS
IN 4-in. CYLINDER TESTS

Expansion Radius (mm)	Wall Velocity B-8208 (mm/μs)	Average Specific Wall Kinetic Energy (mm/μs)²
4	0.984	0.969
5	1.022	1.045
6	1.051	1.104
7	1.074	1.153
8	1.094	1.198
9	1.112	1.237
10	1.128	1.272
11	1.141	1.302
12	1.153	1.329
13	1.163	1.352
14	1.171	1.372
15	1.179	1.390
16	1.186	1.406
17	1.192	1.421
18	1.198	1.435
19	1.203	1.448
20	1.208	1.460
21	1.213	1.471
22	1.217	1.481
23	1.221	1.490
24	1.224	1.499
25	1.228	1.507
26	1.231	1.515
27	1.080	1.523

[a]Also called Destex.

Table 3.25 X-0309[a]
WALL VELOCITY vs EXPANSION RADIUS
IN 2-in. CYLINDER TESTS

Expansion Radius (mm)	Wall Velocity B-8203 (mm/μs)	Average Specific Wall Kinetic Energy $(mm/\mu s)^2$
4	0.985	0.970
5	1.022	1.045
6	1.050	1.103
7	1.074	1.154
8	1.095	1.199
9	1.114	1.241
10	1.130	1.277
11	1.145	1.311
12	1.158	1.341
13	1.168	1.364
14	1.177	1.385
15	1.184	1.402
16	1.190	1.416
17	1.195	1.428
18	1.200	1.440
19	1.206	1.454
20	1.212	1.469
21	1.219	1.486
22	1.225	1.501

[a]Also called Destex.

3.3 Detonation Pressure Determined from Initial Free-Surface Velocity. The detonation pressure is important in any design involving explosives, because it drives inert materials and initiates other explosives. Although detonation pressure has been measured "directly," the most commonly used values are from experiments in which it has been inferred from its measured effects in other materials. The following initial free-surface velocity experiment provides inferential measurements of detonation pressure.

In an initial free-surface velocity experiment, one face of a parallelepiped of test explosive is initiated by a plane-wave lens. In intimate contact with the opposite face is a plate of inert material. The initiated detonation wave traverses the test explosive thickness and transmits a shock wave into the inert material. When this shock wave reaches the free surface of the inert material, it accelerates it. The initial velocity of the free surface is measured. By varying the thickness of the inert plate and measuring the free-surface velocity, one can plot free-surface velocity vs plate thickness and then extrapolate to zero plate thickness. By knowing the plate material equation of state, one can find a corresponding shock velocity and shock

pressure. The "acoustic approximation" is then used to calculate the corresponding explosive pressure from $P_x = P_m (\rho_{0m}U_s + \rho_{0x}D)/2\rho_{0m}U_s$, where P_x = pressure in the explosive, P_m = pressure in the inert plate, ρ_{0m} and ρ_{0x} = initial densities in the inert plate and explosive, respectively, U_s = shock velocity, and D = detonation velocity.

Using an assumed γ-law equation of state for the explosive reaction products, one can then calculate $\gamma = (\rho_{0x}D^2/P_x) - 1$ and $U_{px} = D/(\gamma + 1)$.

The flash-gap technique was used to measure the inert plate's initial free-surface velocities. "Step blocks" of polymethylmethacrylate were mounted on the plate, with 0.1-mm-thick steel shim-covered argon flash gaps as shown in Fig. 3.01. The explosive-accelerated inert plate closed the pair of lateral reference gaps when it began moving, and after traversing the known free-run distance, it closed the other identical gap. The length of this free run was selected to avoid shock reverberation effects on the velocity. Closure of the gaps provided a brilliant, brief flash of light. Images of the flashes were recorded by a streaking camera using multiple slits and yielding multiple determinations of the free-run time, hence velocity. The typical width of a flash gap along the slit length was 19 mm. The initial free-surface velocity technique is described in more detail in "Measurement of Chapman-Jouguet Pressure for Explosives" by W. E. Deal.[1]

Table 3.26 lists the detonation or Chapman-Jouguet (C-J) pressure, P_x; the explosive's particle velocity, U_{px}; and the parameter of the assumed γ-law equation of state, γ, for each explosive.

Subsequent tables give densities, compositions, sample sizes, boosters, and the detailed shock information on each explosive. In the "analysis" section of the tables, t represents plate thickness; ρ, density; P, pressure; U_{fs}, free surface velocity; U_s, shock velocity; U_p, particle velocity; D, detonation velocity; and γ, the parameter of the assumed γ-law equation of state. The subscript "0" refers to initial state, "x" to explosive, and "m" to the plate material. The parameters are given for a linear least squares fit of free-surface velocity vs plate thickness, and the corresponding explosive parameters are derived from the acoustic approximation.

The detonation pressure has been shown to be a function of the charge geometry, and these data are omitted herein.

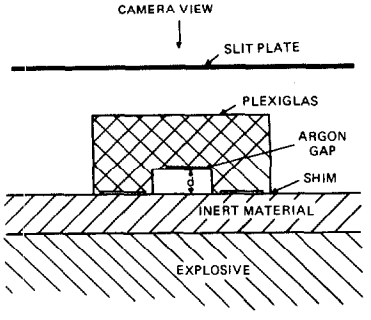

Fig. 3.01. Plexiglas block assembly for measurement of free-surface velocity of an explosive-driven plate.

Table 3.26 DETONATION (C-J) PRESSURE AND OTHER DATA

Explosive	Plate Material	Explosive Density (mg/m³)	Detonation (Chapman-Jouquet) Pressure (GPa)	Explosive Particle Velocity (km/s)	Gamma-Law Equation-of-State Parameter, γ
Comp B	Dural[a]	1.713	29.35	2.134	2.763
Comp B	Brass	1.714	28.54	2.081	2.845
Cyclotol	Dural	1.742	31.24	2.179	2.787
Cyclotol	Plexiglas	1.200	12.36	1.587	3.089
Octol	Dural	1.809	33.84	2.213	2.819
PBX 9206	Dural	1.837	34.62	2.170	3.002
PBX 9207	Dural	1.837	34.35	2.158	3.015
PBX 9401	Dural	1.713	28.63	1.982	3.254
PBX 9402	Dural	1.831	35.35	2.195	2.997
PBX 9404	Dural	1.827	35.72	2.235	2.912
PBX 9405	Dural	1.757	33.70	2.258	2.762
RDX	Dural	1.768	33.16	2.169	2.984
RDX and DNPA	Dural	1.745	31.66	2.153	2.915
RDX and Kel-F	Dural	1.809	33.71	2.248	2.686
TNT	Dural	1.635	17.89-19.35	1.572	3.415
TNT and DNT	Brass	1.579	17.77	1.666	3.055

[a]Aluminum-2024 is known by the name Duraluminum, which we indicate by Dural.

Table 3.27 COMPOSITION B ON DURAL

Explosive

RDX/TNT: 64.0 ± 0.6 wt% RDX. 1.713 ± 0.002 g/cm³. Holston[a] Grade A Composition B. Two 102- by 254-mm pieces to make 203-mm thickness. P-080 booster. $D = 3.127\ \rho_0 + 2.673$ at 65 wt% RDX and increases 0.0134 km/s per 1 wt% RDX increase.

Plate

Dural.

Shot No.	Plate Density (g/cm³)	Plate Thickness (mm)	No. U_{fs} Dets	Free-Surface Velocity (km/s)[b]
[b]	2.793	1.85	3	3.414 ± 0.027
[b]	2.793	2.54	5	3.389 ± 0.028
[b]	2.793	3.16	3	3.378 ± 0.018
[b]	2.794	3.77	3	3.350 ± 0.017
[b]	2.797	4.83	2	3.351 ± 0.013
[b]	2.793	5.08	7	3.330 ± 0.016
8A 579	2.790	6.32	5	3.363 ± 0.011
[b]	2.794	6.34	4	3.304 ± 0.028
8A 665	2.790	6.37	5	3.320 ± 0.017
[b]	2.793	7.61	5	3.290 ± 0.024
[b]	2.797	8.10	2	3.312 ± 0.006
[b]	2.794	8.87	2	3.251 ± 0.021
8A 266	2.793	9.96	24	3.297 ± 0.025
[b]	2.793	10.17	7	3.261 ± 0.032
[b]	2.796	11.31	4	3.256 ± 0.033
[b]	2.793	12.23	4	3.240 ± 0.018
[b]	2.794	12.66	3	3.222 ± 0.042
8A 507	2.784	12.72	5	3.251 ± 0.038
7C 93	2.782	12.73	7	3.262 ± 0.008
8A 260	2.793	12.82	6	3.251 ± 0.024
8A 261	2.793	12.85	6	3.234 ± 0.016
8A 554	2.790	13.06	5	3.210 ± 0.017
8A 666	2.790	19.04	5	3.195 ± 0.018
8A 620	2.790	19.19	5	3.145 ± 0.014
8A 580	2.790	19.20	5	3.207 ± 0.008
8A 344	2.782	23.98	8	3.137 ± 0.032
8A 581	2.790	25.58	5	3.085 ± 0.014
8A 582	2.790	38.33	5	2.961 ± 0.020
8A 684	2.784	50.80	5	2.889 ± 0.034
8A 583	2.790	50.95	5	2.831 ± 0.037

[a]Holston Defense Corp., Kingsport, Tennessee.

[b]Data for this entry were determined on some or all of the following shots: 8A-225, -229, -273, -285, and -325; each was fired using several plate thicknesses.

DETONATION PROPERTIES

Analysis

Linear least squares fitting gives U_{fs} = 3.389 km/s − 0.01079 t (mm). At t = 0, plate U_s = 7.611 km/s and P_m = 35.63 GPa.

Acoustic approximation with D = 8.030 km/s, ρ_{0x} = 1.713 g/cm³, and ρ_{0m} = 2.791 g/cm³ gives corresponding explosive parameters of P_x = 29.35 GPa, U_{px} = 2.134 km/s, and γ = 2.763.

Table 3.28 COMPOSITION B ON DURAL
Charge Length/Diameter = 1

Explosive

RDX/TNT: 65.5 ± 1.5 wt% RDX. Holston Grade A Composition B. 1.713 ± 0.007 g/cm³. Two 76-mm-thick, 152-mm-diam cylinders to make a 152-mm- length. P-080 booster, D = 3.127 ρ_0 + 2.673 at 65 wt% RDX and increases 0.0134 km/s per 1 wt% RDX increase.

Plates

Dural.

Shot No.	Plate Density (g/cm³)	Plate Thickness (mm)	Free-Surface Velocity (km/s)[a]
7C 180	2.774	6.38	3.359 ± 0.027
8A 1314	2.782	12.73	3.259 ± 0.008
8A 1313	2.774	19.07	3.189 ± 0.023
8A 1334	2.782	25.74	3.058 ± 0.016
8A 1319	2.774	38.11	2.933 ± 0.014
8A 1315	2.805	50.86	2.800 ± 0.034

[a]Mean and standard deviation of seven determinations on each shot.

Analysis

Linear least squares fitting gives U_{fs} = 3.421 km/s − 0.01259 t (mm). This intercept is only 0.9% higher than that of the data in Table 3.27 for somewhat larger charges. The slope is steeper. The intercept is 1.6% higher than that in Table 3.29 for charges of the same diameter but ten charge diameters long. The slope is again steeper than found from the data in Table 3.27.

Table 3.29 COMPOSITION B ON DURAL
Charge Length/Diameter = 10

Explosive

RDX/TNT: 65.5 ± 1.5 wt% RDX. Holston Grade A Composition B. 1.713 ± 0.007 g/cm³. Twenty 76-mm-thick, 152-mm-diam cylinders to make a 1524-mm length. P-080 booster, D = 3.127 ρ_0 + 2.673 at 65 wt% RDX and increases 0.0134 km/s per 1 wt% RDX increase.

Plates

Dural.

Shot No.	Plate Density (g/cm³)	Plate Thickness (mm)	Free-Surface Velocity (km/s)[a]
7C 176	2.774	6.35	3.312 ± 0.014
7C 174	2.782	12.73	3.216 ± 0.010
7C 172	2.774	19.10	3.189 ± 0.024
7C 173	2.784	25.39	3.065 ± 0.013
7C 175	2.774	38.13	2.994 ± 0.017
7C 177	2.805	50.85	2.823 ± 0.030

[a]Mean and standard deviation of seven determinations on each shot.

Analysis

Linear least squares fitting gives U_{fs} = 3.368 km/s − 0.01054 t (mm). This intercept is only 0.6% below that for Table 3.27 for somewhat larger diameter but shorter charges. The slope for these long charges is more like that of Table 3.27 than the steeper data of Table 3.28.

Table 3.30 COMPOSITION B ON BRASS

Explosive

RDX/TNT: 64.2 ± 0.4 wt% RDX. 1.714 ± 0.002 g/cm³. Two 102- by 254- by 254-mm pieces to make a 203-mm length. P-080 booster, $D = 3.127\ \rho_0 + 2.673$ at 65 wt% RDX and increases 0.0134 km/s per 1 wt% RDX increase.

Plates

Brass.

Shot No.	Plate Density (g/cm³)	Plate Thickness (mm)	Free-Surface Velocity (km/s)[b]
[a]	8.402	1.97	2.124 ± 0.004
[a]	8.402	3.76	2.068 ± 0.008
[a]	8.402	5.76	2.073 ± 0.027
[a]	8.402	7.68	2.037 ± 0.019
[a]	8.402	9.58	2.033 ± 0.025
[a]	8.402	11.49	2.008 ± 0.015
[a]	8.402	13.41	1.991 ± 0.014
[a]	8.402	15.32	1.969 ± 0.012
8A 700	8.386	25.43	1.872 ± 0.010
8A 769	8.386	38.22	1.781 ± 0.008
8A 699	8.386	48.38	1.717 ± 0.015
8A 766	8.386	48.93	1.711 ± 0.017

[a]Data for this entry were determined on some or all of the following shots: 7C-3, 8A-373, and 8A-374; each was fired using several plate thicknesses.

[b]Mean and standard deviation of five determinations on last four entries, three on the first six and the eighth, and two on the seventh.

Analysis

Linear least squares fitting gives $U_{fs} = 2.107$ km/s − 0.00830 t (mm). At t = 0, plate $U_s = 5.173$ km/s and $P_m = 45.36$ GPa. Acoustic approximation with D = 8.002 km/s, $\rho_{0x} = 1.714$ g/cm³, and $\rho_{0m} = 8.395$ g/cm³ gives corresponding explosive parameters of $P_x = 28.54$ GPa, $U_{px} = 2.081$ km/s, and $\gamma = 2.845$.

Table 3.31 CYCLOTOL ON DURAL

Explosive

RDX/TNT: 77 ± 1.2 wt% RDX. 1.742 ± 0.002 g/cm³. Two 102- by 254-mm pieces to make a 203-mm thickness. P-080 booster. D = 3.193 ρ_0 + 2.702 at 78.1 wt% RDX and increases 0.0134 km/s per 1 wt% RDX increase.

Plates

Dural

Shot No.	Plate Density (g/cm/³)	Plate Thickness (mm)	No. U_{fs} Dets	Free-Surface Velocity (km/s)[b]
[a]	2.793	1.23	2	3.746 ± 0.056
[a]	2.793	1.90	3	3.545 ± 0.012
[a]	2.793	2.53	4	3.528 ± 0.023
[a]	2.793	3.13	5	3.494 ± 0.052
[a]	2.793	3.80	4	3.494 ± 0.023
[a]	2.793	4.70	2	3.500 ± 0.026
[a]	2.793	5.07	3	3.462 ± 0.012
[a]	2.793	6.32	6	3.445 ± 0.021
[a]	2.793	7.61	3	3.437 ± 0.014
[a]	2.793	7.95	2	3.471 ± 0.001
[a]	2.793	8.88	4	3.431 ± 0.042
[a]	2.793	9.57	2	3.425 ± 0.021
[a]	2.793	10.15	3	3.416 ± 0.026
[a]	2.793	10.88	1	3.434
[a]	2.793	11.05	1	3.427
[a]	2.793	11.42	4	3.424 ± 0.007
[a]	2.793	12.04	1	3.343
[a]	2.793	12.56	3	3.378 ± 0.024
7C 145	2.774	19.05	5	3.287 ± 0.022
8A 354	2.788	24.41	6	3.280 ± 0.022
8A 1252	2.805	38.17	5	3.142 ± 0.006
8A 1253	2.799	50.85	5	3.027 ± 0.024

[a]Data for this entry were determined on some or all of the following shots: 8A-238, -302, -305, -306, and -318; each was fired using several plate thicknesses.
[b]Mean and standard deviation of multiple determinations.

Analysis

Linear least squares fitting gives U_{fs} = 3.531 km/s − 0.01029 t (mm). At t = 0, plate U_s = 7.704 km/s and P_m = 37.57 GPa. Acoustic approximation of D = 8.252 km/s, ρ_{0x} = 1.743 g/cm³, and ρ_{0m} = 2.793 g/cm³ gives corresponding explosive parameters of P_x = 31.34 GPa, U_{px} = 2.179 km/s, and γ = 2.787.

Table 3.32 CYCLOTOL ON DURAL

Explosive

RDX/TNT: 76.7 ± 0.8 wt% RDX. 1.756 ± 0.005 g/cm³. 203-mm-diam pieces from 12.7 to 101.6-mm thick in various combinations to give 12.7- to 812.8-mm thicknesses. P-080 booster. D = 3.193 ρ_0 + 2.702 at 78.1 wt% RDX and increases 0.003 km/s per 1 wt% RDX increase.

Plates

Dural, 36.57 ± 0.02 mm thick.

Shot No.	Plate Density (g/cm³)	Plate Thickness (mm)	Explosive Thickness (mm)	Free-Surface Velocity (km/s)[a]
7C 199	2.795	36.59	12.7	1.859 ± 0.025
7C 200	2.793	36.53	25.4	2.240 ± 0.019
7C 201	2.786	36.58	38.1	2.540 ± 0.018
7C 202	2.786	36.58	50.8	2.676 ± 0.010
7C 203	2.790	36.58	76.2	2.875 ± 0.018
7C 204	2.786	36.54	101.6	3.006 ± 0.023
7C 205	2.786	36.57	152.4	3.149 ± 0.018
7C 206	2.793	36.57	203.2	3.194 ± 0.026
7C 207	2.793	36.55	406.4	3.289 ± 0.028
7C 243	2.793	36.58	609.6	3.279 ± 0.030
7C 218	2.786	36.57	812.8	3.237 ± 0.021

[a]Mean and standard deviation of 12 determinations on the first seven entries and on the ninth and tenth, 11 determinations on the eighth, and 3 determinations on the last.

Analysis

As the charge length-to-diameter ratio is increased, the plate free-surface velocity increases continuously and significantly up to an asymptote of 3.29 km/s at about two charge diameters. A small, though possibly significant, decrease is then seen out to four charge diameters. The velocity at one charge diameter is about 3% less than that at two charge diameters.

Table 3.33 CYCLOTOL ON PLEXIGLAS

Explosive

RDX/TNT: 74.99 ± 0.01 wt% RDX. 1.200 ± 0.001 g/cm³. Four 152 ± 0.13-mm-long, 141-mm-diam pieces to make a 610-mm-long charge pressed from ball-milled powder of which 86% passed a 44-μm screen and 12% passed a 96-μm screen. Contained in 5-mm-wall brass tubes. P-080 and 13-mm-thick Comp. B booster. D at infinite diameter and 78 wt% RDX is 6.535 km/s.

Plates

Plexiglas (polymethylmethacrylate), nominal 1.18 g/cm³.

Shot No.	Plate Density (g/cm³)	Plate Thickness (mm)	Free-Surface Velocity (km/s)[a]
7C 239	1.179	6.26	3.613 ± 0.029
7C 240	1.179	12.61	3.451 ± 0.021
7C 242	1.179	19.04	3.342 ± 0.024
7C 241	1.179	24.61	3.322 ± 0.032
7C 238	1.182	38.05	3.305 ± 0.023
7C 237	1.182	48.61	3.173 ± 0.035

[a]Mean and standard deviation of seven determinations on each shot.

Analysis

Linear least squares fitting gives U_{fs} = 3.581 km/s − 0.00858 t (mm). At t = 0, plate U_s = 5.220 km/s and P_m = 10.92 GPa. Acoustic approximation with D = 6.490 km/s, ρ_{0x} = 1.200 g/cm³, and ρ_{0m} = 1.180 g/cm³ gives corresponding explosive parameters of P_x = 12.36 GPa, U_{px} = 1.587 km/s, and γ = 3.089.

Table 3.34 OCTOL ON DURAL

Explosive

HMX/TNT: 76.3 ± 0.8 wt% HMX. 1.809 ± 0.007 g/cm³. 155-mm-thick conical frustum of 279-mm small diameter and 324-mm large diameter with large end toward plate. P-080 and 32-mm-thick Plexiglas booster. D = 8.478 km/s at ρ_0 = 1.814 g/cm³ and 77 wt% HMX. D increases ~0.8031 km/s per 0.001-g/cm³ density increase and ~0.013 km/s per 1 wt% HMX increase.

Plates

Dural.

Shot No.	Plate Density (g/cm³)	Plate Thickness (mm)	Free-Surface Velocity (km/s)[a]
8A 1322	2.774	2.54	3.674 ± 0.035
7C 151	2.782	6.31	3.644 ± 0.064
8A 1337	2.774	6.37	3.698 ± 0.039
7C 117	2.784	12.88	3.476 ± 0.048
8A 1177	2.790	19.15	3.438 ± 0.025
8A 1178	2.782	25.51	3.348 ± 0.021
8A 1189	2.786	38.13	3.232 ± 0.008
8A 1180	2.783	50.88	3.113 ± 0.012
7C 166	2.783	76.76	2.859 ± 0.010

[a]Mean and standard deviation of seven determinations on the first three shots listed, five determinations on the next five, and three determinations on the last.

Analysis

Linear least squares fitting gives U_{fs} = 3.695 km/s − 0.01160 t (mm). At t = 0, plate U_s = 7.811 km/s, and P_m = 39.72 GPa. Acoustic approximation with D = 8.452 km/s, ρ_{0x} = 1.809 g/cm³, and ρ_{0m} = 2.781 g/cm³ gives corresponding explosive parameters of P_x = 33.84 GPa, U_{px} = 2.213 km/s, and γ = 2.819.

Table 3.35 PBX 9206 (HMX/KEL-F) ON DURAL

Explosive

HMX/Kel-F 3700: 92/8. 1.837 ± 0.001 g/cm³. Two 76-mm-thick, 156-mm-diam pieces to make a 152-mm thickness. P-080 booster. D = 8.725 km/s at 41-mm diam and ρ_0 = 1852 g/cm³.

Plates

Dural.

Shot No.	Plate Density (g/cm³)	Plate Thickness (mm)	Free-Surface Velocity (km/s)[a]
7C 225	2.788	6.34	3.658 ± 0.018
7C 210	2.774	12.81	3.560 ± 0.032
7C 211	2.774	19.14	3.487 ± 0.022
7C 212	2.774	25.10	3.511 ± 0.014
7C 254	2.782	25.74	3.445 ± 0.017
7C 214	2.782	38.13	3.307 ± 0.008
7C 215	2.782	50.79	3.195 ± 0.027

[a]Mean and standard deviation of seven determinations on each shot.

Analysis

Linear least squares fitting gives U_{fs} = 3.710 km/s − 0.01016 t (mm). At t = 0, plate U_s =7.821 km/s and P_m = 39.93 GPa. Acoustic approximation with D = 8.685 km/s, ρ_{0x} = 1.837 g/cm³, and ρ_{0m} = 2.779 g/cm³ gives corresponding explosive parameters of P_x = 34.62 GPa, U_{px} = 2.170 km/s, and γ = 3.002.

Table 3.36 PBX 9207 (HMX/EXON/CEF) ON DURAL

Explosive

HMX/Exon 461/CEF: 92/6/2. 1.837 ± 0.002 g/cm³. Two 76-mm-thick, 156-mm-diam pieces to make a 152-mm thickness. P-080 booster. D = 8.677 km/s at 41-mm diam and ρ_0 = 1.843 g/cm³.

Plates

Dural.

Shot No.	Plate Density (g/cm³)	Plate Thickness (mm)	Free-Surface Velocity (km/s)[a]
8A 1449	2.784	5.13	3.599 ± 0.025
7C 231	2.788	6.17	3.728 ± 0.030
7C 226	2.782	12.71	3.553 ± 0.013
7C 227	2.782	19.08	3.499 ± 0.016
7C 228	2.789	24.20	3.439 ± 0.025
7C 229	2.788	38.12	3.334 ± 0.027
7C 244	2.789	50.83	3.215 ± 0.013

[a]Mean and standard deviation of seven determinations on six shots and six determinations on the third one listed.

Analysis

Linear least squares fitting gives U_{fs} = 3.692 km/s − 0.00954 t (mm). At t = 0, plate U_s = 7.809 km/s and P_m = 39.68 GPa. Acoustic approximation with D = 8.665 km/s, ρ_{0x} = 1.837 g/cm³, and ρ_{0m} = 2.786 g/cm³ gives corresponding parameters of P_x = 34.35 GPa, U_{px} = 2.158 km/s, and γ = 3.015.

Table 3.37 PBX 9401 (RDX/PS) ON DURAL

Explosive

RDX/PS/TOF: 94.2/3.6/2.2. 1.713 ± 0.002 g/cm³. A 203-mm-thick conical frustum of 229-mm small diameter and 324-mm large diameter with its small end toward the plate. P-080 booster. D = 8.426 km/s at ρ_0 = 1.711 g/cm³.

Plates

Dural.

Shot No.	Plate Density (g/cm³)	Plate Thickness (mm)	Free-Surface Velocity (km/s)[a]
8A 1191	2.784	6.28	3.229 ± 0.019
7C 92	2.771	12.77	3.171 ± 0.050
7C 91	2.790	19.13	3.183 ± 0.010
7C 94	2.782	25.49	3.156 ± 0.019
7C 95	2.786	38.15	3.095 ± 0.012
7C 96	2.783	50.88	2.990 ± 0.021

[a]Mean and standard deviation of five determinations on each shot.

Analysis

Linear least squares fitting gives U_{fs} = 3.263 km/s − 0.00492 t (mm). At t = 0, plate U_s = 7.529 km/s and P_m = 33.89 GPa. Acoustic approximation with D = 8.432 km/s, ρ_{0x} = 1.713 g/cm³, and ρ_{0m} = 2.783 g/cm³ gives corresponding explosive parameters of P_x = 28.63 GPa, U_{px} = 1.982 km/s, and γ = 3.254.

Table 3.38 PBX 9402 (HMX/NC/CEF) ON DURAL

Explosive

HMX/NC/CEF: 94/3/3. 1.831 ± 0.011 g/cm³. Three 64-mm-thick conical frusta of 279-mm small diameter and 324-mm large diameter with small ends toward plate. P-080 booster. D = 8.732 km/s − 0.037/diam (cm), at ρ_0 = 1.822 g/cm³ and increases approximately 0.003 km/s per 0.001-g/cm³ increase.

Plates

Dural.

Shot No.	Plate Density (g/cm³)	Plate Thickness (mm)	Free-Surface Velocity (km/s)[a]
7C 124	2.782	6.36	3.717 ± 0.013
7C 75	2.771	12.75	3.653 ± 0.021
7C 79	2.790	19.10	3.620 ± 0.009
7C 149	2.805	25.45	3.534 ± 0.022
7C 76	2.782	26.21	3.503 ± 0.042
7C 90	2.786	38.20	3.475 ± 0.038
7C 86	2.783	51.37	3.308 ± 0.005

[a]Mean and standard deviation of five determinations on six shots and three determinations on the second one listed.

Analysis

Linear least squares fitting gives U_{fs} = 3.767 km/s − 0.00870 t(mm). At t = 0, plate U_s = 7.858 km/s and P_m = 40.73 GPa. Acoustic approximation with D = 8.773 km/s, ρ_{0x} = 1.836 g/cm³, and ρ_{0m} = 2.786 g/cm³ gives corresponding explosive parameters of P_x = 35.35 GPa, U_{px} = 2.195 km/s, and γ = 2.997.

Table 3.39 PBX 9404 (HMX/NC/CEF) ON DURAL

Explosive

HMX/NC/CEF: 94/3/3. 1.827 ± 0.001 g/cm³. Two 76-mm-thick, 156-mm-diam pieces to make a 152-mm thickness. P-080 booster. D = 8.732 km/s − 0.037/diam (cm) at ρ_0 = 1.822 g/cm³ and increases approximately 0.003 km/s per 0.001-g/cm³ increase.

Plates

Dural.

Shot No.	Plate Density (g/cm³)	Plate Thickness (mm)	Free-Surface Velocity (km/s)[a]
7C 235	2.788	6.37	3.757 ± 0.024
7C 246	2.782	12.74	3.661 ± 0.019
7C 247	2.789	19.13	3.596 ± 0.029
7C 232	2.782	25.35	3.547 ± 0.025
7C 233	2.788	38.12	3.426 ± 0.003
7C 234	2.789	50.85	3.260 ± 0.022

[a]Mean and standard deviation of seven determinations on each shot.

Analysis

Linear least squares fitting gives U_{fs} = 3.812 km/s − 0.01065 t (mm). At t = 0, plate U_s = 7.88 km/s and P_m = 41.36 GPa. Acoustic approximation with D = 8.745 km/s, ρ_{0x} = 1.827 g/cm³, and ρ_{0m} = 2.786 g/cm³ gives corresponding explosive parameters of P_x = 35.72 GPa, U_{px} = 2.235 km/s, and γ = 2.912.

Table 3.40 PBX-9405 (RDX/NC/CEF) ON DURAL

Explosive

RDX/NC/CEF: 93.7/3.15/3.15. 1.757 ± 0.001 g/cm³. A 203-mm-thick conical frustum of 229-mm small diameter and 326-mm large diameter with its small end toward the plate. P-080 booster, D = 8.489 − 0.157/diam (cm) at ρ_0 = 1.755 g/cm³.

Plates

Dural.

Shot No.	Plate Density (g/cm³)	Plate Thickness (mm)	Free-Surface Velocity (km/s)[a]
8A 1325	2.774	2.54	3.643 ± 0.076
7C 152	2.782	6.35	3.690 ± 0.066
8A 1230	2.782	12.76	3.594 ± 0.013
8A 1231	2.774	19.03	3.517 ± 0.004
8A 1236	2.805	25.41	3.385 ± 0.032
7C 148	2.805	25.53	3.378 ± 0.015
8A 1237	2.805	38.16	3.283 ± 0.019
8A 1238	2.799	50.88	3.129 ± 0.013

[a]Mean and standard deviation of seven determinations on the first two shots listed and five determinations on the other six.

Analysis

Linear least squares fitting gives U_{fs} = 3.718 km/s − 0.01173 t (mm). At t = 0, plate U_s = 7.826 km/s and P_m = 40.04 GPa. Acoustic approximation with D = 8.494 km/s, ρ_{0x} = 1.757 g/cm³ and ρ_{0m} = 2.791 g/cm³ gives corresponding explosive parameters of P_x = 33.70 GPa, U_{px} = 2.258 km/s, and γ = 2.762.

Table 3.41 RDX PRESSED ON DURAL

Explosive

100% RDX pressed without binder. 1.768 ± 0.014 g/cm³. Two 76-mm-thick, 152-mm-diam pieces to make 152-mm thickness. P-080 booster. $D = 3.466\ \rho_0 + 2.515$.

Plates

Dural.

Shot No.	Plate Density (g/cm³)	Plate Thickness (mm)	Free-Surface Velocity (km/s)[c]
[a]	2.790	2.56	3.589 ± 0.019
[a]	2.790	5.11	3.484 ± 0.010
7C 153	2.782	6.31	3.695 ± 0.033
[a]	2.790	7.63	3.470 ± 0.012
[a]	2.790	10.17	3.471 ± 0.015
[b]	2.790	12.61	3.468 ± 0.019
7C 84	2.782	12.69	3.476 ± 0.011
7C 144	2.774	19.09	3.434 ± 0.045
8A 350	2.790	25.37	3.286 ± 0.021
7C 146	2.805	38.13	3.212 ± 0.049
7C 85	2.782	50.80	3.027 ± 0.079

[a]Data for this entry were determined on some or all of the following shots: 8A-326, -331, -332, and -333; each was fired using several plate thicknesses.
[b]Shots 8A-331, -332, and -333.
[c]Mean and standard deviation of seven determinations on the third entry, five each on the last five, four each on the four single-asterisk entries marked a, and three determinations on the entry marked by b.

Analysis

The data at 6.31 mm seem anomalous, but no good reason for discard was found. Linear least squares fitting of all the data gives $U_{fs} = 3.633$ km/s − 0.01184 t (mm). At t = 0, plate $U_s = 7.770$ km/s and $P_m = 38.88$ GPa. Acoustic approximation with $D = 8.642\ \rho_{0x} = 1.768$ g/cm³, and $\rho_{0m} = 2.787$ g/cm³ gives corresponding explosive parameters of $P_x = 33.16$ GPa, $U_{px} = 2.169$ km/s, and $\gamma = 2.984$.

Table 3.42 RDX AND DNPA ON DURAL

Explosive

RDX/DNPA: 90/10. 1.745 ± 0.001 g/cm³. Two 76-mm-thick, 150-mm-diam pieces to make 152-mm thickness. P-080 booster. $D = 3.233\ \rho_0 + 2.785$.

Plates

Dural.

Shot No.	Plate Density (g/cm³)	Plate Thickness (mm)	Free-Surface Velocity (km/s)[b]
[a]	2.790	2.49	3.578 ± 0.016
[a]	2.790	5.04	3.491 ± 0.024
[a]	2.790	6.36	3.466
[a]	2.790	7.58	3.426 ± 0.009
[a]	2.790	10.12	3.421 ± 0.009
[a]	2.790	12.62	3.412 ± 0.021
8A 365	2.793	12.71	3.376
8A 352	2.790	25.35	3.274 ± 0.015
7C 150	2.805	37.97	3.087 ± 0.056
7C 147	2.799	50.87	2.966 ± 0.083

[a]Data for this entry were determined on some or all of the following shots: 8A-315, -334, -335, and -345; each was fired using several plate thicknesses.
[b]Mean and standard deviation of five determinations on the last three entries, four on the second through sixth, three on the first, and one on the third and seventh.

Analysis

Linear least squares fitting gives $U_{fs} = 3.552$ km/s − 0.01171 t (mm). At t = 0, plate $U_s = 7.719$ km/s and $P_m = 37.86$ GPa. Acoustic approximation with D = 8.427 km/s, $\rho_{0x} = 1.745$ g/cm³, and $\rho_{0m} = 2.793$ g/cm³ gives corresponding explosive parameters of $P_x = 31.66$ GPa, $U_{px} = 2.153$ km/s, and $\gamma = 2.915$.

Table 3.43 RDX AND KEL-F ON DURAL

Explosive

RDX/Kel-F 150: 85/15. 1.809 ± 0.004 g/cm³. Two 76-mm-thick, 150-mm-diam pieces to make a 152-mm thickness. P-080 booster. D = 8.280 km/s at ρ_0 = 1.807 g/cm³.

Plates

Dural.

Shot No.	Plate Density (g/cm³)	Plate Thickness (mm)	Free-Surface Velocity (km/s)[b]
[a]	2.790	5.08	3.683 ± 0.020
[a]	2.790	6.35	3.639 ± 0.017
[a]	2.790	7.62	3.616 ± 0.032
[a]	2.790	8.89	3.623 ± 0.008
[a]	2.790	10.16	3.567 ± 0.018
[a]	2.790	12.70	3.517 ± 0.035
8A 404	2.790	13.16	3.505 ± 0.026
8A 403	2.790	25.40	3.388 ± 0.014

[a]Data for this entry were determined on some or all of the following shots: [a]8A-347, -348, -349, -384, -387, -411, and -412; each was fired fired using multiple plate thicknesses.
[b]Mean and standard deviation of seven determinations each on the second and sixth entry, six each on the third and fifth, five each on the first and seventh, four on the last, and two on the fourth.

Analysis

Linear least squares fitting gives U_{fs} = 3.725 km/s − 0.01449 t (mm). At t = 0, plate U_s = 7.831 km/s and P_m = 40.21 GPa. Acoustic approximation with D = 8.287 km/s, ρ_{0x} = 1.809 g/cm³, and ρ_{0m} = 2.790 g/cm³ gives corresponding explosive parameters of P_x = 33.71 GPa, U_{px} = 2.248 km/s, and γ = 2.686.

Table 3.44 TNT PRESSED ON DURAL

Explosive

Granular 400-μm particle-size TNT pressed to a density of 1.635 ± 0.006 g/cm^3. Conical 203-mm-thick frusta of 213-mm minimum and 235-mm maximum diameter. Small end toward plate. D = 2.799 ρ_0 + 2.360.

Plates

Dural.

Shot No.	Plate Density (g/cm^3)	Plate Thickness (mm)	No. U_{fs} Dets	Free-Surface Velocity (km/s)[b]
[a]	2.793	1.79	3	2.470 ± 0.025
[a]	2.793	2.43	3	2.452 ± 0.015
[a]	2.793	3.06	3	2.417 ± 0.004
[a]	2.793	3.70	3	2.409 ± 0.010
[a]	2.791	4.79	6	2.397 ± 0.026
[a]	2.793	5.05	1	2.362
[a]	2.791	6.25	7	2.346 ± 0.011
[a]	2.793	7.51	3	2.336 ± 0.027
[a]	2.790	8.04	4	2.363 ± 0.019
[a]	2.793	8.78	3	2.325 ± 0.020
[a]	2.790	9.63	4	2.312 ± 0.016
[a]	2.793	10.05	3	2.322 ± 0.026
[a]	2.790	11.08	2	2.340 ± 0.025
[a]	2.792	11.29	5	2.323 ± 0.010
[a]	2.793	11.98	2	2.309 ± 0.001
[a]	2.793	12.52	2	2.322 ± 0.004
8A 351	2.788	24.87	6	2.288 ± 0.012
8A 849	2.784	38.1	4	2.193 ± 0.005
8A 850	2.784	50.8	3	2.144 ± 0.003
8A 703	2.784	50.92	5	2.165 ± 0.021

[a]Data for this entry were determined on some or all of the following shots: 8A-251, -255, -311, -312, and -313; each was fired using multiple plate thicknesses.

Analysis

Linear least squares fitting to the data on 6-mm plate thickness gives U_{fs} = 2.510 km/s − 0.02535 t (mm). At t = 0, plate U_s = 7.033 km/s and P_m = 24.49 GPa. Acoustic approximation with D = 6.948 km/s, ρ_{ox} = 1.639 g/cm^3, and ρ_{om} = 2.792 g/cm^3 gives corresponding explosive pressure of P_x = 19.35 GPa. Linear least

squares fitting to the data above 6-mm plate thickness gives U_{fs} = 2.373 km/s − 0.00425 t (mm). The intersection of these two lines at 6.5-mm plate thickness corresponds to a plate U_{fs} = 2.345 km/s, U_s = 6.924 km/s, and P_m = 22.52 GPa. Acoustic approximation with D = 6.942 km/s, ρ_{0x} = 1.637 g/cm³, and ρ_{0m} = 2.789 g/cm³ gives corresponding explosive parameters of P_x = 17.89 GPa, U_{px} = 1.572 km/s, and γ = 3.415.

Table 3.45 TNT AND DNT ON BRASS

Explosive

TNT/DNT: 60.8/39.2. 1.579 ± 0.002 g/cm³. Six 102-mm-high, 150-mm-diam cylinders. P-080 and 13-mm-thick Composition B booster. D = 3.235 ρ_0 + 1.647.

Plates

Brass.

Shot No.	Plate Density (g/cm³)	Plate Thickness (mm)	Free-Surface Velocity (km/s)[a]
8A 1323	8.426	2.54	1.441 ± 0.006
8A 1306	8.426	6.29	1.391 ± 0.007
8A 1179	8.426	12.82	1.313 ± 0.006
8A 1304	8.426	19.04	1.293 ± 0.007
8A 1186	8.426	25.49	1.266 ± 0.006
8A 1303	8.426	38.19	1.202 ± 0.007
7C 109	8.426	51.64	1.085 ± 0.009

[a]Mean and standard deviation of seven determinations on each shot.

Analysis

Linear least squares fitting gives U_{fs} = 1.433 km/s − 0.00666 t (mm). At t = 0, plate U_s = 4.649 km/s and P_m = 27.94 GPa. Acoustic approximation with D = 6.755 km/s, ρ_{0x} = 1.579 g/cm³, and ρ_{0m} = 8.426 g/cm³ gives corresponding explosive parameters of P_x = 17.77 GPa, U_{px} = 1.666 km/s, and γ = 3.055.

3.4 Plate Dent Test. The plate dent test was developed during World War II at the Explosives Research Laboratory at Bruceton, Pennsylvania.[2] It was designed to provide a relative estimate of explosive power. The test involves detonating an unconfined cylindrical charge of high explosive in contact with a heavy steel plate and measuring the depth of the dent produced in the plate. The explosive charges are of a diameter and length that ensure establishment of a steady-state detonation wave of almost infinite-diameter velocity in most explosives. The steel witness plates are massive and strong enough to limit the damage to the area of interest.

The explosive to be tested is prepared in the form of 1 5/8-in.-diam cylinders of varying lengths (see Table 3.46). The test plates are 6-in.-square by 2-in.-thick pieces of 1018 cold-rolled steel, cut from 2- by 6-in. bar stock having a Rockwell hardness of B-74 to B-76.

To eliminate spalling from the rear surface, several test plates are stacked vertically, and the upper surface of the top plate is greased lightly to ensure good coupling with the charge. The test charge is centered on the plate, a booster of adequate size is placed on the charge, and the detonator is put in place. If necessary, a piece of tape may be used to hold the assembly together and maintain good contact among its various components. The assembly ready for firing is shown in Fig. 3.02.

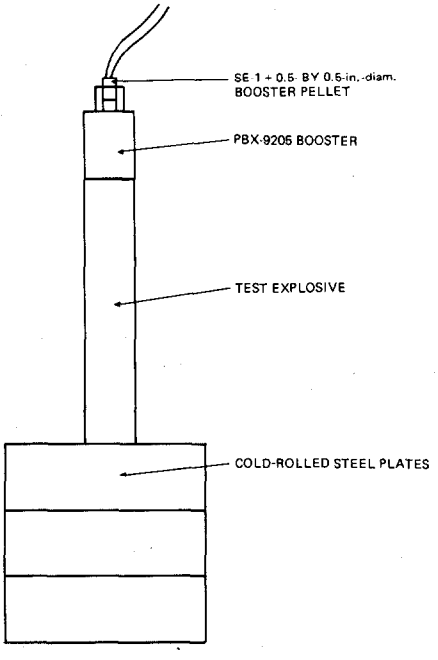

Fig. 3.02. Plate dent test assembly.

Table 3.46 PLATE DENT TEST RESULTS

Explosive	Density (g/cm^3)	Explosive Length (mm)	Dent Depth (mm)	Remarks
BTF	1.838	---	3.05	[a]
HMX	1.730	203	10.07	[b]
Nitromethane	1.133	203	4.15	[b]
NQ	0.25	76.2	0.56	[a] [c]
	0.40	76.2	0.79	[a] [c]
PETN	1.665	203	9.75	[b]
PYX	1.63	203	1.96	[a]
RDX	1.537	203	8.20	[b]
	1.744	203	10.14	[b]
	1.754	203	10.35	[b]
TATB	1.87	203	8.31	[b]
Tetryl	1.681	203	8.10	[b]
TNT - pressed at 65°C	1.629	12.7	1.57	[a]
	1.629	16.9	1.70	[a]
	1.629	25.4	1.93	[a]
	1.629	31.7	1.93	[a]
	1.629	42.4	2.01	[a]
	1.629	84.6	1.93	[a]
	1.629	508	1.93	[a]
	1.631	12.7	1.73	[d]
	1.631	16.9	2.08	[d]

[a] 12.7-mm explosive diameter.
[b] Test explosive diameter 41.3 mm.
[c] 1100 aluminum plate.
[d] 25.4-mm explosive diameter.

Table 3.46 (continued)

Explosive	Density (g/cm^3)	Explosive Length (mm)	Dent Depth (mm)	Remarks
	1.631	25.4	2.90	d
	1.631	31.7	3.20	d
	1.631	42.4	4.04	d
	1.631	50.8	4.19	d
	1.631	63.5	4.27	d
	1.631	72.6	4.14	b
	1.631	84.6	4.19	d
	1.631	101.6	4.09	d
	1.631	127	4.11	d
	1.631	169	4.14	d
	1.631	254	4.06	d
	1.631	508	4.09	d
	1.626	12.7	2.46	b
	1.626	16.9	3.02	b
	1.626	25.4	4.01	b
	1.626	31.7	4.67	b
	1.626	42.4	5.41	b
	1.626	50.8	6.05	b
	1.626	63.5	6.90	b
	1.626	72.6	7.06	b
	1.626	84.61	7.09	b
	1.626	101.6	7.13	b
	1.626	127	7.06	b
	1.626	169	6.88	b
	1.626	254	6.93	b
	1.626	508	6.96	b
	1.626	1016	6.99	b

	1.640	203	6.86	b
	1.620	203	6.68	b
	1.603	127	6.53	b
	1.600	127	6.50	b
	1.583	127	6.43	b
Castable Explosives				
Alex/20				
46 RDX/34 TNT/20 Al	1.762	152	7.34	b
Alex/30				
40 RDX/30 TNT/30 Al	1.864	127	6.76	b
Baratol	2.606	203	3.21	b
Comp B	1.710	203	8.47	b
Comp B-3	1.720	203	8.44	a
Cyclotol 70/30	1.737	203	9.40	b
Cyclotol 75/25	1.740	---	9.53	b
Octol 75/25	1.784	203	9.86	b
	1.784	406	9.86	b
	1.784	508	9.96	b
	1.784	813	9.96	b
	1.802	127	9.99	b
Pentolite 50/50	1.655	127	7.84	54.6 wt% PETN
Tritonol	1.730	---	6.12	80 TNT/20 Al
Plastic-Bonded Explosives				
PBX 9011	1.762	203	9.35	b
PBX 9404	1.840	12.7	4.22	b
	1.840	16.9	5.23	b
	1.840	25.4	7.32	b
	1.840	31.7	8.28	b
	1.840	42.4	9.27	b
	1.840	50.8	9.37	b

Table 3.46 (continued)

Explosive	Density (g/cm³)	Explosive Length (mm)	Dent Depth (mm)	Remarks
	1.840	63.5	9.45	b
	1.840	72.6	9.67	b
	1.840	84.6	9.91	b
	1.840	101.6	10.52	b
	1.840	127	10.54	b
	1.840	169	10.87	b
	1.840	203	11.2	b
	1.840	254	11.3	b
	1.840	305	11.3	b
	1.840	1016	11.3	b
	1.844	203	11.9	b
PBX 9501	1.85	---	10.50	b
X-0007				
86 HMX/14 Estane	1.740	203	8.79	b
X-0009				
93.4 HMX/6.6 Estane	1.798	203	9.98	b
X-0069				
90.2 HMX/9.8 Kel-F 3700	1.874	203	11.10	b
X-0192 (LX-04)				
85 HMX/15 Viton A	1.845	203	10.13	b
X-0204				
83.2 HMX/16.8 Teflon	1.909	203	10.64	b
X-0209				
95.5 HMX/2.5 wax/2.5 Elvax	1.78	203	10.1	b
X-0213	1.79	203	10.2	b
94.6 HMX/2.0 Estane/2.0 BDNPF/ 1.4 wax	1.807	203	10.57	b
X-0217				
94 HMX/4 DNPA/2 NP	1.822	203	10.8	b
	1.824	203	10.8	b

	1.828	203	11.0	b
	1.837	203	10.9	b
X-0234				
94 HMX/4.2 DNPA/1.8 CEF	1.84	203	2.9	a
X-0235				
94 HMX/2 DNPA/2 NP/2 Estane	1.83	203	10.9	b
HMX - DATB Mixture				
X-0143				
85.6 HMX/9.2 DATB/5.4 Estane	1.799	203	10.3	b
HMX - NQ Mixtures				
X-0183				
65.7 HMX/26.4 NQ/7.79 Kel-F	1.814	203	9.8	b
X-0118				
29.7 HMX/64.9 NQ/5.4 Estane	1.709	203	7.4	b
HMX - Tungsten Mixture				
41.6 HMX/5.5 Kel-F/52.9 W	3.532	203	11.00	b
PYX Mixtures				
95 PYX/5 Kel-F	1.696	203	2.11	a
RDX Mixtures				
Comp A-3	1.629	203	8.23	b
PBX 9007	1.636	203	2.29	a
PBX 9010	1.782	12.7	4.24	b
	1.782	25.4	6.99	b
	1.782	50.8	8.81	b
	1.782	76.2	9.22	b
	1.782	102	9.55	b
	1.782	203	10.0	b
	1.782	305	10.3	b
	1.782	406	10.3	b
PBX 9205	1.665	102	8.34	b
	1.675	127	8.50	b
	1.685	102	8.28	h
	1.685	127	8.47	b
	1.685	203	8.69	b

Table 3.46 (continued)

Explosive	Density (g/cm³)	Explosive Length (mm)	Dent Depth (mm)	Remarks
	1.690	12.7	3.61	[b]
	1.690	16.9	4.47	[b]
	1.690	25.4	5.72	[b]
	1.690	31.7	6.78	[b]
	1.690	37.6	7.92	[b]
	1.690	50.8	8.31	[b]
	1.690	63.5	8.43	[b]
	1.690	72.6	8.43	[b]
	1.690	84.6	8.41	[b]
	1.690	102	8.51	[b]
	1.690	127	8.71	[b]
	1.690	169.4	8.94	[b]
	1.690	254	9.12	[b]
	1.690	508	9.20	[b]
	1.690	1016	9.32	[b]
85 RDX/15 Kel-F	1.804	127	9.94	[b]
	1.810	127	9.91	[b]
	1.810	127	10.06	[b]
	1.810	254	10.01	[b]
	1.810	254	9.99	[b]
	1.820	152	9.89	[b]
	1.820	203	10.06	[b]
88 RDX/12 Kel-F	1.79	203	9.78	[b]
94 RDX/3 NC/3 CEF	1.710	203	8.30	[b]
	1.720	203	9.34	[b]
Boron-Filled				
66 RDX/21 Kel-F/13 B	1.850	203	8.10	[b]

Lead-Filled				
19.2 RDX/3.9 Kel-F/76.9 Pb	5.107	203	9.83	b
27.8 RDX/4.9 Kel-F/67.3 Pb	4.164	203	10.36	b
33.8 RDX/5.4 Kel-F/60.8 Pb	3.680	203	10.26	b
41.5 RDX/6.2 Kel-F/52.3 Pb	3.218	203	10.31	b
51.9 RDX/7.3 Kel-F/40.8 Pb	2.748	203	10.38	b
	2.743	203	10.43	b
66.6 RDX/8.7 Kel-F/24.7 Pb	2.274	203	10.24	b
Silicon-Filled				
66.8 RDX/21.3 Kel-F/11.9 Si	1.872	203	8.71	b
Titanium-Hydride-Filled				
65 RDX/13 Kel-F/22 TiH_2	2.018	203	8.87	b
Zirconium-Hydride-Filled				
24.3 RDX/20.3 Kel-F/55.4 ZrH_2	2.920	203	6.36	b
32.6 RDX/18.1 Kel-F/49.3 ZrH_2	2.686	203	7.74	b
41.9 RDX/15.6 Kel-F/42.5 ZrH_2	2.561	203	9.26	b
42.8 RDX/7.3 Kel-F/49.9 ZrH_2	2.630	203	9.43	b
49.3 RDX/7.9 Kel-F/42.8 ZrH_2	2.470	203	9.82	b
52.9 RDX/12.7 Kel-F/34.4 ZrH_2	2.323	203	9.58	b
57.0 RDX/8.5 Kel-F/35.5 ZrH_2	2.328	203	10.03	b
57.0 RDX/18.2 Kel-F/24.8 ZrH_2	2.193	203	9.25	b
	2.188	203	9.53	b
62 RDX/24.7 Kel-F/13.4 ZrH_2	2.048	203	9.09	b
65.8 RDX/9.2 Kel-F/25 ZrH_2	2.144	203	9.86	b
76.4 RDX/10.0 Kel-F/13.6 ZrH_2	1.979	203	10.06	b

Table 3.47 LEAD-LOADED EXPLOSIVE WAFER TEST

A series of plate dent tests were performed in which a wafer of a lead-loaded explosive was placed between the donor explosive and the witness plate. The test results are given below.

Donor Explosive: 90 HMX/10 Exon
Donor Explosive Diameter: 41.3 mm
Donor Length: 203 mm

Wafer Explosive Material	Density (g/cm^3)	Wafer Thickness (mm)	Dent Depth (mm)
[a]	4.84	9.52	11.99
[a]	4.841	12.70	12.64
[a]	4.841	15.87	12.32
[a]	4.841	19.05	12.32

[a] 22.2 HMX/36 Exon/74.2 Pb.

Donor Explosive: 90 RDX/10 Exon
Donor Explosive Diameter: 41.3 mm
Donor Explosive Length: 203 mm
Donor Explosive Density: 1.775 g/cm^3

Wafer Explosive Material	Density (g/cm^3)	Wafer Thickness (mm)	Dent Depth (mm)
None	9.94		
[b]	3.668	9.52	11.12
[b]	3.655	12.7	11.17
[b]	3.654	19.05	11.50
[b]	3.653	25.4	11.45
[c]	4.62	3.17	10.28
[c]	4.62	6.37	10.89
[c]	4.61	9.52	11.66
[c]	4.61	12.70	11.96
[c]	4.61	15.87	12.12
[c]	4.60	19.05	11.77
[c]	4.60	25.04	11.50
[c]	4.60	50.80	10.81

[b] 34.2 RDX/4.6 Exon/61.2 Pb.
[c] 23.3 RDX/3.7 Exon/73.0 Pb.

Table 3.47 (continued)

Wafer Explosive Material	Density (g/cm^3)	Wafer Thickness (mm)	Dent Depth (mm)	Remarks
[d]	5.035	6.37	10.72	
[d]	5.004	9.52	11.18	
[d]	5.025	12.70	11.04	
[d]	5.007	203	8.13	No donor HE
[d]	5.526	6.37	10.86	
[d]	5.537	9.62	11.98	
[d]	5.522	9.52	11.68	
[d]	5.516	15.87	11.73	
[d]	5.537	203	9.75	No donor HE

[d] 16.1 RDX/3.0 Exon/80.6 Pb

3.5 Detonation Failure Thickness. The wedge-shaped explosive sample is confined on the bottom by a 1-in.-thick brass plate and on the sides by 1/4-in.-thick steel bars. The test assembly is shown in Fig. 3.03. The wedge is usually 1 in. wide and, with side confinement, adequately represents a wedge of infinite width. High-density solid explosive samples are prepared most conveniently by gluing a rectangular explosive prism to the brass plate and then forming the wedge by milling. The wedge thickness is measured at various distances from the end of the brass, the side plates are then glued on, and the charge is ready for firing. To minimize damage to the brass, it is backed by a heavy steel plate when the charge is fired. A step in the brass plate indicates the location and thus the thickness of the explosive at the point where detonation fails.

The booster explosive may cause an artificially energetic and rapid detonation, called overdrive, in the sample. To correct for overdrive, wedges with apex angles of 1, 2, 3, 4, and 5° are fired, and the resulting failure thicknesses are plotted vs angle.

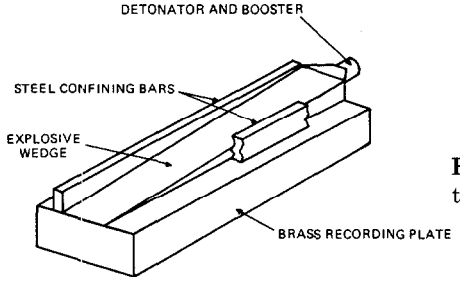

Fig. 3.03. Minimum failure thickness test assembly.

Table 3.48 DETONATION FAILURE THICKNESS

Explosive	Density (g/cm^3)	Failure Thickness (mm)
Pure Explosives		
Ammonium picrate	1.64	3.29
TNT	1.61	1.91[a]
Castable Mixtures		
Comp A-3	1.63	0.57
Comp B-3	1.72	0.94
Cyclotol 75/25	1.75	1.51
Octol 75/25	1.79	1.43
Pentolite	1.70	1.39[b]
Plastic-Bonded Explosives		
HMX-Based		
PBX 9011	1.77	0.61
PBX 9404	1.83	0.46
X-0204	1.922	0.41
RDX-Based		
PBX 9010	1.78	0.52
PBX 9205	1.69	0.57
PBX 9407	1.77	0.30

[a]Pressed at 65°C.
[b]Cast 50-mm wedge.

A linear curve is fitted through the data and extrapolated to 0°, and the failure thickness at 0° is designated the detonation failure thickness.

If the brass plate were completely incompressible, the failure thickness so determined would be half that of an unconfined infinite sheet. The failure thickness of an unconfined sheet is less than the failure diameter of a cylinder because rarefactions in a cylinder enter from all sides of the charge and influence the detonation. Thus, the failure diameter may be several times the failure thickness and may vary from one explosive to another.

More complete details are given in a LASL report.[3]

REFERENCES

1. W. E. Deal, Journal of Chemical Physics **27(1)**, 796-800 (September 1957).
2. Louis C. Smith, Explosivstoffe **15**, 106-110, 130-134 (1967).
3. Manuel J. Urizar, Suzanne W. Peterson, and Louis C. Smith, Los Alamos Scientific Laboratory report LA-7193-MS (April 1978).

4. SHOCK INITIATION PROPERTIES

ORDER OF WEDGE TEST RESULTS

Pure Explosives

HMX
HMX (single crystal)
Nitromethane (NM)
Nitroguanidine (NQ)
PETN (pressed)
PETN (single-crystal)
TATB (purified)
TATB (micronized)
TATB (superfine)
Tetryl
TNT (cast)
TNT (single-crystal)

Castable Mixtures

Baratol (76 barium nitrate, 24 TNT)
Comp B (60 RDX, 40 TNT)
X-0309 (Destex)

Plastic-Bonded Explosives

DATB Base
X-0300 (95 DATB, 5 Estane)

HMX Base
PBX 9501 (95 HMX, 2.5 Estane, 2.5 BDNPFA
PBX 9404 (94 HMX, 3 NC, 3 chloroethylphosphate)
PBX 9011 (90 HMX, 10 Estane)
LX-04 (85 HMX, 15 Viton)
X-0219-50-14-10 (50 HMX, 40 TATB, 10 Kel-F 800)

NQ Base
X-0241 (96 NQ, 2 wax, 2 Elvax)
95 NQ, 5 Estane
X-0228 (90 NQ, 10 Estane)

SHOCK INITIATION PROPERTIES

PETN Base

XTX-8003 (Extex) (80 PETN, 20 Sylgard)

RDX Base

95 RDX, 2.5 wax, 2.5 Elvax
PBX 9407 (94 RDX, 6 Exon)
PBX 9405 (93.7 RDX, 3.15 NC, 3.15 chloroethylphosphate)
X-0224 (74 RDX, 20 Al, 5.4 Elvax, 0.6 wax)
X-0250-40-19 (40.4 RDX, 40.4 cyanuric acid, 19.4 Sylgard)

TATB Base

PBX 9502 (95 TATB, 5 Kel-F 800 (X-0290)
95 TATB, 2.5 Kel-F 800, 2.5 Kel-F 827
94 TATB (coarse), 6 Estane
94 TATB (bimodal), 6 Estane
94 TATB, 3 Elvax, 3 wax
94 TATB, 4.5 polystyrene, 1.5 dioctylphthalate
92 TATB, 6 polystyrene, 2 dioctylphthalate
90 TATB, 10 Estane
X-0219 (90 TATB, 10 Kel-F 800)
90 TATB, 5 Elvax, 5 wax
90 TATB, 5 Kel-F 800, 5 Kel-F 820
85 TATB, 15 Kel-F 800
85 TATB, 7.5 Kel-F 800, 7.5 Kel-F 827

Propellants

FKM Class VII
SPIS-44 Class VII
SPIS-45 Class II
TP-N1028 Class VII
UTP-20930 Class VII
VOP-7 Class VII
VRO Class VII
VRP Class VII
VTG-5A Class VII
VTQ-2 Class VII
VTQ-3 Class VII
VWC-2 Class VII

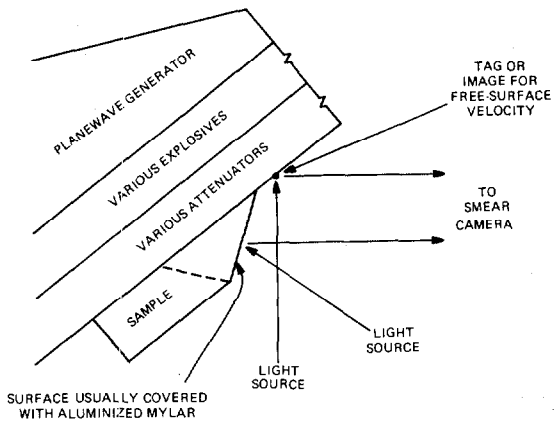

Fig. 4.01. Experimental arrangement for most wedge test shots.

4.1 Wedge-Test Data. Majowicz and Jacobs,[1] and Campbell, Davis, Ramsay, and Travis[2] first used the wedge test to study shock initiation of solid explosives. The test is named for the wedge-shaped explosive sample that is shocked by a booster-and-attenuator system as shown in Fig. 4.01. The explosive is wedge-shaped so that the shock or detonation wave moving through it is visible along the slant face. The slant face and flat of the sample are covered with a thin aluminized plastic and are illuminated by an intense light source. A smear camera is aligned so as to record the light reflecting from the aluminized plastic. As the shock wave proceeds through the explosive, the motion of the explosive mass tilts the reflecting surface on the slant face so that the light is no longer reflected into the camera. This sharp cutoff of light gives a well-defined record of the shock or detonation location vs time. Usually, the shock wave appears to travel through the explosive sample at a slightly increasing velocity and then to travel at a significantly higher velocity when detonation occurs. The point of interest is the distance into the sample, x*, or time, t*, at which detonation occurs.

The booster-and-attenuator system is selected to provide about the desired shock pressure in the sample wedge. In all but a few of the experiments on which data are presented here, the booster-and-attenuator systems consisted of a plane-wave lens, a booster explosive, and an inert metal or plastic shock attenuator. In some instances, the attenuator is composed of several materials. The pressure and particle velocity are assumed to be the same on both sides of the attenuator-and-sample interface. However, because initiation is not a steady state, this boundary condition is not precisely correct. The free-surface velocity of the attenuator is measured, and the particle velocity is assumed to be about half that. The shock Hugoniot of the attenuator is assumed to be known, so the shock pressure and particle velocity in the attenuator can be evaluated using the free-surface velocity measurement. Then, the pressure (P) and particle velocity (U_p) in the explosive sample are found by determining graphically the intersection of the attenuator rarefaction locus and the

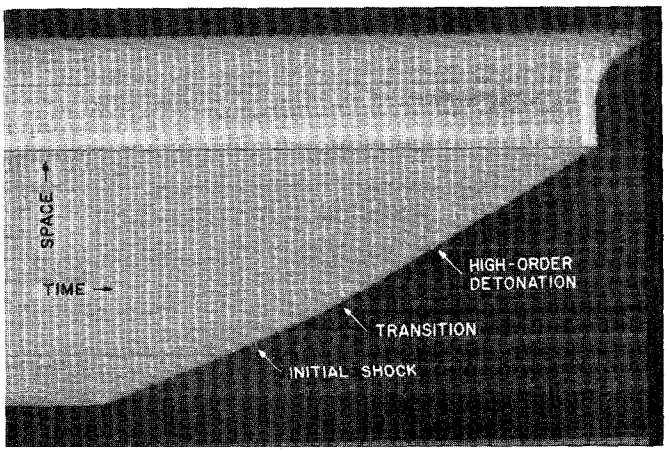

Fig. 4.02.

explosives-state locus given by the conservation-of-momentum relation for the explosive, $P = \rho_0 U_p U_s$, where U_s = shock velocity and ρ_0 = initial density. The attenuator rarefaction locus is approximated by reflecting the attenuator Hugoniot line about a line where the attenuator particle velocity is a constant. Because initiation is not a steady state, the conservation-of-momentum relation does not hold precisely; however, near the sample and attenuator interface, the reaction is slight enough that the accuracy is sufficient. Values of the initial shock parameters, P_0, U_{p0}, and U_{s0}, are given in the tables that follow.

Figure 4.02 shows a typical smear camera wedge record. Characteristically, these traces show the initial shock, the point of transition to high-order detonation, and the high-order detonation. The space and time dimensions are shown. Although the shock and detonation velocities in the explosive can be determined from these records, only the coordinates for the high-order detonation, x^* and t^*, are normally found. Historically, many analysis techniques have been used, including those used here for data analysis.

THE TECHNIQUES

Technique 1. In Technique 1, the *early average* shock velocity is determined from the angle generated on the camera record by the shock-wave progress along the wedge surface, the optical magnification, the wedge angle, the viewing angle, and the camera writing speed. The distance over which this measurement is made is kept as short as is practical. The distance and time of transition to high-order detonation are determined from the film measurements, knowledge of the viewing angle, etc. In all the techniques described here, it is assumed that the shock wave is plane and parallel to the wedge-and-attenuator interface. The initial shock and particle velocity vs pressure in the wedge are obtained from a graphical solution involving the wedge density, early average shock velocity, and pressure in the last attenuator plate.

Technique 2. All wedges analyzed using Technique 2 had a flat portion extending beyond the end of the normal wedge face. The shock position was determined from ratios of disturbed vs undisturbed positions measured on the film image and wedge face. Times were obtained from the known writing speed of the camera and from film measurements. A film trace is obtained when the shock arrives at the free surface of the attenuator plate. Another is obtained when the detonation arrives at the free surface of the flat part of the sample. This latter trace is especially informative about the uniformity of initiation and helps to explain an occasional apparent overshoot. Phase velocities are measured at various positions on the wedge, depending on the specific record, and are analyzed by Technique 1. Each velocity is assigned to a midpoint of the interval over which the measurement is made, and the initial velocity is found by extrapolating the velocity vs thickness curve to zero thickness. The initial pressure and particle velocity are found from a graphical solution as in Technique 1.

Technique 3. In Technique 3, the shock position in the sample, x, is determined from 20-40 points using the same method of proportions as in Technique 2 and considering the wedge thickness and the length of the slant face image. The corresponding times, t, are determined from the known writing speed of the camera and from film measurements. When this technique was used, various equations were tested against the x-t data obtained from the wedge section of the sample. The equation $x = c(e^{kt} + t - 1)$ was chosen to fit the data from the partially reacting run. A plot of t vs ln $(x - ct + c)$ produced a straight line of slope k if the proper c value was selected. Sensitivity of the fit to a chosen c was such that a poor choice was usually recognized, and a questionable choice had only a relatively minor effect on the first derivative evaluated at $t = 0$.

$$\left.\frac{dx}{dt}\right|_{t=0} = c(k + 1) = U_{s0}$$

The c is chosen best from a plot of the data for a shot with a long run to high-order detonation. The data used to evaluate c can come from an experiment in which the shock was accelerating, and high-order detonation need not be observed. The value of c is treated as a constant for that particular explosive formulation and density. This procedure typically gives a lower initial shock velocity value than does Technique 1.

Technique 4. When Technique 4 is used, the lighting of the flat face is adjusted to show particle paths after a shock front has passed. As in Technique 3, the smear camera record is measured and the measurements are converted to real times, t, and distances, x, for the shock traversing the wedge. Average velocities, x/t, are calculated for points before high-order detonation and are plotted against t. (Any inconsistent data near the beginning and end are rejected.) The data are then fitted with $x = U_{s0}t \pm 1/2\ bt^2$ by the least squares method. The derivative evaluated at $t = 0$ is taken as the initial shock velocity. Thereafter, the analysis is like that in Techniques 2 and 3. The single-curve buildup hypothesis is checked by plotting, for

each shot, the shock wave trajectory measured back from the transition to high-order detonation and superimposing the plots using the transition as a fiducial. Detonation velocities are obtained from x-t data measured in the high-order region.

Technique 5. In Technique 5, the driving plate free-surface velocity always is measured with electrical pin contactors. Buildup data from all experiments on a given density of explosive are pooled on the assumption of a single curve buildup and are fitted by the least squares method to the empirical function,

$$D = A_1 T^{(1-A_3)} \left[1 - \exp\left(-A_2 T^{A_3}\right)\right] + (A_4 - A_1 A_2) T \quad ,$$

where D is the distance to detonation, T is the time to detonation at any point on the buildup curve, A_4 is the detonation velocity, and A_1, A_2, and A_3 are arbitrary constants. The shock velocities are evaluated from the derivative of the above function,

$$U_{s0} = A_1(1 - A_3)T^{-A_3}\left[1 - \exp\left(-A_2 T^{A_3}\right)\right] + A_1 A_2 A_3 \exp\left(-A_2 T^{A_3}\right) + A_4 - A_1 A_2 \quad ,$$

using the coefficients fitted to the pooled data and the time to detonation, $T = t^*$, observed in the individual experiments. This shock velocity value is then used with the driving plate free-surface velocity determined as before.

Technique 6. In Technique 6, a flash gap consisting of grooved Lucite blocks is used to measure the driving plate free-surface velocity. Also, shock velocities are determined by reading the average slopes from the streak records. Samples thus analyzed had two phase-velocity regions, the normal high-order detonation and an intermediate velocity region. The two abrupt changes in phase velocity are read from the streak records to give the distance to the intermediate region and the distance to detonation. All other analysis is done using Technique 5.

Technique 7. In Technique 7, the x-t data are digitized into 70 discrete points. A linear fit is made to three adjacent x-t points, and the slope is taken as the velocity at the midpoint of the line. Then one x-t end point is dropped, a new one is added on the other end, a new linear fit is made, and the velocity is found. This running linear least squares process is repeated until all 70 x-t points have been used. The u-x data are then extrapolated to zero thickness (x = 0) to find the initial shock velocity, U_{s0}. All other analysis is done as in Technique 1.

THE DATA TABLES

The data tables indicate the driver-and-attenuator systems used for each experiment. Also given are the LASL shot number; the initial shock pressure, particle velocity, and shock velocity; a fitting parameter, 1/2 b, used in the data reduction where appropriate; the sample density; the distance to detonation, x*, and time to detonation, t*.

Usually the $U_{s0} - U_{p0}$ data are plotted. Also given are equations for these data fitted to one of two functional forms, the most common of which is linear. These equations are given with their coefficients and the standard errors of the coefficients. If the sound speed has been used as a data point in determining the fit, it also is given. For a few explosives, a hyperbolic function is fitted to the data and coefficients without standard errors are given.

For some explosives, a logarithmic function fit to the initiation data, x* or t* vs P_0, is given. Generally, this is done only for the distance to detonation, x*. Usually, if these fits are given, a "Pop" plot also is included. The "Pop" plot functional form traditionally has been a power function with x* or t* as dependent variables and P_0 as the independent variable. However, recent work[3] suggests that the appropriate fitting plane should be log-log, because the measurement errors in x* have been shown to be lognormal, and the t* and P_0 errors may also be lognormal. Since x* and t* are measured quantities and P_0 is based on measurements, all are stochastic variables, and a statistically valid regression analysis cannot be used to estimate a functional relationship. Nevertheless, x* and t* physically occur after the imposition of P_0, and thus it has been argued that they result from (or are dependent on) P_0. Since the error in P_0 data is generally greater than x* and t* error, in finding an "average relationship" between them, it is more appropriate to assume that the variable with the least error is the independent variable.[4] For these reasons, the "Pop" plot functions are given in log form, with log P_0 being the dependent variable.

Table 4.01 WEDGE TEST LENS AND BOOSTER SYSTEMS

The lens and booster explosive systems used for most of the wedge tests are listed below, generally in order of increasing pressure output. All lenses, designated by P-xxx, have plane-wave output. The output face diameter is indicated by the designation number; for instance, P-040 and P-081 and 4 are 8.1 inches in diameter, respectively. The booster explosive thickness also is given.

System	Lens	Booster Thickness (mm)
A	0.25-g/cm^3 NQ PL-38	---
B	P-081	25.4 Baratol
C	P-120	25.4 Baratol
C-1	P-081	50.8 Baratol
D	P-081	6.3 Comp B and 25.4 Baratol
E	P-081	50.8 Baratol
F	P-081	12.7 TNT
G	P-081	25.4 TNT
H	P-081	50.8 TNT
I	P-040	25.4 Comp B
J	P-081	25.4 Comp B
K	P-081	38.1 Comp B
L	P-081	50.8 Comp B
M	P-040	25.4 PBX 9404
N	P-081	25.4 PBX 9404
O	P-120	25.4 PBX 9404
P	P-081	30-32 PBX 9404
Q	P-081	35.5 PBX 9404
R	P-081	38.1 PBX 9404
S	P-081	50.8 PBX 9404
T	P-081	12.7 Plex[a], 16-mesh screen, and 50.8 PBX 9404
U	P-081	101.6 PBX 9404

[a]The following abbreviations are used in describing wedge-test boosters. Plex = Plexiglas; Foam = 0.19-g/cm^3 polyurethane foam; SS = 304 stainless steel; PC = Lexan polycarbonate; PMMA = any of several polymethylmethacrylates, and PE = polyethylene.

Table 4.02 HMX

Composition
100 wt% HMX
Theoretical Maximum Density
1.905 g/cm³
Preparation Method
Solvent pressing
Data Summary
ρ_0 = 1.891 g/cm³. T_0 = 25°C. Technique 1

Shot Number	Initial Shock Parameters			Coordinates for High-Order Detonation		Driving System Thickness (mm)
	P_0 (GPa)	U_{p0} (mm/μs)	U_{s0} (mm/μs)[a]	x^* (mm)	t^* (μs)	
E-2106	4.41	0.592	3.943	7.74	---	B, 6.61 brass, 24.3 Plex
E-2108	4.89	0.593	4.359	6.78	---	B, 6.27 brass, 6.35 Plex
E-2117	4.93	0.632	4.126	6.68	---	E, 6.41 brass, 6.35 Plex
E-2125	7.54	0.884	4.511	2.89	---	B, 36.6 Plex
E-2116	8.02	0.912	4.651	2.59	---	B, 24.8 Plex
E-2099	8.40	0.902	4.924	2.82	---	B, 25.3 Plex
E-2096	9.35	0.952	5.198	2.31	---	B, 6.46 Lucite
E-2118	9.55	1.036	4.877	2.37	---	B, 6.30 Plex

[a]Measured over the first millimeter of run.

Reduced Data
$U_{s0} = (2.901 \pm 0.407) + (2.058 \pm 0.490)\ U_{p0}$.
$\log P = (1.18 \pm 0.02) - (0.59 \pm 0.03) \log x^*$ for $4.41 < P < 9.55$.

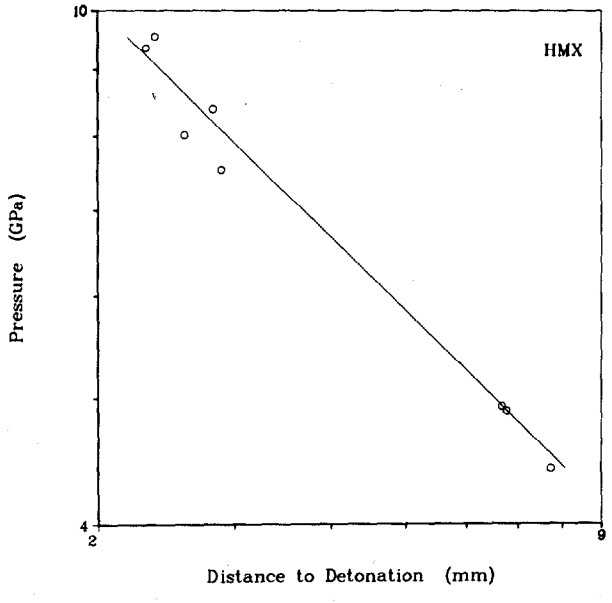
HMX
Pressure (GPa)
10
4
2
9
Distance to Detonation (mm)

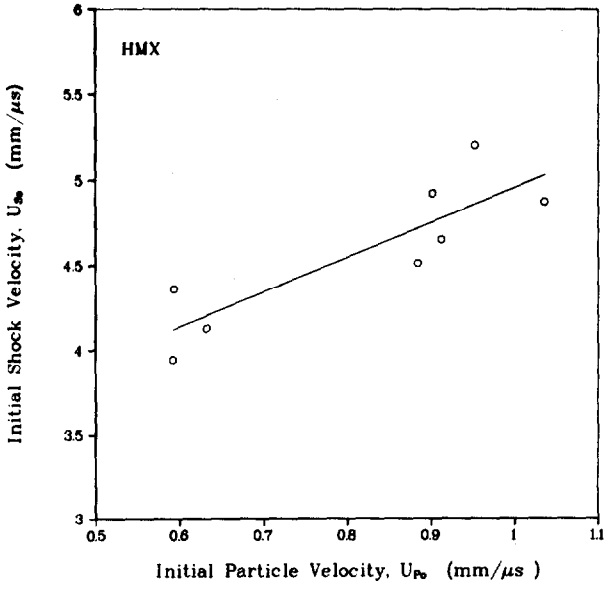
HMX
Initial Shock Velocity, U_{Sb} (mm/μs)
6
5.5
5
4.5
4
3.5
3
0.5
0.6
0.7
0.8
0.9
1
1.1
Initial Particle Velocity, U_{Pb} (mm/μs)

Table 4.03 HMX (SINGLE CRYSTAL)

Composition
100 wt% HMX
Theoretical Maximum Density
1.905 g/cm³
Preparation Method
Controlled solvent evaporation
Data Summary
ρ_0 = 1.90 g/cm³. T_0 = 24°C. Technique 4

Shot Number	Initial Shock Parameters			1/2 b	$\bar{U}_s$	Coordinates for High-Order Detonation		Flyer Plate Thickness
	P_o (GPa)	U_{po} (mm/μs)	U_{so} (mm/μs)	(mm/μs²)	(mm/μs)[a]	x_{0T} (mm)[b]	t_{0T} (μs)[c]	(mm)[d]
E-3794	43.5	2.93	7.812	−2.291	7.55	0.80	0.11	2.52
E-3792	35.6	2.61	7.177	+0.191	7.20	4.40	0.61	3.53
E-3796	34.8	2.49	7.357	−0.016	7.35	>7.4[e]	21.22[e]	4.03

[a] $\bar{U}$ is an estimated initial shock velocity based on the average velocity of the shock in the crystal, the assumption that the shock advanced at a constant velocity, and allowance for experimental complications.
[b] x_{0T} is the average level at which detonation overtook the shock front in the crystal.
[c] t_{0T} is the average time at which detonation overtook the shock front in the crystal.
[d] P-081, 50-mm PBX 9404, 0.25-mm PE, magnesium flyer, 25.4-mm air, 5-mm magnesium.
[e] Overtake occurred after the initial shock had crossed the 7.4-mm-thick crystal. t_{0T} includes the time needed to overtake the crystal's moving free surface.

Table 4.04 NITROMETHANE

Composition
100 wt% NM
Theoretical Maximum Density
1.125 g/cm³
Data Summary
ρ_0 = 1.125 g/cm³. Technique 2

Shot Number	T_0 (°C)	P_0 from Driver (GPa)	U_{s0} (mm/μs)	U_{Px} from Driver (mm/μs)	U_{Px} from Driven (mm/μs)[a]	Δ U_{Px} Driven-Driver	Driving System Thickness (mm/μs)
E-1412	20.4	2.50	2.918	0.762	0.730	−0.032	H, 6.4 Plex, 6.4 brass
E-1395	19.2	3.10	3.080	0.896	0.928	+0.032	C-1, 6.4 brass
E-1397	17.8	5.38	3.670	1.304	1.235	−0.079	H, 6.4 Plex, 6.4 Dural
E-1381	22.0	5.65	3.819	1.315	1.373	+0.058	K, 13 air, 6.4 brass, 6.4 Dural, 13 air, 13 Dural
E-1382	22.0	5.58	3.761	1.319	1.315	−0.004	K, 13 air, 6.4 brass, 6.4 Dural, 13 foam, 13 Dural
E-1402	18.0	5.86	3.885	1.340	1.299	−0.041	H, 13.4 Dural
E-1411	17.2	6.28	4.025	1.387	1.373	−0.014	K, 25.4 Plex, 6.4 brass, 6.4 aluminum
E-1396	19.6	6.07	3.882	1.390	1.338	+0.052	H, 6.4 brass, 6.4 aluminum
E-1383	22.0	6.60	4.016	1.460	1.492	+0.032	K, 9.5 air, 6.4 brass, 6.4 Dural, 13 air, 13 Dural
E-1384	21.6	6.72	4.077	1.465	1.475	+0.010	K, 9.5 air, 6.4 brass, 6.4 Dural, 13 air, 13 Dural

E-1413	17.3	7.35	4.243	1.540	1.446	−0.094	K, 13.4 Micarta, 6.4 brass, 6.4 Dural
E-1386	22.1	9.60	4.639	1.839	Detonation between plates		---
E-1385	22.0	9.59	4.629	1.841	Detonation between plates		---

[a] U_p was deduced from the initial U_{FS} of a Dural plate on a flat of the nitromethane wedge.

Table 4.05 NITROGUANIDINE (NQ)

Composition
100 wt% NQ
Theoretical Maximum Density
1.774 g/cm³
Particle Size Distribution
Large grain and Commercial grain
Preparation Method
Pressing and machining to shape
Data Summary
T_0 = 23°C. Technique 3 or as noted

Shot Number	Initial Shock Parameters P_0 (GPa)	U_{p0} (mm/μs)	U_{s0} (mm/μs)	Coordinates for High-Order Detonation x* (mm)	t* (μs)	Driving System Thickness (mm)
			Large Grain,[a] ρ_0 = 1.659 g/cm³			
E-2838	14.08	1.601	5.300	16.95	2.73	H, 23.4 Plex
E-2840	15.72	1.683	5.630	9.53	1.51	H, 6.4 Plex
E-2864	20.78	2.003	6.251	3.97	0.58	H, 6 Plex
E-2892	24.07	2.184	6.640	2.18	0.30	N, 6 Plex
			ρ_0 = 1.715 g/cm³			
E-2865	13.35	1.368	5.692[b]	>19.01	>3.42	
E-2866	21.30	1.920	6.469	9.42	1.39	J, 6 Plex
E-2867	24.63	2.072	6.932	1.35	0.19	N, 6 Plex
			ρ_0 = 1.723 g/cm³			
E-2868	21.35	1.914	6.473	15.81	2.42	N, 12.2 Plex
E-2869	13.32	1.337	5.780[c]	>18.97	>3.40	G, 13.1 Plex
E-2882	21.39	1.935	6.416[c]	>18.99	>3.06	J, 6 Plex
E-2885	21.90	1.921	6.618[c]	>19.01	>3.02	N, 11.8 Plex
E-2870	25.49	2.215	6.678	4.98	0.72	N, 6 Plex
E-2886[d]	25.85	2.220	6.757	7.24	1.04	N, 5.9 Plex
			Commercial-Grain (needle), ρ_0 = 1.688 g/cm³, Technique 2			
E-1890	10.15	1.172	5.131	>10	---	B, 6.3 Plex
E-1987	---	---	---	>10	---	I, 1.0 D-38
E-1989	11.71	1.320	5.257	>10	---	M, 1.02 D-38
E-1896	16.4	1.650	5.880	>10	---	G, 6.3 Plex
E-1988	21.16	1.982	6.325	4.54	---	U, 25 Plex
E-1891	21.34	1.962	6.445	5.50	---	J, 6 Plex
E-1939	24.25	2.128	6.751	3.04	---	L, 6 Plex

Table 4.05 (continued)

Shot Number	Initial Shock Parameters P_0 (GPa)	U_{p0} (mm/μs)	U_{s0} (mm/μs)	Coordinates for High-Order Detonation x* (mm)	t* (μs)	Driving System Thickness (mm)
E-1897	25.85	2.167	7.067	2.643	---	N, 6 Plex
E-1908	27.28	2.336	6.918	1.954	---	T, 6 Plex

Data from the 10-mm Level[e]

Shot Number	P (GPa)		U_p (mm/μs)	U_s (mm/μs)	Driving System Thickness (mm)
E-1890	10.1		1.207	4.952	B, 6.3 Plex
E-1987	16.3		1.667	5.800	I, 1.0 D-38
E-1989	21.7		2.045	6.278	M, 1.02 D-38
E-1896	21.2		1.979	6.359	G, 6.3 Plex
E-1988		detonated		8.387	U, 25 Plex
E-1891		detonated		8.232	J, 6 Plex
E-1939		detonated		8.268	L, 6 Plex
E-1897		detonated		8.379	N, 6 Plex
E-1908		detonated		8.384	T, 6 Plex

[a]Distributed about 250 μm.
[b]Almost constant.
[c]Decelerates.
[d]Nonuniform initiation produced unrealistically large x*.
[e]P and U_p were deduced from the initial U_{fs} of a 2.26-mm-thick 2024T-4 Dural plate placed on a flat at the 10-mm level of the NQ wedge.

Reduced Data

Large grain, all densities

$U_{s0} = (3.544 \pm 0.524) + (1.459 \pm 0.276)\, U_{p0}$.

$\log P = (1.44 \pm 0.07) - (0.15 \pm 0.08) \log x^*$ for $13.35 < P < 26.28$.

$\log P = (1.32 \pm 0.03) - (0.15 \pm 0.07) \log t^*$.

Commercial grain

$U_{s0} = (3.048 \pm 0.254) + (1.725 \pm 0.135)\, U_{p0}$.

$\log P = (1.51 \pm 0.02) - (0.26 \pm 0.03) \log x^*$ for $21.2 < P < 27.1$.

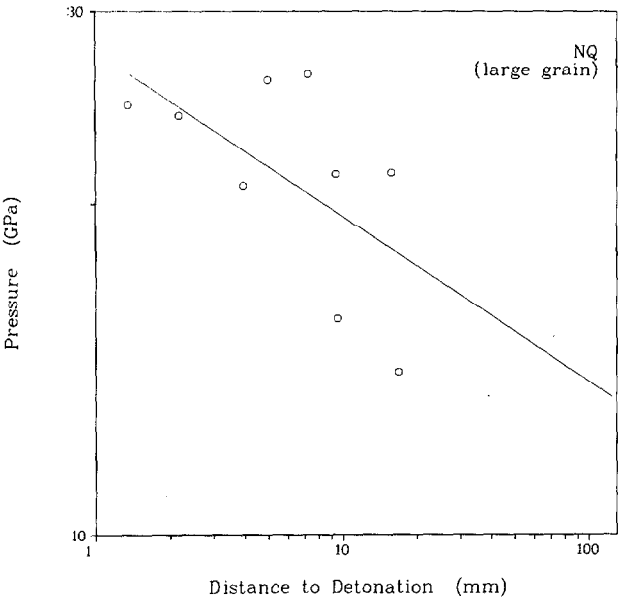
30
10
1
10
100
NQ
(large grain)
Pressure (GPa)
Distance to Detonation (mm)

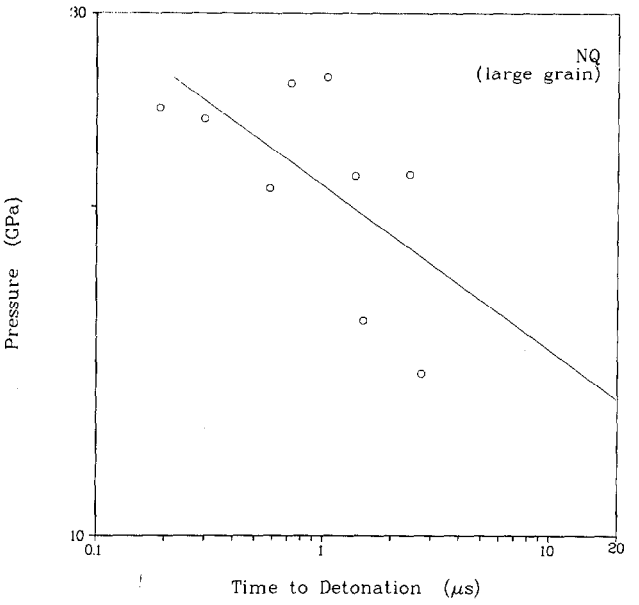
30
10
0.1
1
10
20
NQ
(large grain)
Pressure (GPa)
Time to Detonation (μs)

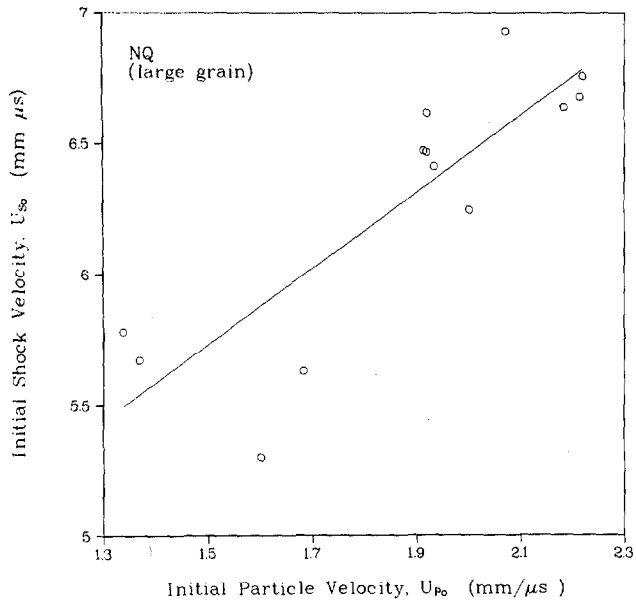
NQ
(large grain)
Initial Shock Velocity, U_{So} (mm μs)
Initial Particle Velocity, U_{Po} (mm/μs)
7
6.5
6
5.5
5
1.3
1.5
1.7
1.9
2.1
2.3

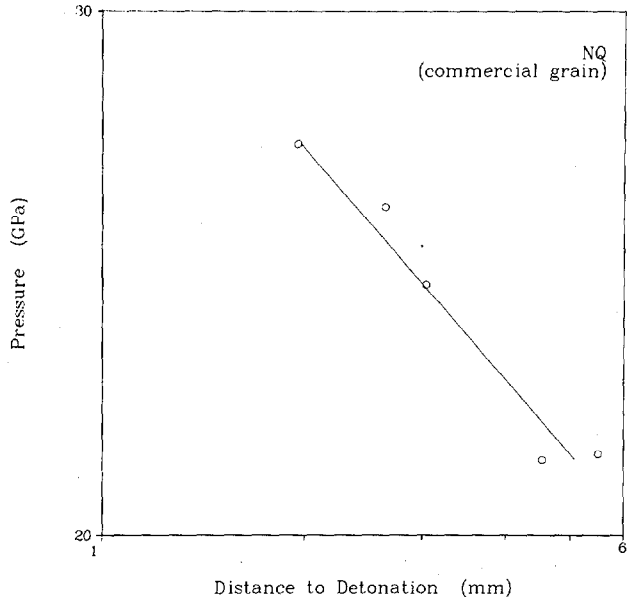
NQ
(commercial grain)
Pressure (GPa)
30
20
1
6
Distance to Detonation (mm)

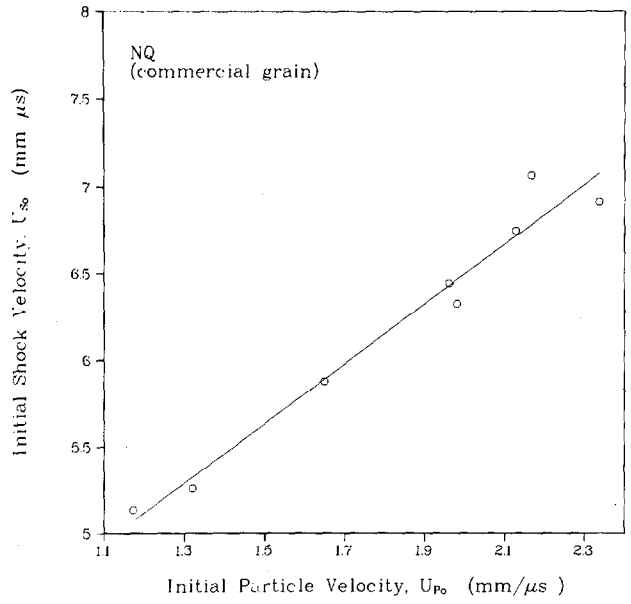
NQ
(commercial grain)
Initial Shock Velocity, U_{s_o} (mm μs)
8
7.5
7
6.5
6
5.5
5
1.1
1.3
1.5
1.7
1.9
2.1
2.3
Initial Particle Velocity, U_{P_o} (mm/μs)

Table 4.06 PETN (PRESSED)

Composition

Pure detonator-grade pentaerythritol tetranitrate

Theoretical Maximum Density

1.778 g/cm^3

Particle Size Distribution

The elongated, prismatic crystals are 130-160 μm long and 10-20 μm across. Air permeation determinations on 1.0-g/cm^3 specimens gave a specific surface of 3300 cm^2/g.

Preparation Method

Cold pressing into pellets and machining into wedges, except for the 1.0-g/cm^3 wedges, which were formed by cutting.

Comments

The experiments and analyses differed from all previous ones as follows.

(a) The Hugoniot relations for 1.72- and 1.6-g/cm^3 PETN were fitted by constraining the intercept of the fitted shock-velocity vs particle-velocity curve to be the bulk sound speed measured in the explosive. This Hugoniot was used to calculate the relations between input shock strength and time and distance to detonation. (See Los Alamos Scientific Laboratory report LA-5131.)

(b) The gas-gun experiment shown in Fig. 4.03 was used to obtain data on 1.4- and 1.75-g/cm^3 PETN. Listed are both the input shock parameters, from the observed shock velocities and impedance match solution with the projectile, and "calculated pressures" obtained from an explosive Hugoniot obtained separately using quartz-gauge experiments and the measured particle velocities. These calculated pressures are used in fitting relations between initial pressure and distance and time to detonation.

Table 4.06 (continued)

Initial Shock Parameters			Coordinates for High-Order Detonation		Driving System[a]	
P_0 (GPa)	U_{p0} (mm/μs)	U_{s0} (mm/μs)	x* (mm)	t* (μs)	No. of Elements	Attenuator System
			$\rho_0 = 1.60$ g/cm³, 90.0% ρ_T			
0.72	0.22	2.05	>9.5	---	4	Brass, ethyl ether
0.95	0.28	2.13	>9.5	---	4	Brass, water
1.2	0.35	2.15	4.03	1.65	4	Brass, carbon tetrachloride
1.3	0.37	2.12	3.79	1.54	4	Brass, carbon tetrachloride
1.4	0.41	2.21	2.30	0.84	3	Brass, carbon tetrachloride
1.8	0.44	2.50	1.94	0.74	4	Brass, mixture 1
1.8	0.42	2.65	2.08	0.78	4	Brass, mixture 1
2.0	0.48	2.58	1.47	0.55	4	Brass, tetrabromoethane

Reduced Data

$\rho_0 = 1.60$ g/cm³, where $1.2 < P < 2.0$.

$\log P = (0.40 \pm 0.03) - (0.54 \pm 0.05) \log x^*$.

$\log P = (0.18 \pm 0.02) - (0.44 \pm 0.09) \log t^*$.

Table 4.06 (continued)

P_0 (GPa)	Initial Shock Parameters: U_{p0} (mm/μs)	U_{s0} (mm/μs)	x* (mm)	Coordinates for High-Order Detonation: t* (μs)	No. of Elements	Driving System[a]: Attenuator System
			$\rho_0 = 1.72$ g/cm³, 96.7% ρ_T			
0.89	0.20	2.59	>9.5	---	4	Brass, ethyl alcohol
1.5	0.29	2.92	>9.5	---	4	Brass, carbon tetrachloride
1.6	0.34	2.79	4.44	1.50	4	Dural, ethyl ether
2.0	0.37	3.10	4.16	1.60	4	Brass, Mixture 1
2.1	0.42	2.83	2.90	0.88	4	Brass, tetrabromocthane
2.2	0.38	3.40	3.69	1.14	4	Brass, tetrabromoethane
2.3	0.42	3.17	3.20	0.96	4	Dural, ethyl alcohol
2.4	0.44	3.18	2.47	0.95	4	Dural, water
2.6	0.46	3.33	2.31	0.69	4	Dural, dichloroethyl ether
2.6	0.42	3.55	2.05	0.61	3	Dural, ethyl alcohol
2.7	0.47	3.39	3.17	1.02	4	Dural, water
3.4	0.49	3.99	1.74	0.49	4	Dural, trichloroethylene
3.5	0.54	3.72	1.46	0.44	3	Dural, water
3.9	0.59	3.83	1.29	0.33	4	Dural, tetrabromoethane
6.8	---	---	<3.6	---	2	Dural, polymethylmethacrylate

[a]Booster system was a P-080 plane-wave lens and 5 cm of Baratol. In three- and four-element attenuators, the third layer was brass and the fourth was one of the polymethylmethacrylates. Mixture 1 consisted of tetrabromoethane and carbon tetrachloride, 2 to 1 by volume.

Reduced Data

$U_{s0} = 2.326 + 2.342\ U_{p0}$.

$\log P = (0.61 \pm 0.03) - (0.49 \pm 0.05) \log x^*$.

$\log P = (0.34 \pm 0.02) - (0.50 \pm 0.09) \log t^*$.

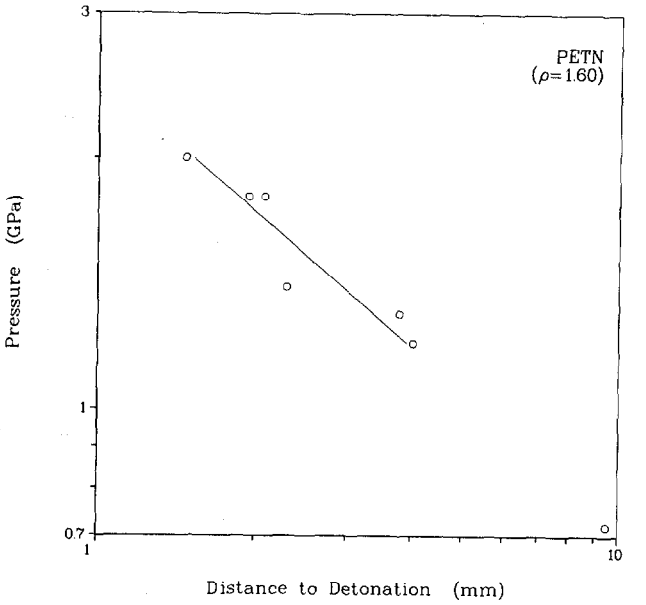
PETN
(ρ=1.60)
Pressure (GPa)
3
1
0.7
1
10
Distance to Detonation (mm)

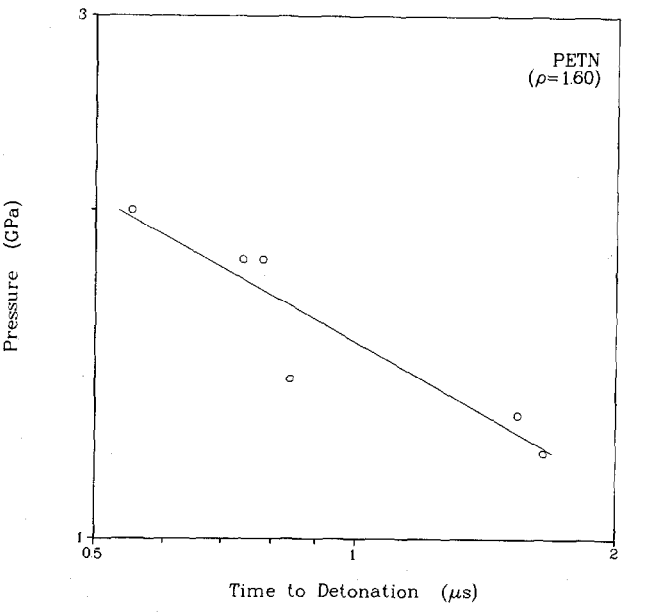
PETN
(ρ=1.60)
Pressure (GPa)
3
1
0.5
1
2
Time to Detonation (μs)

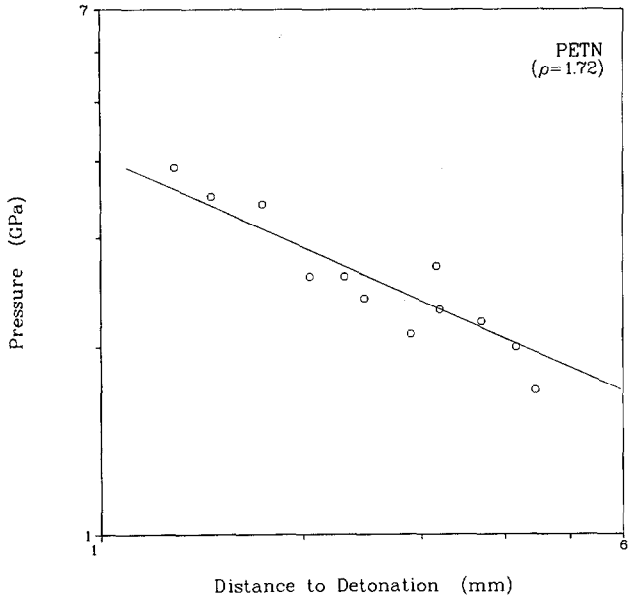
PETN
(ρ=1.72)
Pressure (GPa)
7
1
1
6
Distance to Detonation (mm)

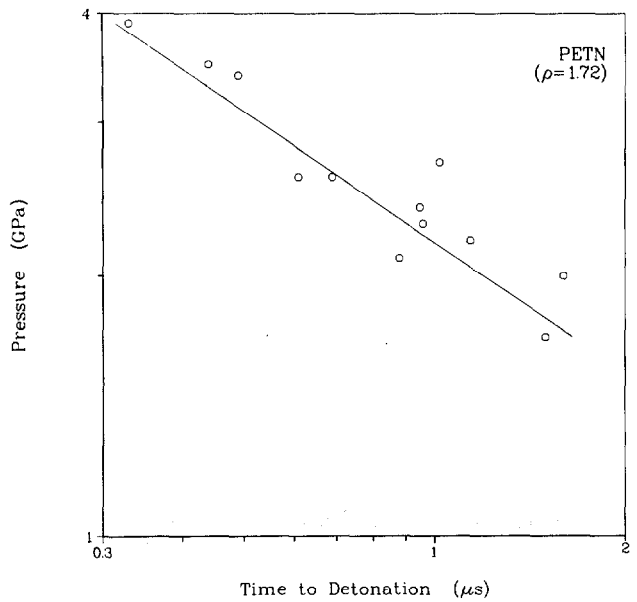
PETN
(ρ=1.72)
Pressure (GPa)
4
1
0.3
1
2
Time to Detonation (μs)

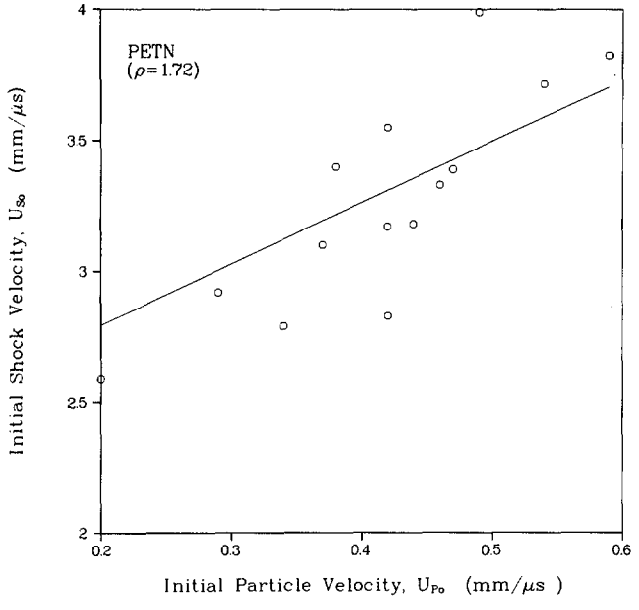
PETN
(ρ=1.72)
Initial Shock Velocity, U_{s_0} (mm/μs)
Initial Particle Velocity, U_{P_0} (mm/μs)
4
3.5
3
2.5
2
0.2
0.3
0.4
0.5
0.6

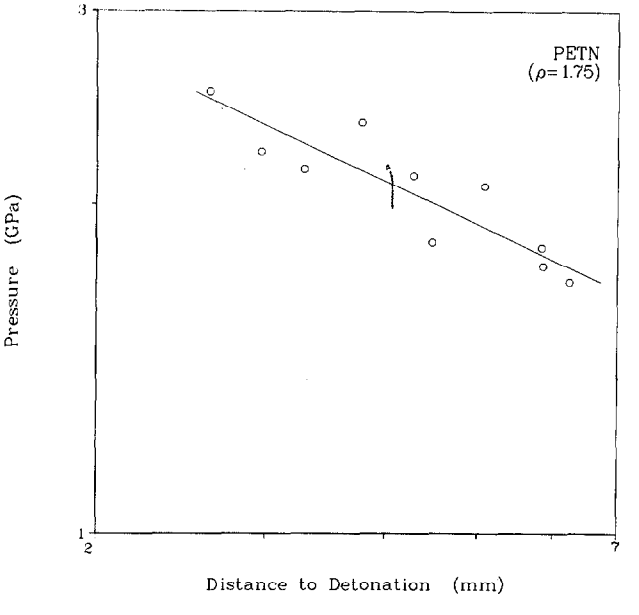
PETN
(ρ=1.75)
Pressure (GPa)
Distance to Detonation (mm)
3
1
2
7

Table 4.06 (continued) PETN (PRESSED), DRIVEN BY A GAS GUN

	Initial Shock Parameters				Coordinates for High-Order Detonation	
v_0[a] (mm/μs)	P_0(calc) (GPa)	P_0 (GPa)	U_{p0} (mm/μs)	U_{s0} (mm/μs)	x* (mm)	t* (μs)
			ρ_0 = 1.75 g/cm^3			
0.418	1.66	1.82	0.300	3.47	>6.4	---
0.426	1.70	---	---	---	6.24	---
0.439	1.76	---	---	---	5.85	---
0.452	1.83	1.47	0.352	2.39	5.83	1.85
0.460	1.85	---	---	---	4.48	---
0.508	2.08	2.15	0.363	3.39	5.08	1.55
0.518	2.13	---	---	---	4.28	---
0.526	2.16	---	---	---	3.29	---
0.540	2.24	2.13	0.397	3.06	2.97	0.95
0.571	2.38	2.52	0.408	3.53	3.78	1.05
0.602	2.54	2.49	0.435	3.27	2.62	0.84
			ρ_0 = 1.4 g/cm^3			
0.313	0.66	0.42	0.284	1.05	7.26	5.2
0.294	0.57	0.37	0.268	1.00	7.84	5.7
0.317	0.67	0.41	0.290	1.02	6.98	4.9
0.357	0.78	0.58	0.318	1.31	4.06	2.7
0.407	0.99	0.79	0.354	1.60	2.35	1.3
0.305	0.62	0.42	0.278	1.07	7.39	5.4

[a]Velocity is that of 7075 aluminum alloy projectile.

Reduced Data

$U_{s0} = 2.26 + 2.32\ U_{p0}$ (mm/μs).

ρ_0 = 1.75 g/cm^3.

For $1.7 < P < 2.54$,

$\log P = (0.57 \pm 0.04) - (0.41 \pm 1\ 0.06) \log x^*$, and

$\log P = (0.33 \pm 0.02) - (0.22 \pm 0.16) \log t^*$,

ρ_0 = 1.4 g/cm^3.

For $0.66 < P < 0.99$,

$\log P = (0.14 \pm 0.03) - (0.4 \pm 0.05) \log x^*$, and

$\log P = (0.04 \pm 0.02) - (0.33 \pm 0.04) \log t^*$.

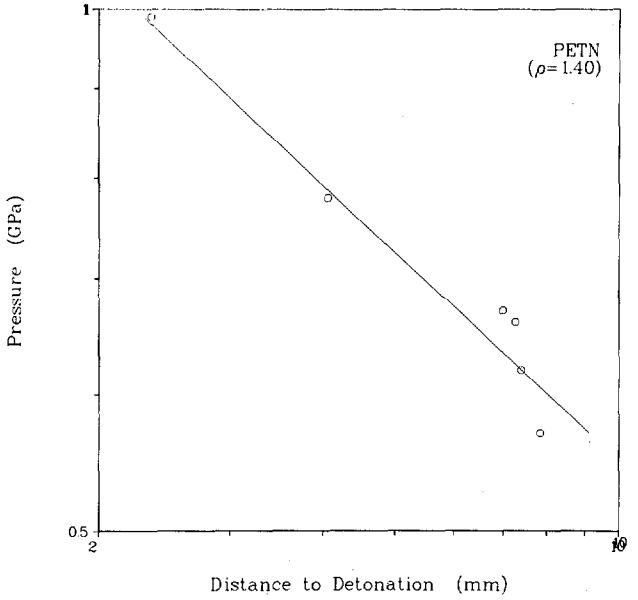
PETN
(ρ=1.40)
Pressure (GPa)
1
0.5
2
10
Distance to Detonation (mm)

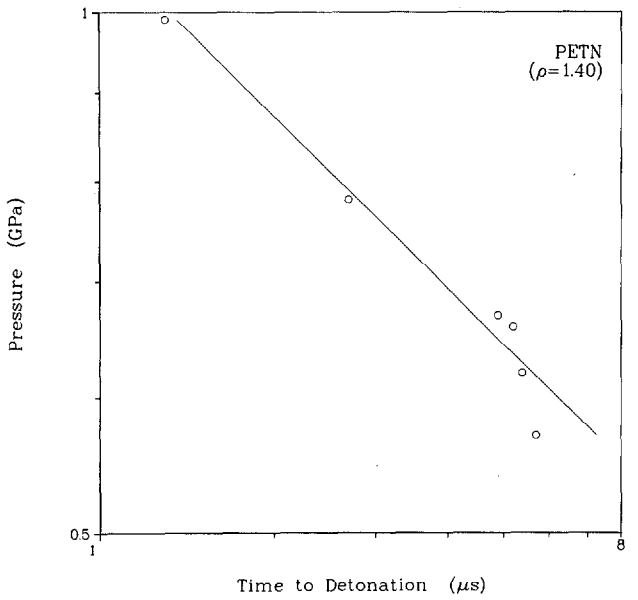
PETN
(ρ=1.40)
Pressure (GPa)
1
0.5
1
8
Time to Detonation (μs)

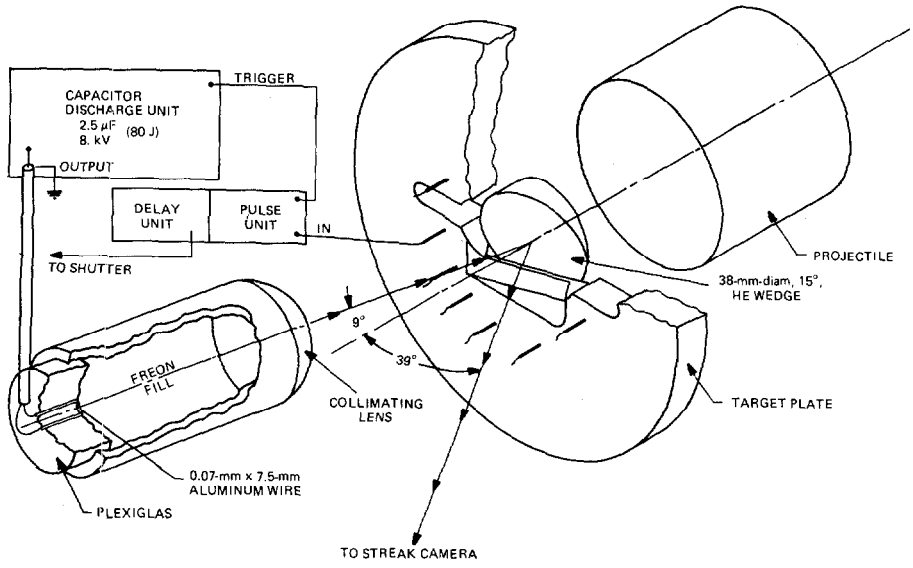

Fig. 4.03. The gas-gun assembly used in PETN testing.

Table 4.07 PETN (SINGLE CRYSTAL)

Composition
100 wt% PETN
Theoretical Maximum Density
1.775 g/cm³
Particle Size Distribution
Single crystal
Preparation Method
Controlled solvent evaporation
Data Summary
ρ_0 = 1.775 g/cm³. T_0 = 24°C. Technique 4

Shot Number	Initial Shock Parameters P_0 (GPa)	U_{p0} (mm/μs)	U_{s0} (mm/μs)	1/2 b (mm/μs²)	$t_0 t$ (μ_s)[a]	t_i (μs)[b]	Driving System Thickness (mm)
E-3799	11.23	1.246	5.078	0.029	1.06	0.28	H, 40.6 Plex
E-3800	10.98	1.240	4.990	0.005	1.03	0.32 − 0.40	H, 45.7 Plex
E-3788	11.05	1.221	5.100	0.063	0.94	0.34 − 0.51	H, 47.5 Plex
E-3787	10.10	1.212	4.696	0.020	1.15	0.61	H, 55.9 Plex
E-3809	8.78	1.068	4.630	0.103	1.58	0.81	B, 9.1 Plex
E-3808	7.19	0.914	4.432	0.020	---	---	B, 48.3 Plex
E-3870	3.95	0.543	4.099	−0.039	---	∞	B, 24.1 SS, 8.9 Plex

[a] t_{0T} is the time at which detonation overtook the shock front in the crystal.
[b] t_i is the induction time.

Reduced Data
U_{s0} = (3.311 ± 0.26) + (1.323 ± 0.238) U_{p0}.

Table 4.08 TATB (PURIFIED)

Composition
100 wt% TATB
Theoretical Maximum Density
1.938 g/cm³
Particle Size Distribution
Wt%: below 10 μm = 4.51; below 25 μm = 41.10; below 30 μm = 53.3; below 45 μm = 77.8.
Surface area over range = 22.62 cm²/g.
Preparation Method
Pressing, and machining to shape
Data Summary
Technique 4

Shot Number	T_0 (°C)	P_0 (GPa)	Initial Shock Parameters U_{p0} (mm/μs)	U_{s0} (mm/μs)	1/2 b (mm/μs²)	Coordinates for High-Order Detonation x* (mm)	t* (μs)	Driving System Thickness (mm)
				ρ_0 = 1.876 g/cm³				
E-3646	~23	0.57	0.152	1.999	−0.0126	≫12.72	≫5.80	A, 11.4 SS, 10.9 Plex
		0.67	0.179					
E-3672	~23	2.89	0.489	3.151	0.0503	≫12.47	≫3.77	B, 17.8 polyethylene, 11.4 SS, 10.9 Acrylite
E-3587	~23	3.02	0.480	3.356	0.0113	≫12.71	≫3.69	B, 17.8 polyethylene, 11.4 SS, 9.7 Acrylite
E-3569	~23	6.74	0.858	4.186	0.049	≫12.65	≫2.92	B, 48.5 Plex
E-3568	~23	9.42	1.063	4.723	0.111	>12.74	>2.44	G, 38.1 Plex
E-3558	~23	11.40	1.208	5.030	0.319	7.66	1.38	G, 18.0 Acrylite
E-3549	~23	13.03	1.340	5.184	0.425	5.80	1.02	G, 12.2 Everkleer
E-3559	~23	16.22	1.471	5.879	0.684	3.23	0.52	G, 6.4 Plex

Table 4.08 (continued)

Shot Number	T_0 (°C)	P_0 (GPA)	U_{p0} (mm/μs)	U_{s0} (mm/μs)	1/2 b (mm/μs²)	x* (mm)	t* (μs)	Driving System Thickness (mm)
				ρ_0 = 1.714 g/cm³				
E-4630	−49	4.47	0.784	3.33	---	16.6	4.32	R, 24.1 SS, 12.2 PC, 6.2 air, 6.1 PC
E-4544	~0	5.36	0.806	3.88	---	6.7	1.37	C, 38.1 PC, 6.2 air, 6.1 PC
E-4535	~8	2.68	0.551	2.84	---	>25.5	>9.5	B, 24.1 SS, 8.9 PC, 6.2 air, 6.1 PC
E-4556	18	3.72	0.657	3.31	---	14.6	3.93	R, 24.1 SS, 12.2 PC, 6.2 air, 6.1 PC
E-4566	23	3.10	0.588	3.08	---	18.7	5.32	N, 24.1 SS, 11.9 PC, 6.2 air, 6.1 PC
E-4596	65	3.86	0.686	3.28	---	12.7	3.18	R, 24.1 SS, 12.2 PC, 6.2 air, 6.1 PC
				ρ_0 = 1.841 g/cm³				
E-4628	−56	6.44	0.845	4.14	---	17.1	3.65	C, 38.1 PC, 6.2 air, 6.1 PC
E-4538	~4	6.05	0.786	4.18	---	12.6	2.72	C, 38.1 PC, 6.2 air, 6.1 PC
E-4567	7	5.34	0.716	4.05	---	~29	~7.0	S, 24.1 SS, 11.9 PC, 6.2 air, 6.1 PC
E-4536	~8	16.80	1.590	5.74	---	2.33	0.38	S, 19.0 PC, 6.2 air, 6.1 PC
E-4562	~11	7.96	0.992	4.36	---	7.71	1.54	G, 31.8 PC, 6.2 air, 6.1 PC
E-4595	65	6.99	0.883	4.3	---	11.5	2.49	C, 38:1 PC, 6.2 air, 6.1 PC

Reduced Data

$C_{Longitudinal}$ = 1.98 ± 0.03 mm/μs, C_{Shear} = 1.16 ± 0.02 mm/μs, and C_0 = 1.46 ± 0.005 mm/μs at ρ = 1.87 g/cm³.

$U_{s0} = (1.663 \pm 0.123) + (2.827 + 0.132)U_{p0}$.

ρ = 1.876 g/cm^3.
For 11.4 < P < 16.22,
log P = (1.42 ± 0.02) − (0.40 ± 0.03) log x*, and
log P = (1.11 ± 0.01) − (0.36 ± 0.03) log t*.
ρ_0 = 1.714 g/cm^3.
For 3.27 < P < 5.64,
log P = (1.09 ± 0.2) − (0.41 ± 0.17) log x*, and
log P = (0.8 ± 0.07) − (0.32 ± 0.12) log t*.
ρ_0 = 1.841 g/cm^3.
For 5.93 < P < 16.5,
log P = (1.39 ± 0.07) − (0.52 ± 0.07) log x*, and
log P = (1.01 ± 0.02) − (0.46 ± 0.05) log t*.

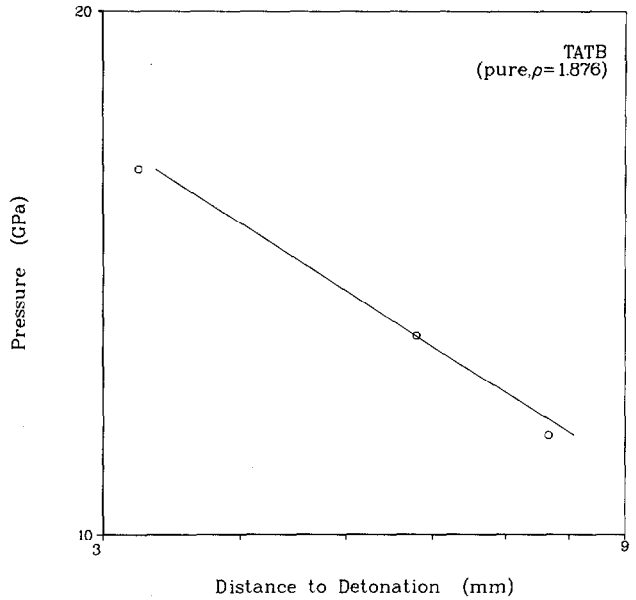
20
10
3
9
TATB
(pure,ρ=1.876)
Pressure (GPa)
Distance to Detonation (mm)

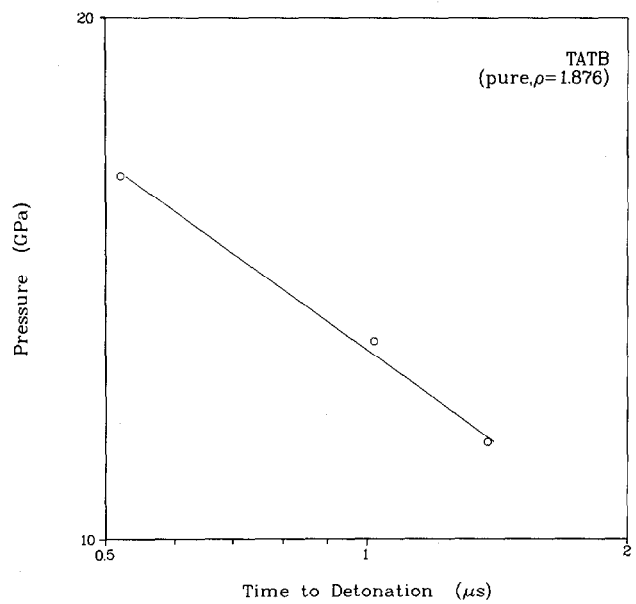
20
10
0.5
1
2
TATB
(pure,ρ=1.876)
Pressure (GPa)
Time to Detonation (μs)

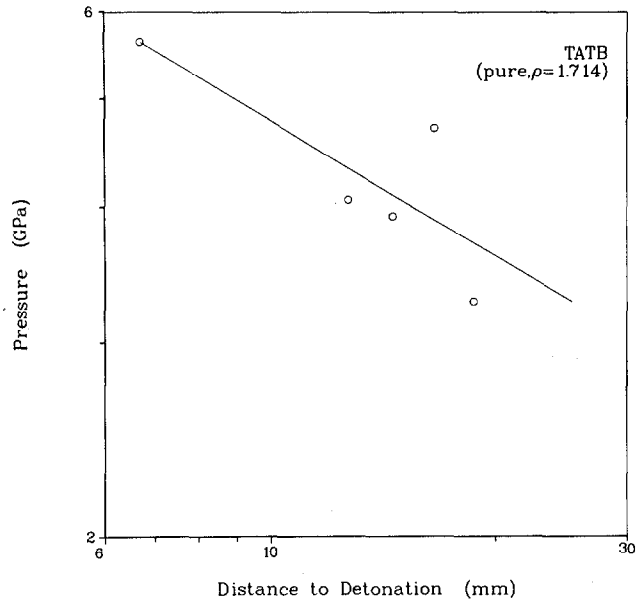
TATB
(pure,ρ=1.714)
Pressure (GPa)
6
2
6
10
30
Distance to Detonation (mm)

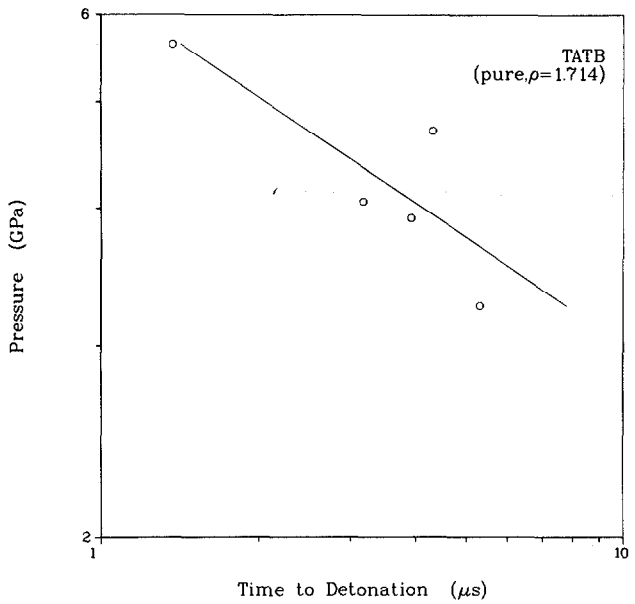
TATB
(pure,ρ=1.714)
Pressure (GPa)
6
2
1
10
Time to Detonation (μs)

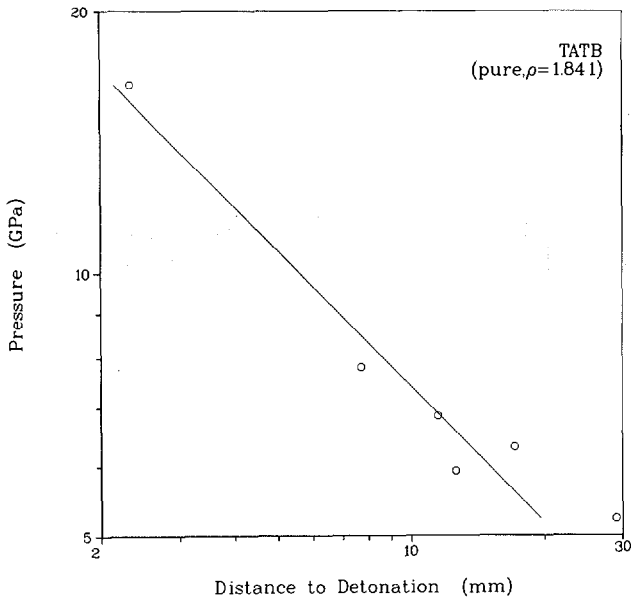
TATB
(pure,ρ=1.84 1)
Pressure (GPa)
20
10
5
2
10
30
Distance to Detonation (mm)

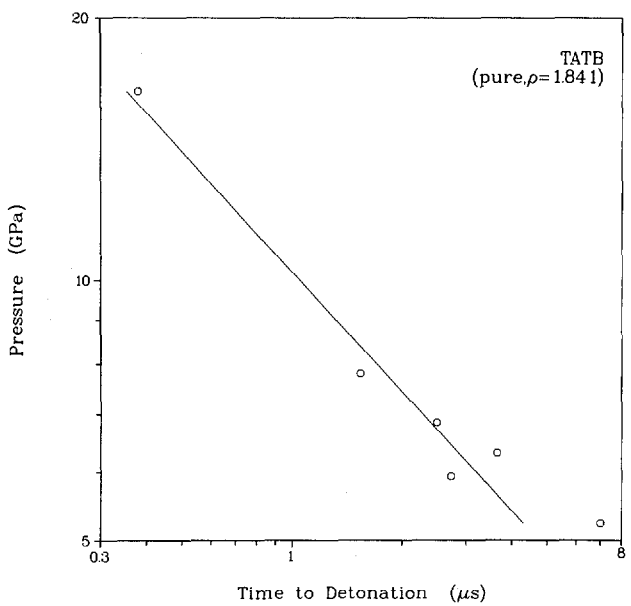
TATB
(pure,ρ=1.84 1)
Pressure (GPa)
20
10
5
0.3
1
8
Time to Detonation (μs)

Table 4.09 TATB (MICRONIZED)

Composition

100 wt% TATB

Theoretical Maximum Density

1.938 g/cm³

Particle Size Distribution

The micronized TATB was prepared by grinding dry aminated superfine TATB, suspended in water. Screen tests showed 89.2% <10-μm and 99.1% <20-μm particles.

Preparation Method

Pellets were dry pressed to a density of 1.808 g/cm³. Wedges were made by abrading the pellets under water.

Data Summary

ρ_0 - 1.808 g/cm³. Technique 6

Initial Shock Parameters			Coordinates for Intermediate Regions		Coordinates for High-Order Detonation		
P_0 (GPa)	U_{p0} (mm/μs)	U_{s0} (mm/μs)	x_i^* (mm)	t_i^* (μs)	x^* (mm)	t^* (μs)	Driving[a] System
14.27	1.4	5.64	1.34	0.206	4.85	0.770	TNT[b]
18.01	1.7	5.86	0.62	0.101	2.15	0.327	TNT
17.79	1.6	6.15	0.55	0.077	2.33	0.331	TNT
22.40	1.9	6.52	0.26	0.039	1.68	0.237	Comp B
23.19	1.9	6.75	0.58	0.069	1.79	0.226	Comp B
23.02	1.9	6.70	0.16	0.035	1.63	0.222	Comp B
25.55	2.1	6.73	---	---	0.86	0.113	Octol
27.84	2.2	7.00	---	---	0.90	0.113	Octol

[a]Driving systems consisted of a plane-wave lens (usually P-081), 50.8 mm of explosive as listed, and 12.7 mm of 6061 aluminum.

[b]This shot had 50.8 mm, rather than 12.7 mm, of 6061 aluminum.

Reduced Data

$U_{s0} = 2.156 + 2.302\ U_{p0}$.

For $14.3 < P < 27.8$,

$\log P = 1.42 - 0.38 \log x^*$, and

$\log P = 0.92 - 0.36 \log t^*$.

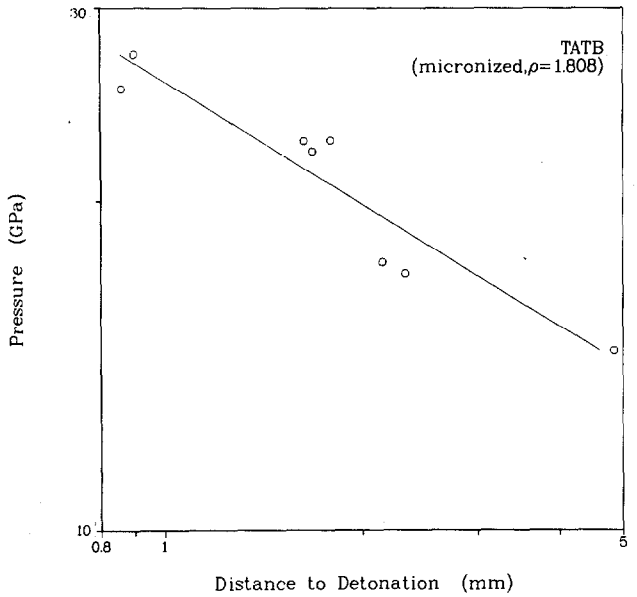
TATB
(micronized,ρ=1.808)
Pressure (GPa)
30
10
0.8
1
5
Distance to Detonation (mm)

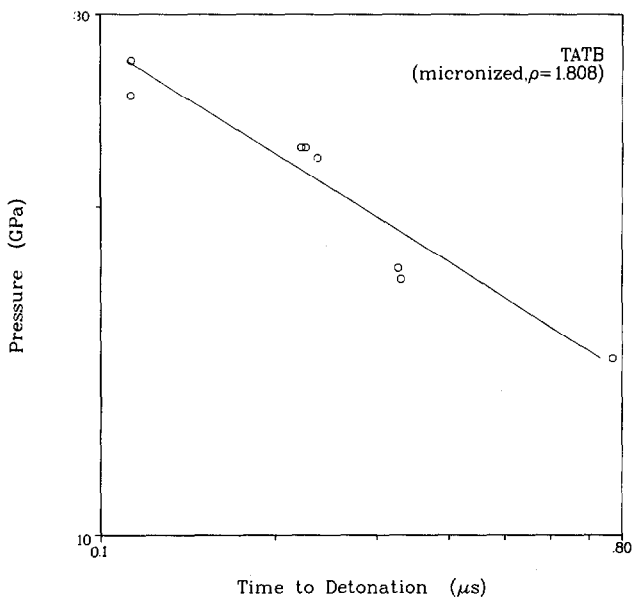
TATB
(micronized,ρ=1.808)
Pressure (GPa)
30
10
0.1
80
Time to Detonation (μs)

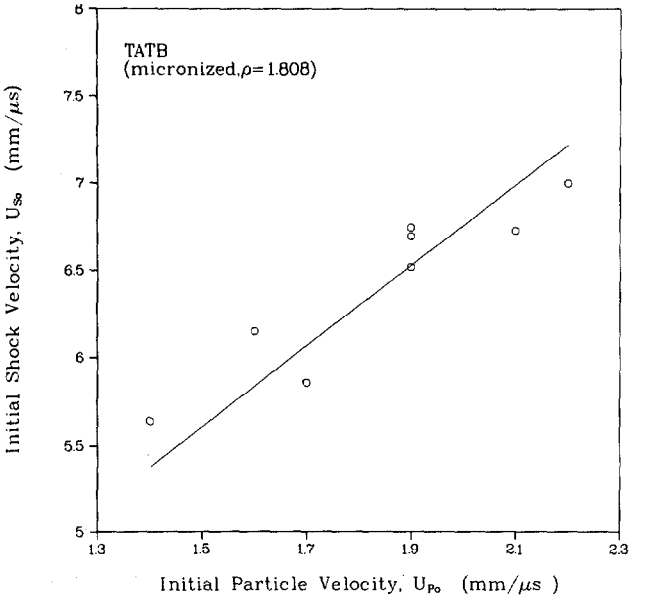
TATB
(micronized,ρ= 1.808)
Initial Shock Velocity, U_{So} (mm/μs)
Initial Particle Velocity, U_{Po} (mm/μs)
8
7.5
7
6.5
6
5.5
5
1.3
1.5
1.7
1.9
2.1
2.3

Table 4.10 TATB (SUPERFINE)

Composition
100 wt% TATB
Theoretical Maximum Density
1.938 g/cm³
Particle Size Distribution
This superfine TATB was dry-aminated, irregular, layer- shaped crystals with many holes and imperfections. A screen test showed 78.7% <20-μm and 99.8% <45-μm particles.
Preparation Method
Pellets were dry pressed to a density of 1.806 g/cm³. Wedges were made by abrading the pellets under water.
Data Summary
ρ_0 = 1.806 g/cm³. Technique 6

Initial Shock Parameters			Coordinates for Intermediate Regions		Coordinates for High-Order Detonation		
P_0 (GPa)	U_{p0} (mm/μs)	U_{s0} (mm/μs)	x_i^* (mm)	t_i^* (μs)	x^* (mm)	t^* (μs)	Driving[a] System
10.1	1.2	4.65	2.00	0.435	5.61	1.113	Baratol
16.0	1.6	5.55	0.90	0.176	1.48	0.260	TNT
16.7	1.5	6.18	0.87	0.146	1.39	0.223	TNT
20.4	2.0	5.64	0.33	0.068	1.12	0.181	Comp B
21.2	1.8	6.52	0.48	0.074	0.93	0.139	Comp B
21.8	1.8	6.70	0.31	0.048	1.00	0.146	Comp B
26.1	2.1	6.89	---	---	0.53	0.063	Octol
26.3	2.1	6.68	---	---	0.49	0.109	Octol
28.1	2.2	7.08	---	---	0.54	0.075	Octol

[a]Driving systems consisted of a plane-wave lens (usually P-081), 50.8 mm of explosive as listed, and 12.7 mm of 6061 aluminum.

Reduced Data
$U_{s0} = 2.156 + 2.302\ U_{p0}$.
For $10.1 < P < 28.1$ (mm/μs),
$\log P = (1.31 \pm 0.01) - (0.43 \pm 0.03) \log x^*$, and
$\log P = (1.00 \pm 0.02) - (0.38 \pm 0.03) \log t^*$.

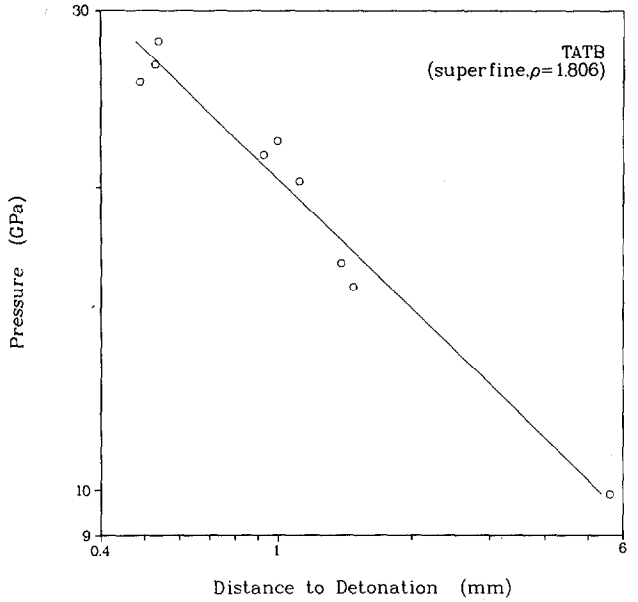
30
10
9
0.4
1
6
TATB
(superfine,ρ=1.806)
Pressure (GPa)
Distance to Detonation (mm)

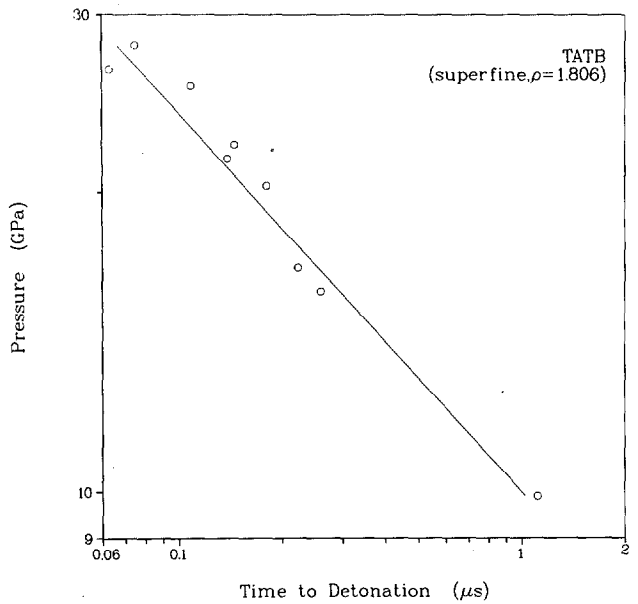
30
10
9
0.06
0.1
1
2
TATB
(superfine,ρ=1.806)
Pressure (GPa)
Time to Detonation (μs)

Table 4.11 TETRYL

Composition
100 wt% tetryl
Theoretical Maximum Density
1.73 g/cm³
Particle Size Distribution
Particles were mostly shapeless, multicrystalline agglomerates, about 0.6 mm in diameter, with a small fraction of 0.1- to 0.2-mm particles.
Preparation Method
Pellets were dry pressed. 1.70-g/cm³ wedges were formed by machining, and the lower density wedges were made by abrading the pellets under water.
Data Summary
Technique 5

Initial Shock Parameters			Coordinates for High-Order Detonation		
P_0 (GPa)	U_{p0} (mm/μs)	U_{s0} (mm/μs)	x* (mm)	t* (μs)	Driving System[a]
		$\rho_0 = 1.7$ g/cm³			
8.53	1.195	4.20	0.52	0.12	1
6.78	1.028	3.88	0.93	0.21	2
5.62	0.876	3.77	1.16	0.27	3
4.98	0.818	3.58	1.76	0.43	5
4.93	0.805	3.60	1.67	0.41	4
3.88	0.664	3.44	2.46	0.63	6
3.31	0.590	3.30	4.15	1.13	7
2.91	0.522	3.28	5.06	1.41	8
2.66	0.490	3.19	7.48	2.19	8
2.41	0.457	3.10	9.71	2.90	8
2.43	0.453	3.15	9.43	2.78	8
2.22	0.429	3.05	11.38	3.31	10
2.22	0.428	3.05	12.95	3.95	10
		$\rho_0 = 1.6$ g/cm³			
8.02	1.232	4.07	0.52	0.13	1
5.82	1.004	3.62	0.87	0.22	2
5.15	0.935	3.44	1.08	0.27	3
4.72	0.867	3.40	1.46	0.36	4
3.52	0.699	3.15	1.89	0.49	6
2.64	0.580	2.85	2.58	0.75	7
2.38	0.548	2.71	3.23	0.99	8
1.98	0.482	2.57	4.61	1.49	9
1.77	0.451	2.45	5.44	1.87	10
1.58	0.414	2.39	6.38	2.21	11
1.49	0.400	2.33	6.82	2.39	13

[a]See "Notes" at end of table.

Table 4.11 (continued)

Initial Shock Parameters			Coordinates for High-Order Detonation		
P_0 (GPa)	U_{p0} (mm/μs)	U_{s0} (mm/μs)	x* (mm)	t* (μs)	Driving System
1.39	0.378	2.30	7.62	2.74	15
1.25	0.363	2.15	9.47	3.65	18
1.25	0.361	2.16	9.27	3.80	18
1.18	0.343	2.15	10.28	3.95	17
1.13	0.330	2.14	11.46	4.55	19
1.08	0.324	2.09	12.28	5.10	20
		$\rho_0 = 1.5$ g/cm^3			
7.09	1.231	3.84	0.83	0.18	1
5.36	1.016	3.52	1.05	0.26	2
4.48	0.902	3.31	1.27	0.34	3
3.05	0.717	2.84	2.34	0.62	6
2.35	0.603	2.60	2.94	0.90	7
2.05	0.569	2.40	3.34	1.08	8
1.74	0.491	2.36	4.03	1.33	9
1.41	0.456	2.06	5.51	1.96	10
1.29	0.411	2.10	5.94	2.19	11
1.19	0.404	1.97	6.21	2.37	13
1.09	0.382	1.90	7.93	3.20	16
0.97	0.367	1.76	8.29	3.44	15
0.82	0.328	1.67	11.42	5.30	21
0.66	0.299	1.48	15.23	7.71	22
0.67	0.293	1.52	13.00	6.32	22
0.62	0.287	1.45	16.09	8.28	22
		$\rho_0 = 1.4$ g/cm^3			
6.84	1.253	3.90	0.93	0.21	1
5.10	1.063	3.43	1.39	0.35	2
4.11	0.946	3.10	1.70	0.49	3
2.75	0.728	2.70	2.80	0.80	6
1.92	0.613	2.24	3.45	1.11	7
1.80	0.563	2.28	4.19	1.36	8
1.48	0.500	2.12	5.06	1.67	9
1.19	0.454	1.87	5.65	2.18	10
1.05	0.415	1.80	6.52	2.59	12
0.94	0.401	1.68	7.18	2.92	14
0.91	0.392	1.65	8.03	3.30	16
0.82	0.364	1.60	8.24	3.61	17
0.66	0.331	1.42	10.82	5.31	21
0.51	0.297	1.22	13.88	7.66	23

Table 4.11 (continued)

Initial Shock Parameters			Coordinates for High-Order Detonation		
P_0 (GPa)	U_{p0} (mm/μs)	U_{s0} (mm/μs)	x* (mm)	t* (μs)	Driving System
		$\rho_0 = 1.3$ g/cm^3			
6.91	1.399	3.80	0.81	0.19	1
4.85	1.140	3.27	1.59	0.39	2
3.68	0.932	3.04	1.88	0.51	3
3.26	0.865	2.90	2.59	0.73	4
1.80	0.632	2.19	3.93	1.35	7
1.12	0.476	1.81	5.98	2.43	10
0.73	0.392	1.43	8.25	3.72	16
0.47	0.332	1.08	10.43	5.54	21
0.37	0.296	0.96	12.46	7.29	23

Reduced Data

Buildup Function Coefficients

$\rho_0 = 1.7$ g/cm^3.

$A_1 = 0.9532$, $A_2 = 5.1388$, $A_3 = 0.4179$, and $A_4 = 7.65$.

$U_{s0} = 2.4763 + 1.4160\ U_{p0}$.

For $2.22 < P < 8.53$,

$\log P = (0.79 \pm 0.01) - (0.42 \pm 0.01) \log x^*$, and

$\log P = (0.55 \pm 0.01) - (0.39 \pm 0.01) \log t^*$.

$\rho_0 = 1.6$ g/cm^3.

$A_1 = 1.7738$, $A_2 = 3.2707$, $A_3 = 0.4182$, and $A_4 = 7.35$.

$U_{s0} = 2.3621 + 1.5285\ U_{p0} - 0.2549/U_{p0}$.

For $1.08 < P < 8.02$,

$\log P = (0.73 \pm 0.01) - (0.65 \pm 0.01) \log x^*$, and

$\log P = (0.4 \pm 0.01) - (0.55 \pm 0.01) \log t^*$.

$\rho_0 = 1.5$ g/cm^3.

$A_1 = 2.8078$, $A_2 = 2.2508$, $A_3 = 0.4027$, and $A_4 = 7.05$.

$U_{s0} = 2.1674 + 1.6225\ U_{p0} - 0.3411/U_{p0}$.

For $0.62 < P < 7.09$,

$\log P = (0.75 \pm 0.01) - (0.81 \pm 0.01) \log x^*$, and

$\log P = (0.35 \pm 0.01) - (0.64 \pm 0.01) \log t^*$.

$\rho_0 = 1.4$ g/cm^3.

$A_1 = 3.3485$, $A_2 = 1.8668$, $A_3 = 0.4564$, and $A_4 = 6.75$.

$U_{s0} = 1.6111 + 1.9658\ U_{p0} - 0.2784/U_{p0}$.

For $0.51 < P < 6.84$,

$\log P = (0.84 \pm 0.01) - (0.99 \pm 0.02) \log x^*$, and

$\log P = (0.35 \pm 0.01) - (0.75 \pm 0.01) \log t^*$.

ρ_0 = 1.3 g/cm³.
A_1 = 6.0649, A_2 = 1.2364, A_3 = 0.3587, and A_4 = 6.45.
$U_{s0} = 2.1620 + 1.4271\ U_{p0} - 0.4993/U_{p0}$.
For $0.37 < P < 6.91$,
$\log P = (0.87 \pm 0.05) - (1.11 \pm 0.07) \log x^*$, and
$\log P = (0.33 \pm 0.02) - (0.83 \pm 0.03) \log t^*$.

Notes on Driving System

Type	Thickness of Each Layer[a] (mm)	First-Layer Metal	Second-Layer Liquid	Free-Surface Velocity (mm/μs)
1	12	Dural	[b]	1.71
2	12	Zinc	[b]	1.27
3	12	Brass	[b]	1.05
4	12	Dural	1,1,2,2,-tetrabromoethane	0.97
5	12	Dural	Carbon tetrachloride-1,1,2,2-tetrabromoethane mixture	0.80-0.97[c]
6	12	Dural	Carbon tetrachloride	0.80
7	12	Brass	Methylene iodide	0.68
8	12	Brass	Carbon tetrachloride-1,1,2,2-tetrabromoethane mixture	0.50-0.64[c]
9	12	Brass	Aqueous zinc-iodide solution[d]	0.54
10	12	Brass	Carbon tetrachloride	0.50
11	12	Brass	Trichloroethylene	0.46
12	16	Brass	Trichloroethylene	0.45
13	12	Brass	β,β'-dichloroethyl ether	0.45
14	16	Brass	β,β'-dichloroethyl ether	0.44
15	12	Brass	Ethyl oxalate	0.43
16	16	Brass	Ethyl oxalate	0.42
17	16	Brass	Water	0.39
18	16	Brass	Toluene-ethyl oxalate mixture	0.36-0.42[c]
19	16	Brass	Ethyl alcohol-water mixture	0.35-0.39[c]
20	16	Brass	Toluene	0.36
21	16	Brass	Ethyl alcohol	0.35
22	16	Brass	Diethyl ether-ethyl alcohol mixture	0.31-0.35[c]
23	16	Brass	Diethyl ether	0.31

[a]All experiments were performed with a P-120, 30-cm-diameter plane-wave lens and a 10-cm thickness of Baratol. Attenuators were made with either one layer or three layers; the third layer was always brass.
[b]This attenuator was a single plate of the "first layer metal."
[c]The value depends on the proportions of the two liquids.
[d]The original solution density was 1.77 g/cm³. The density may have been different at the time of use owing to water evaporation.

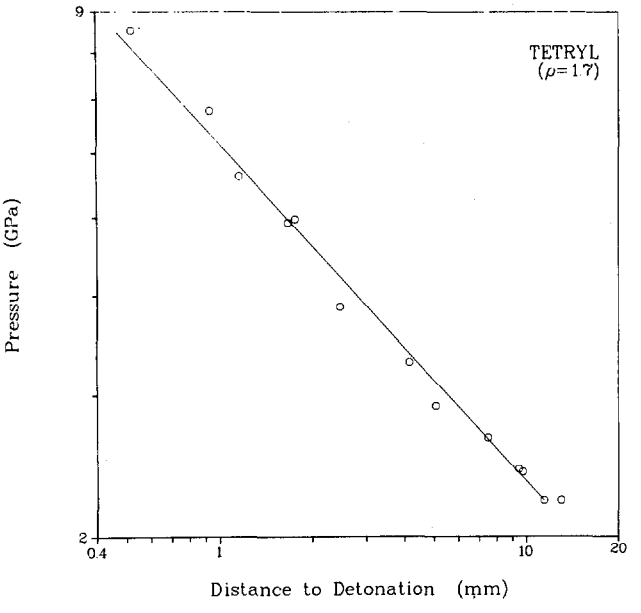
TETRYL
(ρ=1.7)
Pressure (GPa)
9
2
0.4
1
10
20
Distance to Detonation (mm)

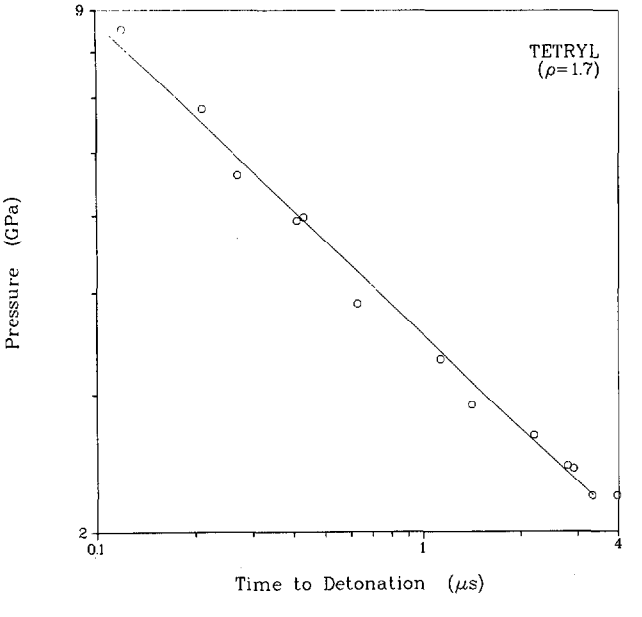
TETRYL
(ρ=1.7)
Pressure (GPa)
9
2
0.1
1
4
Time to Detonation (μs)

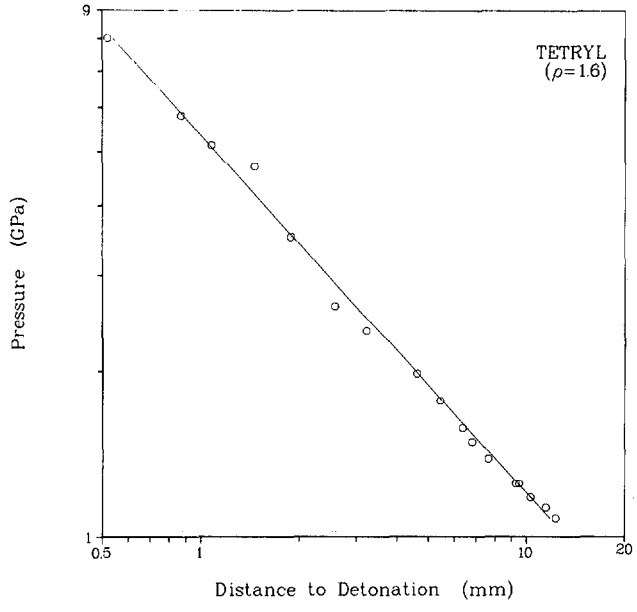
TETRYL
(ρ=1.6)
Pressure (GPa)
9
1
0.5
1
10
20
Distance to Detonation (mm)

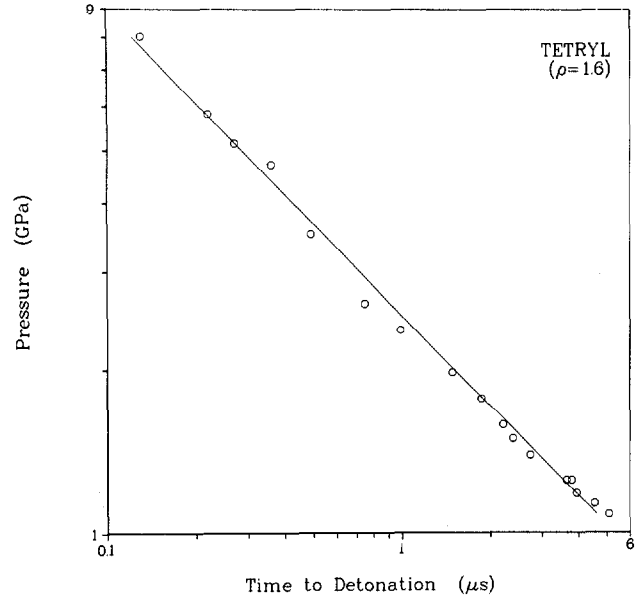
TETRYL
(ρ=1.6)
Pressure (GPa)
9
1
0.1
1
6
Time to Detonation (μs)

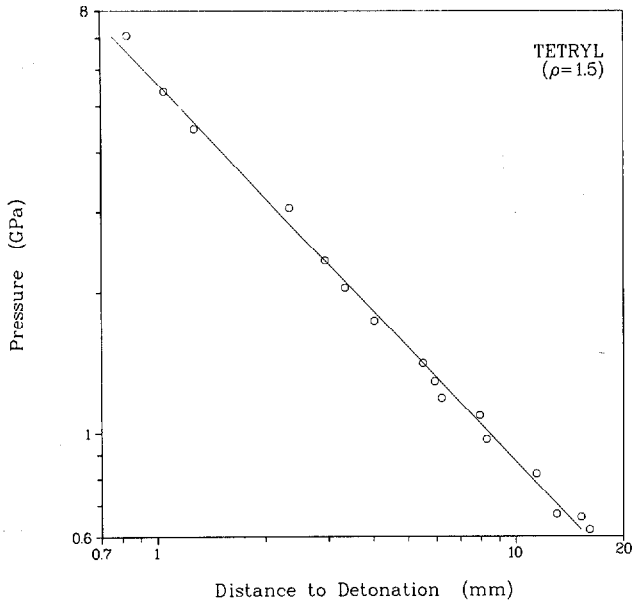
TETRYL
(ρ=1.5)
Pressure (GPa)
8
1
0.6
0.7
1
10
20
Distance to Detonation (mm)

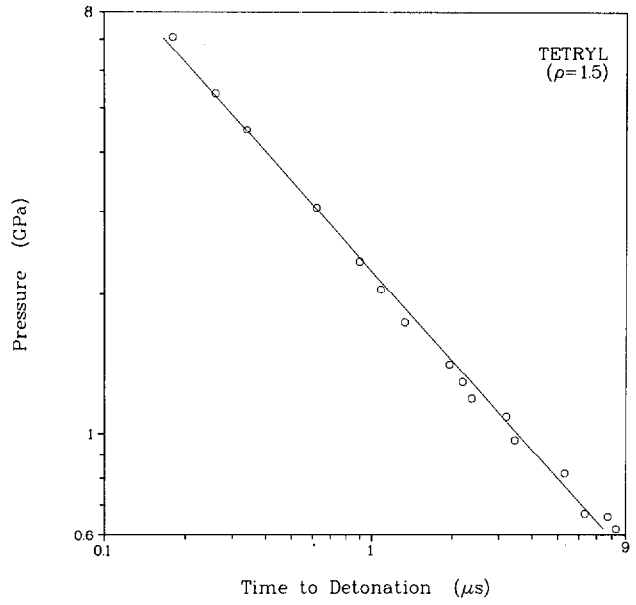
TETRYL
(ρ=1.5)
Pressure (GPa)
8
1
0.6
0.1
1
9
Time to Detonation (μs)

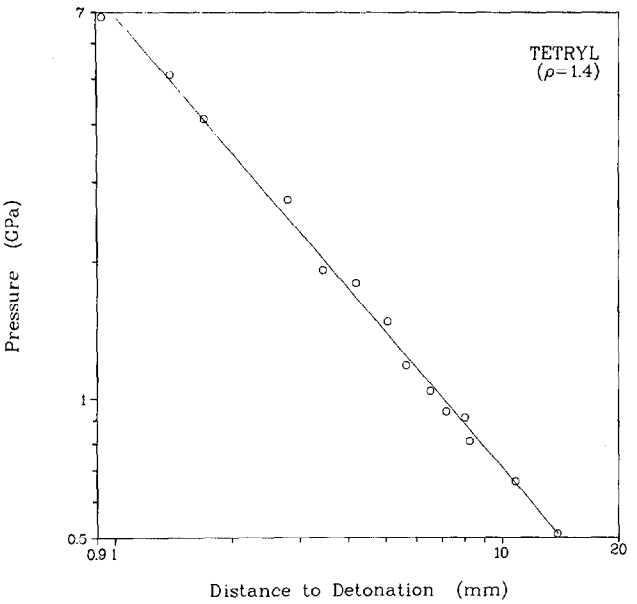
TETRYL
(ρ=1.4)
Pressure (GPa)
7
1
0.5
0.9 1
10
20
Distance to Detonation (mm)

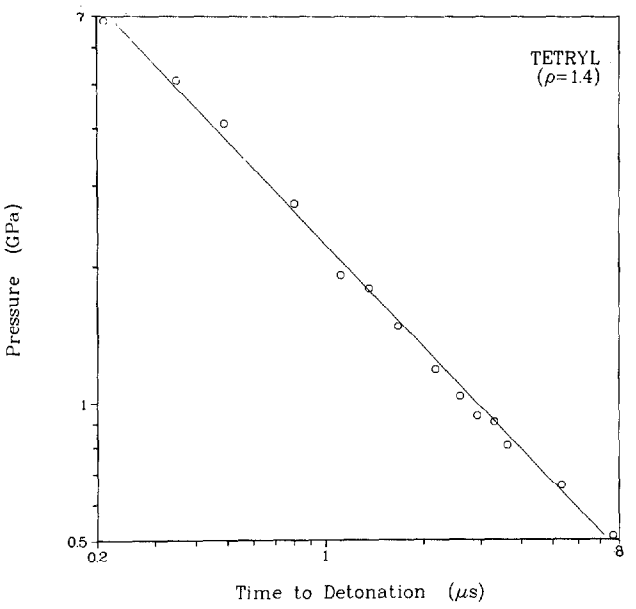
TETRYL
(ρ=1.4)
Pressure (GPa)
7
1
0.5
0.2
1
8
Time to Detonation (μs)

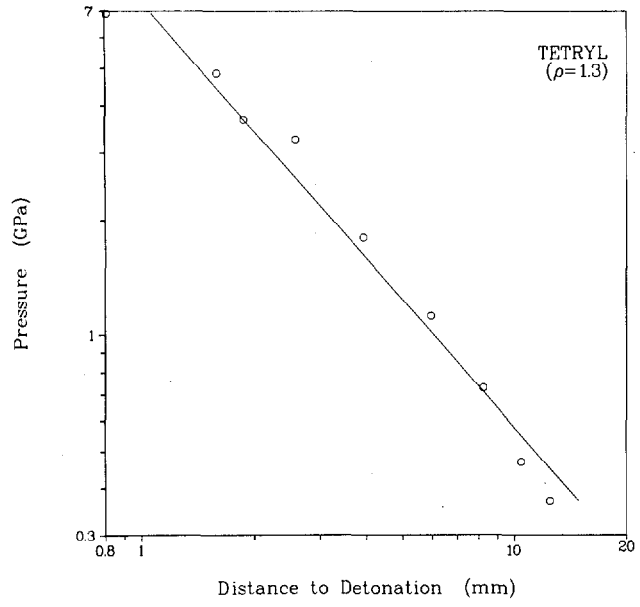
TETRYL
(ρ=1.3)
Pressure (GPa)
7
1
0.3
0.8
1
10
20
Distance to Detonation (mm)

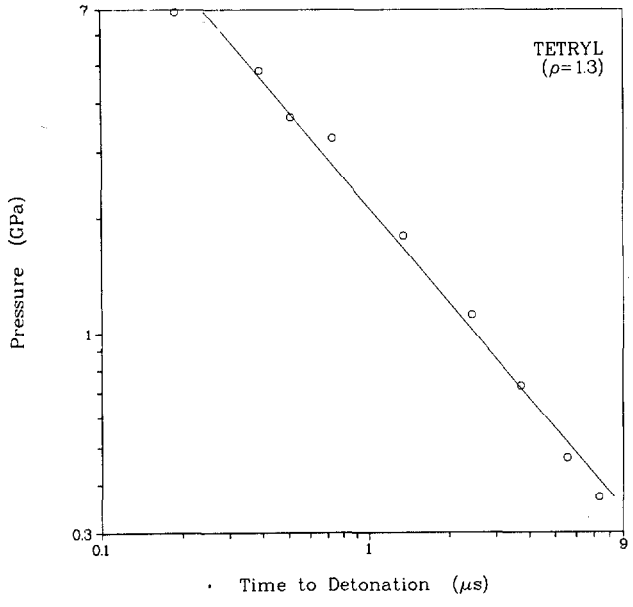
TETRYL
(ρ=1.3)
Pressure (GPa)
7
1
0.3
0.1
1
9
Time to Detonation (μs)

Table 4.12 TNT (CAST)

Composition
100 % TNT
Theoretical Maximum Density
1.654 g/cm³
Preparation Method
Casting
Data Summary
Technique 7

Shot Number	Temp. (°C)	ρ_0 (g/cm³)	Initial Shock Parameters P_o (GPa)	U_{po} (mm/μs)	U_{so} (mm/μs)	Coordinates for High-Order Detonation x* (mm)	t* (μs)	U_{fs} (mm/μs)	Driving System Thickness (mm)
				ρ_0 = 1.62-1.634 g/cm³, T_0 = 25-73°C					
E-4451	25	1.634	7.43	1.03	4.43	>25.4	>5.22	2.407	G, 32 PC, 6.3 air, 6.3 PC
E-4373	25	1.634	9.17	1.16	4.85	22.2	4.30	2.746	N, 32 PC, 6.3 air, 6.3 PC
E-4377	73	1.62	8.80	1.16	4.69	18.9	3.80	2.705	N, 32 PC, 6.3 air, 6.3 PC
E-4393	25	1.634	10.4	1.26	5.05	20.2	3.84	2.992	N, 19 PC, 6.3 air, 6.3 PC
E-4399	73	1.62	10.4	1.34	4.80	14.3	2.77	3.069	N, 19 PC, 6.3 air, 6.3 PC
E-4412	25	1.634	15.1	1.69	5.49	6.96	1.24	3.877	S, 19 PC, 6.3 air, 6.3 PC
E-4414	73	1.62	14.9	1.69	5.44	4.42	0.76	3.867	S, 19 PC, 6.3 air, 6.3 PC
				ρ_0 = 1.624 g/cm³, T_0 = 5-30°C					
E-2187	30	1.624	1.35	0.298	2.80	>10	---	0.661	C, 25.1 brass, 24.5 Plex, 12.7 brass, 11.8 Plex
E-2184	27	1.624	3.31	0.604	3.38	>10	---	1.353	C, 24.4 Plex, 12.6 brass, 11.6 Plex
E-2164	22	1.624	4.36	0.688	3.90	>10	---	1.608	B, 6.35 brass, 6.63 Plex

Table 4.12 (continued)

Shot Number	Temp. (°C)	ρ_0 (g/cm³)	Initial Shock Parameters P_0 (GPa)	U_{p0} (mm/μs)	U_{s0} (mm/μs)	Coordinates for High-Order Detonation x* (mm)	t* (μs)	U_{fs} (mm/μs)	Driving System Thickness (mm)
E-2100	14	1.624	7.63	1.04	4.50	>10	---	2.418	B, 24.8 Plex
E-2097	14	1.624	8.93	1.15	4.77	>10	---	2.684	B, 6.38 Lucite
E-2101	16	1.624	13.4	1.54	5.38	>10	---	3.543	J, 24.8 Plex
E-2102	16	1.624	15.6	1.75	5.50	6.0	---	3.965	G, 5.90 Lucite
E-2114	17	1.624	15.1	1.65	5.65	4.9	---	3.810	J, 18.2 Plex
E-2109	5	1.624	17.0	1.79	5.85	3.6	---	4.121	H, 6.29 Plex
E-2115	14	1.624	17.1	1.81	5.83	2.7	---	4.155	L, 24.6 Plex

Reduced Data

$C_0 = 2.08 \pm 0.13$ mm/μs
at $\rho = 1.635$ g/cm³.

Low pressure

$U_{s0} = (2.109 \pm (0.222) + (2.337 \pm 0.313)\ U_{p0}$.

High pressure

$U_{s0} = (2.974 \pm 0.199) + (1.555 \pm 0.132)\ U_{p0}$.

For both densities, $9.17 < P < 17.1$,

$\log P = (1.40 \pm 0.03) - (0.32 \pm 0.03) \log x^*$, and

$\log P = (1.16 \pm 0.03) - (0.31 \pm 0.05) \log t^*$.

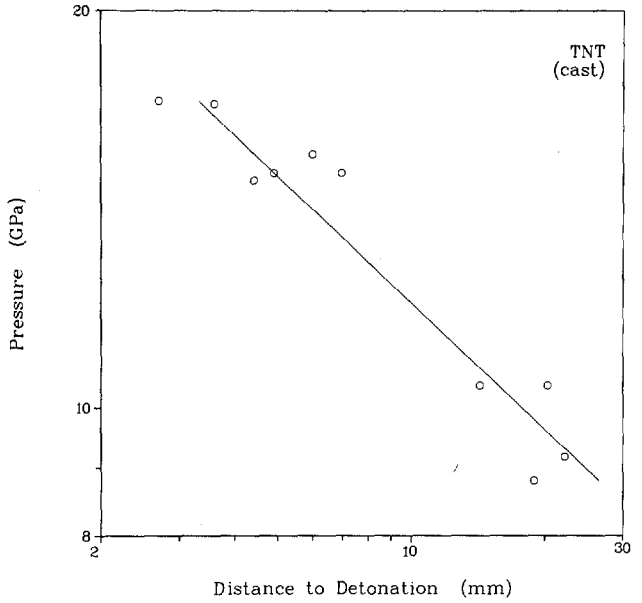
20
10
8
2
10
30
TNT
(cast)
Pressure (GPa)
Distance to Detonation (mm)

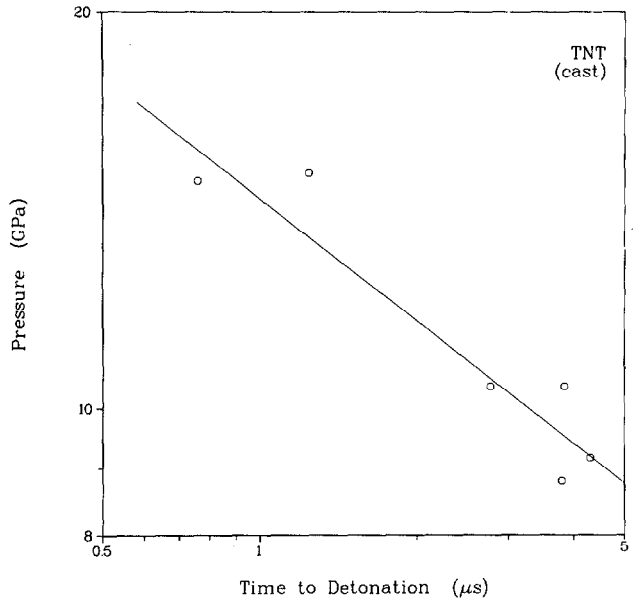
20
10
8
0.5
1
5
TNT
(cast)
Pressure (GPa)
Time to Detonation (μs)

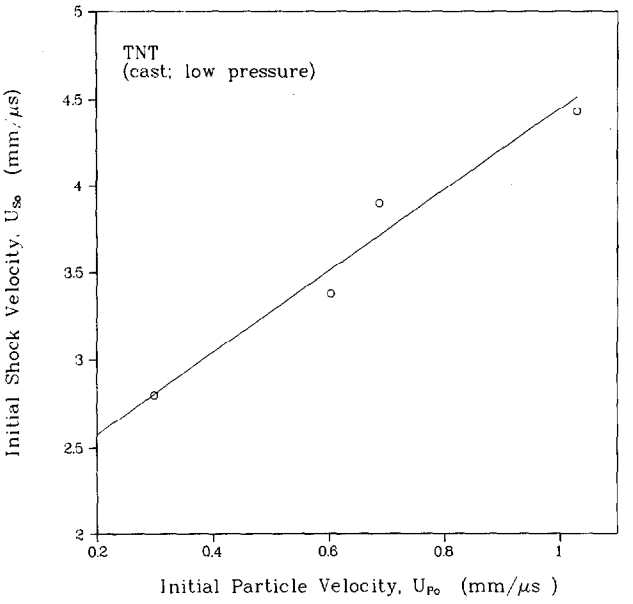
TNT
(cast; low pressure)
Initial Shock Velocity, U_{So} (mm/μs)
Initial Particle Velocity, U_{Po} (mm/μs)
5
4.5
4
3.5
3
2.5
2
0.2
0.4
0.6
0.8
1

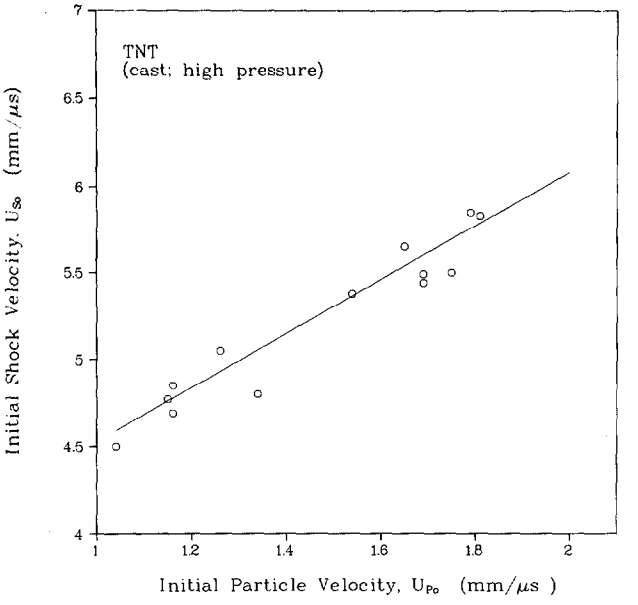
TNT
(cast; high pressure)
Initial Shock Velocity, U_{So} (mm/μs)
Initial Particle Velocity, U_{Po} (mm/μs)
7
6.5
6
5.5
5
4.5
4
1
1.2
1.4
1.6
1.8
2

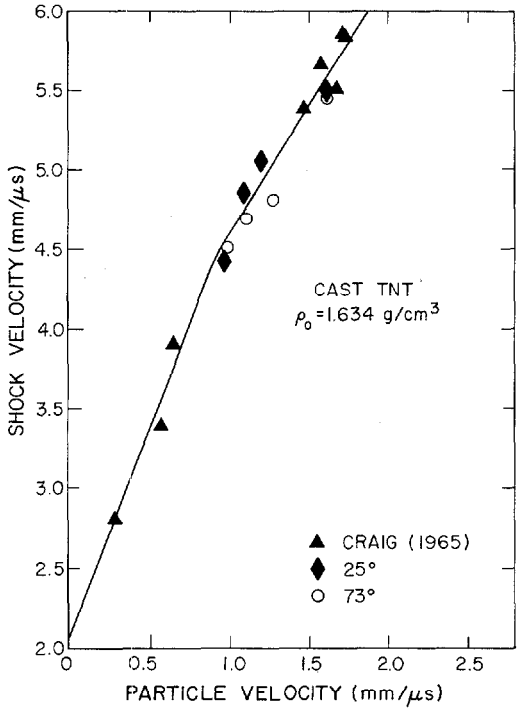

Fig. 4.04. Shock Hugoniot for cast TNT at two temperatures.

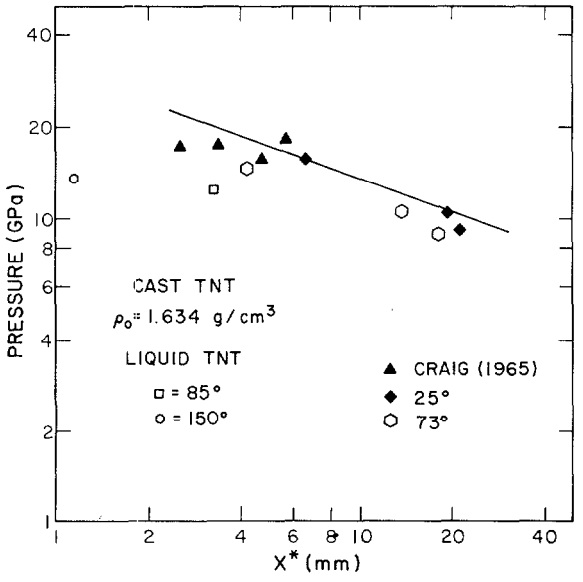

Fig. 4.05. Relationship between initial pressure and distance-to-detonation for cast TNT at 25 and 73°C and liquid TNT at 85 and 150°C.

Table 4.13 TNT (α) (SINGLE CRYSTAL)

Composition
100 wt% TNT
Theoretical Maximum Density
1.654 g/cm^3
Particle Size Distribution
Single crystal
Preparation Method
Controlled solvent evaporation
Data Summary
ρ_o = 1.654 g/cm^3. T_o = 24°C. Technique 4

Shot Number	Initial Shock Parameters P_0 (GPa)	U_{p0} (mm/μs)	U_{s0} (mm/μs)	1/2 b (mm/μs^2)	Driving System Thickness (mm)
E-2257	1.45	0.295	2.976	~0	B, 18.8 brass, 23.9 Plex, 12.2 brass, 5.8 Plex
E-2252	4.35	0.672	3.910	~0	B, 6.4 brass, 6.1 Plex
E-2255	7.80	1.059	4.454	0.192	C-1, 24.1 Plex
E-2262	8.38	1.118	4.532[a]	0.213	B, 11.7 Plex
	8.42	1.107	4.600[a]	0.	
E-2236	8.58	1.083	4.789[a]	0.422	B, 6.1 Plex
	8.67	1.075	4.850[a]	0	
E-2267	10.07	1.324	4.597[a]	0.521	G, 30.5 Plex
	10.7	1.353	4.760[a]	0.	
E-2261	11.8	1.453	4.909	0.095	H, 30.5 Plex
E-2256	13.7	1.536	5.394[a]	0.339	G, 5.8 Plex
	13.9	1.516	5.550[a]	0.	
E-2253	14.3	1.588	5.456	~0.	H, 4.6 aluminum
E-2302	18.1	1.932	5.678	−0.129	L, 18.0 Plex
E-2237	18.0	1.745	6.252	−0.029	L, 24.1 Plex
E-2254	23.3	2.146	6.549	−0.106	L, 6.1 Plex

[a]The first U_{s0} given is that uncorrected for wave tilt as indicated by the large value of 1/2 b; the second U_{s0} given was obtained by forcing 1/2 b to equal zero.

Reduced Data
When the data are corrected for wave tilt,
$U_{s0} = (2.576 \pm 0.229) + (1.822 \pm 0.161)\, U_{p0}$.

Table 4.14 BARATOL

Composition
24 wt% TNT, 76 wt% barium nitrate
Theoretical Maximum Density
2.634 g/cm³
Preparation Method
Casting
Data Summary
$T_0 \approx 23°C$. Technique 4

Shot Number	ρ_0 (g/cm³)	Initial Shock Parameters P_0 (GPa)	U_{p0} (mm/μs)	U_{s0} (mm/μs)	1/2 b (mm/μs²)	Coordinates for High-Order Detonation x* (mm)	t* (μs)	Driving System Thickness (mm)
E-3714	2.608	3.31	0.424	3.011	+0.002	≫25.4	≫8.40	B, 17.7 polyethylene 11.4 SS, 10.9 Plex
E-3645	2.612	5.71	0.627	3.485	+0.008	>25.4	>7.10	J, 20.3 SS, 1.09 Plex
E-3660	2.615	6.86	0.714	3.675	+2.615	16.82	4.39	K, 24.1 SS, 1.09 Plex
E-3643	2.616	8.12	0.836	3.714	+0.081	8.05	2.05	B, 38.1 Plex
E-3674	2.616	9.01	0.959	3.594	+0.311	6.79	1.63	B, 18.7 Plex
E-3712	2.610	9.16	0.983	3.569	+0.389	5.46	1.33	B, 12.7 Plex
E-3713	2.606	11.82	1.140	3.977	+0.780	3.604	0.79	G, 24.5 Plex

Reduced Data
$C_L = 2.95 \pm 0.05$ mm/μs,
$C_S = 1.48 \pm 0.01$ mm/μs, and
$C_0 = 2.40 \pm 0.06$ mm/μs,
all at $\rho = 2.538$ g/cm³.

Table 4.14 (continued)

$U_{s0} = (2.360 \pm 0.08) + (1.773 \pm 0.154)\, U_{p0}$.
$C_0 \leq U_{s0} \leq 3.675$
for $6.86 < P < 11.82$,
$\log P = (1.2 \pm 0.03) - (0.30 \pm 0.03) \log x^*$, and
$\log P = (1.01 \pm 0.01) - (0.27 \pm 0.02) \log t^*$.

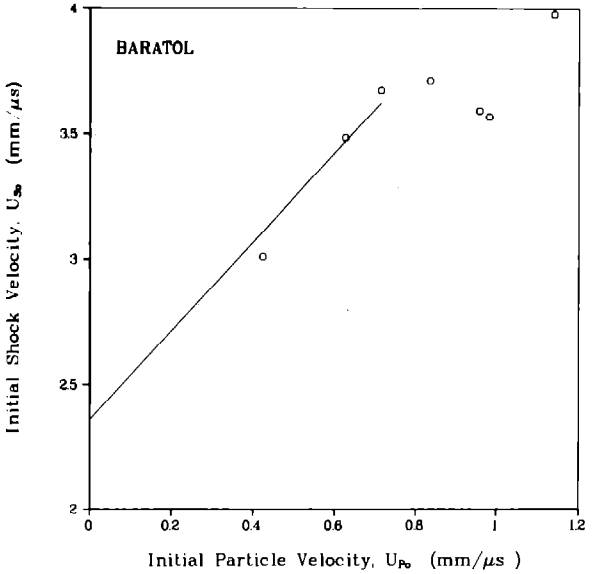

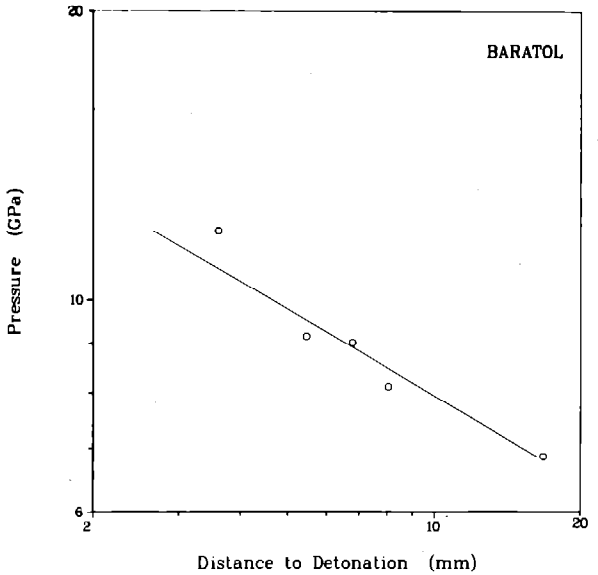

Table 4.15 X-0309 (DESTEX)

Composition

74.6 wt% TNT, 18.7 wt% aluminum, 4.8 wt% wax, 1.9 wt% acetylene black

Preparation Method

Casting and machining to shape

Data Summary

ρ_0 = 1.69 g/cm³. T_0 = 23°C. Technique 4

Shot Number	Initial Shock Parameters			Coordinates for High-Order Detonation		Driving System Thickness (mm)
	P_0 (GPa)	U_{p0} (mm/μs)	U_{s0} (mm/μs)	x* (mm)	t* (μs)	
E-4454	5.79	0.801	4.280	23.48	5.30	R, 24.1 SS, 11:5 Plex
E-4383	6.80	0.930	4.328	12.93	2.74	B, 38.1 Plex
E-4435	7.45	1.014	4.348	11.91	2.45	B, 24.1 Plex
E-4436	9.57	1.198	4.725	6.96	1.33	G, 31.7 Plex
E-4382	10.40	1.224	5.028	5.57	1.05	G, 25.0 Plex
E-4434	11.46	1.370	4.948	3.93	0.72	B, 24.1 Plex
E-4379	13.74	1.537	5.290	2.2	0.39	H, 20.4 Plex

Reduced Data

U_{s0}. = (2.998 ± 0.252) + (1.481 ± 0.214) U_{p0}

For 5.80 < P < 13.73,

log P = (1.28 ± 0.02) − (0.38 ± 0.02) log x*, and

log P = (1.01 ± 0.01) − (0.35 ± 0.02) log t*.

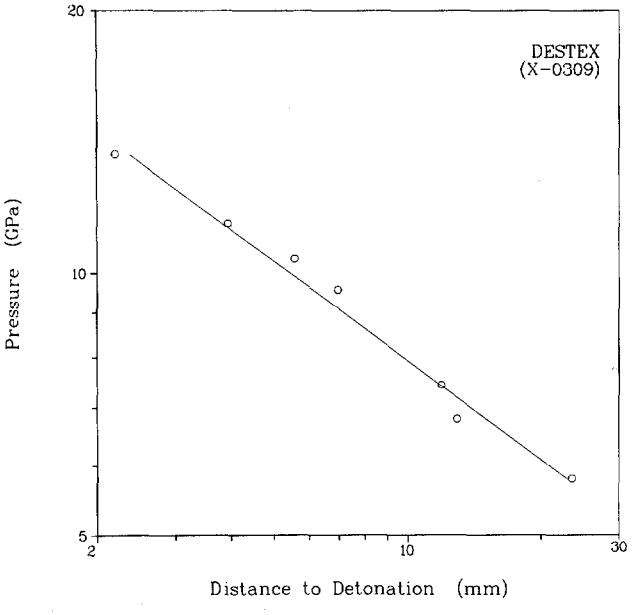
DESTEX
(X-0309)
Pressure (GPa)
20
10
5
2
10
30
Distance to Detonation (mm)

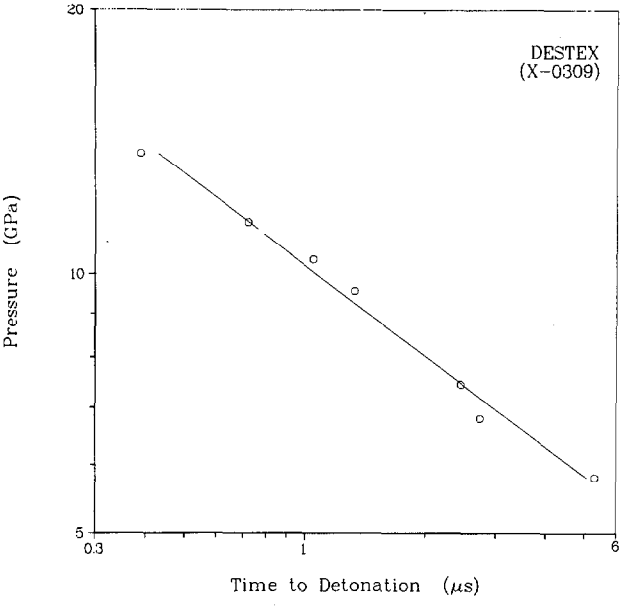
DESTEX
(X-0309)
Pressure (GPa)
20
10
5
0.3
1
6
Time to Detonation (μs)

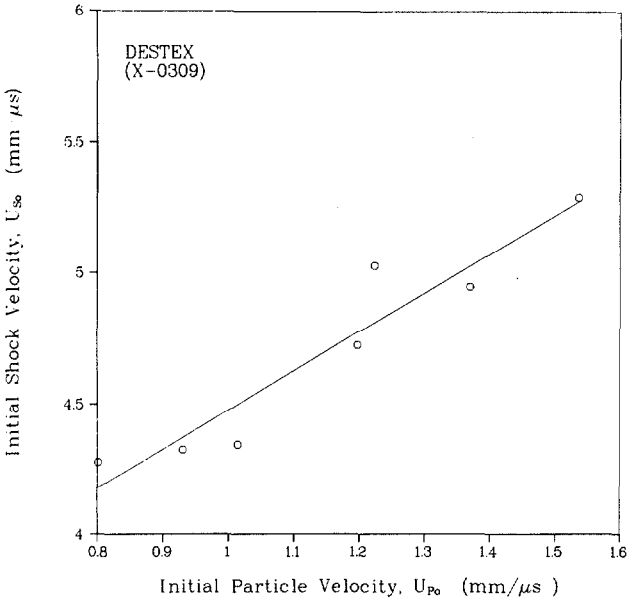
DESTEX
(X-0309)
Initial Shock Velocity, U_{s_0} (mm μs)
Initial Particle Velocity, U_{P_0} (mm/μs)
6
5.5
5
4.5
4
0.8
0.9
1
1.1
1.2
1.3
1.4
1.5
1.6

Table 4.16 95 DATB/5 ESTANE

Composition
95 wt% DATB, 5 wt% Estane
Theoretical Maximum Density
1.835 g/cm³
Particle Size Distribution

Particle Size (μm)	Wt% Retained
125	0.3
90	0.3
60	1.7
45	1.9
30	16.0
20	19.4
20	50.4

Preparation Method
Pressing
Data Summary
ρ_0 = 1.61-1.64 g/cm³. T_0 = 25-150°C. Technique 7

Shot Number	Temp. (°C)	ρ_0 (g/cm³)	Initial Shock Parameters			Coordinates for High-Order Detonation		U_{fs} (mm/μs)	Driving System Thickness (mm)
			P_0 (GPa)	U_{p0} (mm/μs)	U_{s0} (mm/μs)	x^* (mm)	t^* (μs)		
E-4475	26	1.641	1.92	0.47	2.49	>23.2	>11.3	0.982	B, 18 foam, 19 SS, 5.1 PC, 6.3 air, 6.3 PC
E-4495	150	1.61	1.60	0.46	2.16	>16.0	>8.0	0.895	B, 18 foam, 19 SS, 5.1 PC, 6.3 air, 6.3 PC
E-4476	30	1.642	3.48	0.68	3.12	9.59	2.75	1.487	N, 24 SS, 26 PC, 6.3 air, 6.3 PC
E-4492	25	1.641	3.34	0.70	2.91	10.4	3.14	1.488	N, 24 SS, 19 PC, 6.3 air, 6.3 PC
E-4460	25	1.636	3.52	0.71	3.03	9.32	2.83	1.521	N, 24 SS, 19 PC, 6.3 air, 6.3 PC
E-4493	100	1.62	3.13	0.58	3.33	10.9	3.28	1.324	N, 24 SS, 19 PC, 6.3 air, 6.3 PC
E-4479	150	1.61	2.82	0.65	2.71	6.82	2.17	1.335	N, 24 SS, 19 PC, 6.3 air, 6.3 PC
E-4498	22	1.636	3.87	0.75	3.15	8.65	2.42	1.628	L, 24 SS, 19 PC, 6.3 air, 6.3 PC
E-4499	100	1.62	3.36	0.65	3.19	8.15	2.32	1.429	L, 24 SS, 19 PC, 6.3 air, 6.3 PC
E-4500	150	1.61	3.28	0.69	2.95	5.46	1.69	1.466	L, 24 SS, 19 PC, 6.3 air, 6.3 PC

Reduced Data

Combined data for all temperatures

$U_{s0} = (1.296 \pm 0.575) + (2.536 \pm 0.897)U_{p0}$

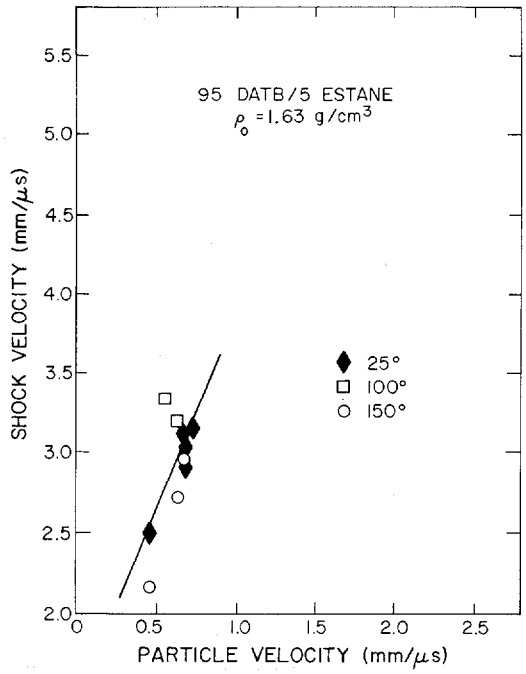

Fig. 4.06. Shock Hugoniot for 95 DATB/5 Estane at three temperatures.

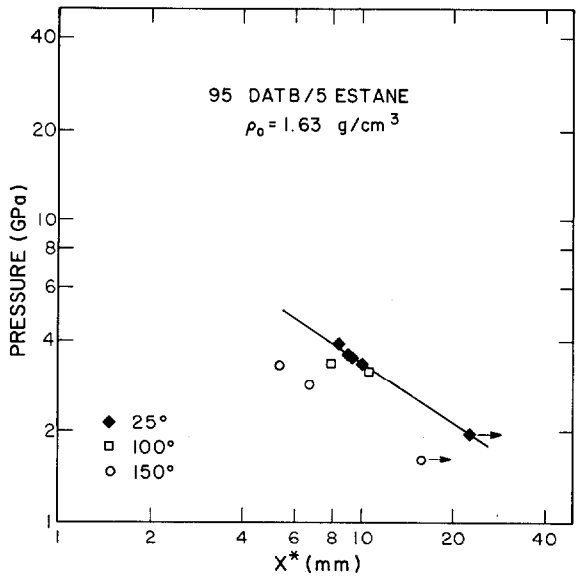

Fig. 4.07. Relationship between initial pressure and distance-to-detonation for DATB at three temperatures. The arrows indicate that the transition was not observed up to the distance where the point is plotted.

Table 4.17 PBX 9501

Composition

95 wt% HMX, 2.5 wt% Estane, 2.5 wt% BDNPF/A

Theoretical Maximum Density

1.855 g/cm³

Particle Size Distribution

HMX: 75%; 90% through USS-50, 50% through USS-100, 20% through USS-200, and 13% through USS-325 sieves. 25%; 100% through USS-50, 98% through USS-120, and 75% min. through USS-325 sieves.

Preparation Method

Slurry mixing, steel die pressing, and machining to shape

Data Summary

Technique 4

Shot Number	Temp (°C)	ρ_0 (g/cm³)	Initial Shock Parameters P_0 (GPa)	U_{p0} (mm/μs)	U_{s0} (mm/μs)	1/2 b (mm/μs²)	Coordinates for High-Order Detonation x* (mm)	t* (μs)	U_{fs} (mm/μs)	Driving System Thickness (mm)
					ρ_0 = 1.833 g/cm³, 98.8% ρ_T, T = 23°C					
E-3710	---	1.832	0.37	0.070	2.87	−0.006	≫25.5	≫9.01	0.183	A, 11.4 SS, 10.9 Acrylite
E-3702	---	1.833	2.38	0.388	3.35	+0.025	14.2	4.15	0.966	B, 17.8 foam, 11.4 SS, 10.9 Acrylite
E-3703	---	1.832	3.08	0.473	3.55	0.049	11.7	3.02	1.181	B, 17.8 polyethylene, 11.4 SS, 10.9 Acrylite
E-3717	---	1.833	3.70	0.553	3.65	0.042	8.6	2.09	1.368	B, 24.1 SS, 15.0 Acrylite
E-3720	----	1.832	7.32	0.887	4.50	0.612	2.70	0.54	2.222	B, 49.5 Plex
					ρ_0 = 1.844 g/cm³, 99.4% ρ_T, T = 23°C					
E-3711	---	1.844	0.57	0.097	3.192	−0.021	≫25.5	≫8.41	---	A, 11.4 SS, 10.9 Acrylite
E-3701	---	1.844	2.47	0.392	3.418	+0.022	22.8	6.14	---	B, 17.8 foam, 11.4 SS, 10.9 Acrylite
E-3705	---	1.844	3.19	0.478	3.617	0.041	16.6	4.21	---	B, 17.8 polyethylene, 11.4 SS, 10.9 Acrylite
E-3707	---	1.845	3.78	0.539	3.803	0.073	11.4	2.75	---	B, 24.1 SS, 15.0 Acrylite
E-3719	---	1.844	7.21	0.897	4.358	0.856	2.96	0.60	---	B, 48.7 Plex

Table 4.17 (continued)

Shot Number	Temp (°C)	ρ_0 (g/cm³)	Initial Shock Parameters P_0 (GPa)	U_{p0} (mm/μs)	U_{s0} (mm/μs)	1/2 b (mm/μs²)	Coordinates for High-Order Detonation x* (mm)	t* (μs)	U_{fs} (mm/μs)	Driving System Thickness (mm)
					ρ_0 = 1.79-1.833 g/cm³, T = 23-150°C					
E-4366	23	1.833	2.14	0.37	3.15	---	17.8	4.98	0.936	B, 18 foam, 11 SS, 51 PC, 6.3 air, 6.3 PC
E-4370	131	1.80	2.10	0.36	3.24	---	16.0	4.60	0.903	B, 18 foam, 11 SS, 51 PC, 6.3 air, 6.3 PC
E-4380	150	1.79	2.05	0.40	2.86	---	12.8	4.02	0.933	B, 18 foam, 11 SS, 51 PC, 6.3 air, 6.3 PC
E-4417	150	1.79	2.13	0.41	2.91	---	12.9	3.87	0.965	B, 18 foam, 11 SS, 51 PC, 6.3 air, 6.3 PC
E-4372	23	1.833	3.24	0.50	3.54	---	9.06	2.26	1.271	B, 38 PC, 6.3 air, 6.3 PC
E-4411	100	1.81	3.57	0.50	3.95	---	9.70	2.39	1.324	B, 38 PC, 6.3 air, 6.3 PC
E-4410	150	1.79	3.03	0.57	2.99	---	8.47	2.20	1.295	B, 38 PC, 6.3 air, 6.3 PC
E-4391	24	1.833	6.77	0.81	4.56	---	3.52	0.72	2.097	B, 24 SS, 8.9 PC, 6.3 air, 6.3 PC
E-4416	100	1.81	6.44	0.80	4.45	---	3.13	0.67	2.052	B, 24 SS, 8.9 PC, 6.3 air, 6.3 PC
E-4415	150	1.79	6.16	0.88	3.91	---	2.48	0.59	2.098	B, 24 SS, 8.9 PC, 6.3 air, 6.3 PC
E-4457	150	1.79	6.42	0.85	4.24	---	3.04	0.61	2.097	B, 24 SS, 8.9 PC, 6.3 air, 6.3 PC

Reduced Data

ρ_0 = 1.833 g/cm³.

$U_{s0} = (2.501 \pm 0.131) + (2.261 \pm 0.233)\ U_{p0}$.

For $2.38 < P < 7.32$,

$\log P = (1.15 \pm 0.05) - (0.64 \pm 0.06) \log x^*$, and

$\log P = (0.73 \pm 0.01) - (0.53 \pm 0.03) \log t^*$.

ρ_0 = 1.844 g/cm³.

$U_{s0} = (2.953 \pm 0.098) + (1.507 \pm 0.179) U_{p0}$.

For $2.47 < P < 7.21$,

$\log P = (1.10 \pm 0.04) - (0.51 \pm 0.03) \log x^*$, and

$\log P = (0.76 \pm 0.01) - (0.45 \pm 0.03) \log t^*$.

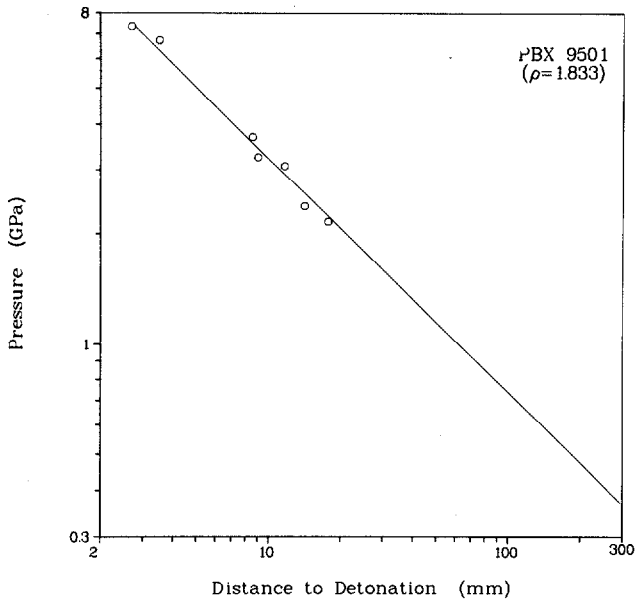
PBX 9501
(ρ=1.833)
Pressure (GPa)
8
1
0.3
2
10
100
300
Distance to Detonation (mm)

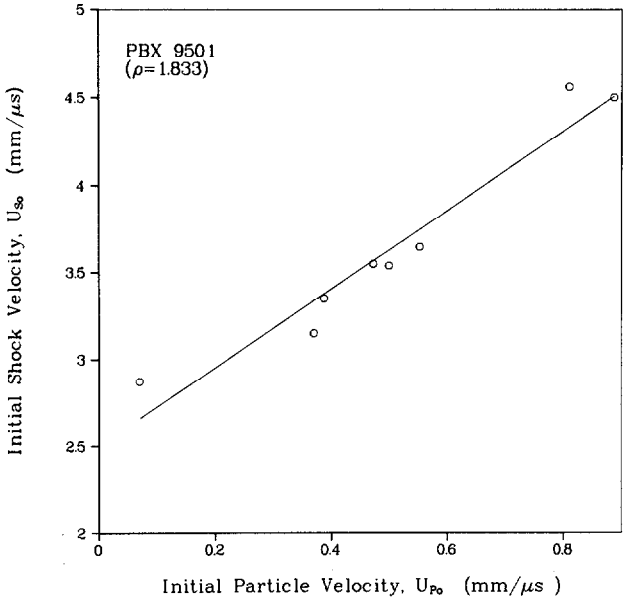
PBX 9501
(ρ=1.833)
Initial Shock Velocity, Us₀ (mm/μs)
5
4.5
4
3.5
3
2.5
2
0
0.2
0.4
0.6
0.8
Initial Particle Velocity, UP₀ (mm/μs)

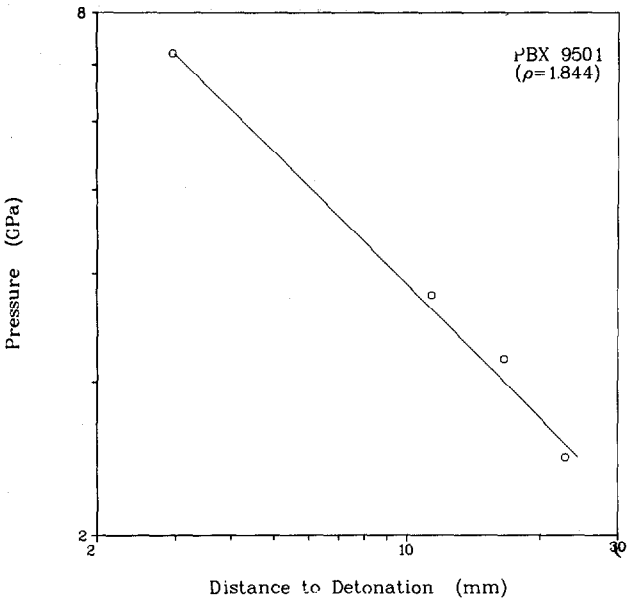
PBX 9501
(ρ=1.844)
Pressure (GPa)
8
2
2
10
30
Distance to Detonation (mm)

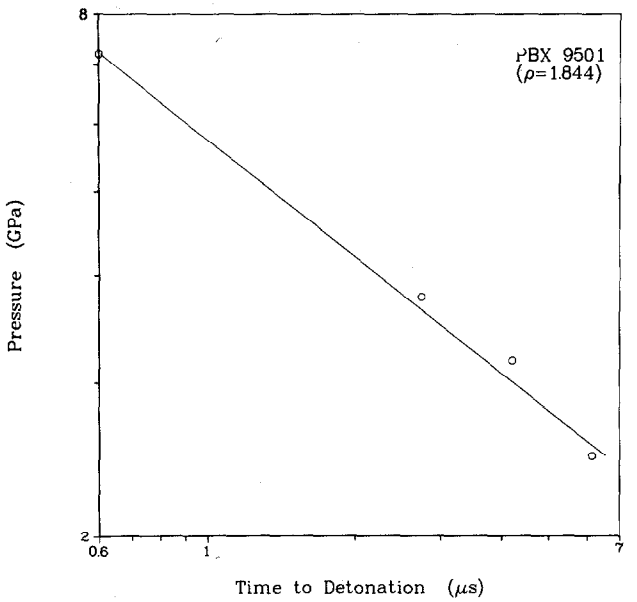
PBX 9501
(ρ=1.844)
Pressure (GPa)
8
2
0.6
1
7
Time to Detonation (μs)

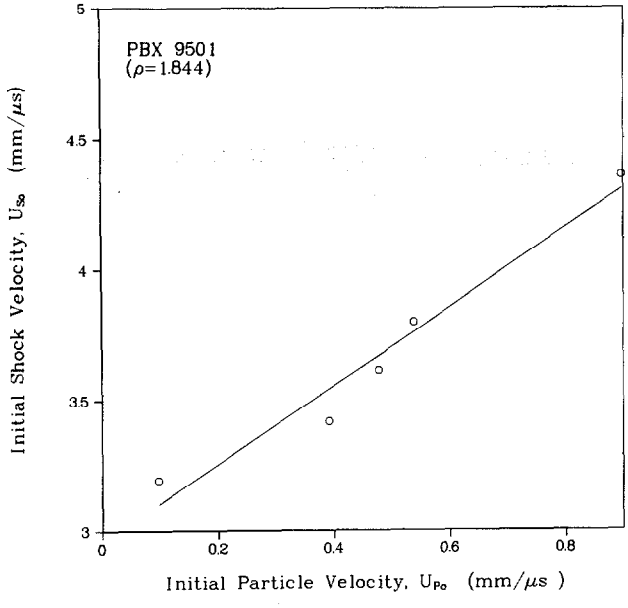
PBX 9501
(ρ=1.844)
Initial Shock Velocity, U_{so} (mm/μs)
Initial Particle Velocity, U_{Po} (mm/μs)
5
4.5
4
3.5
3
0
0.2
0.4
0.6
0.8

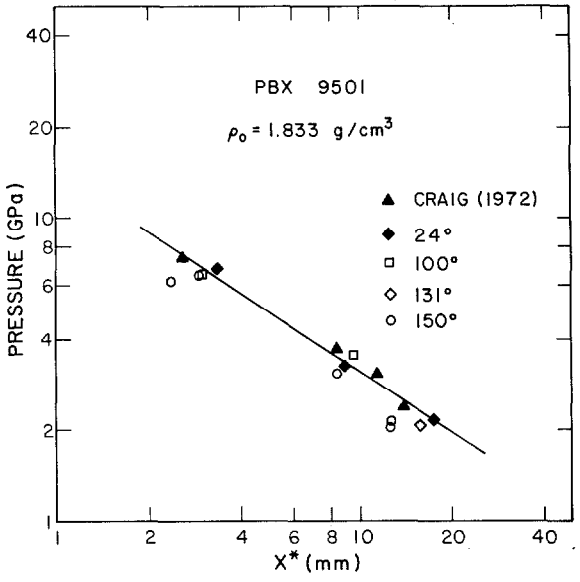

Fig. 4.08. Relationship between initial pressure and distance-to-detonation for PBX 9501 at four temperatures.

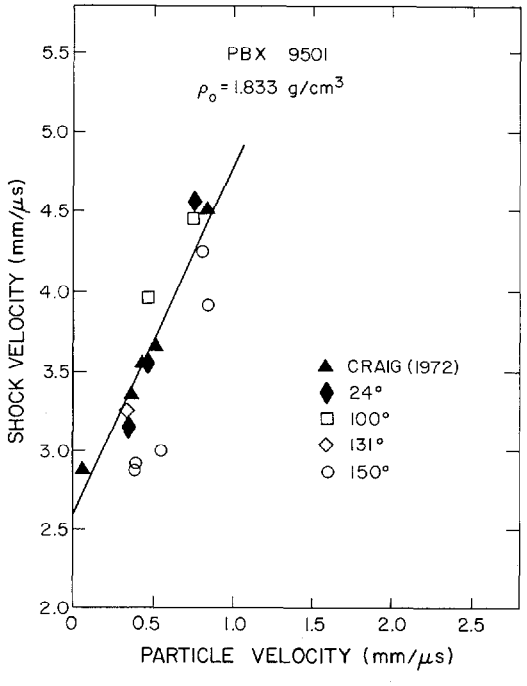

Fig. 4.09. Shock Hugoniot for PBX 9501 at four temperatures.

Table 4.18 PBX 9404

Composition
94 wt% HMX, 3 wt% nitrocellulose, 3 wt% chloroethylphosphate

Theoretical Maximum Density
1.866 g/cm³

Preparation Method
Hydrostatic pressing to 1.839 g/cm³ or ram-pressing to 1.840 ± 0.003 g/cm³

Data Summary
$T_0 \approx 23°C$. Technique 4

Shot Number	Initial Shock Parameters			1/2 b	Coordinates for High-Order Detonation		Driving System Thickness
	P_0 (GPa)	U_{p0} (mm/μs)	U_{s0} (mm/μs)	(mm/μs²)	x* (mm)	t* (μs)	(mm)
	PBX 9404 ram-pressed to ρ_0 = 1.84 g/cm³						
E-3158	0.73	0.133	2.977	−0.021	>25.39	>8.53	NQ lens, 11.43 SS, 10.92 Acrylite
E-3162	1.01	0.190	2.885	−0.003	>25.4	>8.8	NQ lens, 11.43 SS, 10.92 Acrylite
E-3193	1.98	0.340	3.161	−0.006	>25.5	>8.14	NQ lens, 25.4 Acrylite
E-3209	1.80	0.307	3.189	−0.011	>25.5	>8.07	NQ lens, 25.4 Shinkolite
E-3104	2.27	0.380	3.244	+0.034	15.17	4.28	B, 17.78 foam, 11.43 SS, 10.92 Acrylite
E-3246	2.30	0.393	3.183	+0.071	14.366	4.10	B, 17.78 foam, 11.43 SS, 10.92 Acrylite
E-3102	---	---	3.291	+0.069	13.13	3.62	B, 17.78 polyethylene, 11.43 SS, 10.92 H_2O
E-3116	---	---	3.419	+0.014	12.60	3.49	B, 17.78 polyethylene 11.43 SS, 10.92 H_2O

Table 4.18 (continued)

Shot Number	Initial Shock Parameters			1/2 b	Coordinates for High-Order Detonation		Driving System Thickness
	P_0 (GPa)	U_{p0} (mm/μs)	U_{s0} (mm/μs)	(mm/μs²)	x* (mm)	t* (μs)	(mm)
E-3120	---	---	3.370	+0.022	12.63	3.54	B, 17.78 polyethylene, 11.43 SS, 10.92 H_2O
E-3131	2.46	0.407	3.285	+0.098	11.86	3.21	NQ lens, 11.176 Acrylite
E-2984	2.95	0.458	3.504	+0.175	9.94	2.46	B, 17.78 polyethylene, 11.43 SS, 10.92 Acrylite
E-3210	---	---	3.534	+0.068	9.68	2.51	B, 17.78 polyethylene, 11.43 SS, 10.92 Acrylite
E-3211	---	---	3.506	+0.054	9.59	2.51	B, 17.78 polyethylene, 11.43 SS, 10.92 Acrylite
E-2983	3.15	0.481	3.557	+0.090	8.56	2.16	B, 17.78 Acrylite, 11.43 SS, 10.92 Acrylite
E-2966	3.19	0.508	3.413	+0.262	6.80	1.71	B, 25.4 SS, 14.986 Plex
E-3196	3.38	0.488	3.762	+0.271	5.83	1.36	B, 11.43 SS, 10.92 Acrylite
E-2953	3.59	0.538	3.628	+0.186	6.17	1.53	B, 25.4 brass, 24.638 Plex
E-2956	4.02	0.571	3.829	+0.094	6.32	1.55	B, 25.4 brass, 14.986 Plex
E-3173	11.20	1.202	5.062	+2.586	1.227	0.208	A, 25.4 Acrylite
E-3178	12.26	1.256	5.305	+0.397	1.256	0.227	A, 17.78 Acrylite
E-3177	13.31	1.382	5.233	+1.890	1.005	0.179	A, 12.7 Acrylite
E-3115	13.93	1.397	5.420	+6.185	0.782	0.126	R, 0.8636 D-38
E-3212	22.03	1.850	6.473	+10.607	0.471	0.065	N, 12.7 Everkleer
E-3214	25.72	2.063	6.775	+6.608	0.407	0.057	N, 6.35 Acrylite
	PBX-9404 hydrostatically pressed to ρ_0 = 1.839 g/cm³						
E-3183	2.40	0.393	3.317	0.010	15.05	4.26	Like E-3104
E-3184	3.01	0.474	3.454	0.082	10.28	2.70	Like E-2984

E-3185	3.51	0.536	3.564	0.178	8.03	1.99	B, 24.13 SS, 24.384 Acrylite
E-3198	7.18	0.897	4.351	0.950	2.89	0.56	B, 50.8 Acrylite

Shot Number	ρ_0 (g/cm³)	Initial Shock Parameters			1/2 b (mm/μs²)	Coordinates for High-Order Detonation		Driving System Thickness (mm)
		P_0 (GPa)	U_{p0} (mm/μs)	U_{s0} (mm/μs)		x* (mm)	t* (μs)	
	PBX 9404 ram-pressed to ρ_0 = 1.845 ± 0.002 g/cm³							
E-3271	---	2.53	0.417	3.289	0.029	15.98	4.49	Like E-3183
E-3272	---	3.16	0.497	3.447	0.076	10.51	2.78	Like E-3184
E-3273	---	6.59	0.873	4.098	1.097	2.30	0.49	Like E-3198
	PBX-9404 pressed to ρ_0 = 1.721 g/cm³							
E-3555	1.724	6.33	0.995	3.699	2.092	1.67	0.37	B,49.276 Plex
E-3554	1.724	3.04	0.682	2.594	1.082	4.07	1.07	B, 24.13 SS, 13.97 Plex
E-3536	1.728	2.57	0.560	2.664	0.033	6.80	1.82	B, 17.78 polyethylene, 11.43 SS, 10.92 Acrylite
E-3547	1.720	2.51	0.525	2.782	0.124	6.11	1.83	B, 12.7 D-38, 12.7 PMMA
E-3537	1.720	2.02	0.427	2.749	0.061	8.70	2.66	B, 17.78 foam (30 lb/ft³), 11.43 SS, 10.92 Acrylite
E-3539	1.722	1.19	0.297	2.326	0.029	16.50	6.63	A (0.4 g/cm³), 11.43 Dural, 10.922 Acrylite
E-3538	1.722	0.70	0.172	2.365	0.014	>25.4	>10	A (0.4 g/cm³), 11.43 SS, 10.922 Acrylite
E-3567	1.714	1.53	0.387	2.294	0.017	12.81	4.74	A, 25.4 Plex

D ≈ 8.3 mm/μs

Table 4.18 (continued)

Shot Number	ρ_0 (g/cm³)	Initial Shock Parameters P_0 (GPa)	U_{p0} (mm/μs)	U_{s0} (mm/μs)	1/2 b (mm/μs²)	Coordinates for High-Order Detonation x* (mm)	t* (μs)
			Additional Data PBX-9404				
E-771	1.84	4.0	0.49	4.41	---	2.67	0.56
E-781	1.84	2.4	0.37	3.47	---	13.9	3.78
B-4481	1.84	3.8	0.53	3.82	---	6.76	1.60
B-4677	1.84	2.5	0.40	3.45	---	14.0	3.80
D-6837	1.84	2.9	0.43	3.66	---	10.6	2.73
B-4688	1.84	2.9	0.44	3.59	---	10.8	3.05
E-1558[a,b]	1.845	---	---	3.6	---	3.12	0.72
D-7697[b]	1.847	5.66	0.737	4.16	---	3.34	0.73
E-1559[b]	1.845	5.42	0.691	4.25	---	3.63	0.78
E-1560[b]	1.844	5.97	0.718	4.51	---	2.85	0.58
D-7742[b]	1.85	5.87	0.723	4.39	---	2.66	0.55
B-5543	1.84	2.2	0.37	3.23	---	20.2	5.79
B-5550	1.84	2.19	0.36	3.30	---	19.6	5.56
B-5538	1.84	15.9	1.43	6.03	---	0.49	0.08
B-5555	1.84	15.7	1.45	5.89	---	0.56	0.10
			PBX-9404-00				
E-663	1.82	6.8	0.81	4.65	---	2.56	0.44
E-707	1.83	1.7	0.28	3.27	---	>17	---
E-711	1.83	2.2	0.38	3.27	---	15.8	4.51
E-743	1.83	3.6	0.53	3.67	---	8.2	2.00
B-4317	1.82	5.7	0.71	4.38	---	3.47	0.66

B-4615	1.83	3.6	0.51	3.87	---	7.65	1.76
D-6514	1.84	3.7	0.52	3.85	---	7.61	1.74

[a]Very poor record.
[b]Five replicate shots were fired without simultaneously measuring the driver pressure. However, the driver free-surface velocity had been measured in eight shots. Data for the driver and the reported U_{s0} were used to deduce P_0 and U_{p0}.

Reduced Data

For $\rho_0 = 1.84$ g/cm³.
$U_{s0} = (2.494 \pm 0.039) + (2.093 + 0.045)U_{p0}$.
For $2.27 < P < 25.72$,
$\log P = (1.11 \pm 0.01) - (0.65 \pm 0.02) \log x^*$, and
$\log P = (0.69 \pm 0.01) - (0.54 \pm 0.01) \log t^*$.
$D = 8.81$ mm/μs.

For $\rho_0 = 1.72$ g/cm³.
$U_{s0} = (1.890 \pm 0.197) + (1.565 \pm 0.353)U_{p0}$.
For $1.19 < P < 6.34$,
$\log P = (0.96 + 0.03) - (0.71 \pm 0.04) \log x^*$, and
$\log P = (0.54 \pm 0.01) - (0.57 \pm 0.02) \log t^*$.

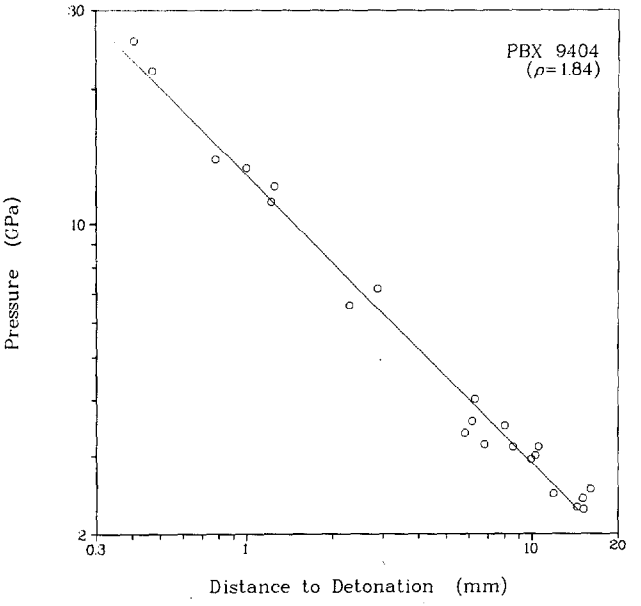
PBX 9404
(ρ=1.84)
30
10
2
0.3
1
10
20
Pressure (GPa)
Distance to Detonation (mm)

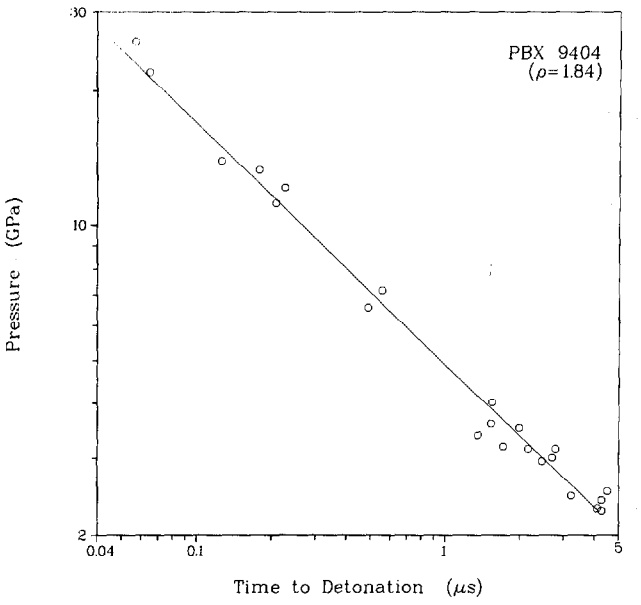
PBX 9404
(ρ=1.84)
30
10
2
0.04
0.1
1
5
Pressure (GPa)
Time to Detonation (μs)

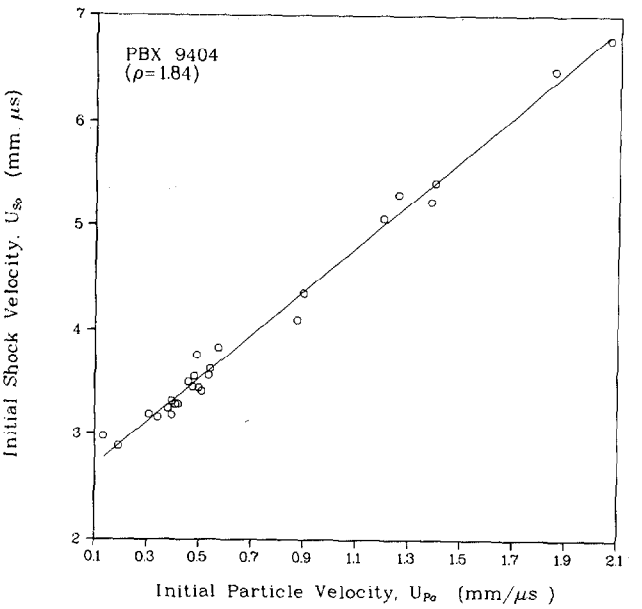
PBX 9404
(ρ=1.84)
Initial Shock Velocity, U_{So} (mm/μs)
Initial Particle Velocity, U_{Po} (mm/μs)
7
6
5
4
3
2
0.1
0.3
0.5
0.7
0.9
1.1
1.3
1.5
1.7
1.9
2.1

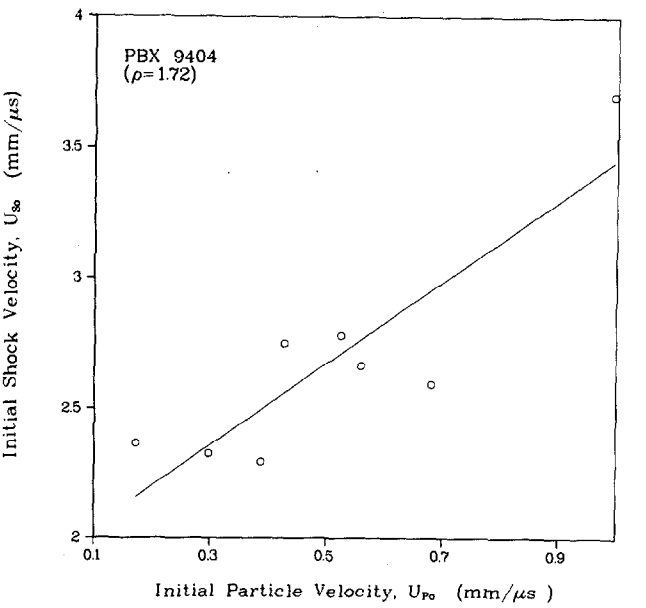
PBX 9404
(ρ=1.72)
Initial Shock Velocity, U_{So} (mm/μs)
Initial Particle Velocity, U_{Po} (mm/μs)
4
3.5
3
2.5
2
0.1
0.3
0.5
0.7
0.9

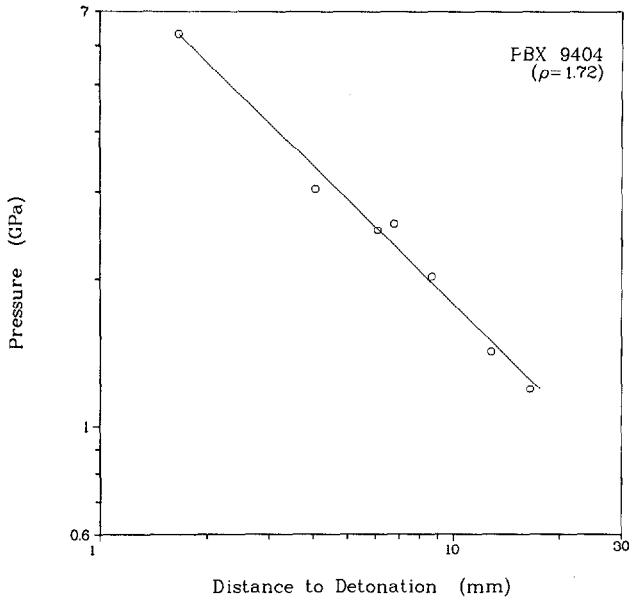
PBX 9404
(ρ=1.72)
Pressure (GPa)
7
1
0.6
1
10
30
Distance to Detonation (mm)

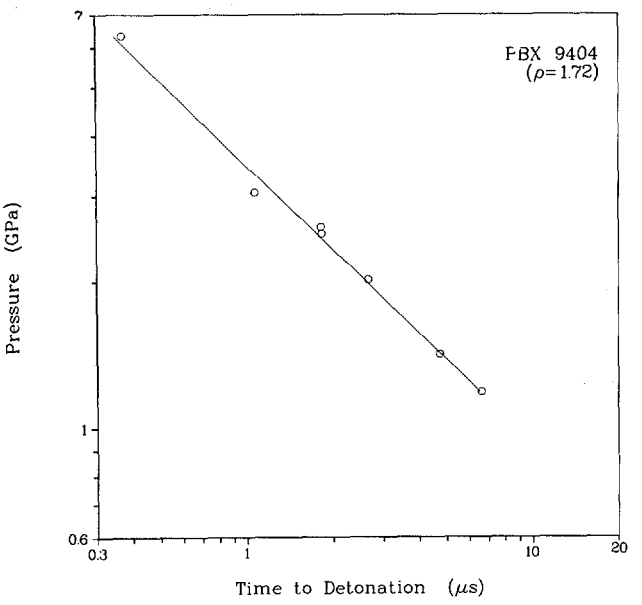
PBX 9404
(ρ=1.72)
Pressure (GPa)
7
1
0.6
0.3
1
10
20
Time to Detonation (μs)

Table 4.19 PBX 9011

Composition

90 wt% HMX, 10 wt% Estane

Theoretical Maximum Density

1.795 g/cm^3

Particle Size Distribution

HMX: 100% through USS-50 sieve, 98% min. through USS-120 sieve, and 75% min. through USS-325 sieve

Preparation Method

Slurring mixing, hydrostatic pressing, and machining to shape

Data Summary

ρ = 1.790 g/cm^3. $T_0 \approx 23°C$. Technique 4

Shot Number	Initial Shock Parameters			1/2 b	Coordinates for High-Order Detonation		Driving System Thickness
	P_0 (GPa)	U_{p0} (mm/μs)	U_{s0} (mm/μs)	(mm/μs^2)	x* (mm)	t* (μs)	(mm)
E-2415	15.65	1.427	6.126	+2.320	0.995	0.155	L, 6.096 brass
E-2398	9.81	1.096	5.001	+1.029	1.893	0.344	H, 6.096 brass
E-2399	7.55	0.932	4.528	+0.738	2.930	0.578	H, 25.4 Plex, 11.176 brass
E-2396	6.24	0.803	4.340	+0.483	3.719	0.769	B, 6.096 brass
E-2416	4.82	0.654	4.115	+0.191	6.043	1.342	B, 13.208 Plex, 6.096 brass

Reduced Data

$C_L = 2.89 \pm 0.03$ mm/μs,

$C_S = 1.38 \pm 0.02$ mm/μs, and

$C_0 = 2.41 \pm 0.04$ mm/μs.

ρ = 1.77 g/cm^3.

$U_{s0} = (2.363 \pm 0.131) + (2.513 \pm 0.141)U_{p0}$.

For $4.82 < P < 15.65$,

$\log P = (1.18 \pm 0.01) - (0.66 \pm 0.02) \log x^*$, and

$\log P = (0.74 \pm 0.01) - (0.55 \pm 0.01) \log t^*$.

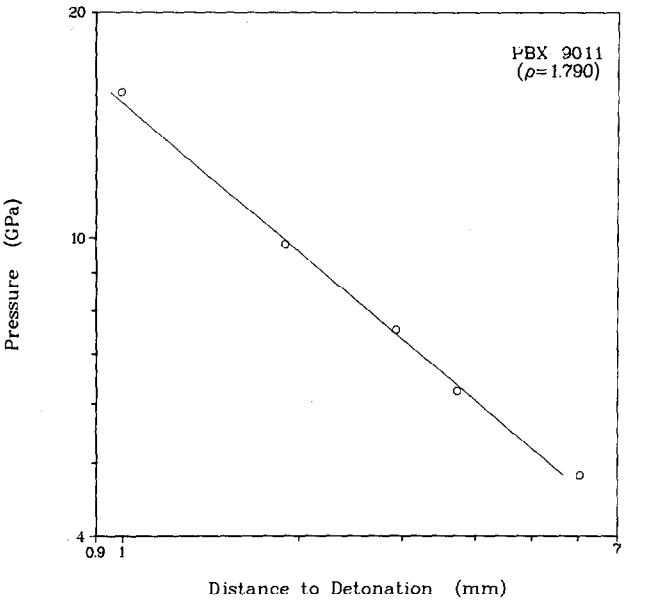
PBX 9011
(ρ=1.790)
Pressure (GPa)
20
10
4
0.9
1
7
Distance to Detonation (mm)

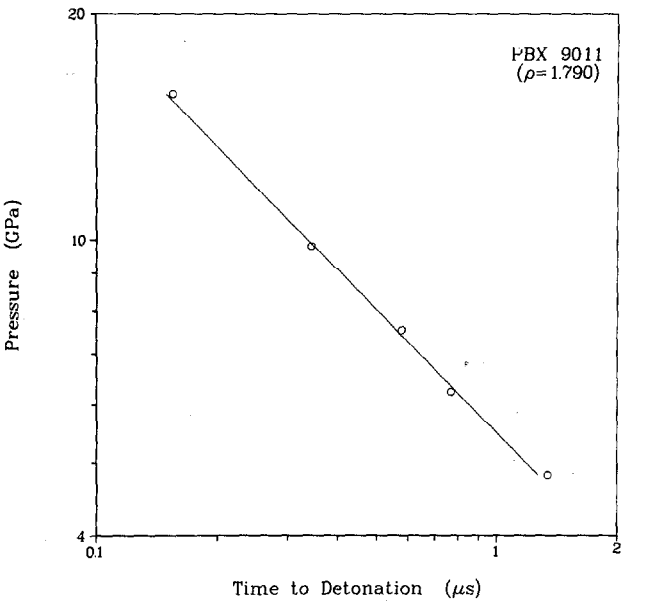
PBX 9011
(ρ=1.790)
Pressure (GPa)
20
10
4
0.1
1
2
Time to Detonation (μs)

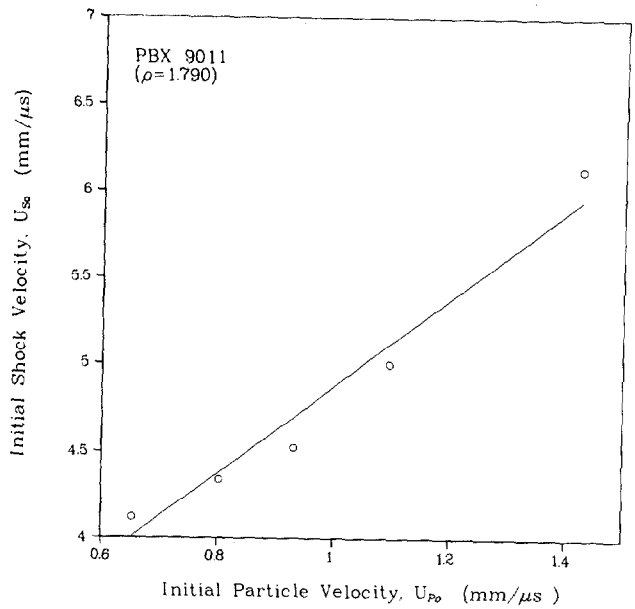
PBX 9011
(ρ=1.790)
Initial Shock Velocity, U_{So} (mm/μs)
Initial Particle Velocity, U_{Po} (mm/μs)
7
6.5
6
5.5
5
4.5
4
0.6
0.8
1
1.2
1.4

Table 4.20 LX-04

Composition
85 wt% HMX, 15 wt% Viton
Particle Size Distribution
"Fine-grain" HMX
Preparation Method
Pressing and machining to shape
Data Summary
ρ_0 = 1.859 g/cm³. Technique 1

Shot Number	Initial Shock Parameters			Coordinates for High-Order Detonation		Driving System Thickness (mm)
	P_0 (GPa)	U_{p0} (mm/μs)	U_{s0} (mm/μs)	x* (mm)	t* (μs)	
E-1887	6.74	0.832	4.354	2.39	---	B, 6.1 brass
E-1889	4.44	0.611	3.895	6.42	---	B, 6.4 brass, 6.4 PMMA
E-1894	4.06	0.577	3.785	6.36	---	B, 6.4 Plex, 6.1 brass, 6.4 Plex

Reduced Data
$U_{s0} = (2.546 \pm 0.089) + (2.176 \pm 0.131)U_{p0}$.
For $4.06 < P < 6.74$,
$\log P = (1.01 \pm 0.06) - (0.47 \pm 0.08) \log x^*$.

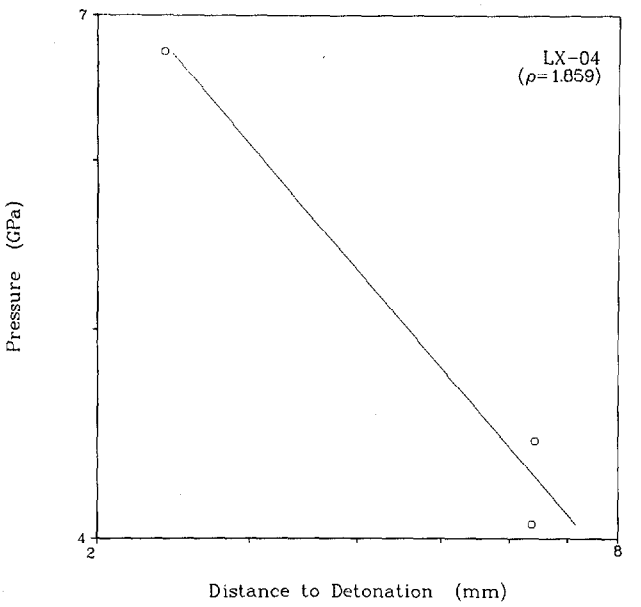
LX-04
(ρ=1.859)
Pressure (GPa)
7
4
2
8
Distance to Detonation (mm)

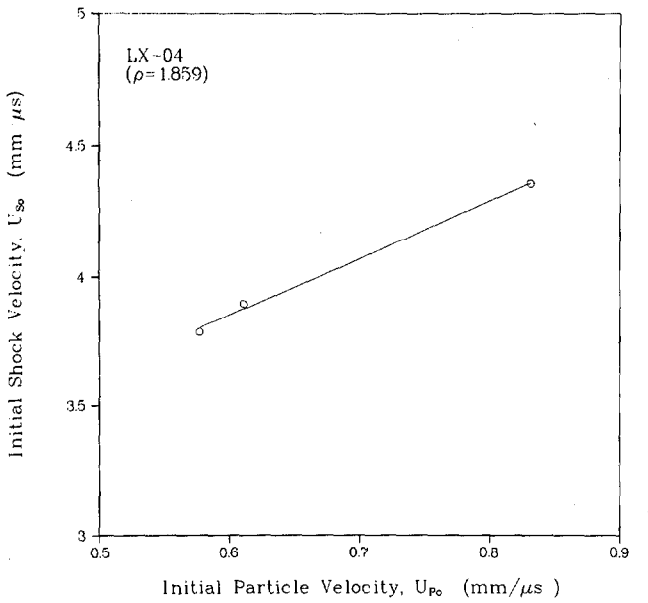
LX-04
(ρ=1.859)
Initial Shock Velocity, U_{s_0} (mm μs)
5
4.5
4
3.5
3
0.5
0.6
0.7
0.8
0.9
Initial Particle Velocity, U_{P_0} (mm/μs)

Table 4.21 X-0219-50-14-10

Composition
50 wt% HMX, 40 wt% TATB, 10 wt% Kel-F 800
Theoretical Maximum Density
1.927 g/cm³
Preparation Method
Slurry mixing, pressing, and machining to shape
Data Summary
ρ_0 = 1.912 g/cm³. $T_0 \approx 23°C$. Technique 4

Shot Number	Initial Shock Parameters			1/2 b	Coordinates for High-Order Detonation		Driving System Thickness
	P_0 (GPa)	U_{p0} (mm/μs)	U_{s0} mm/μs)	(mm/μs²)	x* (mm)	t* (μs)	(mm)
E-3591	3.90	0.554	3.683	0.035	>12.7	>3.23	B, 25.4 brass, 18.542 Plex
E-3596	7.15	0.883	4.237	0.436	4.18	0.86	B, 49.53 Plex
E-3604	6.89	0.831	4.336	0.581	3.500	0.722	L, 24.13 SS, 10.92 Plex
E-3642	6.30	0.811	4.062	0.061	8.476	1.946	H, 24.13 SS, 10.92 Plex

Reduced Data
$U_{s0} = (2.674 \pm 0.387) + (1.826 \pm 0.497)U_{p0}$.
For $3.9 < P < 7.15$.
$\log P = (0.92 \pm 0.05) + (0.12 \pm 0.06) \log x^*$, and
$\log P = (0.83 \pm 0.01) - (0.11 \pm 0.05) \log t^*$.

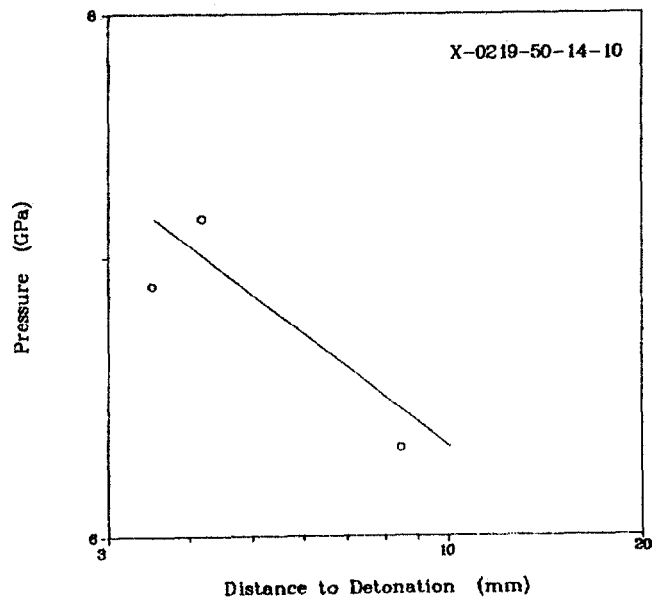
X-0219-50-14-10
Pressure (GPa)
8
6
3
10
20
Distance to Detonation (mm)

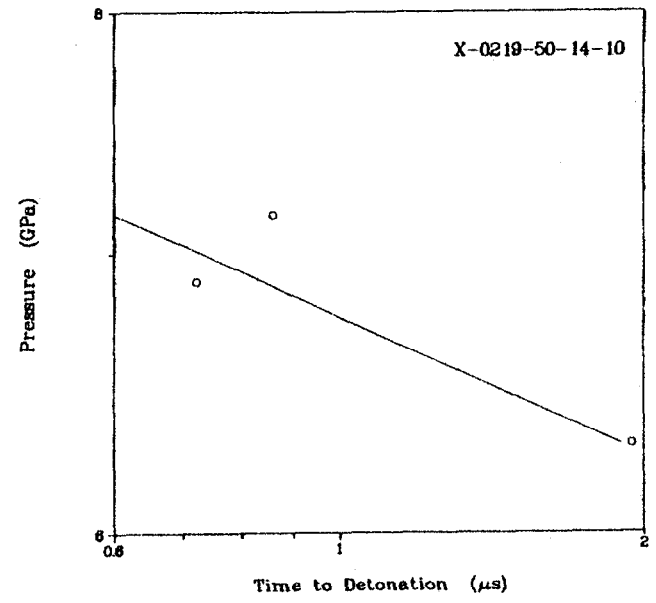
X-0219-50-14-10
Pressure (GPa)
8
6
0.6
1
2
Time to Detonation (μs)

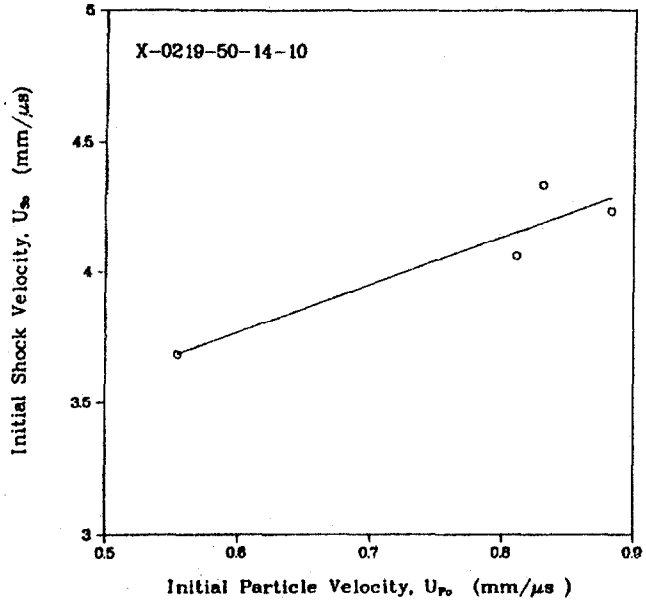
X-0219-50-14-10
Initial Shock Velocity, U_{Si} (mm/μs)
Initial Particle Velocity, U_{Po} (mm/μs)
5
4.5
4
3.5
3
0.5
0.6
0.7
0.8
0.9

Table 4.22 X-0241-96

Composition
96 wt% NQ, 2 wt% wax, 2 wt% Elvax
Theoretical Maximum Density
1.720 g/cm³
Preparation Method
Slurry mixing, pressing, and machining to shape
Data Summary
ρ_0 = 1.676 g/cm³. $T_0 \approx 23°C$. Technique 4

Shot Number	Initial Shock Parameters			1/2 b	Coordinates for High-Order Detonation		Driving System Thickness
	P_0 (GPa)	U_{p0} (mm/μs)	U_{s0} (mm/μs)	(mm/μs²)	x* (mm)	t* (μs)	(mm)
E-3284	24.29	2.216	6.539	+0.742	4.23	0.60	N, 6.096 Everkleer
E-3279	20.30	1.898	6.380	+0.058	15.14	2.29	N, 14.986 Plex
E-3285	18.66	1.794	6.206	+0.056	24.52	3.80	N, 16.51 Plex
E-3352	9.05	1.136	4.753	+0.019	>25.40	>5.24	B, 17.78 Acrylite

Reduced Data
$U_{s0} = (2.88 \pm 0.58) + (1.755 \pm 0.321)U_{p0}$.
For $9.05 < P < 24.29$,
$\log P = (1.48 \pm 0.01) - (0.15 \pm 0.01) \log x^*$, and
$\log P = (1.35 \pm 0.003) - (0.14 \pm 0.01) \log t^*$.

Table 4.23 95 NQ/5 ESTANE

Composition
95 wt% NQ, 5 wt% Estane
Theoretical Maximum Density
1.738 g/cm³
Particle Size Distribution
Standard
Preparation Method
Pressing and machining to shape
Data Summary
T = 23°C. Technique 3

Shot Number	Initial Shock Parameters			Coordinates for High-Order Detonation		Driving System Thickness (mm)
	P_0 (GPa)	U_{p0} (mm/μs)	U_{s0} (mm/μs)	x* (mm)	t* (μs)	
	ρ_0 = 1.699 g/cm³					
E-2977	8.59	1.041	4.859[a]	≫29.2	≫5.95	B, 12.9 Plex
E-2936	15.87	1.603	5.828	>28.23	>4.78	N, 23.5 Plex
E-3050	18.70	1.746	6.303	23+	3+	O, 17.9 PMMA
E-2939	18.75	1.778	6.208	16.03	2.50	N, 18.3 PMMA
E-2938	21.00	1.920	6.438	7.253	1.09	N, 11.4 PMMA
	ρ_0 = 1.663 g/cm³					
E-2927	14.24	1.571	5.449	12.64	2.10	J, 18.6 Plex
E-2925	15.50	1.672	5.576	9.94	1.62	N, 24.3 Plex
E-2910	26.32	2.302	6.874	1.03	0.15	N, 5.9 Plex

			ρ_0 = 1.653 g/cm³			
E-2930[b]	14.73	1.565	5.695	12.23	1.99	J, 18.1 Plex
E-2932[c]	14.50	---	---	>9.42	---	J, 18.5 Plex

[a]Decelerates.
[b]This wedge had a tight butt joint in the direction of propagation.
[c]The butt joint for this shot was spaced open by 0.005 in. A multi-slit technique was used to show that high-order detonation first occurred about 7.5 mm on each side of the joint.

Shot Number	P_0 (GPa)	U_{p0} (mm/μs)	U_{p0} (mm/μs)	1/2 b (mm/μs²)	x* (mm)	t* (μs)	Driving System Thickness (mm)
			Large-Grain NQ, ρ_0 = 1.700 g/cm³				
E-3051	18.52	1.772	6.147	0.0	>25.4	>4.15	N, 18.3 PMMA
E-3052	19.91	1.820	6.434	0.001	11.08	1.67	N, 11.4 PMMA
E-3054	24.43	2.125	6.764	0.020	5.59	0.80	N, 6.02 Plex

Table 4.23 (continued)

Shot Number	P_1 (GPa)	U_{s1} (mm/μs)	$1/2\,b_1$ (mm/μs²)	x_{0T} (mm)	t_{0T} (μs)	P_2[a] (GPa)	U_{s2} (mm/μs)	x* (mm)	Driving System Thickness (mm)
	Multiple-Shock, Large-Grain NQ, ρ_0 = 1.700 g/cm³								
E-3245	16.2	5.904	−0.013	15.24	2.62	18.8	6.256	>25.4	R, 3.0 SS
E-3220	15.7	5.787	+0.025	8.45	1.46	18.9	6.215	>25.4	N, 1.73 SS
E-3423	16.9	5.988	−0.106	19.88	3.54	11.4[b]	5.276	>25.4	F, 2.96 Plex
E-3442	19.1	6.232	−0.042	17.56	2.88	20.7	6.399	>25.4	R, 1.91 Pb
E-2960	15.7	5.89	−0.162	15.45	2.80	16.6	6.19	>29.2	P, 2.87 Ni
E-2961	13.5	5.54	−0.01	15.89	2.94	---	5.75	>29.2	Q, 1.93 U
E-2962	12.6	5.43	−0.01	6.5/13.8/ 19.1[c]	1.2/2.4/ 3.25[c]	17.9	6.09	23.3[d]	P, 0.89 U
E-2963	---	5.85	−0.05	15.15	2.63	---	6.03	>29.2	Q, 2.89 Ni

[a]From P vs U_s data for a single shock and observed U_{s2}.
[b]Probably low owing to edge effect.
[c]Three overtakes.
[d]Total distance including overtakes.

Reduced Data

Standard NQ only.

$U_{s0} = (3.022 \pm 0.376) + (1.713 \pm 0.219)U_{p0}$.

For $14.24 < P < 18.75$,

$\log P = (1.42 \pm 0.07) - (0.19 \pm 0.07) \log x^*$, and

$\log P = (1.27 \pm 0.03) - (0.19 \pm 0.02) \log t^*$.

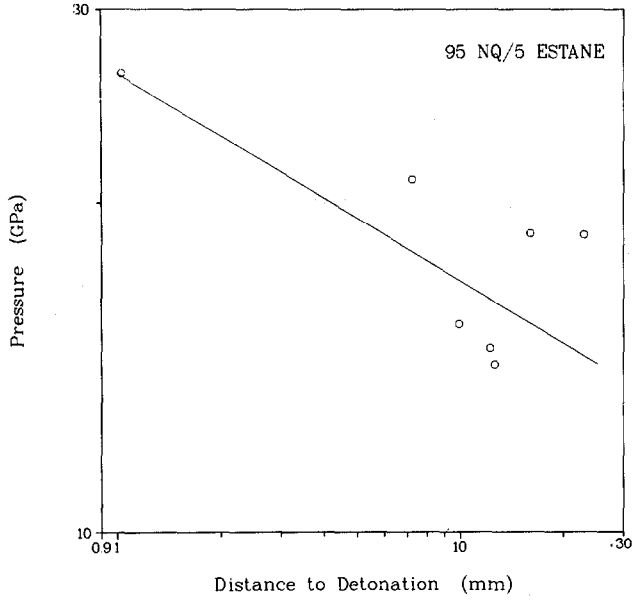
30
95 NQ/5 ESTANE
Pressure (GPa)
10
0.9 1
10
30
Distance to Detonation (mm)

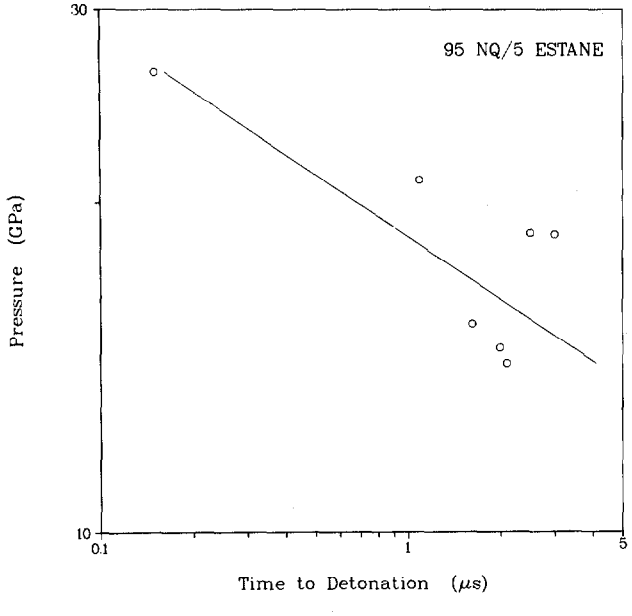
30
95 NQ/5 ESTANE
Pressure (GPa)
10
0.1
1
5
Time to Detonation (μs)

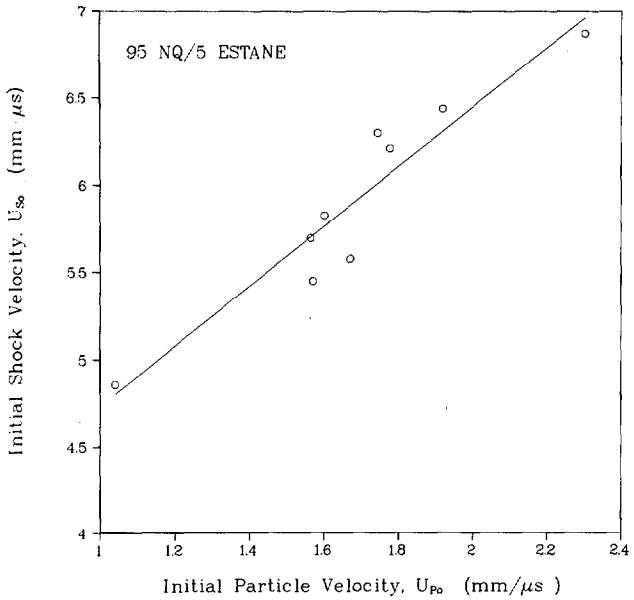
95 NQ/5 ESTANE
Initial Shock Velocity, U_{So} (mm μs)
Initial Particle Velocity, U_{Po} (mm/μs)
7
6.5
6
5.5
5
4.5
4
1
1.2
1.4
1.6
1.8
2
2.2
2.4

Table 4.24 X-0228-90

Composition
90 wt% NQ, 10 wt% Estane
Theoretical Maximum Density
1.698 g/cm³
Preparation Method
Slurry mixing, pressing, and machining to shape
Data Summary
$T_0 \approx 23°C$. Technique 4

Shot Number	Initial Shock Parameters			1/2 b	Coordinates for High-Order Detonation		Driving System Thickness
	P_0 (GPa)	U_{p0} (mm/μs)	U_{s0} (mm/μs)	(mm/μs²)	x* (mm)	t* (μs)	(mm)
	$\rho_0 = 1.667$ g/cm³ "Large" Grain						
E-3278	27.24	2.274	7.186	+0.659	2.07	0.28	S, 6.35 Everkleer
E-3275	24.58	2.181	6.761	+0.293	5.05	0.72	N, 6.096 Everkleer
E-3276	22.61	2.068	6.558	+0.117	13.39	1.91	N, 9.652 Plex
E-3277	20.90	2.001	6.266	−0.000	>25.42	>4.04	N, 12.954 Everkleer
E-3353	8.15	1.018	4.804	+0.003	>25.42	>5.274	B, 18.78 Acrylite
	$\rho_0 = 1.666$ g/cm³ "Commercial" Grain						
E-2941	20.27	1.924	6.325	---	14.35	2.20	N, 12.192 Acrylite
	$\rho_0 = 1.647$ g/cm³ "Commercial" Grain						
E-2909	24.83	2.083	7.238	---	2.21	0.30	N, 6.096 Plex
E-2926	17.32	1.766	5.954	---	12.09	1.90	N, 19.05 Plex
E-2916	15.03	1.628	5.606	---	>24.93	>4.08	N, 25.4 Plex
E-2929	~13.1	---	~5.5	---	>31.42	>4.94	J, 19.05 Plex

Table 4.24 (continued)

Reduced Data

Combined densities.

$U_{s0} = (2.68 \pm 0.477) + (1.923 \pm 0.249)U_{p0}$.

For $17.32 < P < 27.24$,

$\log P = (1.35 \pm 0.02) - (0.14 \pm 0.05) \log t^*$, and

$\log P = (1.47 \pm 0.05) - (0.15 \pm 0.05) \log x^*$.

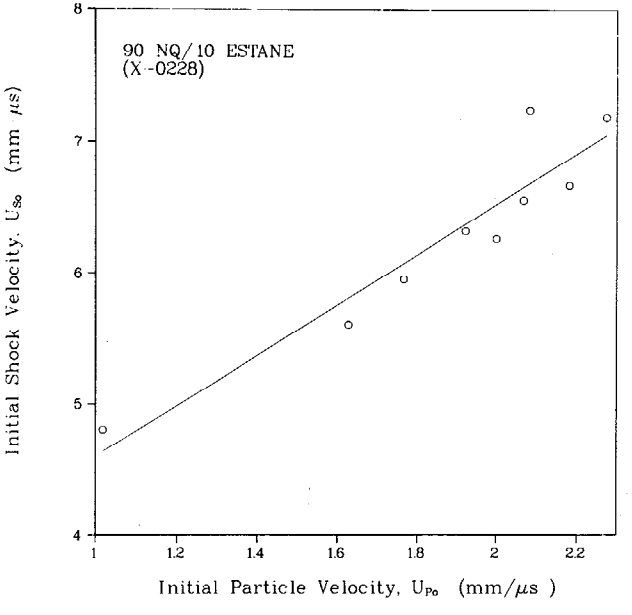

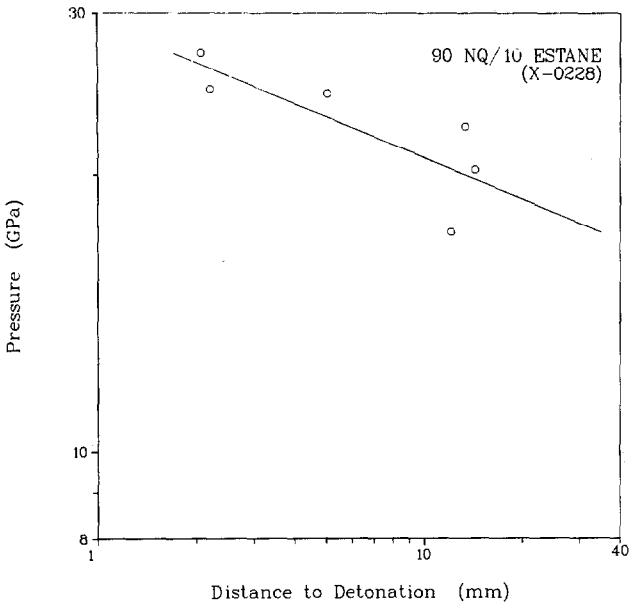
90 NQ/10 ESTANE
(X-0228)
Pressure (GPa)
30
10
8
1
10
40
Distance to Detonation (mm)

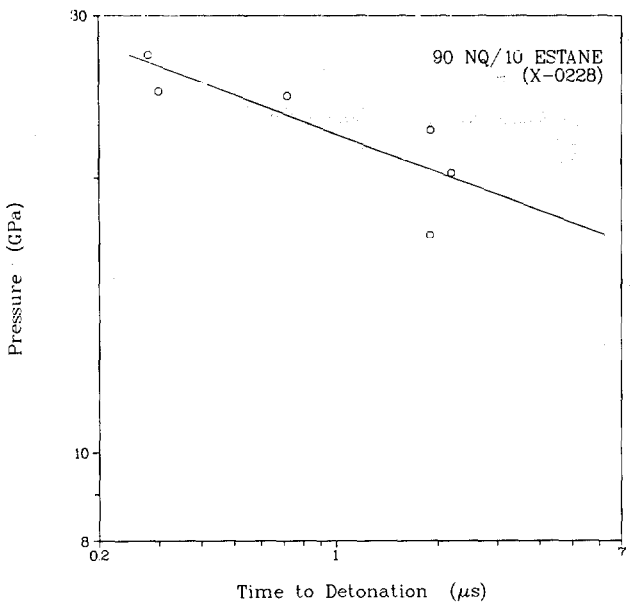
90 NQ/10 ESTANE
(X-0228)
Pressure (GPa)
30
10
8
0.2
1
7
Time to Detonation (μs)

Table 4.25 XTX-8003 (EXTEX)

Composition

80 wt% PETN, 20 wt% Sylgard silicone rubber

Theoretical Maximum Density

1.556 g/cm^3

Particle Size Distribution

Prepared with irregular 10- to 30-μm PETN crystals.

Preparation Method

Pellets were made by extruding the explosive into evacuated forms, and wedges were cut with a razor blade.

Data Summary

ρ_0 = 1.53 g/cm^3. Technique 5

Initial Shock Parameters			Coordinates for High-Order Detonation		Driving System[a]	
P_0 (GPa)	U_{p0} (mm/μs)	U_{s0} (mm/μs)	x* (mm)	t* (μs)	No. of Elements	Attenuator System
2.3	0.48	3.11	>6.2	---	3	Brass, methylene iodide
2.5	0.50	3.30	6.84	2.06	4	Brass, mixture 2
2.9	0.58	3.28	5.21	1.52	4	Dural, carbon tetrachloride
3.2	0.58	3.65	4.40	1.31	3	Dural, carbon tetrachloride
3.4	---	---	4.15	1.14	4	Dural, carbon tetrachloride
4.2	0.73	3.81	1.87	0.58	3	Dural, methylene iodide
5.1	0.78	4.25	1.33	0.31	2	Zinc, PMMA
8.2	---	---	0.31	0.06	2	Magnesium, PMMA

[a]Booster system was a P-80 plane-wave lens and 5 cm of Baratol. In three- and four-element attenuators, the third layer was brass and the fourth was PMMA. Mixture 2 consisted of equal volumes of methylene iodide and tetrabromoethane.

Reduced Data

$U_{s0} = (1.59 \pm 0.39) + (3.24 \pm 0.63)U_{p0}$.

For $2.5 < P < 8.2$,

$\log P = (0.74 \pm 0.01) - (0.37 \pm 0.02) \log x^*$, and

$\log P = (0.53 \pm 0.008) - (0.33 \pm 0.02) \log t^*$.

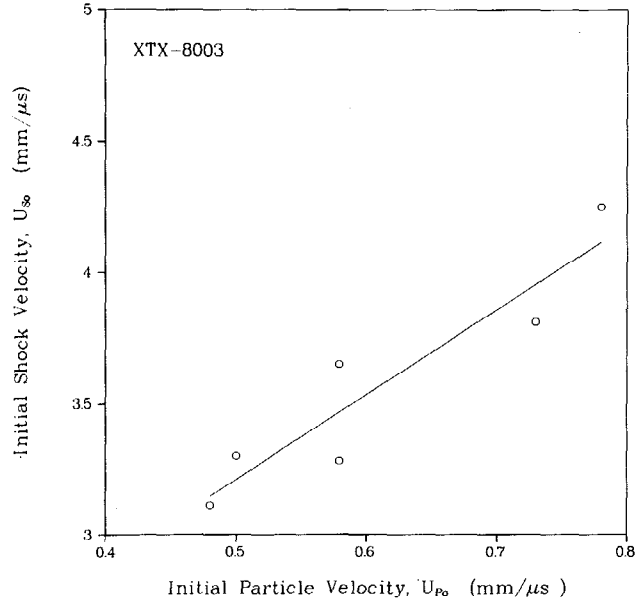

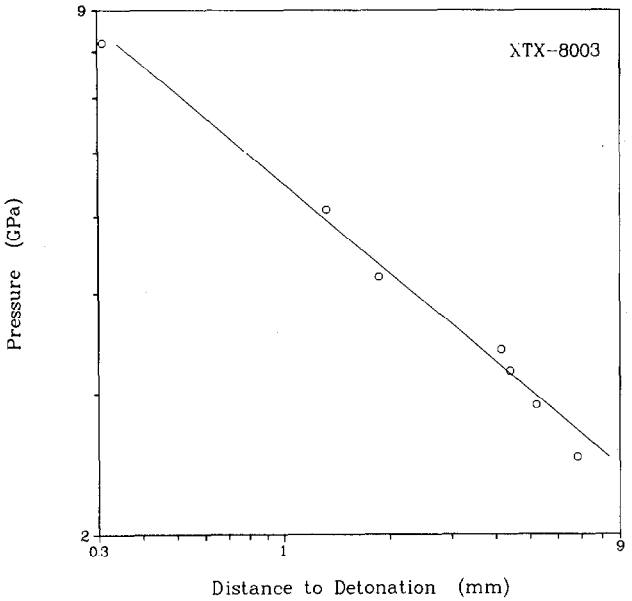
XTX-8003
Pressure (GPa)
9
2
0.3
1
9
Distance to Detonation (mm)

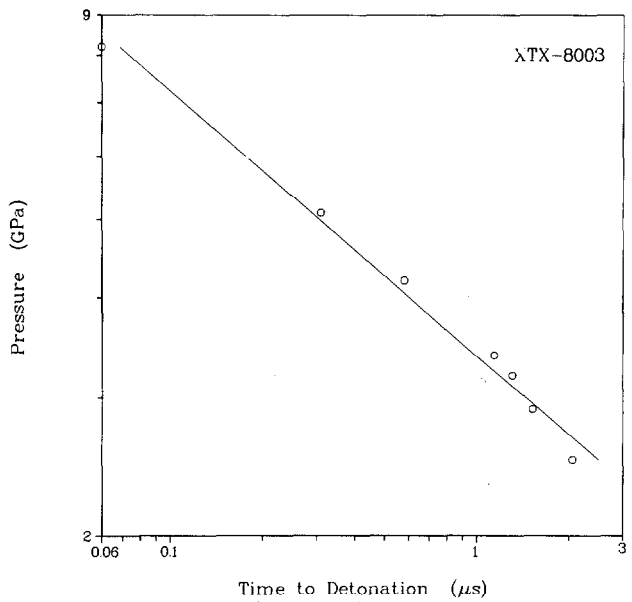
XTX-8003
Pressure (GPa)
9
2
0.06
0.1
1
3
Time to Detonation (μs)

Table 4.26 RDX/2.5 WAX/2.5 ELVAX

Composition
95 wt% RDX, 2.5 wt% wax, 2.5 wt% Elvax
Theoretical Maximum Density
1.726 g/cm^3
Particle Size Distribution
98% 62 to 350 μm
Preparation Method
Slurry mixing, pressing, and machining to shape
Data Summary
ρ_0 = 1.711. $T_0 \approx 23°C$. Technique 4

Shot Number	Initial Shock Parameters			Coordinates for High-Order Detonation		t*	Driving System Thickness
	P_0 (GPa)	U_{p0} (mm/μs)	U_{s0} (mm/μs)	1/2 b (mm/μs^2)	x* (mm)	(μs)	(mm)
E-3239	2.96	0.473	3.662	0.014	21.5	5.56	B, 11.43 SS, 12.7 Plex
E-3234	7.00	0.899	4.599	0.167	5.18	1.06	B, 25.4 Plex
E-3249	11.64	1.371	4.963	0.137	3.71	0.72	C-1, 12.7 Plex

Reduced Data
$U_{s0} = (3.094 \pm 0.405) + (1.437 \pm 0.411)U_{p0}$.
$2.96 < P < 11.71$.
$\log P = (1.43 \pm 0.14) - (0.73 \pm 0.15) \log x^*$, and
$\log P = (0.93 \pm 0.06) - (0.63 \pm 0.13) \log t^*$.

Table 4.27 PBX 9407

Compositon

94 wt% RDX, 6 wt% Exon

Theoretical Maximum Density

1.81 g/cm³

Particle Size Distribution

Roughly spherical RDX particles, 10-50 μm in diameter

Preparation Method

RDX fines were coated with Exon and cold pressed to the 1.6-g/cm³ specimen density. Wedges were machined.

Data Summary

ρ_0 = 1.60 g/cm³. Technique 5

Initial Shock Parameters			Coordinates for High-Order Detonation		Driving[a] System Thickness (mm)
P_0 (GPa)	U_{p0} (mm/μs)	U_{s0} (mm/μs)	x* (mm)	t* (μs)	
1.14	0.349	2.033	15.519	7.022	16 brass, 16 water
1.18	0.359	2.046	11.091	4.8473	16 brass, 16 water
1.37	0.406	2.110	6.873	2.8099	12 brass, 12 diethanolamine
1.47	0.426	2.152	5.634	2.2283	12 brass, 12 β β'-dichlorethyl ether
1.50	0.433	2.171	5.216	2.0305	12 brass, 12 trichlorethylene
1.80	0.487	2.310	3.346	1.1964	12 brass, 12 aqueous solution
2.21	0.558	2.475	2.278	0.7480	12 brass, 12 organic mixture
2.44	0.597	2.557	1.943	0.6148	12 brass, 12 methylene iodide
3.49	0.783	2.783	1.334	0.3858	12 Dural, 12 carbon tetrachloride

4.17	0.860	3.032	0.943	0.2508	12 Dural, twelve 1,1,2,2-tetrabromoethane
4.69	0.928	3.163	0.801	0.2047	12 brass

[a] Explosives for all experiments were a 30-cm-diam plane-wave lens and 10 cm of Baratol. All except the highest pressure shot used three-layer attenuator systems. The final attenuator element was a 12-mm-thick brass layer in all cases.

Reduced Data

Buildup function coefficients

$A_1 = 1.404$, $A_2 = 4.713$, $A_3 = 0.398$, and $A_4 = 0.011$.

$U_{s0} = 1.328 + 1.993\ U_{p0}$.

For $1.4 < P < 4.69$,

$\log P = (0.57 \pm 0.02) - (0.49 \pm 0.03) \log x^*$, and

$\log P = (0.33 \pm 0.13) - (0.41 \pm 0.03) \log t^*$.

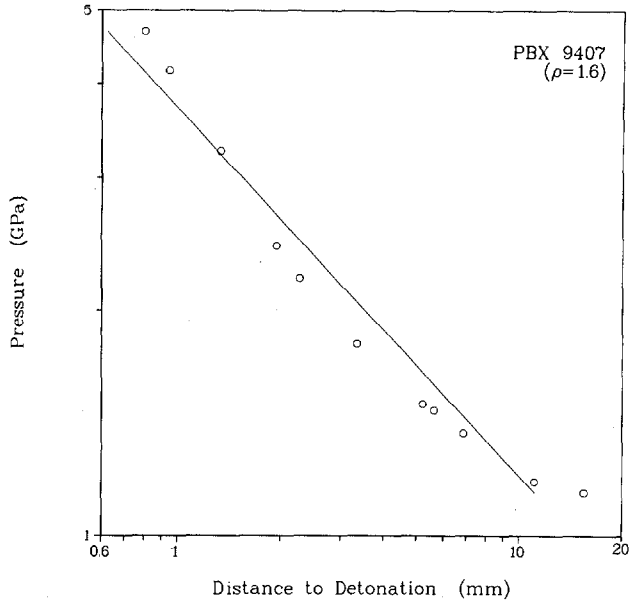
PBX 9407
(ρ=1.6)
Pressure (GPa)
5
1
0.6
1
10
20
Distance to Detonation (mm)

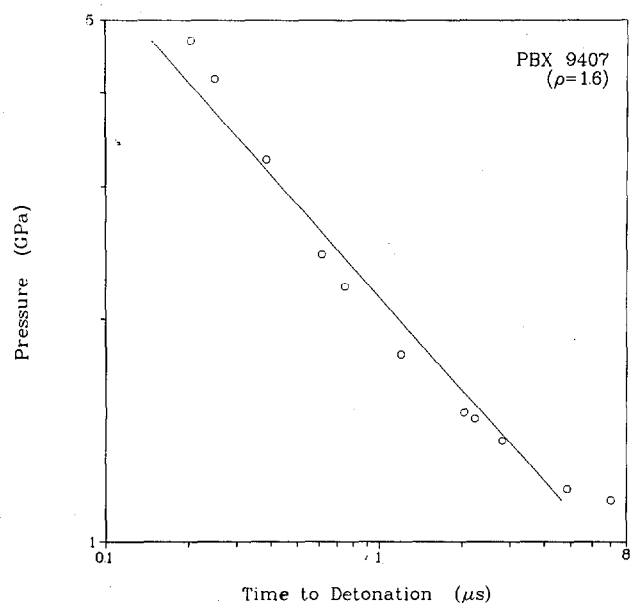
PBX 9407
(ρ=1.6)
Pressure (GPa)
5
1
0.1
1
8
Time to Detonation (μs)

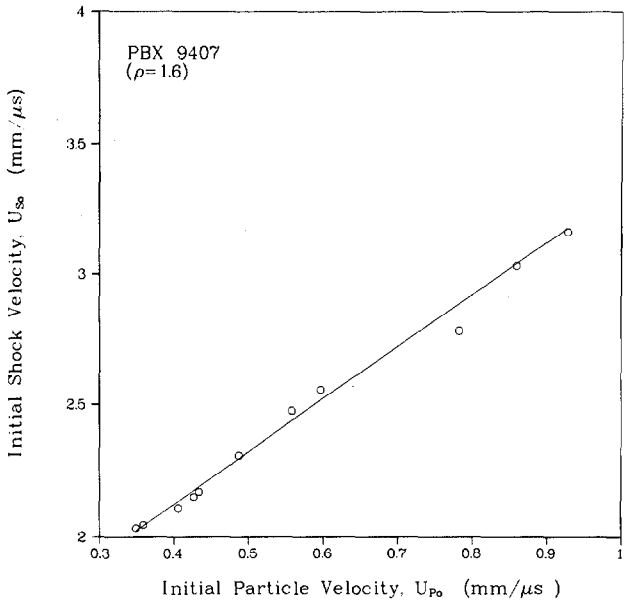
PBX 9407
(ρ=1.6)
Initial Shock Velocity, U_{So} (mm/μs)
Initial Particle Velocity, U_{Po} (mm/μs)
4
3.5
3
2.5
2
0.3
0.4
0.5
0.6
0.7
0.8
0.9
1

Table 4.28 PBX 9405

Composition

93.7 wt% RDX, 3.15 wt% nitrocellulose, 3.15 wt% chloroethylphosphate

Theoretical Maximum Density

1.789 g/cm^3

Particle Size Distribution

RDX: 25%, less than 44 μm (average 25 μm);
75%, of which 98% pass through USS-50 sieves, 90% pass through USS-100 sieves, and 46% pass through USS-200 sieves.

Preparation Method

Slurry mixing, steel die pressing, and machining to shape

Data Summary

ρ_0 = 1.761 g/cm^3. $T_0 \approx 23°C$. Technique 4

Shot Number	Initial Shock Parameters			1/2 b	Coordinates for High-Order Detonation		Driving System Thickness
	P_0 (GPa)	U_{p0} (mm/μs)	U_{s0} (mm/μs)	(mm/μs^2)	x* (mm)	t* (μs)	(mm)
E-3709	0.5	0.087	3.276	−0.010	≫25.5	≫7.95	A, 11.4 SS, 10.9 Acrylite
E-3700	2.19	0.394	3.152	+0.028	13.09	3.99	B, 17.8 foam, 11.4 SS, 10.9 Acrylite
E-3708	2.27	0.404	3.195	+0.040	12.74	3.78	B, 17.8 foam, 11.4 SS, 10.9 Acrylite
E-3704	2.84	0.496	3.255	+0.119	10.23	2.81	B, 17.8 Polyethylene, 11.4 SS, 10.9 Acrylite
E-3723	2.92	0.488	3.400	+0.027	11.15	2.13	A, (0.4 g/cm^3) 10.9 Acrylite

E-3706	3.59	0.567	3.594	+0.032	8.78	2.27	B, 24.9 SS, 15.0 Plex
E-3724	4.93	0.730	3.841	+0.138	5.01	1.17	H, 24.1 SS, 10.9 Acrylite
E-3718	6.81	0.932	4.152	+0.675	2.72	0.58	B, 49.4 Plex

Reduced Data (without Shot E-3709)

$U_{s0} = (2.433 \pm 0.092) + (1.88 \pm 0.153)\ U_{p0}$.

For $2.19 < P < 6.81$.

$\log P = (1.16 \pm 0.06) - (0.70 \pm 0.06) \log x^*$, and

$\log P = (0.71 \pm 0.02) - (0.59 \pm 0.05) \log t^*$.

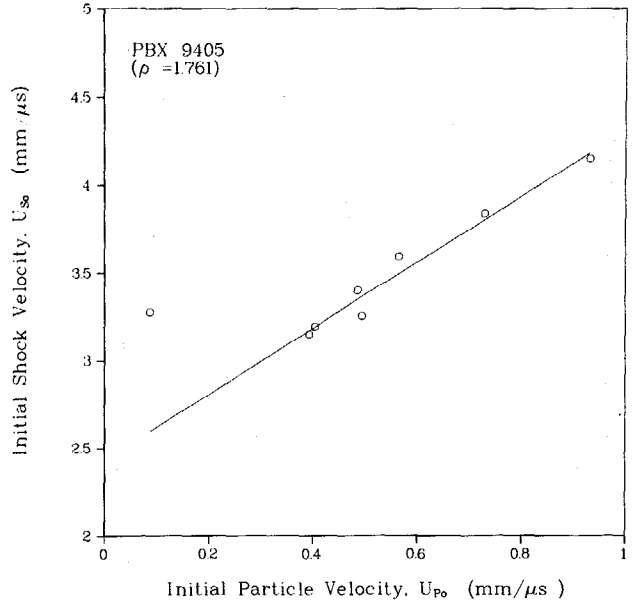

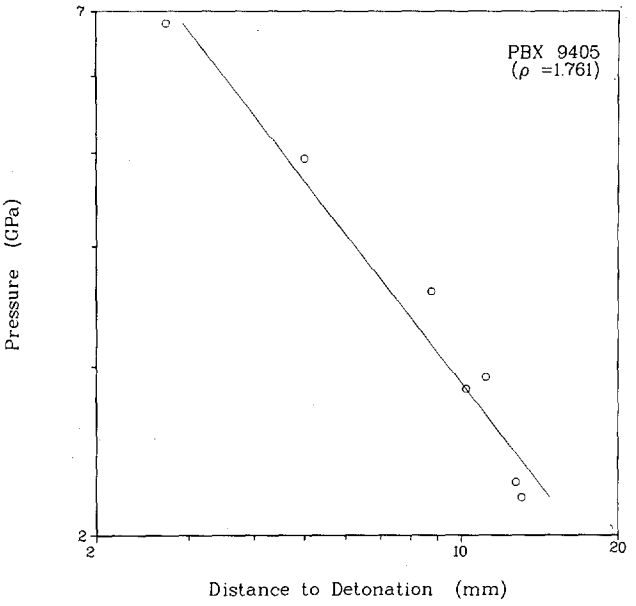
PBX 9405
(ρ =1.761)
Pressure (GPa)
7
2
2
10
20
Distance to Detonation (mm)

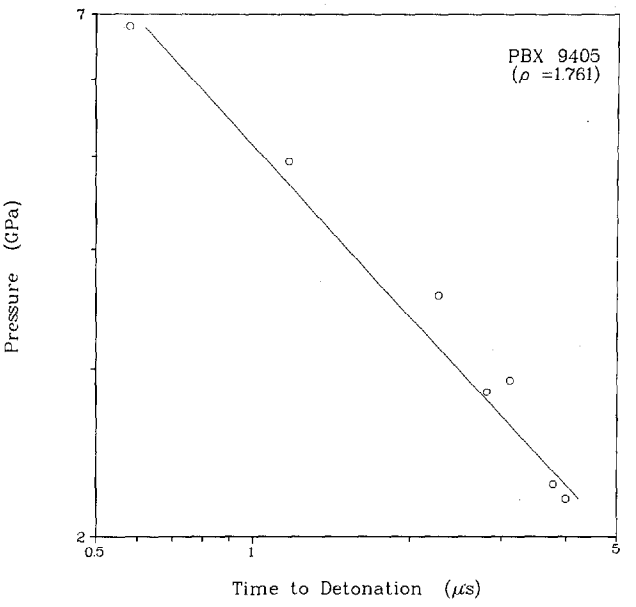
PBX 9405
(ρ =1.761)
Pressure (GPa)
7
2
0.5
1
5
Time to Detonation (μs)

Table 4.29 X-0224

Composition

74 wt% RDX, 20 wt% aluminum, 5.4 wt% Elvax, 0.6 wt% wax

Theoretical Maximum Density

1.818 g/cm³

Particle Size Distribution

Mean aluminum particle size ~30 μm; 96.1 wt% passed through 90-μm screen; 33 wt% passed through 20-μm screen

Preparation Method

Slurry mixing, pressing, and machining to shape

Data Summary

ρ_0 = 1.812 g/cm³. $T_0 \approx 23°C$. Technique 4

Shot Number	Initial Shock Parameters			1/2 b	Coordinates for High-Order Detonation		Driving System Thickness
	P_0 (GPa)	U_{p0} (mm/μs)	U_{s0} (mm/μs)	(mm/μs²)	x* (mm)	t* (μs)	(mm)
E-3570	7.25	0.997	4.016	0.910	3.242	0.676	B, 23.62 Plex
E-3573	3.71	0.565	3.627	0.093	11.150	2.799	B, 25.4 brass, 17.78 Plex
E-3574	2.41	0.394	3.377	0.018	>25.52	>7.20	B, 17.78 foam, 11.43 SS, 10.92 Plex
E-3580	3.02	0.468	3.564	0.010	19.262	5.139	B, 17.78 Polyethylene, 11.43 SS, 10.82 Plex
E-3608	~8.0	~1.05	~4.2	---	1.923	0.344	A, (1.0 g/cm³) 0.729 Plex

Reduced Data

$U_{s0} = (2.999 \pm 0.083) + (1.091 \pm 0.111)U_{p0}$.

For $2.41 < P < 8.0$,

$\log P = (1.05 \pm 0.03) - (0.45 \pm 0.04) \log x^*$, and

$\log P = (0.75 \pm 0.02) - (0.38 \pm 0.04) \log t^*$.

Table 4.30 X-0250-40-19

Composition
40.2 wt% RDX, 40.4 wt% cyanuric acid, 19.4 wt% Sylgard

Theoretical Maximum Density
1.573 g/cm³

Particle Size Distribution
Avg. 25 μm, all less than 44 μm

Material Preparation
Extrusion

Data Summary
ρ_0 = 1.45 g/cm³. $T_0 \approx 23°C$. Technique 4
D = 5.37 mm/μs

Shot Number	ρ_0 (g/cm³)	Initial Shock Parameters P_0 (GPa)	U_{p0} (mm/μs)	U_{s0} (mm/μs)	1/2 b (mm/μs²)	Coordinates for High-Order Detonation x* (mm)	t* (μs)	Driving System System Thickness (mm)
E-3548	1.433	6.48	1.228	3.682	0.538	2.73	0.66	B, 24.38 PMMA
E-3560	1.442	3.06	0.710	2.990	0.066	18.36	5.20	B, 24.13 SS, 13.208 Plex
E-3576	1.453	2.82	0.711	2.731	0.062	18.43	5.83	B, 24.13 SS, 17.78 Plex
E-3566	1.447	5.08	1.126	3.117	0.403	~2.85	~0.82	B, 48.514 Plex
				Multiple Shock				
E-3553	1.473	2.18	0.592	2.502	0.040	>24.25	8.39	B, 0.7 polyethylene, 0.45 SS, 0.45 Acrylite

Reduced Data
Single shock
$U_{s0} = (1.944 \pm 0.528) + (1.257 \pm 0.543)U_{p0}$.
For $2.82 < P < 6.48$,
$\log P = (0.92 \pm 0.06) - (0.36 \pm 0.06) \log x^*$, and
$\log P = (0.72 \pm 0.02) - (0.34 \pm 0.04) \log t^*$.

Table 4.31 PBX 9502 (X-0290)

Composition
95 wt% TATB, 5 wt% Kel-F 800
Theoretical Maximum Density
1.942 g/cm³
Particle Size Distribution
Pantex standard
Preparation Method
Slurry mixing, pressing, and machining to shape
Data Summary
ρ_0 = 1.896 g/cm³. Technique 4

Shot Number	Initial Shock Parameters			1/2 b	Coordinates for High-Order Detonation		Driving System Thickness
	P_0 (GPa)	U_{p0} (mm/μs)	U_{s0} (mm/μs)	(mm/μs²)	x* (mm)	t* (μs)	(mm)
E-4122	10.05	1.083	4.894	0.101	15.38	2.893	G, 38.07 Plex
E-4106	11.76	1.148	5.401	0.034	12.78	2.243	G, 24.16 Plex
E-4121	14.31	1.349	5.595	0.278	5.88	0.994	H, 19.34 Plex
E-4105	14.96	1.421	5.552	0.697	4.64	0.756	H, 12.69 Plex

Reduced Data
$U_{s0} = (3.263 \pm 0.977) + (1.678 \pm 0.777)U_{p0}$.
For $10.05 < P < 14.95$,
$\log P = (1.39 \pm 0.05) - (0.31 \pm 0.05) \log x^*$, and
$\log P = (1.15 \pm 0.01) - (0.28 \pm 0.04) \log t^*$.

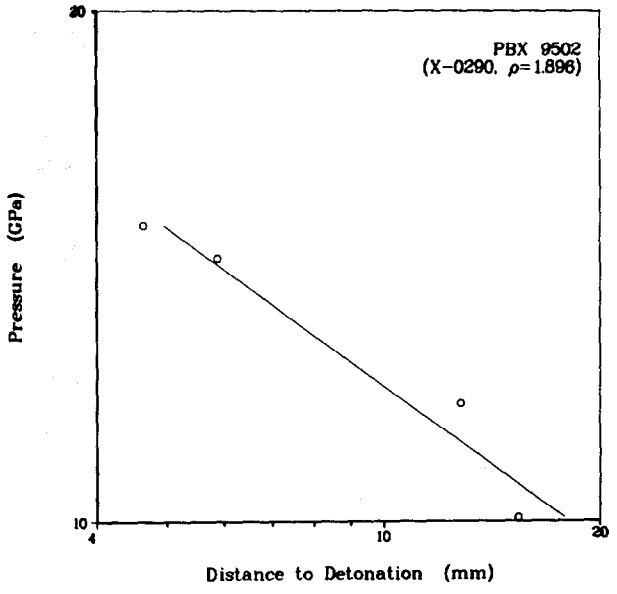
PBX 9502
(X-0290, ρ=1.896)
Pressure (GPa)
20
10
4
10
20
Distance to Detonation (mm)

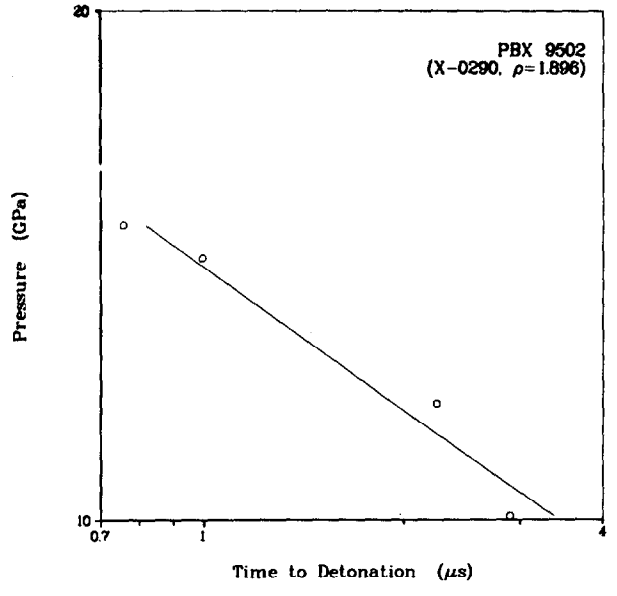
PBX 9502
(X-0290, ρ=1.896)
Pressure (GPa)
20
10
0.7
1
4
Time to Detonation (μs)

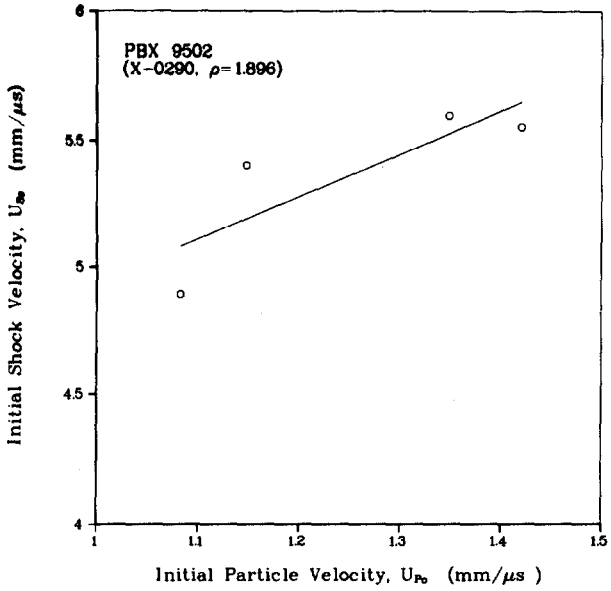
PBX 9502
(X-0290, ρ=1.896)
Initial Shock Velocity, U_{s_0} (mm/μs)
Initial Particle Velocity, U_{P_0} (mm/μs)
6
5.5
5
4.5
4
1
1.1
1.2
1.3
1.4
1.5

Table 4.32 95 TATB/2.5 Kel-F 800/2.5 Kel-F 827

Composition
95 wt% TATB, 2.5 wt% Kel-F 800, 2.5 wt% Kel-F 827
Theoretical Maximum Density
1.941 g/cm³
Particle Size Distribution
Standard
Preparation Method
Hot pressing and machining to shape
Data Summary
ρ_0 = 1.883 g/cm³. $T_0 \approx$ 23°C. Technique 3

Shot Number	Initial Shock Parameters			Coordinates for High-Order Detonation		Driving System Thickness (mm)
	P_0 (GPa)	U_{p0} (mm/μs)	U_{s0} (mmμs)	x* (mm)	t* (μs)	
E-2897	8.77	1.030	4.524	>19.06	>3.95	B, 12.3 PMMA
E-2815	13.70	1.339	5.434	6.05	1.05	H, 23.7 Plex
E-2813	15.64	1.462	5.683	3.86	0.63	H, 12.9 Plex
E-2814	17.50	1.545	6.014	3.10	0.49	H, 6.05 Plex

Reduced Data
$U_{s0} = (1.620 \pm 0.195) + (2.823 \pm 0.144)U_{p0}$.
For $13.7 < P < 17.49$,
$\log P = (1.41 \pm 0.03) - (0.35 \pm 0.05) \log x^*$, and
$\log P = (1.14 \pm 0.01) - (0.31 \pm 0.05) \log t^*$.

Table 4.33 94 TATB (COARSE)/6 ESTANE

Composition
94 wt% TATB (coarse), 6 wt% Estane
Theoretical Maximum Density
1.868 g/cm³
Particle Size Distribution
Coarse, 65-μm median particle diameter
Preparation Method
Hot pressing and machining to shape
Data Summary
ρ_0 = 1.846 g/cm³. $T_0 \approx 23°C$. Technique 3

Shot Number	Initial Shock Parameters			Coordinates for High-Order Detonation		Driving System Thickness (mm)
	P_0 (GPa)	U_{p0} (mm/μs)	U_{s0} (mm/μs)	x* (mm)	t* (μs)	
E-2891	15.33	1.506	5.515	13.82	2.33	H, 11.8 Plex
E-2912	17.94	1.652	5.882	8.15	1.31	J, 11.8 PMMA
E-2893	25.86	2.040	6.867	1.93	0.28	N, 6.3 Plex

Reduced Data
$U_{s0} = (1.699 \pm 0.009) + (2.533 \pm 0.005)U_{p0}$.
$\log P = (1.49 \pm 0.01) - (0.27 \pm 0.01) \log x^*$.
$\log P = (1.28 \pm 0.003) - (0.25 \pm 0.01) \log t^*$.

Table 4.34 94 TATB (BIMODAL)/6 ESTANE

Composition
94 wt% TATB (bimodal), 6 wt% Estane
Theoretical Maximum Density
1.869 g/cm^3
Particle Size Distribution
Bimodal
Preparation Method
Hot pressing and machining to shape
Data Summary
ρ_0 = 1.833 g/cm^3. $T_0 \approx 23°C$. Technique 3

Shot Number	Initial Shock Parameters			Coordinates for High-Order Detonation		Driving System Thickness (mm)
	P_0 (GPa)	U_{p0} (mm/μs)	U_{s0} (mm/μs)	x* (mm)	t* (μs)	
E-2915	12.00	1.299	5.040	17.14	3.04	G, 12.2 PMMA
E-2889	13.40	1.350	5.414	10.16	1.70	H, 11.9 Plex
E-2913	17.82	1.677	5.796	5.25	0.84	J, 12.1 PMMA
E-2890	25.72	2.139	6.560	1.46	0.21	N, 6.1 Plex

Reduced Data
$U_{s0} = (3.032 \pm 0.358) + (1.652 \pm 0.217)U_{p0}$.
$\log P = (1.47 \pm 0.02) - (0.32 \pm 0.02) \log x^*$.
$\log P = (1.21 \pm 0.81) - (0.29 \pm 0.02) \log t^*$.

Table 4.35 94 TATB/3 ELVAX/3 WAX

Composition
94 wt% TATB, 3 wt% Elvax, 3 wt% wax
Theoretical Maximum Density
1.822 g/cm^3
Particle Size Distribution
Standard
Preparation Method
Hot pressing and machining to shape
Data Summary
ρ_0 = 1.802 g/cm^3. $T_0 \approx 23°C$. Technique 3

Shot Number	Initial Shock Parameters P_0 (GPa)	U_{p0} (mm/μs)	U_{s0} (mm/μs)	Coordinates for High-Order Detonation x* (mm)	t* (μs)	Driving System Thickness (mm)
E-2899	14.98	1.482	5.610	>19.09	>3.312	H, 13.4 PMMA
E-2904	17.13	1.660	5.725	17.59	2.951	J, 13.2 PMMA
E-2905	21.22	1.847	6.375	5.32	0.80	G, 6.3 Plex
E-2898	26.17	2.105	6.908	1.92	0.28	N, 6.1 Plex

Reduced Data
$U_{s0} = (2.215 \pm 0.585) + (2.221 \pm 0.327)U_{p0}$.
$\log P = (1.47 \pm 0.01) - (0.19 \pm 0.01) \log x^*$.
$\log P = (1.32 \pm 0.004) - (0.18 \pm 0.01) \log t^*$.

Table 4.36 94 TATB/4.5 PS/1.5 DOP

Composition
94 wt% TATB, 4.5 wt% polystyrene, 1.5 wt% dioctylphthalate (DOP)
Theoretical Maximum Density
1.841 g/cm^3
Particle Size Distribution
Standard
Preparation Method
Hot pressing and machining to shape
Data Summary
$T_0 \approx 23°C$. Technique 3

Shot Number	Initial Shock Parameters			Coordinates for High-Order Detonation		Driving System Thickness (mm)
	P_0 (GPa)	U_{p0} (mm/μs)	U_{s0} (mm/μs)	x* (mm)	t* (μs)	
			ρ_0 = 1.817 g/cm^3			
E-2906	12.88	1.403	5.054	16.84	2.97	F, 12.3 Plex
E-2851	15.24	1.523	5.508	9.06	1.49	H, 6.2 Plex
E-2914	17.40	1.674	5.719	7.22	1.15	J, 12.1 PMMA
E-2887	25.62	2.083	6.768	1.60	0.22	N, 6.0 Plex
			ρ_0 = 1.825 g/cm^3			
E-2903	15.32	1.526	5.498	14.43	2.45	H, 12.2 Plex
E-2850	17.01	1.642	5.675	10.72	1.77	H, 6.1 Plex
E-2888	25.86	2.080	6.813	1.78	0.23	N, 6.0 Plex

Reduced Data
$U_{s0} = (1.69 \pm 0.185) + (2.448 \pm 0.107)U_{p0}$.
$\log P = (1.47 \pm 0.03) - (0.27 \pm 0.03) \log x^*$.
$\log P = (1.25 \pm 0.01) - (0.24 \pm 0.02) \log t^*$.

Table 4.37 92 TATB/6 PS/2 DOP

Composition
92 wt% TATB, 6 wt% polystyrene, 2 wt% dioctylphthalate
Theoretical Maximum Density
1.811 g/cm^3
Particle Size Distribution
Standard
Preparation Method
Hot pressing and maching to shape
Data Summary
ρ_0 = 1.797 g/cm^3. $T_0 \approx 23°C$. Technique 3

Shot Number	Initial Shock Parameters			Coordinates for High-Order Detonation		Driving System Thickness (mm)
	P_0 (GPa)	U_{p0} (mm/μs)	U_{s0} (mm/μs)	x* (mm)	t* (μs)	
E-2920	13.35	1.420	5.231	>25.46	>4.64	G, 11.8 PMMA
E-2945	13.75	1.452	5.270	19.25	3.38	H, 18.1 PMMA
E-2924	15.25	1.529	5.549	14.37	2.44	H, 12.0 PMMA
E-2917	17.93	1.693	5.895	7.98	1.29	L, 24.8 Plex

Reduced Data
$U_{s0} = (1.676 \pm 0.325) + (2.501 \pm 0.213)U_{p0}$.

Table 4.38 90 TATB/10 ESTANE

Composition
90 wt% TATB, 10 wt% Estane
Theoretical Maximum Density
1.827 g/cm^3
Particle Size Distribution
Standard
Preparation Method
Hot pressing and machining to shape
Data Summary
ρ_0 = 1.805 g/cm^3. $T_0 \approx 23°C$. Technique 3

Shot Number	Initial Shock Parameters			Coordinates for High-Order Detonation		Driving System Thickness (mm)
	P_0 (GPa)	U_{p0} (mm/μs)	U_{s0} (mm/μs)	x* (mm)	t* (μs)	
E-2911	17.04	1.646	5.734	14.37	2.40	J, 13.1 PMMA
E-2908	24.48	2.049	6.620	1.83	0.27	N, 6.5 Plex

Table 4.39 X-0219

Composition
90 wt% TATB, 10 wt% Kel-F 800
Theoretical Maximum Density
1.943 g/cm³
Particle Size Distribution
See table captions below
Preparation Method
Hot pressing and machining to shape
Data Summary
$T_0 \approx 23°C$. Technique 3

Shot Number	Initial Shock Parameters				Coordinates for High-Order Detonation		Driving System Thickness (mm)
	P_0 (GPa)	U_{p0} (mm/μs)	U_{s0} (mm/μs)	1/2 b (mm/μs²)	x* (mm)	t* (μs)	
	ρ_0 = 1.896 g/cm³, Pantex standard						
E-4122	10.05	1.083	4.894	0.101	15.38	2.89	G, 38.07 Plex
E-4106	11.76	1.148	5.401	0.034	12.78	2.24	G, 24.16 Plex
E-4121	14.31	1.349	5.595	0.278	5.88	0.99	H, 19.34 Plex
E-4105	14.96	1.421	5.552	0.697	4.64	0.76	H, 12.69 Plex
	ρ_0 = 1.898 g/cm³, Pantex standard						
E-4073	7.80	0.942	4.363	0.063	>25.5	>5.32	C, 23.97 Plex
E-4068	9.80	1.125	4.590	0.163	18.50	3.53	G, 38.61 Plex
E-4047	11.40	1.218	4.931	0.225	11.72	2.12	G, 22.61 Plex
E-4069	14.40	1.369	5.543	0.325	6.20	1.04	H, 18.59 Plex
E-4048	15.15	1.458	5.473	0.429	5.21	0.87	H, 11.45 Plex

Table 4.39 (continued)

Shot Number	Initial Shock Parameters			1/2 b	Coordinates for High-Order Detonation		Driving System Thickness
	P_0 (GPa)	U_{po} (mm/μs)	U_{so} (mm/μs)	(mm/μs^2)	x* (mm)	t* (μs)	(mm)
			ρ_0 = 1.898 g/cm^3, Pantex fine				
E-4068	9.80	1.125	4.590	0.163	18.49	3.53	G, 38.61 Plex
			ρ_0 = 1.905 g/cm^3, Pantex fine				
E-4043	9.68	1.110	4.579	0.148	19.22	3.69	G, 38.65 Plex
E-4027	11.21	1.213	4.850	0.316	12.11	2.18	H, 37.80 Plex
E-4024	13.95	1.395	5.250	0.374	7.36	1.27	H, 17.55 Plex
E-4023	15.69	1.447	5.692	0.460	5.69	0.93	H, 11.23 Plex
			ρ_0 = 1.912 g/cm^3, reprocessed				
E-4044	9.71	1.074	4.728	0.056	22.62	4.43	G, 38.66 Plex
E-4025	11.62	1.239	4.905	0.178	14.31	2.63	H, 36.79 Plex
E-4019	13.80	1.449	4.982	0.636	6.54	1.15	H, 18.39 Plex
E-4018	15.30	1.522	5.259	0.872	4.68	0.79	H, 11.81 Plex
			ρ_0 = 1.914 g/cm^3, Pantex standard				
E-4049	9.80	1.114	4.596	0.143	19.14	3.677	G, 36.37 Plex
E-4026	11.43	1.256	4.755	0.324	12.38	2.254	H, 36.02 Plex
E-4022	14.21	1.390	5.340	0.329	7.80	1.337	H, 18.14 Plex
E-4020	15.77	1.455	5.664	0.301	5.70	0.945	H, 11.43 Plex

			ρ_0 = 1.920 g/cm³, standard				
E-2896	13.07	1.360	5.005	---	16.48	2.92	H, 25.4 Plex
E-2849	15.80	1.545	5.328	---	9.99	1.71	H, 7.4 Plex
E-2863	16.58	1.582	5.460	---	9.42	1.55	G, 6.3 Plex
E-2845	18.72	1.776	5.491	---	5.47	0.92	H, 6.0 Plex
			ρ_0 = 1.929 g/cm³, Pantex standard				
E-4091	13.50	1.302	5.375	0.070	20.17	3.545	H, 23.5 Plex
E-4088	14.20	1.388	5.302	0.175	16.10	2.763	H, 18.59 Plex
E-4089	15.35	1.470	5.413	0.186	15.13	2.543	H, 12.80 Plex
E-4090	16.10	1.532	5.448	0.442	8.374	1.358	H, 6.38 Plex

Reduced Data

$U_{s0} = (3.178 \pm 0.340) + (1.483 \pm 0.253)\ U_{p0}$.

For $9.68 < P < 18.72$,

$\log P = (1.40 \pm 0.05) - (0.28 \pm 0.05) \log x^*$, and

$\log P = (1.19 \pm 0.01) - (0.27 \pm 0.04) \log t^*$.

Table 4.40 90 TATB/5 KEL-F 800/5 KEL-F 820

Composition
90 wt% TATB, 5 wt% Kel-F 800, 5 wt% Kel-F 820
Theoretical Maximum Density
1.944 g/cm^3
Particle Size Distribution
Standard
Preparation Method
Hot pressing and machining to shape
Data Summary
ρ_0 = 1.917 g/cm^3. $T_0 \approx 23°C$. Technique 2

Shot Number	Initial Shock Parameters			Coordinates for High-Order Detonation		Driving System Thickness (mm)
	P_0 (GPa)	U_{p0} (mm/μs)	U_{s0} (mm/μs)	x* (mm)	t* (μs)	
E-2260	10.16	1.105	4.796[a]	>20.73	---	B, 5.5 Plex
E-2263	13.86	1.342	5.387[a]	>20.82	---	G, 24.5 Plex
E-2266	16.19	1.499	5.635[b]	9.60	---	H, 12.2 Plex
E-2258	18.99	1.625	6.096	3.7	---	H, 5.9 Plex

	Multiple Shock							
Shot Number	P_1 (GPa)	U_{p1} (mm/μs)	U_{s1} (mm/μs)	x_{OT} (mm)	P_2 (GPa)	U_{s2} (mm/μs)	x* (mm)	Driving System Thickness (mm)
E-2265	12.2	~1.22	5.058	6.65	~18.2	5.985	10.7[c]	P, 1.05 D-38

[a]Decelerates.
[b]Poor record.
[c]4.05 mm downstream from overtake.

Table 4.41 90 TATB/5 ELVAX/5 WAX

Composition
90 wt% TATB, 5 wt% Elvax, 5 wt% wax
Theoretical Maximum Density
1.751 g/cm^3
Particle Size Distribution
Standard
Preparation Method
Hot pressing and machining to shape
Data Summary
ρ_0 = 1.739 g/cm^3. $T_0 \approx 23°C$. Technique 3

Shot Number	Initial Shock Parameters			Coordinates for High-Order Detonation		Driving System Thickness (mm)
	P_0 (GPa)	U_{p0} (mm/μs)	U_{s0} (mm/μs)	x* (mm)	t* (μs)	
E-2918	18.32	1.672	6.302	25.52	3.73	L, 24.6 Plex
E-2931	19.85	1.834	6.224[a]	8.72	1.36	L, 18.2 PMMA
E-2928	21.38	1.909	6.441	4.73	0.73	L, 12.3 PMMA

[a]The input wave was tilted significantly in a direction that caused low initial shock velocity.

Reduced Data
Fit not made owing to nature of the data.

Table 4.42 85 TATB/15 KEL-F 800

Composition
85 wt% TATB, 15 wt% Kel-F 800
Theoretical Maximum Density
1.948 g/cm³
Particle Size Distribution
Standard
Preparation Method
Hot pressing and machining to shape
Data Summary
ρ_0 = 1.930 g/cm³. T_0 = 23°C. Technique 3

Shot Number	Initial Shock Parameters			Coordinates for High-Order Detonation		Driving System Thickness (mm)
	P_0 (GPa)	U_{p0} (mm/μs)	U_{s0} (mm/μs)	x* (mm)	t* (μs)	
E-2900	14.31	1.380	5.371	16.60	2.88	H, 18.8 PMMA
E-2848	15.60	1.476	5.477	12.35	2.12	H, 13.1 Plex
E-2852	17.14	1.575	5.638	8.72	1.46	H, 6.3 Plex
E-2846	18.68	1.684	5.749	6.73	1.11	H, 6.0 PMMA

Reduced Data
$U_{s0} = (3.603 \pm 0.125) + (1.279 \pm 0.082)U_{p0}$.

Table 4.43 85 TATB/7.5 KEL-F 800/7.5 KEL-F 827

Composition
85 wt% TATB, 7.5 wt% Kel-F 800, 7.5 wt% Kel-F 827
Theoretical Maximum Density
1.947 g/cm^3
Particle Size Distribution
Standard
Preparation Method
Hot pressing and machining to shape
Data Summary
ρ_0 = 1.912 g/cm^3. $T_0 \approx 23°C$. Technique 3

Shot Number	Initial Shock Parameters			Coordinates for High-Order Detonation		Driving System Thickness (mm)
	P_0 (GPa)	U_{p0} (mm/μs)	U_{s0} (mm/μs)	x* (mm)	t* (μs)	
E-2895	13.18	1.341	5.141	12.27	2.16	H, 23.9 Plex
E-2818[a]	~13.6	---	---	9.59	---	H, 23.7 PMMA
E-2819	14.42	1.381	5.462	7.21	1.22	H, 13.4 PMMA
E-2820	18.67	1.707	5.722	4.57	0.73	H, 6.0 PMMA

[a]Very poor record.

Reduced Data
$U_{s0} = (0.944 \pm 0.828) + (3.179 \pm 0.632)U_{p0}$.

Table 4.44 FKM CLASS VII PROPELLANT

Theoretical Maximum Density
1.814 g/cm³

Preparation Method
Vacuum casting and pressure curing

Data Summary
ρ_0 = 1.814 g/cm³. T_0 = 25°C. Technique 4

Shot Number	Initial Shock Parameters P_0 (GPa)	U_{p0} (mm/μs)	U_{s0} (mm/μs)	1/2 b (mm/μs²)	Coordinates for High-Order Detonation x* (mm)	t* (μs)	Driving System Thickness (mm)	Comments
E-4289	1.30	0.263	2.726	+0.0003	≫ 25.4	---	C, 24.4 brass, 24.6 Plex, 11.8 brass, 14.9 Plex	
E-4276	2.29	0.427	2.956	+0.003	>25.4	---	B, 17.8 foam, 11.4 SS, 10.9 Plex	Almost transited to high order within 25.4-mm-thick sample
E-4279	3.30	0.568	3.205	+0.061	14.74	4.13	B, 25.4 SS, 15.0 Plex	
E-4277	2.86	0.484	3.256	+0.001	---	---	B, 17.7 PC, 11.4 SS, 10.9 Plex	Second shock overtook shock wave thereby invalidating measurement
E-4287	3.57	0.586	3.355	+0.050	12.85	3.53	B, 25.4 brass, 17.8 Plex	
E-4285	3.30	0.535	3.398	−0.003	19.29	5.16	B, 25.4 SS, 25.2 Plex	Nonsimultaneous arrival caused larger than usual errors
E-4286	4.79	0.689	3.831	+0.009	6.16	1.52	J, 20.4 SS, 12.7 Plex	

E-4291	6.73	0.902	4.111	+0.095	3.51	0.81	B, 48.2 Plex	No decomposition signal observed, miniwedge
E-4280	---	---	---	---	≈3.8	≈0.8	B, 49.1 Plex	x* too short for accurate measurement of parameters with standard wedge

Reduced Data

$U_{s0} = (2.079 + 0.146) + 2.292 \pm 0.249)U_{p0}$

$\log P = 1.06 - 0.47 \log x^*.$

Table 4.45 SPIS-44 CLASS II PROPELLANT

Composition

49 wt% AP, 20 wt% HMX, 21 wt% Al, 7.27 wt% R45M, 2 wt% INDOPOL, 0.51 wt% IPDI, 0.15 wt% Tepanol, 0.07 wt% CAO-14

Theoretical Maximum Density

1.831 g/cm^3

Particle Size Distribution

9-μm HMX, 200-μm AP (28%), 6-μm AP (21%), 6-μm Al

Preparation Method

Casting, curing, and machining to shape

Data Summary

ρ_0 = 1.830 g/cm^3. T_0 = 24°C. Technique 7

Shot Number	Initial Shock Parameters			Coordinates for High-Order Detonation		Driving System Thickness (mm)
	P_0 (GPa)	U_{p0} (mm/μs)	U_{s0} (mm/μs)	x* (mm)	t* (μs)	
E-4527	3.63	0.536	3.70	[a]	---	C, 24.1 SS, 18.3 Plex
E-4554	7.05	0.864	4.46	[a]	---	L, 24.1 SS, 10.9 Plex
E-4563	22.3	1.92	6.36	[a]	---	L, 17.8 Plex
E-4561	25.7	2.11	6.65	[a]	---	S, 10.9 Plex

[a]No transition to detonation was observed within 25.4 mm, but a violent reaction trailed the shock wave at a time that depended on the shock pressure.

Reduced Data

$U_{s0} = (2.774 \pm 0.093) + (1.855 \pm 0.062)U_{p0}$.

Table 4.46 SPIS-45 CLASS II PROPELLANT

Composition
72.7 wt% R45M, 0.07 wt% CAO-14, 2.00 wt% INDOPOL, 0.15 wt% Tepanol, 0.51 wt% IPDI, 21 wt% Al, 12 wt% HMX, 57 wt% AP

Theoretical Maximum Density
1.832 g/cm³

Particle Size Distribution
9-μm HMX, 200-μm AP (36%), 6-μm AP (21%), 6-μm Al

Preparation Method
Casting and curing

Data Summary
ρ_0 = 1.831 g/cm³. $T_0 \approx 24°C$. Technique 7

Shot Number	Initial Shock Parameters			Coordinates for High-Order Detonation		Driving System Thickness (mm)
	P_0 (GPa)	U_{p0} (mm/μs)	U_{s0} (mm/μs)	x* (mm)	t* (μs)	
E-4553	5.47	0.723	4.13	[a]	---	H, 19.0 SS, 10.9 Plex
E-4559	18.7	1.69	6.05	[a]	---	L, 24.1 Plex

[a]No transition to detonation was observed within 25.4 mm, but a violent reaction trailed the shock wave at a time that depended on the shock pressure.

Table 4.47 TP-N1028 CLASS VII PROPELLANT

Data Summary

ρ_0 = 1.846 g/cm³. T_0 = 24°C. Technique 7

Shot Number	Initial Shock Parameters			Coordinates for High-Order Detonation		Driving System Thickness (mm)
	P_0 (GPa)	U_{p0} (mm/μs)	U_{s0} (mm/μs)	x* (mm)	t* (μs)	
E-4609	3.20	0.501	3.46	>26.	---	B, 17.8 PC,11.4 SS, 10.9 PMMA
E-4597	3.76	0.604	3.37	22.0	5.57	B, 19.1 SS, 10.9 PMMA
E-4606	3.97	0.601	3.58	23.0	5.91	B, 19.1 SS, 10.9 PMMA
E-4593	4.66	0.632	4.00	16.9	4.06	D, 19.1 SS, 10.9 PMMA
E-4588	5.38	0.678	4.30	12.2	2.79	H, 19.0 SS, 10.9 PMMA
E-4607	5.26	0.723	3.94	11.3	2.59	H, 19.0 SS, 10.9 PMMA
E-4599	6.70	0.794	4.57	7.0	1.42	K, 19.1 SS, 10.9 PMMA
E-4604	7.60	0.879	4.68	5.3	1.06	L, 19.1 SS, 10.9 PMMA
E-4610	7.86	0.906	4.70	5.2	1.08	L, 19.1 SS, 10.9 PMMA
E-4612	8.85	1.008	4.76	3.6	0.71	B, 22.9 PMMA

Reduced Data

ρ = 1.846 g/cm³.

$U_{s0} = (2.20 \pm 0.199) + (2.659 \pm 0.279)U_{p0}$.

C_L = 2.36 mm/μs, C_S = 0.35 mm/μs, and C_0 = 2.33 mm/μs.

Table 4.48 UTP-20930 CLASS VII PROPELLANT

Data Summary

ρ_0 = 1.838 g/cm³. T_0 = 24°C. Technique 7

Shot Number	Initial Shock Parameters			Coordinates for High-Order Detonation		Driving System Thickness (mm)
	P_0 (GPa)	U_{p0} (mm/μs)	U_{s0} (mm/μs)	x* (mm)	t* (μs)	
E-4608	3.13	0.494	3.45	>26	---	B, 17.8 PC, 12.7 SS, 10.9 PMMA
E-4603	4.46	0.613	3.96	24.3	5.73	H, 24.1 SS, 18.0 PMMA
E-4598	4.58	0.635	3.92	26.5	6.2	D, 19 SS, 10.9 PMMA
E-4594	5.18	0.705	4.00	17.3	4.05	H, 19 SS, 10.9 PMMA
E-4602	5.39	0.714	4.11	18.3	4.18	H, 19 SS, 10.9 PMMA
E-4600	6.50	0.830	4.26	10.9	2.33	K, 19 SS, 10.9 PMMA
E-4605	7.41	0.892	4.52	6.5	1.37	L, 19 SS, 10.9 PMMA
E-4601	7.41	0.942	4.28	7.0	1.53	L, 19 SS, 10.9 PMMA
E-4611	8.8	0.98	4.9 ± 0.1	4.6	0.91	B, 20.3, PMMA

Reduced Data

ρ = 1.838 g/cm³.

$U_{s0} = (2.529 \pm 0.133) + (2.157 \pm 0.181)U_{p0}$.

C_L = 2.61 mm/μs, C_S = 0.41 mm/μs, and C_0 = 2.57 mm/μs.

Table 4.49 VOP-7 CLASS VII PROPELLANT

Theoretical Maximum Density

>1.910 g/cm³

Preparation Method

Vacuum casting and pressure curing

Data Summary

ρ_0 = 1.910 g/cm³. T_0 = 25°C. Technique 4

Shot Number	Initial Shock Parameters			1/2 b	Coordinates for High-Order Detonation		Driving System Thickness
	P_0 (GPa)	U_{p0} (mm/μs)	U_{s0} (mm/μs)	(mm/μs²)	x* (mm)	t* (μs)	(mm)
E-4213	0.5	0.093	2.811	−0.030	≫25.3	≫9.93	A, 11.4 SS, 10.9 Plex
E-4209	2.40	0.394	3.186	0.015	>25.2	>8.13	A, 25.4 Plex
E-4193	2.49	0.392	3.323	0.032	21.49	5.90	B, 10.9 Plex
E-4207	2.35	0.385	3.195	0.054	21.04	5.84	B, 10.9 Plex
E-4194	4.44	0.643	3.615	0.070	11.64	2.90	B, 12.7 Plex
E-4208	5.20	0.710	3.835	0.292	6.17	1.43	J, 11.4 Plex
E-4202	6.75	0.858	4.121	1.077	3.95	0.78	B, 24.7 Plex
E-4203	4.80	0.706	3.561	0.515	6.06	1.41	J, 11.4 Plex
E-4225	12.2	1.081	5.911	−0.395	1.914	0.33	J, 48.6 Plex
E-4221	10.20	1.157	4.614	1.578	1.49	0.29	J, 50.7 Plex
E-4218 and E-4219	≈15 GPa expected, but results are not consistent with those of other experiments. It is not clear whether the inconsistency is caused by the poor records obtained or by the unusually large change in slope of the U_s-U_p curve.						J, 24.2 Plex J, 24.2 Plex

Reduced Data

$U_{s0} = (2.571 \pm 0.080) + (1.708 \pm 0.1211)U_{p0}$.

Table 4.50 VRO CLASS VII PROPELLANT

Preparation Method

Vacuum casting, pressure curing, and machining to shape

Data Summary

ρ_0 = 1.833 g/cm³. T_0 = 25°C. Technique 4

Shot Number	Initial Shock Parameters			1/2 b	Coordinates for High-Order Detonation		Driving System Thickness
	P_0 (GPa)	U_{p0} (mm/μs)	U_{s0} (mm/μs)	(mm/μs²)	x* (mm)	t* (μs)	(mm)
E-4473	7.26	0.903	4.385	0.109	4.21	0.92	L, 24.1 SS, 10.9 PMMA
E-4461	6.45	0.844	4.170	0.104	6.10	1.36	K, 24.1 SS, 10.9 PMMA
E-4472	4.93	0.703	3.823	0.084	10.74	2.59	H, 24.2 SS, 10.9 PMMA
E-4450	4.70	0.677	3.790	0.098	10.59	2.58	H, 24.2 SS, 10.9 PMMA
E-4448	3.75	0.583	3.508	0.040	20.26	5.32	B, 15.3 SS, 15.2 PMMA
E-4442	3.75	0.584	3.506	0.033	23.31	6.11	B, 24.2 SS, 17.8 PMMA
E-4441	3.25	0.522	3.395	0.039	>25.50	>6.82	B, 23.9 SS, 25.5 PMMA
E-4471	2.54	0.446	3.109	0.013	>25.47	>7.85	B, 17.8 foam, 11.5 SS, 10.9 PMMA

Table 4.51 VRP CLASS VII PROPELLANT

Preparation Method

Vacuum casting, pressure curing, and machining to shape

Data Summary

ρ_0 = 1.836 g/cm³. T_0 = 24°C. Technique 7

Shot Number	Initial Shock Parameters			Coordinates for High-Order Detonation		Driving System Thicknness (mm)
	P_0 (GPa)	U_{p0} (mm/μs)	U_{s0} (mm/μs)	x* (mm)	t* (μs)	
E-4513	3.42	0.548	3.40	>25.5	>7.15	B, 24.1 SS, 23.3 PMMA
E-4514	5.27	0.718	4.0	8.55	2.17	H, 19 SS, 19.0 PMMA
E-4524	3.65	0.542	3.67	22.6	5.81	B, 24.1 SS, 14.8 PMMA
E-4526	6.27	0.835	4.09	5.69	1.28	K, 24.1 SS, 10.9 PMMA
E-4533	5.42	0.738	4.00	9.40	2.21	G, 19 SS, 10.9 PMMA
E-4534	4.35	0.653	3.63	21.1	5.48	B, 19 SS, 10.9 PMMA
E-4541	6.26	0.784	4.35	5.75	1.27	K, 24.1 SS, 10.9 PMMA
E-4545	7.20	0.872	4.5	5.21	1.03	L, 24.1 SS, 10.9 PMMA

Reduced Data

$U_{s0} = (1.992 \pm 0.365) + (2.761 \pm 0.507)U_{p0}$.

Table 4.52 VTG-5A CLASS VII PROPELLANT

Preparation Method

Vacuum casting and pressure curing

Data Summary

ρ_0 = 1.839 g/cm³. T_0 = 24°C. Technique 7

Shot Number	Initial Shock Parameters			Coordinates for High-Order Detonation		Driving System Thickness (mm)
	P_0 (GPa)	U_{p0} (mm/μs)	U_{s0} (mm/μs)	x* (mm)	t* (μs)	
E-4506	6.01	0.760	4.3	7.08	1.82	H, 24.1 SS, 10.9 PMMA
E-4515	5.52	0.728	4.12	7.53	1.76	H, 19.0 SS, 10.9 PMMA
E-4516	5.79	0.749	4.20	7.64	1.80	L, 24.1 SS, 23.7 PMMA
E-4518	3.53	0.545	3.52	>25.5	>6.79	C-1, 24.1 SS, 23.7 PMMA
E-4532	3.68	0.572	3.50	23.0	6.05	B, 19 SS, 10.9 PMMA
E-4537	7.25	0.876	4.5	4.68	0.97	L, 24.1 SS, 10.9 PMMA
E-4546	4.45	0.637	3.80	14.9	3.70	D, 19.0 SS, 10.9 PMMA

Reduced Data

$U_{s0} = (1.703 \pm 0.177) + (3.292 \pm 0.251)U_{p0}$.

Table 4.53 VTQ-2 CLASS VII PROPELLANT

Preparation Method

Vacuum casting, pressure curing, and machining to shape

Data Summary

ρ_0 = 1.852 g/cm³. T_0 = 24°C. Technique 7

Shot Number	Initial Shock Parameters P_0 (GPa)	U_{p0} (mm/μs)	U_{s0} (mm/μs)	Coordinates for High-Order Detonation x* (mm)	t* (μs)	Driving System Thickness (mm)
			Lot 1			
E-4470	2.50	0.43	3.14	>25.5	>7.37	B, 18 foam, 11 SS, 11 PMMA
E-4447	2.48	0.42	3.19	>25.4	>7.34	B, 18 foam, 11 SS, 11 PMMA
E-4480	2.99	0.47	3.44	22.5	6.13	B, 18 PE, 12 SS, 11 PMMA
E-4462	2.85	0.46	3.35	22.4	6.15	B, 18 PE, 12 SS, 11 PMMA
E-4440	3.50	0.54	3.50	17.8	4.66	B, 24 SS, 23 PMMA
E-4443	3.72	0.58	3.46	15.9	4.18	B, 24 SS, 18 PMMA
E-4449	5.16	0.64	4.35	9.47	2.07	H, 24 SS, 11 PMMA
E-4474	7.73	0.84	4.97	3.74	0.76	L, 24 SS, 11 PMMA
E-4446	11.4	1.07	5.73	1.4	0.24	J, 51 PMMA
			Lot 2			
E-4522	3.07	0.48	3.45	22.5	6.02	B, 18 PE, 12 SS, 11 PMMA
E-4501	3.55	0.53	3.62	16.7	4.38	B, 24 SS, 23 PMMA
E-4502	5.04	0.67	4.06	7.32	1.72	H, 24 SS, 11 PMMA
E-4503	5.89	0.77	4.13	4.85	1.09	L, 24 SS, 19 PMMA

Reduced Data

$U_{s0} = (1.514 \pm 0.192) + (3.887 + 0.303)U_{p0}$.

Table 4.54 VTQ-3 CLASS VII PROPELLANT

Preparation Method

Vacuum casting and pressure curing

Data Summary

ρ_0 = 1.857 g/cm³. $T_0 \approx 24°C$. Technique 7

Shot Number	Initial Shock Parameters			Coordinates for High-Order Detonation		Driving System Thickness (mm)
	P_0 (GPa)	U_{p0} (mm/μs)	U_{s0} (mm/μs)	x* (mm)	t* (μs)	
E-4555	3.21	0.500	3.46	26.0	7.1	B, 17.8 PC, 12.7 SS, 10.9 PMMA
E-4560	3.88	0.571	3.66	15.8	3.96	B, 19.1 SS, 10.9 PMMA
E-4551	4.21	0.625	3.63	12.6	3.12	D, 24.0 SS, 18.5 PMMA
E-4550	5.12	0.673	4.1	8.50	1.95	H, 24.1 SS, 10.9 PMMA
E-4540	5.74	0.773	4.0	5.98	1.37	H, 19 SS, 10.9 PMMA
E-4558	7.15	0.877	4.39	3.95	0.82	J, 24.1 SS, 10.9 PMMA

Reduced Data

$U_{s0} = (2.287 \pm 0.318) + (2.368 \pm 0.466)U_{p0}$.

C_0 = 2.20 mm/μs.

Table 4.55 VWC-2 CLASS VII PROPELLANT

Preparation Method

Vacuum casting, pressure curing, and machining to shape

Data Summary

ρ_0 = 1.835 g/cm³. T_0 = 24°C. Technique 7

Shot Number	Initial Shock Parameters			Coordinates for High-Order Detonation		Driving System Thickness (mm)
	P_0 (GPa)	U_{p0} (mm/μs)	U_{s0} (mm/μs)	x* (mm)	t* (μs)	
E-4564	3.87	0.596	3.54	23.4	6.16	B, 24.1 SS, 18.3 PMMA
E-4552	3.92	0.597	3.58	20.9	5.44	B, 24.1 SS, 18.3 PMMA
E-4548	4.47	0.640	3.81	14.3	3.58	D, 24.0 SS, 10.9 PMMA
E-4547	4.79	0.706	3.7 ± 0.2	14.1	3.48	D, 19.0 SS, 10.9 PMMA
E-4565	5.13	0.718	3.89	9.0	2.15	H, 19.0 SS, 10.9 PMMA
E-4539	5.19	0.702	4.03	9.2	2.17	H, 19.0 SS, 10.9 PMMA
E-4557	6.44	0.811	4.33	6.1	1.34	K, 24.1 SS, 10.9 PMMA
E-4549	7.30	0.878	4.53	4.3	0.93	L, 19.1 SS, 10.9 PMMA

Reduced Data

ρ = 1.835 g/cm³.

$U_{s0} = (1.989 \pm 0.121) + (2.754 \pm 0.180)U_{p0}$.

C_L = 2.13 mm/μs, C_S = 0.49 mm/μs, and C_0 = 2.05 mm/μs.

4.2 Small- and Large-Scale Gap Thicknesses. Gap tests are explosive shock tests. A standard donor explosive produces a shock pressure of uniform magnitude which is transmitted to the test explosive through an attenuating inert barrier or gap. By varying the thickness of the barrier between the donor and test (acceptor) explosives, one can determine the barrier thickness required to inhibit detonation in the test explosive half the time (G_{50}).

A variety of gap tests have been used to qualitatively measure the shock wave amplitude required to initiate detonation in explosives. LASL has used two test configurations that differ only in scale. The diameter of the cylindrical acceptor charge in the small-scale test is 12.7 mm; that in the large-scale test is 41.3 mm. An explosive whose detonation failure diameter is near to or greater than the diameter of the acceptor charge cannot be tested in the small-scale test so the large-scale test is used. Figures 4.10 and 4.11 show the configuration of both gap tests. The test procedure is to fire a few preliminary shots to determine the spacer thickness that allows detonation in the test explosive. Shots are fired with the spacer thickness alternately increased and decreased until the spacer thickness that allows detonation in the acceptor explosive in half of the trials is determined. A deep, sharply defined dent in the steel witness plate indicates that the test explosive detonated.

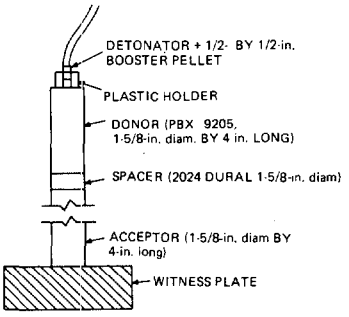

Fig. 4.10. Large-scale gap test assembly.

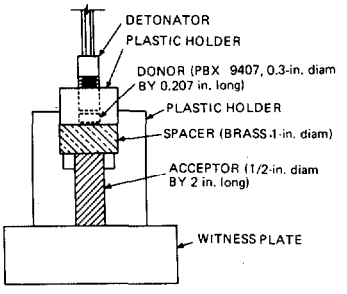

Fig. 4.11. Small-scale gap test assembly.

Table 4.56 SMALL- AND LARGE-SCALE GAP TEST RESULTS

Explosive	Density (g/cm^3)	Small G_{50} (mm)	Large G_{50} (mm)	Remarks
		Pure Explosives		
Ammonium picrate	1.0	No go	35.7	Pressed
	1.604	0.13	43.0	Pressed
	1.635	0.36	43.0	Pressed
	1.65	0.33	42.5	Pressed
Baratol (76/24) mixture	2.597	No go	22.2	Cast
DATB	1.77	0.75	41.7	Pressed
HMX	0.72	6.32	---	
	1.07	---	70.7	Pressed
	1.18	2.46	38.7	Water-filled voids
	1.18	2.77	---	Saturated ZnCl solution-filled voids
	1.02	2.11	---	Ball-milled to d_m 15 μm
NQ	1.63	No go	5.0	Pressed
PETN				See Figs. 4.12-4.18
RDX	0.70	6.94	69.4	
	1.73	5.08	61.8	
	1.15	1.35	---	Water-filled voids
				See Figs. 4.19 and 4.20
TATB	1.87	0.127	21.9	
	0.8	1.02	---	S_0^p 3300 cm^2/g
	1.0	0.76	---	S_0^p 3300 cm^2/g
	1.4	0.51	---	S_0^p 3300 cm^2/g
	1.6	0.51	---	S_0^p 3300 cm^2/g
	1.7	0.51	---	S_0^p 3300 cm^2/g
	1.8	0.25	---	S_0^p 3300 cm^2/g
	1.87	0.127	21.9	Particle size undefined
	1.197	15.80 ± 0.18[a]		Superfine
	1.350	14.32 ± 0.23[a]		
	1.500	17.02 ± 0.05[a]		Superfine

	1.700	14.73 ± 0.38[a]		Superfine
	1.700	15.29 ± 0.08[a]		
	1.791	11.73 ± 0.18[a]		Superfine
	1.806	12.47 ± 0.13[a]		
	1.894	12.36 ± 0.10[a]		
Tetryl	1.68	3.90	60.6	
	1.18	15.53	---	Water-filled voids
	0.96		47.9	
	1.0	3.04	---	S_o^g = 2300 cm²/g
	1.0	3.30	---	S_o^g = 2900 cm²/g
	1.0	2.79	---	S_o^g = 4650
	1.0	3.04	---	S_o^g = 7100
	1.0	3.30	---	S_o^g = 8500
	1.01	---	60	Pressed at 25°C
	1.49	---	53.3	Pressed at 25°C
	1.56	---	52.3	Pressed at 45°C
	1.62	0.33	48.2	Pressed at 65°C
	1.52	---	61.9	Pressed at 75°C
	1.62	0.29	49.4	Pressed, granular
Castable Mixtures				
Comp B-3	1.717	23.2 ± 0.22	---	
	1.72	1.22	45.7	Cast
Comp C-3	0.82	---	27.4	Bulk density
	1.61	---	48.5	Pressed
Cyclotol(75/25)	1.75	1.24	44.3	Cast
Cyclotol(70/30)	1.74	0.38	47.0	Cast
Octol	1.80	0.54	---	Cast
Pentolite	0.75	4.80	61.4	
	1.66	2.31	68.7	
	1.70	0.86	64.7	
TATB/TNT (50/50)	1.76	---	35.1	Cast, 1% voids

[a]Tested at 25.4-mm diam.

Table 4.56 (continued)

Explosive	Density (g/cm^3)	Small G_{50} (mm)	Large G_{50} (mm)	Remarks
Plastic-Bonded Explosives				
HMX-Based				
PBX 9011	1.76	1.37	52.4	
PBX 9404	0.95	2.35	64.5	
	1.84	2.56	95.4	
	1.846	27.3 ± 0.25	---	
PBX-9501	0.64	6.63	62.0	
X-0217	1.83	1.86	51.0	
X-0234	1.84	2.84	---	
RDX-Based				
Comp A-3	0.8	---	51.9	Bulk density
	1.62	2.16	54.6	Pressed
PBX 9007	0.74	4.80	64.2	
	1.77	1.96	54.5	
	1.78	2.39	52.3	
PBX 9010	0.85	5.16	67.13	Bulk density
	1.77	2.28	56.2	Pressed
PBX 9205	0.90	7.52	68.6	Bulk density
	1.69	1.40	50.8	Pressed
PBX 9407	0.64	6.63	62.0	
	1.66	4.19	56.3	
TATB-Based				
PBX 9502[a]	1.92	---	3.78	25°C
		---	2.34	−78°C
		---	5.54	80°C
X-0219[a]	1.499	7.75 ± 0.43[a]		
	1.700	10.69 ± 0.08[a]		
	1.801	8.51 ± 0.05[a]		

	1.890	3.35 ± 0.18[a]	
	1.913	1.73 ± 0.08[a]	
	1.914	1.63 ± 0.05[a]	
	1.914	1.65 ± 0.05[a]	
X-0290[a]	1.349	11.76 ± 0.18[a]	
	1.498	13.46 ± 0.05[a]	
	1.700	13.54 ± 0.05[a]	
	1.803	11.50 ± 0.08[a]	
	1.845	9.22 ± 0.08[a]	
	1.846	8.89 ± 0.25[a]	Reworked TATB
	1.895	3.38 ± 0.15[a]	
	1.908	1.93 ± 0.23[a]	
X-0291	1.501	11.10 ± 0.36[a]	
	1.700	12.65	
	1.701	12.14 ± 0.18[a]	
	1.905	2.06 ± 0.64[a]	

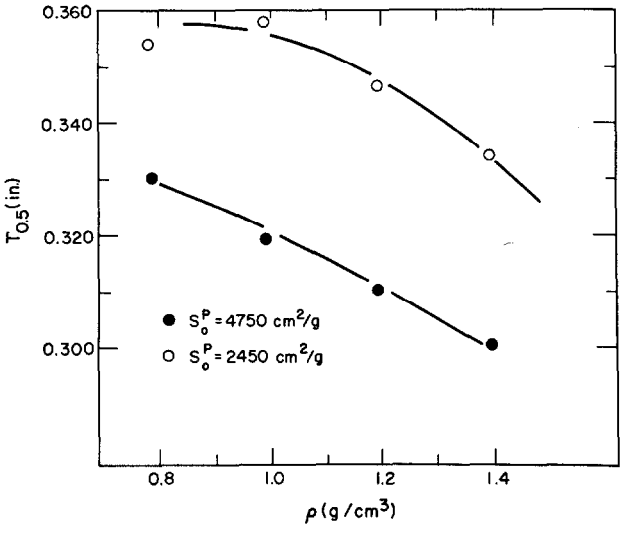

Fig. 4.12. Small-scale gap test sensitivity of PETN vs loading density.

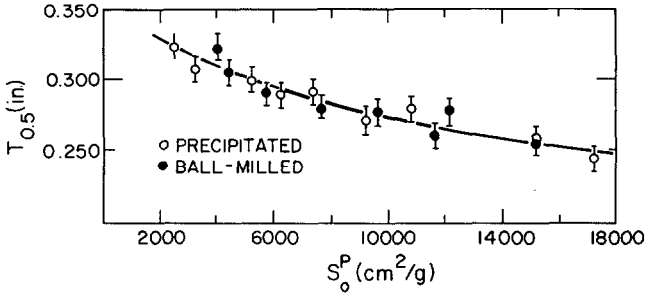

Fig. 4.13 Small-scale gap test sensitivity of 0.95-g/cm³ PETN vs specific surface.

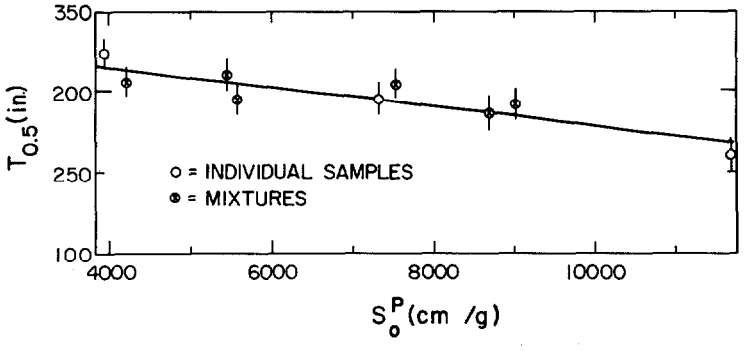

Fig. 4.14. Small-scale gap test sensitivity of 0.95-g/cm³ PETN vs specific surface.

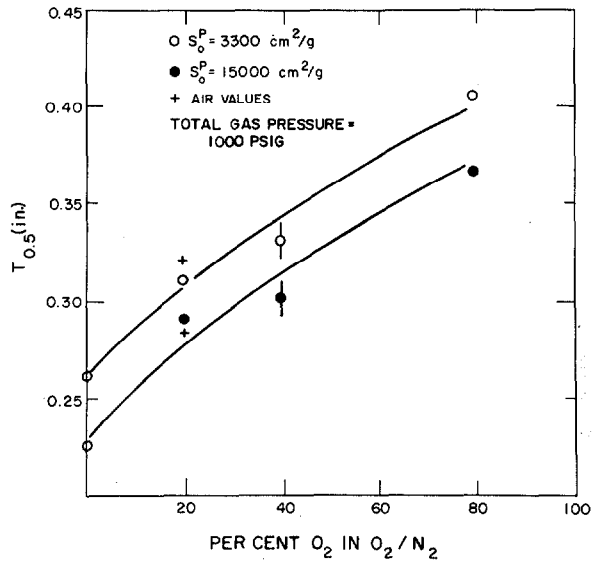

Fig. 4.15. Small-scale gap test sensitivity of PETN vs oxygen concentration.

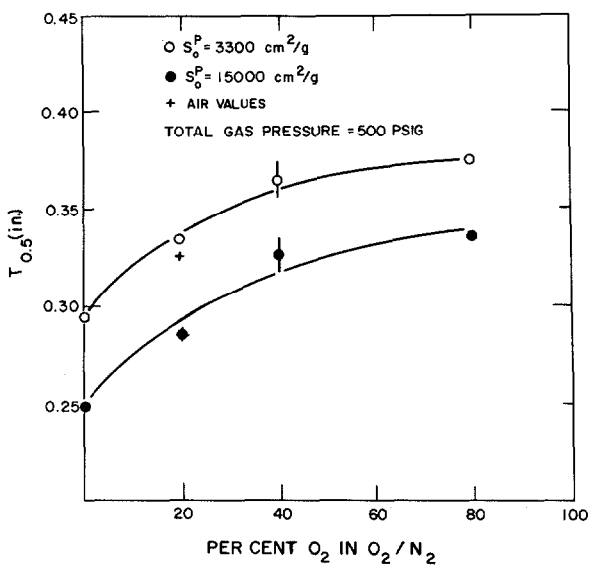

Fig. 4.16. Small-scale gap test sensitivy of PETN vs oxygen concentration.

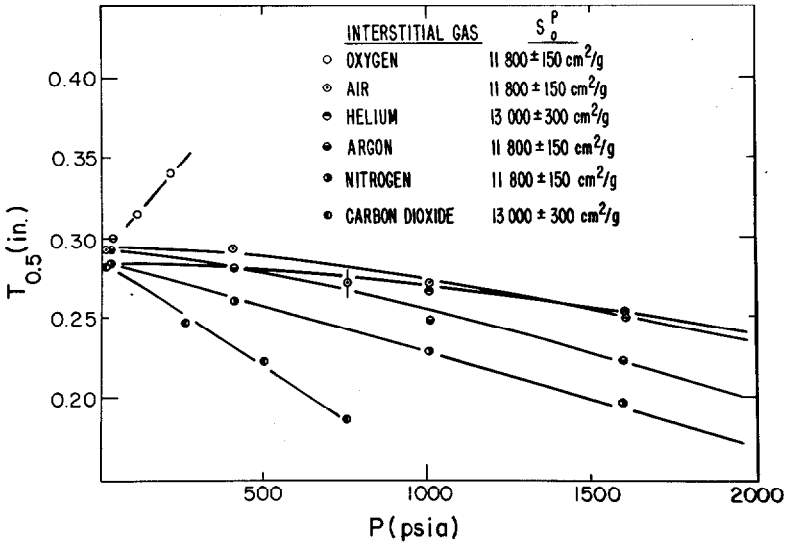

Fig. 4.17. Small-scale gap test sensitivity of PETN vs interstitial gas pressure.

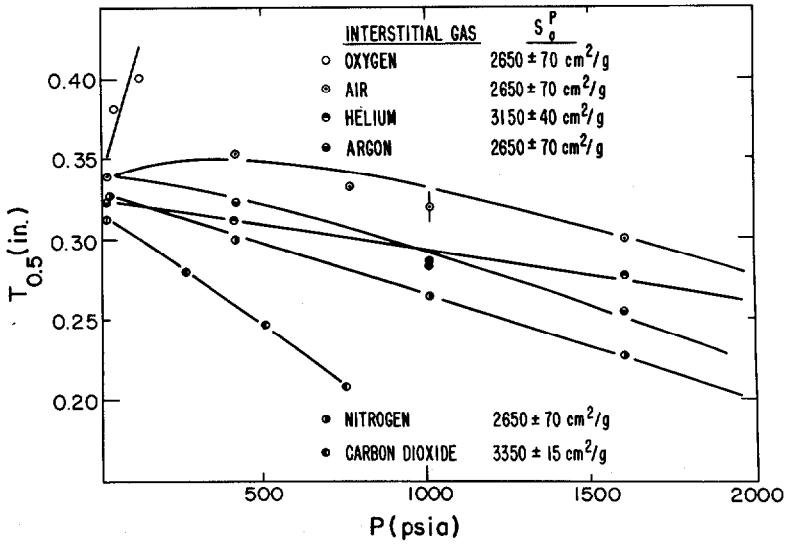

Fig. 4.18. Small-scale gap test sensitivity of PETN vs interstitial gas pressure.

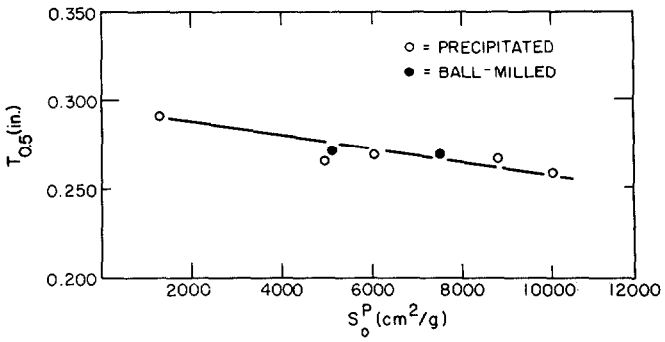

Fig. 4.19. Small-scale gap test sensitivity of RDX vs specific surface at loading density = 0.80 g/cm³.

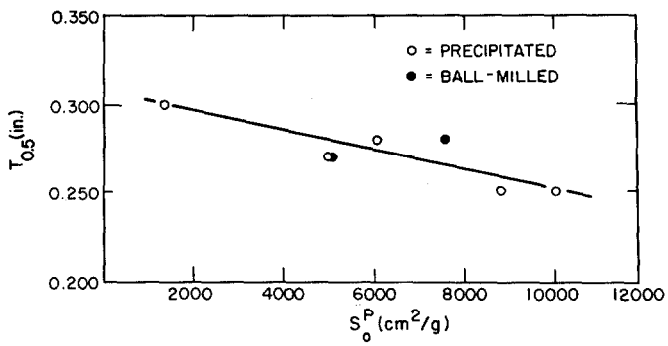

Fig. 4.20. Small-scale gap test sensitivity of RDX vs specific surface at loading density = 1.00 g/cm³.

4.3. Minimum Priming Charge. The minimum priming charge test determines the quantity of some initiator or booster explosive that will cause high-order detonation in the test explosive in half the trials. This test has been used to determine both the relative effectiveness of various initiator explosives and the relative sensitivities of various test explosives. The basic property of the test explosive is its ability to build up to a high-order detonation after a short, intense, geometrically small, and usually highly divergent shock wave is induced from the priming charge.

Figure 4.21 shows the LASL version of this test. The test charge is a 2-in.-diam by 2-in.-high cylinder. A hemispherical cavity milled into one face is filled with a putty-like explosive, XTX 8003, prepared by roll-milling 80 parts of a specially recrystallized PETN with 20 parts of an uncatalyzed silicone resin (Dow Corning

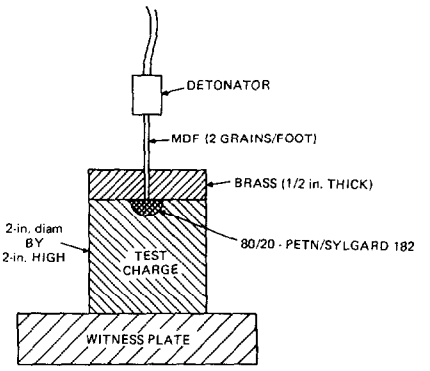

Fig. 4.21. Minimum priming charge test assembly.

Resin 93-022, Sylgard 182). This material was chosen because it can be loaded readily into the cavity, and it propagates a detonation in quite small diameters of test explosives. The 1/2-in.-thick brass plate that covers the assembly partly confines the explosive reaction and also serves as a locating ring for the 2-grain/ft mild detonating fuse (MDF) that carries the detonation from the detonator to the XTX 8003.

The quantity varied is the diameter of the hemispherical cavity, and hence the volume and weight of the XTX 8003 booster. This is done by using a set of end mills whose tips have been ground so that they form cavities of the desired sizes. The cavity is filled by weighing out the required quantity of XTX 8003 (1.53-g/cm^3 loading density), rolling it into a ball, and pressing it into place.

The weight of XTX 8003 is increased and decreased in logarithmic steps of 0.1 log units, starting with 1.53 mg, until the quantity of XTX 8003 required to detonate the test charge in half the trials is found.

4.4 Rifle Bullet Test. Three tests have been used at LASL to determine the response of explosives to attack by rifle bullets.

In the first test, a bare, 2-in.-diam by 3-in.-long cylinder is placed in the V-notch of a plastic holder that rests on a steel plate. The projectile, a 90-grain steel cylinder, roughly 0.3 in. in diameter and 0.5 in. long, is fired at the end of the charge by a .30 caliber rifle. The approximate bullet velocity is measured with velocity screens. A microphone or pressure transducer that measures the overpressure created by an event usually indicates either no overpressure or a pressure characteristic of a detonation. Results are expressed in terms of a critical velocity, V_{crit}; the minimum velocity at which detonations were observed, $V_{det\ min}$; and the maximum velocity at which no reactions were observed, $V_{inert\ max}$. This test is another shock sensitivity test. The bullet velocity is an indirect indicator of the shock pressure required to initiate detonation.

In the second and third tests, the explosive is confined in a 1- by 1.5-in. pipe nipple or a 1-pint cardboard carton, respectively. Standard .30 and .50 caliber bullets weighing 153 and 700 grains are fired at velocities of 2755 and 2840 ft/s to attack the explosive. (In these tests the pipe nipple confinement is used for explosives cast or pressed to more than 95% of their crystal densities. The cardboard carton confine-

ment is used to test explosives at their bulk densities.) In each case the bullet is fired at the cylindrical surface of the confinement vessel with the bullet velocity and caliber held constant.

The results are expressed as follows: no explosion (NE), in which there is no explosive reaction; partial explosion (PE), in which some unconsumed explosive is recovered; explosion (E), in which no explosive is recovered; and complete explosion (CE), in which no explosive is recovered and the steel pipe nipple is recovered in small fragments. The difference between an explosion and complete explosion is subjective in that it depends upon the amplitude of the sound produced by the event and recovery of the debris.

A test series usually consists of 10 to 20 shots, and the results are given as the probability of no explosion, P_{NE}, and the probability of a complete explosion, P_{CE}.

Table 4.57 MINIMUM PRIMING CHARGE

Explosive	Density (g/cm³)	Minimum Priming Weight, W_{50} (mg)
Pure Explosives		
Ammonium picrate	1.646	1790
DATB	1.707	26
TNT[a]	1.59	394
	1.63	1260
Tetryl	1.692	<5
Castable Mixtures		
Comp A-3	1.63	51
Comp B-3	1.725	623
Cyclotol (70/30)	1.739	898
Cyclotol (75/25)	1.749	785
Octol	1.818	292
Plastic-Bonded Explosives		
HMX-Based		
PBX 9011	1.77	88.8
PBX 9404	1.830	22.8
X-0234	1.847	24.0
RDX-Based		
PBX 9007	1.649	14.4
PBX 9010	1.782	58.1
PBX 9205	1.690	78.5
PBX 9407	1.764	6.3
TATB-Based		
PBX 9502	1.915	>4835

[a]Pressed at 65°C.

Table 4.58 UNCONFINED EXPLOSIVES (except as noted)

Explosive	Density (g/cm^3)	$V_{det\ min}$ (ft/s)	$V_{inert\ max}$ (ft/s)	Remarks
Pure Explosives				
Tetryl	1.677	2077	2116	---
Castable Mixtures				
Comp B-3	1.728	3410	3395	---
	1.728	3420	3390	Confined in 1/8-in.-thick brass tube
	1.728	3405	3433	Confined in 1/4-in.-thick brass tube
	1.728	3364	3395	Confined in 3/8-in.-thick brass tube
Octol 75/25	1.807	3861	3842	---
Plastic-Bonded Explosives				
HMX-Based				
PBX 9404	1.826	3058	3085	[a]
	1.825	3028	3098	[a]
	1.824	3129	3178	[a]
	1.843	2870	2970	[b]
	1.830	2830	2976	Unimodal HMX 25-μm median diameter
	1.837	2738	2878	[b]
	1.836	2896	2991	[b]
	1.837	2640	2830	[b]
HMX and wax	1.767	3086	3102	88 wt% HMX/12 wt% Elvax
	1.763	3267	3190	88 wt% HMX/6 wt% Elvax/6 wt% wax
	1.767	3086	3111	88 wt% HMX/12 wt%
RDX-Based				
PBX 9010	1.786	2965	3070	
RDX and wax	1.666	2900	2890	94 wt% RDX/6 wt% wax
	1.696	2900	2920	96 wt% RDX/3.7 wt% wax/0.3 wt% rubber
	1.680	2400	2340	98 wt% RDX/1.7 wt% wax/0.3 wt% rubber

[a]Unimodal HMX 125-μm median diameter.
[b]Standard HMX particle size distribution.

Table 4.59 CONFINED EXPLOSIVES

Confinement: 1- by 1.5-in. pipe nipple
Bullet Type: .30 Caliber
Bullet Weight: 153 grains
Bullet Velocity: 2755 ft/s

Explosive	Density (g/cm^3)	NE	PE	E	CE	P_{NE}	P_{CE}
Castable Mixtures							
Comp B	1.720	20	0	0	0	100	0
Cyclotol 75/25	1.757	20	0	0	0	100	0
Octol 25/25	1.815	20	0	0	0	100	0
Plastic-Bonded Explosives							
HMX-Based							
PBX 9404	1.840	0	1	18	1	0	5
	1.844	6	7	7	0	30	0
	1.827	1	4	14	1	5	5
	1.825	1	3	15	1	5	5
	1.823	0	13	5	0	0	0
	1.840	7	9	4	0	35	0
	1.839	3	1	15	1	15	5
	1.840	1	7	12	1	5	5
97 wt% HMX/3 wt% wax	1.773	19	1	0	0	95	0
RDX-Based							
PBX 9007	1.642	5	13	2	0	25	0
PBX 9407	1.772	0	0	10	0	0	0
	1.744	0	0	10	0	0	0

Confinement: 1- by 1.5-in. pipe nipple
Bullet Type: .50 Caliber
Bullet Weight: 153 grains
Bullet Vellocity: 2840 ft/s

Pure Explosives							
Tetryl	1.682	10	8	2	0	50	0
Castable Mixtures							
Comp B	1.71	18	2	0	0	90	0
Cyclotol 75/25	1.74	10	0	0	0	100	0
Plastic-Bonded Explosives							
HMX-Based							
PBX 9404	1.844	10	6	4	0	50	0
RDX-Based							
PBX 9010	1.783	0	0	20	0	0	0

Table 4.59 (continued)

Explosive	Density (g/cm^3)	NE	PE	E	CE	P_{NE}	P_{CE}
Confinement: Cardboard Carton, 3-5/16-in. i.d. by 3-3/16-in.-high by 1/32-in.-wall							
Bullet Type: .30 Caliber							
Bullet Weight: 153 grains							
Bullet Velocity: 2755 ft/s							
Pure Explosives							
Tetryl	0.85	0	0	---	20	0	100
Plastic-Bonded Explosives							
HMX-Based							
PBX 9404	1.00	0	2	---	18	0	90
	0.96	0	1	---	19	0	95
	0.98	0	3	---	17	0	85
	1.09	---	17	---	3	0	15
	1.10	0	20	---	0	0	0
	1.09	0	20	---	0	0	0
	---	10	0	---	0	100	0
RDX-Based							
PBX 9007	0.77	10	0	---	0	100	0
PBX 9407	0.60	0	0	---	10	0	100
	0.63	2	0	0	18	10	90
Confinement: Cardboard, 3.312-in.-i.d. by 3.187-in.-high by .30-in.-wall							
Bullet Type: .30 Caliber							
Bullet Weight: 153 grains							
Bullet Velocity: 2000 ft/s							
Pure Explosives							
Tetryl	0.89	18	0	---	2	90	10
Plastic-Bonded Explosives							
HMX-Based							
PBX 9404	1.00	12	3	---	5	60	25
	0.98	20	0	---	0	100	0
	0.96	20	0	---	0	100	0
RDX-Based							
PBX 9010	0.89	18	0	---	2	90	10

Table 4.59 (continued)

Explosive	Density (g/cm^3)	NE	PE	E	CE	P_{NE}	P_{CE}
Confinement: Cardboard, 3.312-in.-i.d. by 3.187-in.-high by 0.030-in.-wall Bullet Type: .30 Caliber Bullet Weight: 153 grains Bullet Velocity: 2250 ft/s							
Pure Explosives							
Tetryl	0.89	1	0	---	19	5	95
Plastic-Bonded Explosives							
HMX-Based							
PBX 9404	1.00	7	0	---	10	41	59
	0.96	9	1	---	0	90	0
RDX-Based							
PBX 9010	---	10	0	---	0	100	0

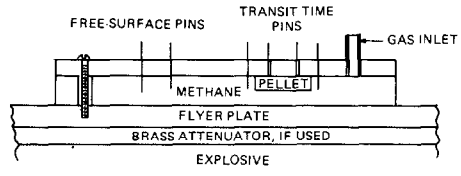

Fig. 4.22. Experimental arrangement for initiation by sustained shocks.

4.5 Miscellaneous Tests.

4.5.1 Initiation of Detonation by a Sustained Shock. A common way to initiate detonation in an explosive is to transmit a shock wave into it. The shock enters at a velocity less than the explosive's detonation velocity and travels for a time, t_s, before detonation occurs. The detonation would require a different time, t_D to travel the same distance. The difference between the detonation and shock travel time is $t_s - t_D$, the excess transit time is t_e. It is related inversely to the strength of the input shock. If the shock is produced by hitting the explosive with a flying plate, the shock pressure induced in the explosive is proportional to the plate velocity, and the shock duration is proportional to the plate weight, and hence, thickness. Thus, production of a "sustained" shock requires a "thick" flying plate or flyer.

In the test used to produce the data that follow, a plane, square wave-shaped shock was transmitted to the various explosives by an explosive-propelled flyer whose thickness was selected so that the induced shock always lasted longer than the time required to initiate a steady-state detonation. The flyer was propelled by an explosive driver consisting of a 305-mm-diam plane-wave generator, a 50- or 100-mm explosive charge, and an attenuator. After traversing a methane-filled space, the flyer collided with the 25.4-mm-diam by 6.35-mm-high right circular cylinder of explosive. Figure 4.22 shows the experimental setup.

The flyer velocity was adjusted by varying the explosive and attenuator. The free-surface velocity of the flyer and the shock transit time through the explosive sample were measured with ionization switches. Premature, ionization-caused, switch discharge was prevented by the methane atmosphere. The explosive detonation velocity and thus the detonation transit time, t_D is known from other experiments. The difference between the measured time and t_D is the excess transit time t_e. The free-surface velocity of the flyer has been correlated with t_e, t_e has been correlated with the free-surface velocity of the flyer, and functions have been found.

4.5.2 Initiation of Detonation by Short-Duration Shocks. Short-duration shocks in the test explosives were produced by striking them with a thin flying foil. The thin foils were driven from the surface of a material of higher impedance by shocking it with an explosive driver. Figure 4.23 shows the experimental setup. The shock duration was adjusted by varying the foil thickness, and the free-surface velocity was adjusted by varying the explosive driver. The thin foils flew through vacuum (10-mm Hg) and struck the 25.4-mm-diam by 6.35-mm-thick test explosives. Transit times through the test explosives and free-surface velocities of the foils were determined using ionization switches.

The unreduced data from all of the experiments are given in Table 4.61.

Table 4.60 INITIATION OF DETONATION BY A SUSTAINED SHOCK

Explosive	Density (g/cm³)	Assumed Detonation Velocity (mm/μs)	Flyer	Number of Observations	Least Squares Fit Experimental Data Log t_e =	Valid U_{fs} Range (mm/μs)
Pure Explosives						
Tetryl	---	7.453	2024 Al	21	$(2.30 \pm 0.07) - (3.30 \pm 0.24) \log U_{fs}$	1.00-3.34
Castable Explosives						
Comp B	1.715 ± 0.003	8.00	2024 Al	---	$(3.14 \pm 0.03) - (3.08 \pm 0.09) \log U_{fs}$	1.06-3.31
Comp B-3	1.726 ± 0.002	7.95	2024 Al	32	$(2.89 \pm 0.02) - (3.33 \pm 0.07) \log U_{fs}$	1.07-2.85
Cyclotol 75/25	1.755 ± 0.003	8.3	2024 Al	117	$(3.20 \pm 0.02) - (2.98 \pm 0.07) \log U_{fs}$	1.17-3.37
Cyclotol 75/25	1.755 ± 0.002	8.30	Mild steel	12	$(3.35 \pm 0.08) - (4.40 \pm 0.23) \log U_{fs}$	1.72-2.73
Octol 75/25	1.815	8.475	2024 Al	17	$(3.00 \pm 0.01) - (2.80 \pm 0.04) \log U_{fs}$	1.17-2.82
Octol 75/25	1.815 ± 0.001	8.475	Mild steel	15	$(2.71 \pm 0.01) - (2.64 \pm 0.05) \log U_{fs}$	1.02-2.03
EDC-1	1.770 ± 0.010	8.310	2024 Al	15	$(3.02 \pm 0.02) - (2.69 \pm 0.06) \log U_{fs}$	1.19-2.86
EDC-1	1.790 ± 0.005	8.380	2024 Al	15	$(3.10 \pm 0.02) - (2.86 \pm 0.08) \log U_{fs}$	1.19-2.84
Plastic-Bonded Explosives						
PBX 9010	1.781 ± 0.004	8.33	2024 Al	33	$(2.82 \pm 0.02) - (3.38 \pm 0.09) \log U_{fs}$	1.01-3.06
PBX 9011	1.764 ± 0.001	8.50	2024 Al	21	$(2.89 \pm 0.01) - (3.09 \pm 0.04) \log U_{fs}$	1.13-2.29
PBX 9404	1.789 ± 0.002	8.650	2024 Al	9	$(2.63 \pm 0.01) - (2.68 \pm 0.03) \log U_{fs}$	0.99-1.50
PBX 9404	1.821 ± 0.002	8.720	2024 Al	6	$(2.63 \pm 0.02) - (2.79 \pm 0.24) \log U_{fs}$	1.00-1.50
PBX 9404	1.844	8.80	2024 Al	43	$(2.77 \pm 0.01) - (2.99 \pm 0.04) \log U_{fs}$	0.68-3.10
PBX 9404	1.843 ± 0.001	8.80	Magnesium	18	$(3.00 \pm 0.01) - (2.92 \pm 0.03) \log U_{fs}$	1.17-2.92
PBX 9404	1.843 ± 0.001	8.80	Mild steel	21.	$(2.43 \pm 0.02) - (3.27 \pm 0.12) \log U_{fs}$	0.65-1.90
PBX 9404[a]	Variable	Variable	Mild steel	12.	$(2.06 \pm 0.09) + (1.70 \pm 0.37) \log \rho_o$	1.584-1.837

[a]The effect shown is that of the explosive initial density on the excess transit time, where the steel flyer U_{fs} = 1.23 mm/μs.

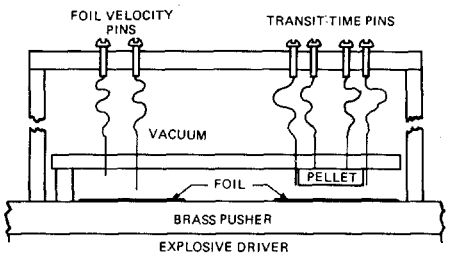

Fig. 4.23. Experimental arrangement for producing short-duration shocks.

Table 4.61 INITIATION OF DETONATION BY SHORT-DURATION SHOCKS

Explosive: PBX 9404
Density: 1.842 ± 0.003 g/cm^3
Assumed Detonation Velocity: 8.80 mm/μs
Flyer Material: 2024 Aluminum

Foil Thickness (mm)	Foil Velocity (mm/μs)	Observed Transit Time (ns)	Excess Transit Time (ns)
1.26	0.75	4585[a]	2845
1.26	0.75	4574[a]	2852
1.58	0.78	2868	1137
1.58	0.78	2853	1122
0.26	1.40	1123	395
0.26	1.40	1208	483
0.26	1.39	1404	681
0.30	1.39	1089	368
0.30	1.42	1301	584
0.20	1.66	1076	355
0.20	1.64	968	244
0.20	1.61	994	271
0.14	1.78	1093	369
0.14	1.77	1407	323
0.14	1.77	948	224
0.14	1.78	972	248
0.14	1.82	1446	362
0.14	1.82	962	239
0.14	1.82	1363	279
0.14	1.82	1027	304
0.21	1.80	863	139
0.21	1.80	824	100
0.25	1.80	805	83
0.21	1.80	836	113
0.31	1.76	854	130
0.31	1.76	847	122

[a]A slowly rising pulse indicated marginal initiation.

4.5.3 Partial Reaction in Shocked Explosives. As a shock wave passes through an explosive, some reaction usually occurs behind the wave front. If the shock wave is strong enough, the decomposition can build up to a detonation. There are few experimental data or theories that describe this process, but the following data give evidence of its effect in one configuration.

Figure 4.24 shows the experimental arrangement. A plane-wave shock of known amplitude was transmitted into one side of the test explosive, and the free-surface velocity of a witness plate on the opposite side was measured. The explosive thickness was varied for each input shock amplitude. If the explosive were totally inert, the witness plate free-surface velocity would be expected to decrease slightly with increasing explosive thickness and constant input shock. Instead, as the data show, the velocity increases, indicating that energy is added to the transmitted shock from shock-induced reaction in the explosive. Unfortunately, there are no similar data with the explosive as an inert. They would allow the reaction to be characterized quantitatively as a free-surface velocity increase for a particular shock pressure and run distance in the explosive. These data were included with the hope that they can be useful and perhaps encourage further study of shock-induced reaction.

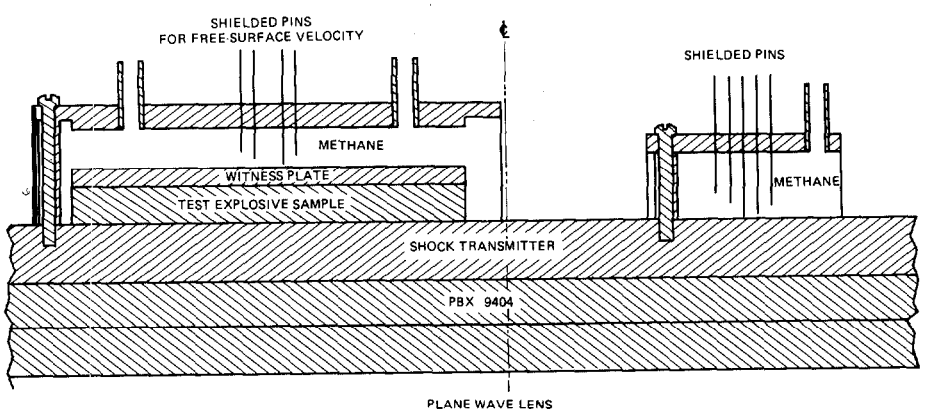

Fig. 4.24. Experimental arrangement for producing partial reaction in shocked explosives.

Table 4.62 DATA ON PARTIAL REACTION IN SHOCKED EXPLOSIVES

Explosive: PBX 9404
Density: 1.847 ± 0.001 g/cm³
Shock Transmitter: 2024 Aluminum
Witness Plate: Lucite

Transmitter Free-Surface Velocity (mm/μs)	Test Explosive Thickness (mm)	Witness Plate	
		Thickness (mm)	Free-Surface Velocity (mm/μs)
1.108	0.00	5.08	1.717
1.109	1.03	5.08	2.346
1.103	1.96	5.05	2.964
1.108	2.56	5.06	3.251
1.109	4.01	5.09	3.574
1.103	6.36	5.05	4.121
1.124	2.54	3.19	3.612
1.124	2.53	6.35	3.075

Explosive: PBX 9404
Density: 1.843 ± 0.001 g/cm³
Shock Transmitter: 2024 Aluminum
Witness Plate: Magnesium

1.048	1.92	2.54	2.393
---	3.82	2.54	3.734
1.063	7.62	2.55	3.800
---	7.62	2.53	3.838

Explosive: Nitroguanidine
Density: 1.700 ± 0.001 g/cm³
Shock Transmitter: Polymethylmethacrylate
Witness Plate: Plexiglas

4.450	0.00	5.09	4.229
4.475	5.02	5.07	4.356
4.450	10.02	5.09	4.763
4.475	14.01	5.08	5.408

Table 4.62 (continued)

Explosive: Comp B
Density: 1.700 ± 0.003 g/cm³
Shock Transmitter: 2024 Aluminum
Witness Plate: 2024 Aluminum
Witness Plate Thickness: 4.75 ± 0.05 mm

Transmitter Free-Surface Velocity (mm/μs)	Test Explosive Thickness (mm)	Witness Plate	
		Thickness (mm)	Free-Surface Velocity (mm/μs)
1.07	2.08	4.70	1.43
1.07	2.55	4.81	1.43
1.07	3.83	4.81	1.56
1.07	3.85	4.80	1.56
1.07	5.08	4.81	1.69
1.07	5.10	4.80	1.71
1.07	7.66	4.79	2.23
1.07	10.19	4.80	2.63
1.07	10.19	4.72	2.58
1.07	12.71	4.78	2.59
1.07	15.26	4.80	2.70
1.07	20.33	4.78	2.76
1.17	3.85	4.82	1.86
1.17	5.06	4.80	2.08
1.51	3.80	4.80	2.30
1.51	5.11	4.80	2.51
1.97	3.84	4.78	2.49
1.97	5.08	4.80	2.57
2.43	5.15	4.83	2.60
2.82	3.84	4.83	2.75
2.82	5.11	4.80	2.72
3.12	5.11	4.74	2.99

REFERENCES

1. J. M. Majowicz and S. J. Jacobs, American Physical Society Bulletin **3**, 293 (1958).

2. A. W. Campbell, W. C. Davis, J. B. Ramsay, and J. R. Travis, Physics of Fluids **4**, 511-521 (1961).

3. J. B. Ramsay and J. J. Dick, Los Alamos Scientific Laboratory, personal communication.

4. Anders Hald, *Statistical Theory with Engineering Applications,* (John Wiley & Sons, Inc., New York, 1952), p. 622.

5. SENSITIVITY TESTS

5.1 Drop Weight Impact Text. The drop weight impact machine used at LASL is based on the design that the Explosive Research Laboratory at Bruceton, Pennsylvania developed during World War II. It consists of a free-falling weight, tooling to hold the explosive sample, and a supporting frame (Fig. 5.01).

An electronic monitoring circuit is used to distinguish between events and failures. The noise that the event creates is picked up by a microphone or pressure transducer whose output is fed to a triggering circuit. The threshold of this circuit is adjusted to place one of the standard explosives, usually TNT, at a fixed point on the drop weight impact scale.

The sample to be tested is dried, usually under vacuum, and loaded into a dimple in the center of a 6.5-cm^2 sheet of 5/0 garnet paper. That is the Type 12 sample configuration. A variation, the Type 12B without garnet paper, also is used.

In it the striker and anvil surfaces are roughened by sandblasting with No. 40 carborundum, and the explosive is placed on the roughened surface of the anvil. Depending on the bulk density, the sample weight varies from 30 to 40 mg. Explosives that are normally received in granular form, such as PETN, RDX, and the plastic-bonded molding powders, are tested as received. Cast explosives, such as Comp B, are ground, and the test sample is a 50/50 mixture of material that passes through a USS 16 but is retained on a USS 30 sieve and that passes through a USS 30 but is retained on a USS 50 sieve. A third sample configuration, called Type 13, is used to test liquids. A drop of liquid is placed on the anvil surface, and the lower surface of the striker is positioned approximately 3 mm above the sample. A wooden shear pin is used to locate the striker.

A standard test consists of 25 shots performed by following the 'up-and-down' testing techniques normally used in sensitivity testing, and results are reported in terms of the height at which an event is obtained 50% of the time (H_{50}). The intervals between drop heights used at LASL are 0.05 ~~times the logarithm (base 10) of the preceding drop height~~. The logarithmic scale is used on the assumption that the heights at which events occur follow a lognormal distribution. The interval size in this method of testing is based on the standard deviation of the mean, or 50%, point.

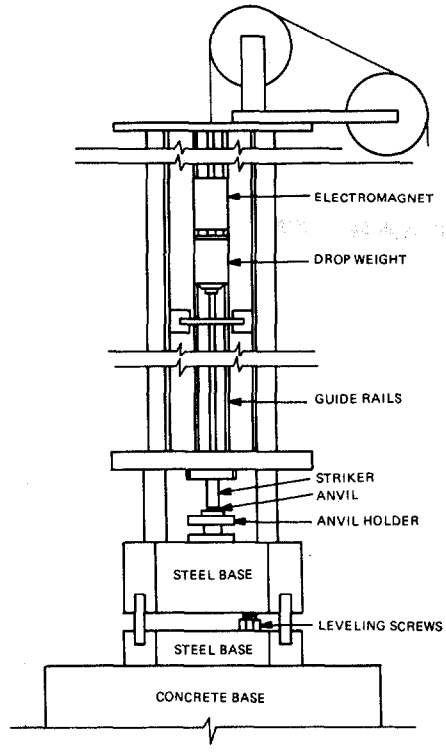

Fig. 5.01. Drop weight impact machine, based on Explosives Research Laboratory model with Type 12 tooling.

Table 5.01 DROP WEIGHT IMPACT RESULTS

Explosive	Result				Remarks
	Type 12		Type 12B		
	H_{50} (cm)	σ (log)	H_{50} (cm)	σ (log)	
Pure Explosives					
Ammonium nitrate	2 go's at 320		>320		
Ammonium picrate	136	± 0.05	220	± 0.05	Also known as Explosive D
	137 to >320[a]		220 to >320[a]		
BTF	22.7	± 0.17	---		Fine powder
	45.2	± 0.09	---		Fine powder
	13.8	± 0.05	---		Blend of needles and powder
DATB	>320		>320		
DINA	41.1	± 0.03			
DIPAM	85.1	± 0.06	95.5	± 0.04	
DIREHAN	25.8	± 0.11	32.8	± 0.06	
EDNA	42.7	± 0.04	---		
HMX	26.1	± 0.03[a]	36.0	± 0.04[a]	
	31.7	± 0.05[a]	29.9	± 0.05[a]	
HNAB	36.6	± 0.07	32.3	± 0.11	
HNB	15.6	± 0.03	16.8	± 0.04	
HNS	53.7	± 0.07	66.3	± 0.04	
MAN	64.2	± 0.03	242		
NC	49.8	± 0.02	56.6	± 0.04	11.8-12.2% N
NM			>320[b]		
NP			284	± 0.01[b]	
NQ	>320		>320		
PETN	12.5	± 0.02[a]	13.9	± 0.08[a]	
	16.2	± 0.05[a]	20.1	± 0.05[a]	
PNA	19.3	± 0.08	20.6	± 0.03	

Picrates		
Cesium	29.0 ± 0.12	30.2 ± 0.23
Lithium	36.3 ± 0.05	110.0 ± 0.06
Potassium	37.3 ± 0.05	55.9 ± 0.04
Rubidium	37.2 ± 0.01	---
Sodium	58.0 ± 0.06	180 ± 0.01
Picric acid	73.0 ± 0.03	191 ± 0.11
Picryl azide	12.1 ± 0.04	52.6 ± 0.13
PYX	122 ± 0.07	---
QMAN	>320	>320
RDX	23.3 ± 0.03[a]	66 ± 0.05[a]
	27.9 ± 0.09[a]	31.8 ± 0.07[a]
TATB	>320	>320.
Tetryl	38.5 ± 0.10	42.3 ± 0.10
TNT	157 ± 0.03	>320
TPM	>320[a]	>320[a]
	>320[a]	161 ± 0.25[a]
TNS	1 go in 8 trials at 320	

Castable Mixtures

Amatex/20	76 ± 0.02	132 ± 0.07	40 AN/40 TNT/20 RDX wt%
Baratol	68 ± 0.04[a]	98 ± 0.02[a]	
	140 ± 0.13[a]	182 ± 0.12[a]	
Boracitol	>320	>320	
Comp B	48.7 ± 0.01[a]	72 ± 0.04[a]	
	85 ± 0.08[a]	300 ± 0.18[a]	
Comp B-3	45.6 ± 0.02[a]	68.9 ± 0.02[a]	
	80.4 ± 0.10[a]	123 ± 0.10[a]	

[a]Range of values obtained for various lots of explosive manufactured to the same material specification.
[b]Type 13 tool used for liquid.

Table 5.01 (continued)

Explosive	Result				Remarks
	Type 12		Type 12B		
	H_{50} (cm)	σ (log)	H_{50} (cm)	σ (log)	
Cyclotol 75/25	41.9 ± 0.02[a]		98.6 ± 0.02[a]		
	52.0 ± 0.13[a]		129 ± 0.11[a]		
Cyclotol 70/30	36.6 ± 0.05		52.7 ± 0.05		
Destex	299 ± 0.05		>320		80 TNT/20 Al/5 wax/2 carbon/0.1 lecithin wt%
Octol 75/25	35.0 ± 0.01[a]		48.9 ± 0.01[a]		
	52.2 ± 0.08[a]		274. ± 0.17[a]		
Plastic-Bonded Explosives					
DATB-Based					
95 DATB/5 Viton	>320		>320		
95 DATB/2.5 PS/2.5 DOP	>320		>320		
95 DATB/5 Estane	>320		>320		
95 DATB/5 Kel-F	>320		>320		
HMX-Based					
PBX 9011[a]	44.8 ± 0.01		53.2 ± 0.01		90 HMX/10 Estane wt%
	88.8 ± 0.08		97.5 ± 0.11		
PBX 9404[a]	33.0 ± 0.02		35.0 ± 0.02		
	48.3 ± 0.06		57.0 ± 0.10		
PBX 9501[a]	41.5 ± 0.01		41.1 ± 0.03		
	57.4 ± 0.10		84.3 ± 0.13		
86.4 HMX/13.6 Estane[a]	56		55		
	80		129		
93.4 HMX/6.6 Estane[a]	44		50		
	60		70		

83 HMX/17 Teflon[a]	32.2 ± 0.01	55.3 ± 0.01	
	61.4 ± 0.1	154 ± 0.11	
94 HMX/3.6 DNPA/2.4 NP	37.7 ± 0.04	39.8 ± 0.05	
94 HMX/3 DNPA/3 CEF	44.3 ± 0.03	45.2 ± 0.05	
94 HMX/3.6 DNPA/2.4 CEF	45.6 ± 0.06	62.9 ± 0.06	
94 HMX/4.2 DNPA/1.8 CEF	43.6 ± 0.05	48.2 ± 0.10	
94 HMX/4.8 DNPA/1.2 CEF	43.7 ± 0.04	46.2 ± 0.12	
97 HMX/1.35 Kraton/1.65 oil	49.7 ± 0.05	59.1 ± 0.05	
97 HMX/1.9 Kraton/ 1.1 wax	48.3 ± 0.07	66.0 ± 0.05	
75 HMX/25 Nitroso rubber	49.7 ± 0.03	101 ± 0.04	
80 HMX/20 Nitroso rubber	53.7 ± 0.04	42.7 ± 0.03	
85 HMX/15 Nitroso rubber	41.0 ± 0.04	39.7 ± 0.05	
90 HMX/10 Nitroso rubber	38.2 ± 0.03	87 ± 0.04	
95 HMX/5 Nitroso rubber	36.2 ± 0.02	46 ± 0.04	
HMX-Based with Metal Fill			
77.5 HMX/20 Al/2.5 Kraton oil	41.5 ± 0.03	48.3 ± 0.04	
77.6 HMX/20.4 Pb/2.0 Exon	40.3 ± 0.06	---	
13.2 HMX/85.3 W/1.5 Estane	74.2 ± 0.05[a]	134 ± 0.03[a]	
	>320[a]	>320[a]	
87 HMX/5 UO_2/8 Teflon	47.9 ± 0.1	73 ± 0.05	
RDX-Based			
PBX 9001	39.1 ± 0.05	43.9 ± 0.03	90 RDX/8.5 PS/1.5 DOP
PBX 9007	39.1	---	90 RDX/9.1 PS/0.5 DOP/0.4 resin
PBX 9010	30.8 ± 0.03[a]	30.8 ± 0.03[a]	
	41.1 ± 0.10[a]	91.6 ± 0.07[a]	
Comp C	41.7 ± 0.05	36.3 ± 0.05	88 RDX/12 wax
PBX 9205	44.3 ± 0.04[a]	47.9 ± 0.05[a]	92 RDX/6 PS/2 DOP
	59.6 ± 0.18[a]	55.8 ± 0.15[a]	
PBX 9401	43.5 ± 0.04	56.6 ± 0.09	94.2 RDX/3.2 PS/2.2 TOF
PBX 9407	37. ± 0.03[a]	49 ± 0.05[a]	
	45.6 ± 0.06[a]	46 ± 0.08[a]	
XTX 8004	41.9 ± 0.02	39.1 ± 0.02	
	80.4 ± 0.13	180 ± 0.25	
95 RDX/5 Viton wt%	39.5 ± 0.04	39.0 ± 0.06	

Table 5.01 (continued)

Explosive	Result				Remarks
	Type 12		Type 12B		
	H_{50} (cm)	σ (log)	H_{50} (cm)	σ (log)	
RDX-Based with Metal Fill					
81.8 RDX/9.1 Kel-F/0.1 Al	39.1	± 0.04			Aluminized PBX 9010
85.5 RDX/5.4 Exon/9.1 Al	19.4	± 0.05			Aluminized PBX 9407
74 RDX/20 Al/5.4 Wax/0.6 Elvax	50.3	± 0.04	83.8	± 0.05	
74 RDX/20 Al/6 Wax	44.8	± 0.04	80.0	± 0.04	
74 RDX/20 Al/6 Wax	54.8	± 0.17	81.1	± 0.14	
0.5 Stearic Acid/16.2 RDX/81.5 Pb/ 1.4 PS/0.5 DOP	>320		>320		
10.3 RDX/88.1 W/1.3 PS/0.3 DOP	>320		>320		
15.4 RDX/82.6 W/1.6 PS/0.4 DOP	305	± 0.06	---		
23.9 RDX/73.4 W/2.2 PS/0.5 DOP	170	± 0.08			
HMX-TATB Mixtures					
3 TATB/95 HMX/2 Estane	39	± 0.04	61	± 0.04	
3 TATB/92 HMX/5 Kel-F	39.9	± 0.02	65	± 0.06	
38 TATB/57 HMX/5 Kel-F	58	± 0.05	82	± 0.06	
18 TATB/72 HMX/10 Kel-F	52.7	± 0.04	62	± 0.15	
20 TATB/70 HMX/10 Kel-F	74	± 0.04	58	± 0.05	
36 TATB/54 HMX/10 Kel-F	67	± 0.06	80	± 0.08	
45 TATB/45 HMX/10 Kel-F	156	± 0.04	145	± 0.05	
45 TATB/40 HMX/10 Kel-F	74	± 0.10	87	± 0.05	
63 TATB/27 HMX/10 Kel-F	>320		185	± 0.12	
70 TATB/20 HMX/10 Kel-F	>320		254	± 0.04	
RDX-Oxidizer Mixtures					
40 RDX/60 AN	45.6	± 0.04	71.2	± 0.12	
40 RDX/60 MAN	60.3	± 0.04	71.0	± 0.09	
20 RDX/80 MAN	68.9	± 0.07	125	± 0.17	
40 RDX/45 AN/15 MAN	51	± 0.04	125	± 0.05	

40 RDX/48 AN/12 QMAN	55.8 ± 0.07	56.6 ± 0.08	
40 RDX/40 AN/20 QMAN	73.7 ± 0.05	92.8 ± 0.07	
40 RDX/30 AN/30 MAN	60 ± 0.03	114 ± 0.04	
40 RDX/30 AN/30 QMAN	78.8 ± 0.05	82 ± 0.07	
40 RDX/15 AN/45 MAN	58.4 ± 0.06	117 ± 0.06	
	Oxidizer Mixtures		
50 AN/50 MAN	81.9 ± 0.06	180 ± 0.01	
75 AN/25 MAN	104 ± 0.05	~225	
ANFO	1 go at 320	1 go at 320	94 AN/d diesel oil

5.2 Skid Test. The skid test used at LASL is a modification of one designed by the Atomic Weapons Research Establishment in cooperation with the Explosives Research and Development Establishment, both of the United Kingdom. The intent of this test, sometimes called the oblique impact test, is to simulate a bare explosive charge accidentally hitting a rigid surface at an oblique angle during handling. In these circumstances, combined impact, friction, and shearing forces generate thermal energy.

In the most common version of this test, an uncased hemispherical charge, 254 mm in diameter, is dropped vertically in free fall onto a rigid target inclined at a 45° angle. In a second version, the hemispherical charge swings down in a harness on the end of a cable and strikes a rigid horizontal target at a predetermined angle.

In either version, the variables are the drop height, the angle of impact between target and explosive, and the target surface.

Two target surfaces have been used. The first is a thin (10-gauge) steel pad painted with epoxy resin sprinkled with sea sand. After curing, this surface resembles coarse sandpaper. Closekote, 80D-grit garnet paper bonded with epoxy resin to the surface of a 6.3-mm-thick Dural plate has also been used. The steel or aluminum target is placed on a rigid steel pad, 114.3 mm thick.

A standard test consists of 10 to 15 drops performed by following the up and down techniques normally used in sensitivity testing. The overpressure at a distance of 10 ft is measured with an Atlantic Research Model LC-13 pressure gauge. Results reported are the drop height that produces events in 50% of the trials and the average overpressure. This test measures each of initiation (drop height) and ease of detonation growth (overpressure).

Table 5.02 SKID TEST RESULTS

Explosive	Density (g/cm³)	Impact Angle (°)	Target Surface	H_{50} (ft)	Over-pressure (psi)	Remarks
Castable Explosives						
Comp A-3	---	45	Sand + epoxy	>150	---	
Comp B-3	1.727	15	Sand + epoxy	9.8	<0.5	
Cyclotol 75/25	1.758	15	Sand+ epoxy	4	<1.0	
Octol	1.810	45	Sand + epoxy	~75	<0.1	
Octol + 1 wt% wax	1.805	45	Sand + epoxy	>150	---	
HMX-Based Plastic-Bonded Explosives						
LX-09	1.840	45	Garnet paper	5.7	~9	
PBX 9011	1.773	45	Garnet paper	78	<0.5	75 Class A/25 Class B HMX
PBX 9011	1.773	45	Garnet paper	4	<0.5	HE cooled to −20°F
PBX 9011-03	1.773	45	Garnet paper	11	<0.5	HMX particle-size study - 75 Class B/ 25 Class A HMX
PBX 9011-04	1.773	45	Garnet paper	4	<0.5	25 Class B/75 Class C HMX
PBX 9011-05	1.773	45	Garnet paper	45	<0.5	50 Class B/50 Class C HMX
PBX 9404	1.847	45	Sand + epoxy	~4.5	>20	
PBX 9404 + 10 wt% wax	1.820	45	Sand + epoxy	23.1	---	93 HMX/3 NC/3 CEF/1 wax
PBX 9404	1.837	45	Garnet paper	4	15	
PBX 9404	1.866	45	Garnet paper	3	11	High density
PBX 9404	1.828	45	Garnet paper	4.8	8	Low density
PBX 9404	1.837	15	Garnet paper	3.0	~15	Nominal density
PBX 9501	1.830	45	Garnet paper	26	~1.0	
PBX 9501	1.830	45	Garnet paper	25	~1.0	PBX 9501 with 0.5 wt% calcium stearate

Table 5.02 (continued)

Explosive	Density (g/cm^3)	Impact Angle (°)	Target Surface	H_{50} (ft)	Over-pressure (psi)	Remarks
Effect of Target Surface						
Comp A-3	1.638	45	Sand + epoxy	>150	---	
PBX 9010	1.786	45	Garnet paper	2.5	~13	
PBX 9404	1.838	15	Quartz	1.8	~15	Target surface finish 1.2-2.0 μm
PBX 9404	1.838	15	Alumina	~11	~15	Target surface finish 1.2-2.0 μm
PBX 9404	1.838	15	Alumina	~19	~15	Target surface finish 0.5-0.9 μm
PBX 9404	1.838	45	Gold	>150	---	Smooth target surface
PBX 9501	1.830	45	Garnet	26	~1.0	
PBX 9501	1.830	15	Quartz	~14	---	Target surface finish 200 μin.
Experimental Formulations						
HMX-Estane Systems						
X-0009	---	45	Sand + epoxy	19.7	---	93.4 HMX/6.6 Estane
LX-14	---	45	Garnet	4	1.5	95.5 HMX/4.5 Estane
X-0282	---	45	Garnet	7.1	0.9	95.5 HMX/4.5 Estane
X-0242	---	45	Garnet	6.1	1.45	95.0 HMX/5 Estane
HMX-Teflon Systems						
X-0204	---	45	Garnet	4.9	---	83 HMX/17 Teflon
HMX-Viton Systems						
X-0215	1.829	45	Garnet	11	2.5	90 HMX/8.5 Viton/1.5 wax/
HMX-Kraton Formulations						
X-0298	1.820	45	Garnet	12.5	1.0	97.5 HMX/1.12 Kraton/1.38 high-vacuum oil
X-0287	1.820	45	Garnet	9.2	1.0	97.4 HMX/1.43 Kraton/1.17 wax

HMX-DNPA-NP Formulations						
X-0217-90-04-60	1.832	45	Garnet	~4	7	90 HMX/6 DNPA/4 NP
X-0217-93-01-60	1.835	45	Garnet	~5	8-23	93 HMX/4.2 DNPA/2.8 NP
X-0217-93-01-60	1.837	45	Garnet	2.5	17	93 HMX/5.25 DNPA/1.75 NP
X-0217-94-01-75	1.839	45	Garnet	~3	22.5	94 HMX/4.5 DNPA/1.5 NP
X-0217-94-01-75	1.824	15	Garnet	~1	>20	94 HMX/4.5 DNPA/1.5 NP
X-0217-94-01-63	1.818	45	Garnet	~2	8.5	94 HMX/3.75 DNPA/1.25 NP/ 1.0 wax
X-0127-94-04-50	1.821	45	Garnet	~8	5.4	94 coarse HMX/3 DNPA/2 NP/ 1 wax
X-0217-94-04-60	1.834	45	Garnet	~4	26	94 coarse HMX/3.6 DNPA/2.4 NP
HMX-DNPA-CEF Formulations						
X-0234-94-01-80	1.841	45	Garnet	3.2	14	94 HMX/4.8 DNPA/1.2 CEF
X-0234-94-01-70	1.842	45	Garnet	8.6	9.4	94 HMX/4.2 DNPA/1.8 CEF/
X-0234-94-01-70	1.841	45	Garnet	~4	~8	94 HMX/4.2 /DNPA/1.8 CEF (2nd series)
X-0234-94-01-60	1.844	45	Garnet	18	~1.8	94 HMX/3.6 DNPA/2.4 CEF
X-0234-94-01-60	1.845	45	Garnet	17	~1.9	94 HMX/3.6 DNPA/2.4 CEF (2nd series)
X-0234-94-01-50	1.847	45	Garnet	36	~1.3	94 HMX/3 DNPA/3 CEF
HMX-TATB-Kel-F 800 Systems						
X-0219-90	1.869	45	Garnet	<1	<0.5	90 HMX/10 Kel-F 800
X-0219-70	1.873	45	Garnet	~3	<0.5	70 HMX/20 TATB/10 Kel-F 800
X-0219-50	1.878	45	Garnet	>64	---	50 HMX/40 TATB/10 Kel-F 800
HMX-TATB-Estane Systems						
X-0272	1.844	45	Garnet	5	~2	93 HMX/5 TATB/3 Estane

5.3 Large-Scale Drop Test or Spigot Test. This test, developed by LASL, is used to help assess the safety of large explosive charges subjected to combined mechanical impact and shearing and, possibly, adiabatic heating. A 6-in.-diam, 4-in.-high right circular cylinder of high explosive weighing 7-9 lb, and usually at its working density, is glued into the counterbore of an inert plastic-bonded material that has about the same shock impedance characteristics. The inert material is an 8-3/4-in.-high truncated cone with diameters of 12-3/4 in. at the top and 8-3/4 in. at the bottom. A 1/2-in.-thick Micarta plate is glued to its top surface to hold a wire sling that is used to raise the assembly. A 1/2-in.-thick steel plate glued to the bottom surface has a 3/4-in.-diam hole in its center and a 1-3/16-in.-diam, 1/4-in.-deep counterbore cut from the surface facing the HE. A steel pin with a 1-1/8-in.-diam, 1/4-in.-thick head and a 1-1/4-in.-long, 3/4-in.-diam shaft is placed through this hole so that its shaft protrudes from the bottom of the HE. As assembled, the head of the steel pin is separated from the bottom surface of the explosive by a 0.35- to 0.50-mm gap and the shaft extends 25 mm beyond the bottom surface of the steel plate.

A test normally consists of 20 drops performed by following the up-and-down technique. The results are reported in terms of the drop height that produces events in half of the trials and of the magnitude of the event.

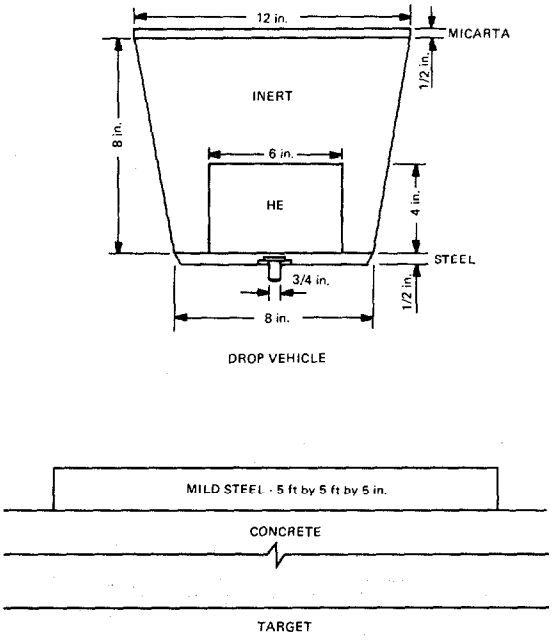

Fig. 5.02. Drop test assembly.

Table 5.03 LARGE-SCALE DROP OR SPIGOT TEST RESULTS

Explosive	Density (g/cm³)	H_{50} (ft)	Type of Event[a]	Over-pressure (psi)	Average Air Gap[b] (mils)	Remarks
Castable Explosives						
Comp B-3	1.725	85	P	---	---	
EDC-1	1.766	110	P	---	---	U.K. Octol with 1 wt% wax
Octol	1.810	45	P	---	---	
Octol + 1 wt% wax	1.805	~150	P	---	---	Very low order, partial
Plastic-Bonded HMX						
PBX 9011	1.773	96	P	~0.2	0.040	
PBX 9404	1.835	49	E	---	---	
PBX 9404 + 1 wt% wax	1.820	~110	D	---	0.030	Detonation
PBX 9501	1.830	>150	P	---	0.030	1 partial in 8 drops from 150 ft
LX-10	1.863	75	D	30.0	0.030	Events were detonation
LX-09	1.842	~90	D	27.0	0.040	Events were detonation
Plastic-Bonded RDX						
Comp A-3	1.638	>150	P	---	---	2 events in 18 trials from 150 ft
PBX 9010	1.786	66	E	---	---	
Experimental Formulations						
HMX-DATB Systems						
X-0143	---	~106	D	---	0.020	85.6 HMX/9.2 DATB/5.2 Estane
HMX-DATB-Viton	1.839	~130	E	5.0	---	70 HMX/20 DATB/10 Viton
HMX-NP-DNPA Systems						
X-0217-94-04-60	---	~150	E	---	---	94 HMX/3.6 NP/2.4 DNPA
HMX-Teflon Systems						
X-0204	---	~53	P	---	---	85 HMX/15 Teflon

[a]P - partial explosion with most of the explosive unreacted. E = explosion with some of the explosive unreacted. D = detonation with all of the explosive reacted.
[b]Air gap between the head of the pin and the explosive.

5.4 Spark Sensitivity. The spark sensitivity of an explosive is determined by subjecting the explosive to a high-voltage discharge from a capacitor. The discharge energy is increased and decreased until the spark energy that produces initiation in half, and only half, of the explosive samples is found.

The explosive sample is placed in a holder like that shown in Fig. 5.03. A polystyrene sleeve is cemented around a steel dowel leaving a 3/16-in.-diam by 1/4-in.-high space to contain the sample. The sample is placed in the sleeve and covered with a lead-foil disk. A polystyrene ring is then clamped over the polystyrene sleeve to hold the foil and sample in place.

The steel dowel provides the ground plane for the electrical circuit. To induce a spark, a needle, charged at high voltage, moves toward and penetrates the lead disk and then is retracted. The discharge takes place when the needle has penetrated the disk and a spark passes through the explosive to the grounded steel dowel. Spark initiation of the explosive is evidenced by a ruptured lead disk; otherwise, the disk is intact except for a single puncture.

The charged needle is moved in and out by a sewing-machine-like mechanism with a stroke duration of about 0.04 seconds. The needle is electrically connected to a variable-capacitance capacitor bank that is, in turn, connected to a variable power supply. Various combinations of voltage and capacitance can be selected to produce the variable spark energy required for the test. The energies given in the tables are found using $E = 1/2\ CV^2$, where C = capacitance in farads, V = potential in volts, and E = spark energy in joules.

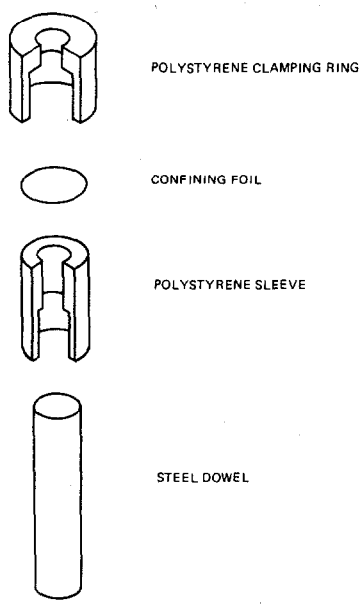

Fig. 5.03. Exploded view of sample holder.

Table 5.04 SPARK SENSITIVITY

Explosive	Energy, (J) 0.076-mm Foil	0.254-mm Foil	Comments
Pure Explosives			
ABH	0.82	2.92	
HMX	0.23	1.42	23% explosions
	0.20	1.03	Brass electrode
	0.11	1.40	
ICCP	1.93	4.04	
Lead chromate	1.03	6.50	Tested at 125°C
PADP	0.42	1.90	
HNAB	0.37	1.38	
PETN	0.19	0.75	8% explosions
	0.19	0.36	Brass electrode
	---	0.41	
Potassium picrate	0.73	0.54	
PYX	1.17	---	
RDX	---	0.87	
	0.22	0.55	Brass electrode
TACOT	---	16.83	
TCTNB	0.38	1.95	
Tetryl	---	3.83	
	0.54	2.79	Brass electrode
TNT	---	4.00	
	0.46	3.75	6% explosions
	0.46	2.75	Brass electrode
Castable Mixtures			
Composition A	0.63	4.38	0% explosions
Cyclotol (75/25)	0.38	3.29	23% explosions
Octol (75/25)	0.82	4.63	17% explosions
Pentolite (50/50)	---	3.33	
	0.32	1.96	15% explosions
	0.44	2.10	Brass electrode
Other Mixtures			
Ball Powder	1.46	7.42	
Detasheet	1.13	16.7	
Plastic-Bonded Explosives			
HMX-based			
PBX 9011	1.09	2.77	33% explosions
PBX 9404	0.42	3.13	0% explosions
X-0298	0.5	3.9	
PETN-Based			
LX-04	1.04	2.58	
RDX-based			
PBX 9010	0.79	1.53	54% explosions
PBX 9205	0.53	1.37	42% explosions
PBX 9407	0.42	3.13	0% explosions

GLOSSARY

ABH	Azo-bis (2,2',4,4',6,6'-hexanitrobiphenyl), $C_{24}H_6N_{14}O_{24}$
Amatex-20	X-0284
ATNI	Ammonium 2,4,5-trinitroimidazole, $C_3H_4N_6O_6$
BDNPA	Bis-dinitropropyl acetal
BDNPF	Bis-dinitropropyl formal
BTF	Benzotrifuroxane (Benzotris-1,2,5-oxadiazole-1-oxide), $C_6N_6O_6$
CEF	Tris-beta chloroethylphosphate
Cell parameters	a,b,c Lengths of unit cell edges along x, y, z axis α, β, γ Interaxial angles α(b,c,), β(a,c), γ(a,b)
Destex	74.8 wt% TNT, 18.7 wt% aluminum 4.7 wt% wax, and 1.9 wt% graphite; also called X-0309
DINA	Di(nitroethyl) nitramine, $C_4H_8N_4O_8$
DNPA	2,2-Dinitropropyl acrylate, $C_6H_8N_2O_6$
DNT	Dinitrotoluene
DODECA	2,2',2'',2''',4,4',4'',4''',6,6',6'',6''' -Dodeca-nitro-m-m'-quatraphenyl, $C_{24}H_6N_{12}O_{24}$
DOP	Di-2-ethylhexyl phthalate, $C_{24}H_{38}O_4$
EDC-1	Another name for octol
EDNA	Ethylene dinitramine, $C_2H_6N_4O_4$
Elvax	A copolymer of ethylene and vinyl acetate

Estane	A polyester polyurethane
EXON-461	A fluorinated thermoplastic resin
FEFO	Bis(1-fluoro-2,2-dinitroethyl) formal, $C_5H_6N_4O_{10}F_2$
HNAB	2,2',4,4',6,6'-Hexanitroazobenzene, $C_{12}H_4N_8O_{12}$
Bis-HNAB	2,2',2'',2''',4,4',4'',4''',6,6',6'',6'''- Dodecanitro-3,3'-bis(phenylazo) biphenyl, $C_{24}H_6N_{16}O_{24}$
HNB	Hexanitrobenzene, $C_6N_6O_{12}$
HNBP	2,2',4,4',6,6'-Hexanitrobiphenyl, $C_{12}H_4N_6O_{12}$
Indices of refraction	The ratio of the velocity of light in two contrasting substances is a constant and is called the refractive index. The absolute refractive index of a substance is its index with respect to a vacuum; this has practically the same value as the index against air. Solid crystalline materials are either isotropic or anisotropic. Isotropic materials have a single index of refraction. Anisotropic crystals of hexagonal or tetragonal systems exhibit, for monochromatic light vibrating parallel to the 'c' axis, a unique index of refraction customarily symbolized as epsilon. For all vibrations directed at 90° to the 'c' axis the refractive indices all equal a common value symbolized as omega. Anisotropic biaxial crystals belong to the orthorhombic, monoclinic, or triclinic system and possess three significant indices of refraction symbolized as alpha, beta, and gamma.
Kel-F 800 Kel-F 827	Chlorofluoroethylene polymers
LX-09	A high-explosive formulation developed by the Lawrence Livermore Laboratory consisting of 93 wt% HMX, 2.4 wt% FEFO, and 4.6 wt% DNPA
LX-14	A high-explosive formulation developed by the Lawrence Livermore Laboratory consisting of 95.5 wt% HMX and 4.5 wt% Estane
MAN	Methyl amine nitrate, $CH_6N_2O_3$
NC	Nitrocellulose
NONA	2,2',2'',4,4',4'',6,6',6''-Nonanitroterphenyl, $C_{18}H_5N_9O_{12}$

NP	Nitroplasticizer
OFHC	Oxygen-free high conductivity
ONT	2,2',4,4',4'',6,6',6''- Octanitro-m-terphenyl, $C_{18}H_6N_8O_{16}$
P-16	A conical explosive lens with a base of 1.6 inches, designed to generate a plane detonation
P-22	A conical explosive lens with a base of 2.2 inches, designed to generate a plane detonation
P-40	A conical explosive lens with a base of 4.0 inches, designed to generate a plane detonation
P-80	A conical explosive lens with a base of 8.0 inches, designed to generate a plane detonation
P-120	A conical explosive lens with a base of 12.0 inches, designed to generate a plane detonation
PADP	2,6-Bis(picrylazo)-3,5-dinitropyridine, $C_{17}H_5N_{13}O_{16}$
PATO	3-Picrylamino-1,2,4-triazole, $C_8H_5N_7O_6$
PC	A thermoplastic polycarbonate
PENCO	2,2',4,4',6-Pentanitrobenzophenone, $C_{13}H_5N_5O_{11}$
PMMA	Any of several polymethylmethacrylates
PS	Polystyrene
PYX	2,6-Bis(picrylamino)-3,5-dinitropyridine, $C_{17}H_7N_{11}O_{16}$
QMAN	Tetramethylammonium nitrate, $C_4H_{12}N_2O_3$
Sauereisen	A brand name of an acid-proof cement
Susan Test	This projectile impact sensitivity test was developed by the Lawrence Livermore Laboratory. The high-explosive test sample configured in the form of a right circular cylinder and weighing about 0.45 kg is loaded into an aluminum cap, which becomes the head of a steel-bodied projectile. Projectiles containing the test explosive in the nose cap are fired from a gun at progressively increasing velocities against a rigid steel target. The overpressure resulting from the impact or from subsequent events such as explosions or detonations are determined. Results are generally reported as a single sensitivity curve with overpressure, normalized

	to a point source detonation, plotted as a function of the projectile velocity. A more complete description of the test may be obtained in a paper by L. G. Green and G. D. Dorough published in the *Fourth Symposium (International) on Detonation* (Office of Naval Research, ACR-126, October 1965).
Sylgard	Low-temperature vulcanizing silicone resin
T-TACOT	1,3,8,10-Tetranitrobenzotriazolo-1,2a-benzotriazole, $C_{12}H_4N_8O_8$
Z-TACOT	1,3,7,9-Tetranitrobenzotriazolo-2,1a-benzotriazole, $C_{12}H_4N_8O_8$
TCTNB	Trichlorotrinitrobenzene, $C_6N_3O_6Cl_3$
TNN	1,4,5,8-Tetranitronaphthalene, $C_{10}H_4N_4O_8$
TNS	Trinitrostilbene, $C_{14}H_{11}N_3O_6$
TOF	Trioctylphosphate, a plasticizer
TPB	1,3,5-Tripicrylbenzene, $C_{29}H_9N_9O_{18}$
TPM	Tripicrylmelamine, $C_{21}H_9N_{15}O_{18}$
TPT	2,4,6-Tripicryl-s-triazine, $C_{21}H_6N_{12}O_{18}$
Viton	A fluoroelastomer
Wax	Any of a series of petroleum-based paraffins
XTX	E*XT*rudable e*X*plosive

AUTHOR INDEX

SUBJECT INDEX